IN TWO SECTIONS—SECTION ONE

Transactions

of the

ASME

JANUARY, 1951

VOL. 73, NO. 1

Transactions

of The American Society of Mechanical Engineers

Published on the tenth of every month, except March, June, September, and December

---

Published monthly by The American Society of Mechanical Engineers. Publication office at 20th and Northampton Streets, Easton, Pa. The editorial department is located at the headquarters of the Society, 29 West Thirty-Ninth Street, New York 18, N. Y. Cable address, "Dynamic," New York. Price $1.50 a copy, $12.00 a year for Transactions and the *Journal of Applied Mechanics*; to members and affiliates, $1.00 a copy, $6.00 a year. Changes of address must be received at Society headquarters three weeks before they are to be effective on the mailing list. Please send old as well as new address. . . . By-Law: The Society shall not be responsible for statements or opinions advanced in papers or . . . printed in its publications (B13, Par. 4). . . . Entered as second-class matter March 2, 1928, at the Post Office at Easton, Pa., under the Act of August 24, 1912. . . . Copyrighted, 1951, by The American Society of Mechanical Engineers. Reprints from this publication may be made on condition that full credit be given the Transactions of the ASME and the author, and that date of publication be stated.

Investigations of Axial-Flow Compressors

By J. T. BOWEN,[1] R. H. SABERSKY,[2] AND W. D. RANNIE,[3] PASADENA, CALIF.

An approximate theory of the general perfect fluid flow in axial turbomachines is presented. The validity of the simplifying assumptions of the theory is justified by comparison with flow patterns measured in a large, low-speed, axial-flow compressor. It is concluded that the theory is convenient to apply and is sufficiently accurate for most engineering purposes. Performance data on blading designed for two and three-dimensional flow show that the blade types have comparable efficiencies. It is suggested that the advantages of unconventional blade types be exploited by designers. The flow regions in which fluid viscosity is important are shown. Experimental studies of cascade losses in the compressor indicate these losses to be greater than those measured in a cascade test tunnel. Measurements show that the rate of growth of the wall boundary layer need not be unusually great in an axial-flow compressor.

Nomenclature

The following nomenclature is used in this paper and is illustrated in part by Fig. 1:

- A = compressor-annulus area
- C = velocity at any point; airfoil chord length
- C_a = axial-velocity component
- C_u = circumferential-velocity component
- H = boundary-layer shape parameter $\left(\frac{\delta^*}{\vartheta}\right)$
- i^* = flow-incidence angle relative to leading-edge camber line
- n = an exponent
- p = static pressure
- p_t = total pressure (static plus dynamic)
- r = radius of a particular stream tube
- r_i = hub radius
- r_0 = tip radius
- S = cascade pitch
- u_0 = velocity of rotor-blade tip
- α = a constant
- β = relative flow direction measured from plane of rotation
- δ = trailing-edge deviation angle; boundary-layer thickness
- β' = rotor-blade stagger angle
- γ = absolute flow direction measured from plane of rotation
- γ' = stator-blade stagger angle
- δ^* = boundary-layer displacement thickness
- Δ = change of a quantity
- η = compressor efficiency
- ϑ = boundary-layer momentum thickness
- θ = airfoil-camber angle
- θ^* = fluid turning angle, e.g., $\beta_2 - \beta_1$
- ρ = fluid density
- ϕ = local axial-velocity coefficient
- $\bar{\phi}$ = average flow coefficient
- $\bar{\phi}'$ = average flow coefficient omitting boundary-layer and wake effects
- ψ = local power coefficient
- $\bar{\psi}$ = average power coefficient
- $\bar{\psi}'$ = average total pressure increase coefficient
- ω = rotor angular velocity
- Ω = mean cascade loss coefficient

Subscripts

- 1, 2, 3, etc. = various axial stations
- $\bar{x}$ = average value
- x^* = characteristic value

Introduction

During the past few years the multistage axial-flow air compressor has become a frequently used component in gas-turbine systems. Single-stage axial-flow pumps and fans had previously found numerous industrial applications. However, much of the development work on such devices has taken place under conditions which require that a working machine be produced in the shortest possible time, and relatively few fundamental investigations of internal flow patterns have been made. Perhaps the most extensive work has been done by British investigators and by the NACA in this country.

Prior to the inception of this experimental program, a theory of perfect fluid flow in axial turbomachines had been developed by the senior author. One of the principal objects of the experimental work was to determine the correctness of the theory. This theory has not been widely available and therefore is summarized in this paper.

It was believed that verification of the validity of the compressor theory and considerable information on the location and magnitude of major losses could be obtained from tests in the low-speed, low Mach number regime of operation. The minor influence of fluid compressibility up to the first appearance of sonic velocity can be predicted satisfactorily from low-speed data. Hence a relatively large, low-speed compressor of one to three stages was constructed. Since the main emphasis of the program is on the study of internal flow, considerable attention has been devoted to internal instrumentation. The results obtained in the first two years of testing are summarized in this paper. More detailed accounts of the work and descriptions of the equipment are given in references (1) and (2).[4]

Axial-Flow Compressor Theory

Determination of Flow Pattern for Given Blading. Consider the flow of an incompressible fluid through a single isolated blade row in an annular duct. A rotor will be considered first; hence the blade row is assumed to have a constant angular velocity. Further, it is assumed that the blades are sufficiently close together so that there is complete symmetry in the flow outside of the blade row. The elementary stream tubes then are bounded by surfaces of revolution and, in a section through the axis of the

---

[1] Research Assistant, Mechanical Engineering, California Institute of Technology; now Research Engineer, Union Carbide and Carbon Corporation, New York, N. Y. Jun. ASME.

[2] Assistant Professor, Mechanical Engineering, California Institute of Technology. Jun. ASME.

[3] Assistant Professor, Mechanical Engineering, California Institute of Technology.

Contributed by the Hydraulic Division and presented at the Annual Meeting, New York, N. Y., November 27–December 2, 1949, of The American Society of Mechanical Engineers.

Note: Statements and opinions advanced in papers are to be understood as individual expressions of their authors and not those of the Society. Paper No. 49—A-102.

[4] Numbers in parentheses refer to the Bibliography at the end of the paper.

compressor, they will appear as in Fig. 1. At great distances upstream or downstream from the blade row, the streamlines must lie on cylindrical surfaces since this is the only possible flow. The radius of a stream surface will, in general, change after passing through the blade row. As shown in Fig. 1, the radius of a stream tube far upstream is denoted by r_1 and the radius of the same stream tube far downstream by r_2.

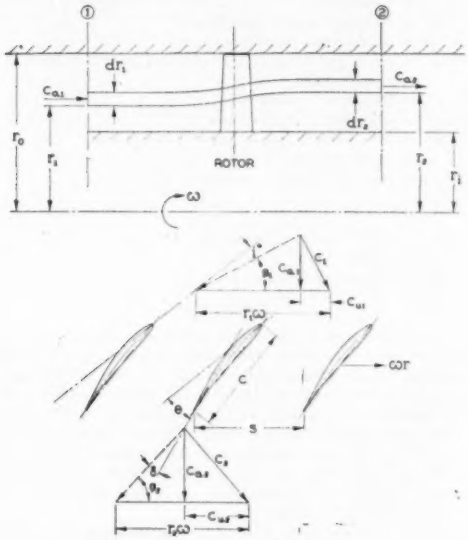

FIG. 1 ILLUSTRATION OF NOMENCLATURE

Consider two stations, one far upstream and one far downstream. For these stations the equations of motion reduce to the radial equilibrium conditions

$$\rho \frac{C_{u1}^2}{r_1} = \frac{dp_1}{dr_1}, \quad \rho \frac{C_{u2}^2}{r_2} = \frac{dp_2}{dr_2} \quad \ldots\ldots\ldots\ldots [1]$$

where ρ is the density, p the pressure, and C_u the circumferential or whirl component of velocity. The equation corresponding to the Bernoulli equation is obtained by integrating the Eulerian equations of motion in a system rotating with angular velocity ω and hence

$$p_1 + \frac{\rho}{2}(C_{u1}^2 + C_{a1}^2 - 2\omega r_1 C_{u1}) = p_2 + \frac{\rho}{2}(C_{u2}^2 + C_{a2}^2 - 2\omega r_2 C_{u2}) \ldots\ldots [2]$$

where C_a is the axial component of velocity. For a stator blade the terms with ω vanish. The continuity equation is

$$C_{a1} r_1 dr_1 = C_{a2} r_2 dr_2 \ldots\ldots\ldots\ldots\ldots [3]$$

If the upstream flow pattern is completely known, Equations [1], [2], and [3] involve the four unknowns p_2, C_{u2}, C_{a2} (as functions of r_2, say), and r_2 as a function of r_1. The fourth equation, to make the solution determinate, must introduce the geometry or physical characteristics of the blades.

By considering only stations far upstream and far downstream it has so far been possible to avoid any consideration of radial velocity components, since these are confined to the immediate vicinity of the blade row. The simplest way of introducing the blade characteristics is to assume that the angle of flow leaving the blade row is a known function of r_2 and is independent of the upstream conditions. This assumption is very good for closely spaced blades (high solidity) and is surprisingly good for solidities (C/S) as low as 0.70. If β_2 is the angle relative to the moving blades between the exit flow direction and the plane of rotation, then the influence of the blade row on the flow is given by the relation

$$C_{u2} = \omega r_2 - C_{a2} \cot \beta_2 \ldots\ldots\ldots\ldots\ldots [4]$$

This relation is assumed to hold far downstream so that it is implied that the radial shift takes place entirely within the blade row, that is, the radius r_2 of the streamline is constant downstream of the trailing edges of the blades. Even if the radial shift outside the blade row is appreciable, however, the error introduced is relatively small, as will be shown.

By differentiating Equation [2] and substituting from Equations [1] and [4] there results, after some rearrangement

$$\frac{(\omega r_2 - C_{a2}\cot\beta_2)^2}{r_2} + \frac{1}{2}\frac{d}{dr_2}\left[-\omega^2 r_2^2 + \frac{C_{a2}^2}{\sin^2\beta_2}\right] = \left[\frac{C_{u1}^2}{r_1} + \frac{1}{2}\frac{d}{dr_1}(C_{a1}^2 + C_{u1}^2) - \omega\frac{d}{dr_1}(r_1 C_{u1})\right]\frac{dr_1}{dr_2}$$

The ratio dr_1/dr_2 is now eliminated by substituting from Equation [3], giving, with further rearrangement

$$\frac{dC_{a2}}{dr_2} + \left[\frac{\cos^2\beta_2}{r_2} - \frac{d}{dr_2}(\ln \sin\beta_2)\right] C_{a2} = \omega\left[2\sin\beta_2\cos\beta_2 - \frac{r_2}{C_{a1}r_1}\sin^2\beta_2\frac{d}{dr_1}(r_1 C_{u1})\right] + \frac{r_2}{C_{a1}r_1}\left[\frac{C_{u1}^2}{r_1} + \frac{1}{2}\frac{d}{dr_1}(C_{a1}^2 + C_{u1}^2)\right]\sin^2\beta_2 \ldots [5]$$

This differential equation for C_{a2} is nonlinear because the right-hand side contains functions of r_1 as well as of r_2. The coefficient of C_{a2} is a known function of r_2, and the right-hand side of the equation is composed of known functions of r_1 and r_2. The exact solution requires simultaneous solving of Equations [5] and [3], but because of the nonlinearity, approximate methods must be employed.

To obtain an approximate solution of Equation [5] a linearization is made by putting $r_1 = r_2 = r$. The right-hand side then becomes a known function of r, and the equation becomes a linear first-order differential equation for C_{a2}. It is reasonable to suppose that the error thus introduced is small because $r_1 = r_2$ at the annulus walls and the maximum difference $|r_1 - r_2|$, which occurs somewhere near the middle of the annulus, is small compared to r_1 or r_2 in any problem of engineering interest. With the assumption that $r_1 = r_2$, Equation [3] in its differential form is no longer required. The integrated form, however, will be necessary for evaluation of the constants of integration which arise in the solution of Equation [5].

It is important to recognize that the foregoing linearization process must be carried out in a definite manner. If r_1 is set equal to r_2 in the original equations, Equation [3] yields the result $C_{a1} = C_{a2}$. This approximation is the usual one hitherto employed, and is equivalent to assuming "two-dimensional" flow. It is applicable, however, only in very restricted cases. When used beyond its range of applicability it leads to quite erroneous results. The improved linearization method described makes use of the fact that, although $r_2/r_1 = 1$, the ratio dr_2/dr_1 can be very different from unity. Since the approximation $r_2 = r_1$ is

introduced only after Equation [5] is derived, the procedure is seen to give a more nearly correct accounting of the variation dr_1/dr_2. The approximation is valid only when the outer and inner streamlines lie on fixed boundaries; it cannot be used where ducting is absent, as for instance, in heavily loaded windmills or propellers.

Equation [5] can now be integrated formally, giving

$$C_{a2} = \sin\beta_2\, e^{-\int \frac{\cos^2\beta_1}{r_2}\,dr_2} \left\{ \int \left[\omega \left(2\cos\beta_2 - \frac{\sin\beta_2}{C_{a1}} \frac{d}{dr_1}(r_1 C_{a1}) \right) + \frac{\left[\frac{C_{a1}^2}{r_1} + \frac{1}{2}\frac{d}{dr_1}(C_{a1}^2 + C_{a1}^2) \right]}{C_{a1}} \sin\beta_2 \right] e^{\int \frac{\cos^2\beta_1}{r_2}\,dr_2} dr_2 + K \right\} \quad \ldots\ldots [6]$$

The constant K is evaluated by means of the continuity equation, Equation [3], integrated over the annulus area. The expression for C_{a2} cannot, in general, be evaluated in closed form; it can, however, be evaluated easily by numerical processes. Ordinarily the numerical integrations can be carried out with simply the trapezoidal rule, and five or six radial stations will be found to give sufficient accuracy. Having determined C_{a2}, the velocity component C_{w2} is obtained immediately from Equation [4], and other quantities, such as pressures and work input can be computed. The corresponding calculation for the flow through a stator-blade row is accomplished simply by letting $\omega = 0$ in Equation [6]. With C_{a1} and C_{a2} determined, the streamline shifts and, therefore, r_2/r_1 can be computed from the continuity equation. This ratio may then be substituted into Equation [5] and a second approximation may be obtained for C_{a2}. This process of iteration can be continued, and in all examples worked has been found to converge rapidly; however, for moderate hub ratios (say 0.5) and physically realizable blade loading, the first approximation (Equation [6]) is usually satisfactory for engineering purposes.

The foregoing calculations have referred to isolated blade rows, but if it is assumed that conditions similar to those far upstream and far downstream exist between adjacent blade rows, the methods can be applied to any multistage machine. For compressible fluids, the flow can be treated as incompressible through a blade row and then corrected for the average density change before proceeding to the next row. If an appreciable fraction of the radial shift in the streamlines takes place outside the blade row, then the leaving-flow angle, as introduced in Equation [4], will not be quite correct in the middle of the channel, and, further, for closely spaced blade rows, the radial shift of any one row will influence the flow through adjacent rows. In such cases, a more elaborate analysis is required and the reader is referred to the work of F. E. Marble (3). Numerical comparisons of the results of the approximate method described here have been made with the more nearly correct treatment for several different examples. In all cases the simpler methods were found sufficiently accurate for engineering purposes. In actual compressor flow, the real fluid effects tend to mask any further refinement to the calculation of perfect fluid flow.

Determination of Blading for Given Flow Pattern. The foregoing derivation indicates a method by which the flow pattern through an arbitrary blade row may be determined. The inverse problem, i.e., the determination of the blade angles to yield a prescribed flow pattern, will be discussed next. To limit the treatment somewhat, a design will be considered for which the entering fluid is of constant total energy and for which the flow pattern repeats in successive stages (a stage consists of one rotor row and one stator row).

For this case the Bernoulli equation for the flow through the rotor is identical with Equation [2], and the equation for the flow through the following stator becomes

$$p_2 + \frac{1}{2}\rho(C_{a2}^2 + C_{w2}^2) = p_3 + \frac{1}{2}\rho(C_{a3}^2 + C_{w3}^2) \quad \ldots [7]$$

The equations of motion for the radial direction are

$$\frac{dp_1}{dr_1} = \rho\frac{C_{w1}^2}{r_1} = \frac{dp_2}{dr_1}, \quad \frac{dp_2}{dr_2} = \rho\frac{C_{w2}^2}{r_2} \quad \ldots\ldots [8]$$

From Equations [2] and [7] the pressure rise across a stage is seen to be

$$\Delta p = p_3 - p_1 = \rho\omega(C_{w2}r_2 - C_{w1}r_1)$$

or, within the approximation previously introduced ($r_1 = r_2 = r$)

$$\Delta p = \rho\omega r(C_{w2} - C_{w1}) \quad \ldots\ldots [9]$$

Since the flow pattern repeats, the kinetic energy of the air leaving the stage is the same as that of the entering air, so that the pressure difference (Δp) is proportional to the energy added by the rotor. As a consequence of the repeating flow pattern and Equation [8], the energy addition is independent of the radius.

Differentiating Equation [7] and substituting Equation [8], one obtains the relation

$$\frac{C_{w2}^2}{r_1} + \frac{1}{2}\frac{d}{dr_1}(C_{a1}^2 + C_{w1}^2) = \left[\frac{C_{w2}^2}{r_2} + \frac{1}{2}\frac{d}{dr_2}(C_{a2}^2 + C_{w2}^2) \right] \frac{dr_2}{dr_1} \quad \ldots\ldots [10]$$

The left-hand side of this equation represents the radial-energy gradient of the entering fluid. In the case under discussion this is equal to zero, and Equation [10] may be separated into two equations

$$\frac{C_{w1}^2}{r_1} + \frac{1}{2}\frac{d}{dr_1}(C_{a1}^2 + C_{w1}^2) = 0 \quad \ldots\ldots [10a]$$

and

$$\frac{C_{w2}^2}{r_2} + \frac{1}{2}\frac{d}{dr_2}(C_{a2}^2 + C_{w2}^2) = 0 \quad \ldots\ldots [10b]$$

For evaluation of the constants of integration that occur in the solutions of Equations [10a] and [10b], the integral form of the continuity equation is introduced, i.e.

$$\int_{r_1}^{r_2} C_{a1} r_1 dr_1 = \int_{r_1}^{r_2} C_{a2} r_2 dr_1 = \frac{1}{2}\overline{C}_a(r_2^2 - r_1^2) \ldots [3a]$$

The quantity Δp, being independent of radius, is equal to the specific energy addition per stage, and the quantity $\overline{C}_a$, the average axial velocity component, determines the flow rate. Δp and $\overline{C}_a$ together, therefore, determine the over-all performance of the compressor at the design condition and are the design parameters which are usually specified. Having selected Δp and $\overline{C}_a$, there are three equations, Equations [10a], [10b], and [9], available for the solution of the inverse problem. The number of unknowns involved is four, and a further assumption may, therefore, be introduced. It is convenient to specify the radial distribution of the circumferential velocity, $C_{w1}(r_1)$. With C_{w1} specified, Equation [10a] can be solved directly for C_{a1}. The velocity C_{w2} is determined from Equation [9], and knowing C_{w2}, C_{a2} is easily obtained from Equation [10b]. The constants of integration are determined from Equation [3a].

Investigation of Various Blade Types. It is to be noticed that a different flow pattern, and therefore different blade shapes,

corresponds to each selection of $C_{u1}(r_1)$. Nevertheless, the overall performance as given by Δp and $\bar{C}_a$ is not changed. This means that entirely different blade shapes may produce the same design performance. Since the internal flow pattern is different for each shape, the blade types will exhibit different properties. Some of the more important properties are the following:

1 The maximum velocity (either absolute or relative) that occurs in the flow pattern. This quantity is of importance in high-speed compressors if detrimental compressibility effects are to be avoided.

2 The maximum fluid turning required of any blade section. This quantity is related to the lift coefficient. Large losses are frequently associated with large turning angles or lift coefficients.

3 The blade twist. This quantity is of importance in blade manufacture and for strength considerations.

A number of blade types were investigated and compared on the basis of these and similar criteria. Types were investigated which resulted from assuming $C_{u1} = \alpha u_0 \left(\frac{r}{r_0}\right)^n$, where α is some constant and n was taken equal to -2, -1, 0, 1, and 2. To obtain a more uniform basis of comparison α was selected so that C_{u1} at the mid-radius would be equal for all types, a restriction which can be shown to have, in general, only a minor influence on the results of the comparison.

The study shows that significant differences in the properties of the various types result. Therefore it should be possible to select a most suitable type for each particular application.

A blade type which is frequently used in compressors is the so-called "free-vortex" blading. This type results from assuming $C_{u1} = \alpha u_0 (r_0/r)$. The name of the blading comes from the fact that the assumed distribution of the circumferential-velocity component C_{u1} is the same as that of a free vortex. An inspection of Equations [9], [10a], and [10b] shows that considerable simplifications occur in the analytical work for this case; for example, the axial velocity is uniform and the flow essentially two-dimensional. On the basis of some of the properties mentioned, however, other blade types show significant improvement over the free-vortex blading. If, for example, compressibility effects are of importance, a reduction of about 10 per cent in the maximum relative velocity component may be obtained by changing from a free-vortex design to a so-called "solid-body-rotation" design, i.e., one in which C_{u1} is proportional to the radius. For the same value of the maximum relative velocity the change in blade type allows a reduction in hub-to-tip ratio equivalent to about a 20 per cent decrease in the frontal area. Such improvements are of interest in the design of compressors for aircraft applications. Similar improvements are likely to be possible for other applications. In this connection, it should be pointed out that none of the assumptions restricts the theory to air as a working fluid, and the results apply to axial-flow pumps equally well.

From the foregoing study, the free-vortex and the solid-body blading were selected for the experimental work. The free-vortex blading was selected because it was desired to measure in detail the flow pattern of this more conventional set at its design point, and to determine its efficiency in order to establish a basis of comparison with other blade types. Off the design point, this blading does not possess any properties which simplify the flow pattern, and the experiments at those flow rates lend themselves very well to checks on the theory. The solid-body set is of general interest because it has a number of desirable properties as, for example, the low diagram velocity mentioned previously. It is of special interest here, because it represents a blade shape very different from the free-vortex blades and leads to a three-dimensional flow at the design point as well as off the design point. This will give further checks on the proposed compressor theory, and it will show whether or not such a blading has a comparable efficiency at its design point.

Determination of Blade-Section Characteristics. So far the blade rows have been treated as if they consisted of an infinite number of closely spaced blades. The direction of the air leaving a row would then be equal to the direction of the trailing-edge tangent and would be independent of the entrance direction.

To find the direction of the flow through a cascade of blades of finite spacing and thickness, various techniques may be employed. Where test data of two-dimensional cascades (having the same cross sections as the compressor blade at the radius in question) are available, they may be used with satisfactory accuracy, provided the axial-velocity component remains approximately constant for the flow through the section of the blade row in question. If large changes in this component occur, the static pressure change (amount of diffusion) through the compressor blade row is different from that in the purely two-dimensional case and the cascade characteristics are expected to be influenced. On the basis of some preliminary test results it seems that it is mainly the magnitude of the incidence angle at which the real fluid effects become considerable which is changed. For the region of incidence angles for which real fluid effects are small, however, the leaving angle seems to be well predicted by the two-dimensional data even for three-dimensional flow.

The leaving angle also may be predicted on the basis of a conformal transformation of the flow of a perfect fluid about an infinite cylinder. This method accurately predicts two-dimensional cascade performance if real fluid effects are small, but in application to compressor design, the method is subject to the several restrictions of two-dimensional test data.

Another method is a rule derived by H. Constant (4) based again upon two-dimensional cascade data. According to this rule, the deviation of the direction of the leaving fluid from the trailing-edge tangent is equal to $\delta = 0.26\,\theta\sqrt{S/C}$ at the design condition. Over the range of incidence angles for which losses are relatively low (the region of most interest in compressor design), this deviation may be taken as constant.

For the cases in which the three methods could be compared, the results were in good agreement, again of course only in the region of low losses.

Test Equipment

A test program was initiated with the objectives of evaluating the assumptions and range of applicability of the turbomachine theory and of investigating the location and extent of viscosity effects in a compressor flow stream. The test compressor was designed to simulate internal flow patterns commonly employed in modern, high-performance compressors. The entire test installation is also adaptable to investigation of other compressor phenomena.

A general view of the test compressor is given in Fig. 2. A cross section of the entire installation is shown in Fig. 3 where the principal dimensions are also summarized. Air from the laboratory room enters the cylindrical entrance duct through a bell mouth. The wall static pressure of the entrance duct is calibrated to give total air-flow rate. The air stream acquires an initial circumferential component in flowing through the entrance or prerotation vanes. It then passes through successive rows of rotating and fixed compressor blades as shown in Fig. 3. It should be noted that each row of blades is separately removable, hence one to three full or partial stages may be installed. Each blade can be rotated about its shank center and be accurately located by a simple indexing mechanism. By this means, all blade angles may be adjusted in $^1/_2$-deg increments.

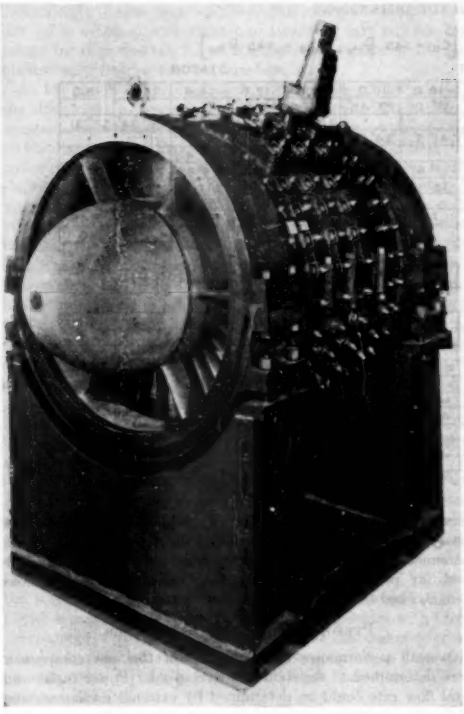

FIG. 2 TEST COMPRESSOR

Six rectangular ports are provided near the top of the outer case through which an instrument survey carriage can be inserted. Using the survey carriage, instruments can be placed accurately at any point within a 15-deg sector of an annular section. An instrument probe also can be rotated about its own center line, thus allowing flow-direction measurement. Axial locations of the ports make possible flow surveys downstream of each rotor and stator-blade row. A set of access holes is provided for making radial surveys between blade rows. Measurements of local total pressure, static pressure, velocity, and flow direction are made through the access holes and ports. The average total pressure rise through a given number of stages, hence the power input to the air stream, is determined by flow surveys downstream of the last blade row. Downstream of the last measuring plane, two sets of vanes are provided to remove the whirl velocity and thus minimize duct loss. The air stream passes out of the test installation through a vaned elbow and a rectangular, adjustable throttling orifice. The throttle is used to vary flow resistance and thus the total air-flow rate.

A 125-hp electric dynamometer drives the compressor by means of a shaft which passes through the rear duct. Accurate measurements of rotative speed and driving torque are possible. Thus the power input to the compressor can be computed. Windage and bearing-friction torques proved to be so low that it is unnecessary to correct for their effect.

Both sets of compressor blading (free-vortex and solid-body) were designed for repeating flow patterns throughout the three stages and for an average power coefficient $\bar{\psi} = 0.40$ at a flow coefficient $\bar{\phi} = 0.45$ (Equations [11] and [12]). The blade sets are shown in Fig. 4. The design method previously outlined was used. Geometric properties of the blade sets are summarized in Table 1. All blade sections have circular arc camber lines which are tangent to the incident velocity direction at the design condition. The empirical rule of Constant was used to determine leaving angles. A thickness distribution similar to that of modern high-speed airfoils (maximum thickness at 35 per cent C) was distributed about the camber lines. The actual blades were sand-cast of 356 aluminum alloy and finished by hand. Careful

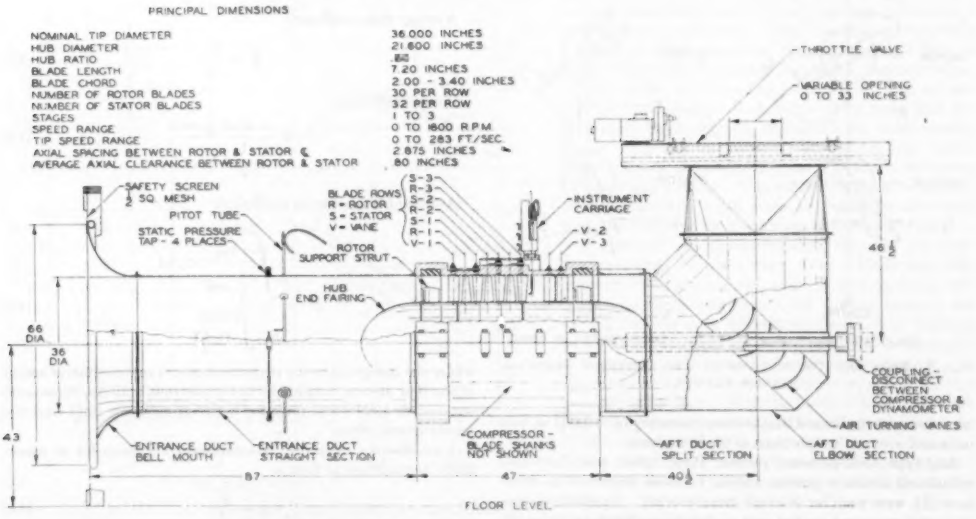

FIG. 3 ASSEMBLY DRAWING OF THE TEST INSTALLATION

TABLE 1 COMPRESSOR BLADE DIMENSIONS

FREE VORTEX $\left[C_{u1} = .145\ \bar{P} u_0;\ C_{u2} = .345\ \bar{P} u_0\right]$

	ROTOR					STATOR				
SECTION LOCATION - r - INCHES	10.8	12.6	14.4	16.2	18.0	10.8	12.6	14.4	16.2	18.0
DESIGN ENT. ANGLE - ROTOR - β_1 - DEG.	51° 21′	42° 24′	36° 2′	31° 21′	27° 45′					
DESIGN ENT. ANGLE - STATOR - γ_2 - DEG.						38° 3′	42° 24′	46° 13′	49° 34′	52° 31′
DESIGN EXIT ANGLE - ROTOR - β_2 - DEG.	86° 49′	85° 17′	50° 40′	41° 3′	34° 29′					
DESIGN EXIT ANGLE - STATOR - γ_1 - DEG.						61° 46′	65° 17′	68° 4′	70° 16′	72° 8′
SECTION CAMBER - θ - DEGREES	46° 40′	31° 0′	20° 19′	13° 47′	9° 46′	31° 53′	31° 6′	29° 59′	28° 41′	27° 20′
CASCADE STAGGER ANGLE - β' - DEG.	74° 48′	57° 54′	46° 12′	36° 15′	32° 36′					
CASCADE STAGGER ANGLE - γ - DEG.						54° 0′	57° 57′	61° 12′	63° 55′	66° 11′
SOLIDITY - C/S	1.150	.985	.862	.766	.690	1.035	.970	.920	.880	.849
MAXIMUM THICKNESS - % C	12	11	10	9	8	10	10	10	10	10

SOLID BODY $\left[C_{u1} = .325\ \frac{r}{r_0} u_0;\ C_{u2} = \left(.325\ \frac{r}{r_0} + .200\ \bar{P}\right) u_0\right]$

	ROTOR					STATOR				
SECTION LOCATION - r - INCHES	10.8	12.6	14.4	16.2	18.0	10.8	12.6	14.4	16.2	18.0
DESIGN ENT. ANGLE - ROTOR - β_1 - DEG.	52° 10′	46° 18′	40° 30′	34° 42′	28° 43′					
DESIGN ENT. ANGLE - STATOR - γ_2 - DEG.						46° 22′	46° 15′	42° 40′	37° 21′	29° 18′
DESIGN EXIT ANGLE - ROTOR - β_2 - DEG.	83° 7′	70° 47′	58° 19′	45° 33′	31° 48′					
DESIGN EXIT ANGLE - STATOR - γ_1 - DEG.						69° 30′	65° 16′	60° 36′	55° 11′	48° 41′
SECTION CAMBER - θ - DEGREES	40° 52′	32° 45′	24° 6′	14° 49′	4° 15′	28° 23′	25° 53′	24° 37′	24° 42′	27° 0′
CASCADE STAGGER ANGLE - β' - DEG.	72° 36′	62° 41′	52° 33′	42° 7′	30° 51′					
CASCADE STAGGER ANGLE - γ - DEG.						62° 34′	59° 12′	54° 59′	49° 42′	42° 46′
SOLIDITY - C/S	1.150	1.061	.995	.944	.903	1.039	.970	.920	.880	.850
MAXIMUM THICKNESS - % C	12	11	10	9	8	10	10	10	10	10

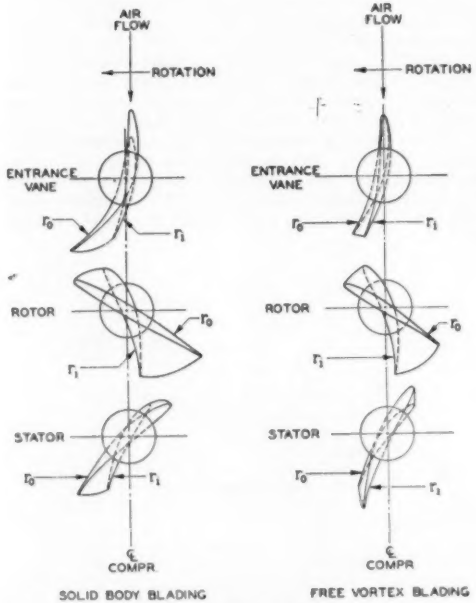

FIG. 4 ROOT AND TIP SECTIONS OF TWO TYPES OF TEST-COMPRESSOR BLADING

measurements indicated that contour accuracy of ±0.003 in. was obtained over critical portions of blade surfaces.

Kiel-type total-pressure probes, Pitot tubes, and three-hole cylindrical direction probes, similar to those described in reference (5), were used for internal measurement. In addition, special total pressures probes and a claw-type direction probe (6) were constructed from 0.020-in. hypodermic tubing for flow measurements near bounding surfaces. Inclined-tube water manometers and an electric strain-gage pressure pickup were used for pressure measurement. All instrument calibrations were checked frequently in a 1-in. calibration jet.

PERFORMANCE OF TEST COMPRESSOR

Over-all performance characteristics of the test compressor were determined at constant rotative speed. Power input and total flow rate could be determined by external measurements, while the air-stream pressure rise was obtained from complete internal survey data. The results are presented in terms of dimensionless coefficients, as follows

Average flow coefficient

$$\bar{\phi} = \frac{\bar{C}_a}{u_0} \qquad [11]$$

Power coefficient

$$\bar{\psi} = \frac{\text{shaft power}}{\frac{1}{2}\rho A \bar{C}_a u_0^3} \qquad [12]$$

Average total pressure coefficient

$$\bar{\psi}' = \frac{\int_{\text{Sector}} \frac{\Delta p_t}{\frac{1}{2}\rho u_0^2} C_a dA}{\int_{\text{Sector}} C_a dA} \qquad [13]$$

where the integrations are performed over a representative sector of the flow stream behind the last blade row, and Δp_t represents the rise in local total pressure between entrance duct and the measurement plane.

A satisfactory definition of compressor efficiency for an essentially incompressible flow is

$$\eta = \frac{\bar{\psi}'}{\bar{\psi}} \qquad [14]$$

According to the previous definitions, it is seen that efficiency thus defined is weighted with respect to local flow rate but not corrected for compressibility,[4] mixing loss downstream of the last blade row, or bearing and windage loss.

In Fig. 5 the power coefficient, the pressure coefficient, and the efficiency are shown as functions of the flow coefficient for a constant rotative speed of 750 rpm. In addition to the experimental curves for free-vortex and solid-body blading, the power-input curve predicted by the turbomachine theory is also shown. It will be recalled that both blade sets were designed for a power coefficient $\bar{\Psi} = 0.40$ at a flow coefficient of $\bar{\phi} = 0.45$. It is seen that in each case, $\bar{\Psi} = 0.40$ at a lower flow, $\bar{\phi} = 0.43$, but that the measured and calculated performance curves are nearly parallel. Displacement of the design point to a lower flow rate was expected, since in designing the compressor for test work it was unnecessary to consider the effective area reduction due to wall and blade-surface boundary layers. The performance of the compressor is largely determined by flow in the center-passage areas. These portions of the flow attain design velocities at an over-all flow rate approximately 4½ per cent lower than that of a perfect fluid. Compressor designers are usually able to estimate this effect with satisfactory accuracy. With this adjustment the measured and calculated power curves become almost identical near the design condition.

The pressure-rise curves $\bar{\Psi}'$, lie somewhat below the power curves. The efficiency attains its maximum value near the design point in all cases, the maximum values being, respectively, 89 per cent and 88 per cent for single stages of vortex and solid-body blading and somewhat lower for three stages of vortex blading. It should be noted that at the test speed of 750 rpm, the Reynolds number is rather low. A few tests conducted at higher speeds indicated significant efficiency increase with Reynolds number, a maximum efficiency of 92 per cent being obtained when a single stage of vortex blading was tested at 1500 rpm. This increase is in close agreement with that predicted by reference (7).

[4] Measurements with three stages of vortex blading at 750 rpm show a maximum air density change of ½ per cent.

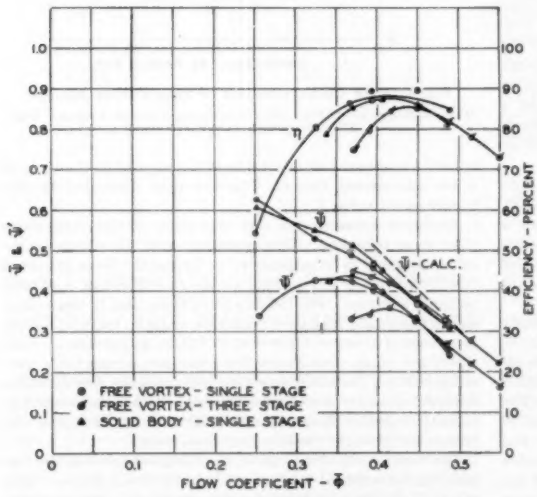

FIG. 5 OVER-ALL PERFORMANCE OF FREE-VORTEX AND SOLID-BODY BLADING

Above the design flow rate, the power, pressure rise, and the efficiency decrease moderately and the compressor operation is quite stable. Below the design condition, the pressure rise increases somewhat, but then begins to decrease. This range of operation is sometimes designated as "stalling" by analogy with the lift characteristics of single airfoils. In different portions of this range, violent and audible flow pulsations occur for both blade types, and the compressor operation even becomes unstable. These effects are believed to be associated with complete or intermittent flow separation over portions of the blades. It is seen that single-stage performance of the two blade types is quite similar even in the stalled range. However, the stall condition is more abrupt and comes at higher flow rates for three-stage operation. This effect has been observed frequently and is one factor which seriously limits the usefulness of single-stage data for predicting multistage axial-flow compressor performance. Probably both viscous phenomena and mutual interference between blade rows are operative, but no complete explanation for the effect is known.

Shift of the design point, pressure loss, and stalling are all attributable to fluid viscosity effects. However, it is clear that the theory satisfactorily predicts the design performance of blade types with either two or three-dimensional flow patterns. The two blade types, which are widely different in appearance, do yield approximately the same over-all performance. These facts support the assumptions made in the turbomachine theory and establish the fact that a compressor designed for three-dimensional flow can have high efficiency.

COMPARISON OF MEASURED AND CALCULATED INTERNAL-FLOW PATTERNS

In a previous section a theory for computing the flow through an axial compressor was proposed. It is desirable to verify experimentally this theory in detail before it is used for design.

In the derivation of the flow theory a number of assumptions were made. The principal assumptions were of different types, and their role in the development of the theory is as follows:

The first type of assumption concerned the nature of the working fluid; the fluid was postulated to be perfect, i.e., homogeneous and without friction, and the fluid was also taken as incompressible. These assumptions are very common in fluid dynamics, and it is believed that at normal flow conditions, pressure and flow characteristics, as well as the corresponding blade shapes, can be calculated on this basis. It is on this same basis that the lift and induced drag are calculated for airplane-wing shapes. For the computation of efficiency and "stall" characteristics, the viscosity of the fluid has of course to be taken into account. The perfect-fluid and constant-density assumptions are made so frequently that they were not regarded as peculiar to the present theory.

The second type of assumptions concerned the leaving angle from the blade rows. For a blade row with infinitely close spacing this angle is determined by the tangent to the trailing edge. For a finite spacing, the leaving angle is more difficult to predict. The methods which have been used for determining the leaving angles in this case were discussed in a previous paragraph. In the development of the theory, however, this angle was assumed to be given, and the methods of determining the properties of a cascade with finite blade spacing were considered as auxiliary assumptions.

The third type of assumptions consists of those peculiar to the theory. These assumptions include the following:

(a) The ratio of the radius of a particular stream tube

in front of a blade row to the radius of the same stream tube behind the blade row is assumed in the first approximation to be equal to unity.

(*b*) The equilibrium flow pattern, which theoretically is reached only at an infinite distance behind the blade row, is assumed to be fully developed at the trailing edge of the blade row.

(*c*) The flow is assumed axially symmetrical.

It is upon these assumptions that the simplifications of the theory are based, and it is these assumptions in particular which were to be checked against the experimental results. For the comparison of measured and computed data, operating conditions, therefore, were selected for which the first two types of assumptions were satisfied. Agreement between experiment and theory under these conditions was then interpreted to mean that the special assumptions of the theory are valid.

For the investigation, single-stage tests with free-vortex and solid-body blading were carried out. A set of entrance vanes and a rotor were installed, and detail measurements of the velocity and the total head in front and behind this rotor were obtained. In the case of the free-vortex blading, the following stator was also installed for some of the tests, and similar measurements were made in front of and behind this blade row. These detail measurements between stages constitute a very severe check on the theory, much more severe, of course, than a check of over-all performance only.

Since the theory assumes a perfect working fluid, it cannot be expected that the flow pattern will be predicted near the compressor wall or in a wake. The average flow coefficient, $\bar{\phi}$, used as the basis of comparison with the calculated results, was therefore computed from the measured data by omitting these regions. The results of the measurements behind the free-vortex rotor are shown in Fig. 6. In Fig. 6 the axial-velocity component is plotted as a function of the radius, the solid line giving the measured values and the dashed line giving the calculated ones. The flow rate is about 10 per cent above the design flow rate. Fig. 6 shows that the agreement between the calculated and measured velocity components is nearly perfect, with the exception, of course, of the boundary regions. Fig. 6 shows equally good agreement for the axial-velocity components behind the free-vortex stator. The comparison for the total head behind the rotor is also shown in Fig. 6. The two curves are perfectly parallel. The small difference in magnitude is accounted for by the loss through the blade rows. Since there is no increase in total head through the stator, the corresponding measurements behind this blade row are practically identical to those behind the rotor, and this curve is therefore not shown.

Because the afore-mentioned tests were carried out at "off-design" conditions, the free-vortex blading yields no especially simple flow pattern. The agreement obtained is, therefore, a significant indication of the validity of the compressor theory. The results which were obtained with the solid-body blading are shown in Figs. 7 and 8. These experiments were also made at about 10 per cent above design flow rate.

For this type of flow pattern, the change of the axial-velocity component with the radius is very large, the axial velocity at the hub being about twice that at the tip. The flow is therefore far from two-dimensional, and the measurements at this condition therefore constitute a very severe check on the theory. The results of these measurements are presented in Figs. 7 and 8. They show that even in this case, agreement between theory and experiment is extremely close, both for the axial-velocity profile as well as for the total-head distribution. A prediction of the flow characteristics to this accuracy probably would be sufficient for most engineering work. Quite an erroneous total-head distribution is obtained if the total head is computed on the basis of a two-dimensional theory. This has been illustrated by the broken curve in Fig. 8.

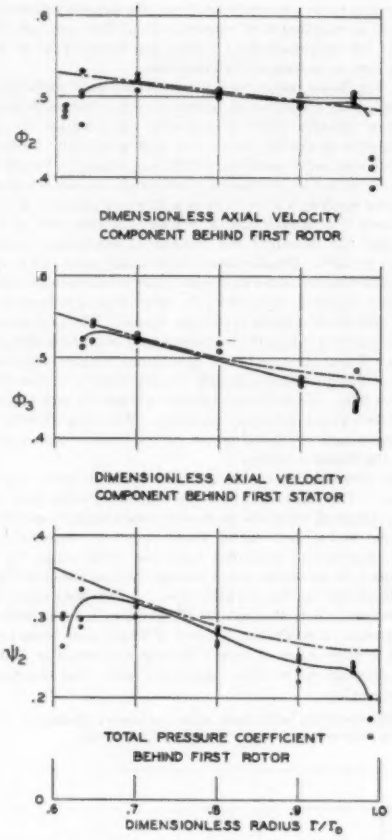

FIG. 6 FLOW CHARACTERISTICS OF FREE-VORTEX BLADING
(Flow coefficient, $\bar{\phi}' = 0.504$. Solid lines represent measured values. Dash-dot lines represent calculated values.)

Extensive measurements also were made at flow rates other than those presented. The agreement with the calculated results was found to be satisfactory as long as the losses remained reasonably small, and as long as the flow direction had been correctly assumed. For the two-blade types used in the experiments this meant that good prediction could be made in a flow-rate range of about ± 10 per cent off the design condition. Outside of this range, considerable flow separation occurred over part of the blade. The losses were then high, and the flow direction deviated seriously from that predicted. As a consequence the calculated profiles disagreed more with the measured ones the further the flow rate was from the above range.

The experiments described in the foregoing sections are believed to be sufficient to show the validity of the theory. The theory is therefore available for immediate use to the engineer. It is now possible to solve by relatively simple means the prob-

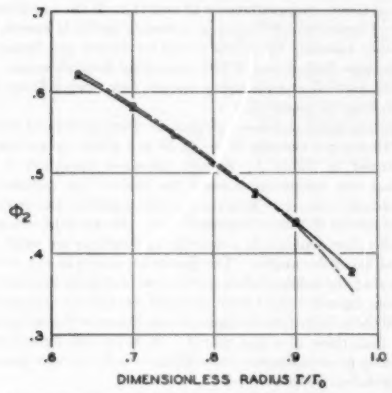

FIG. 7 DIMENSIONLESS AXIAL-VELOCITY COMPONENTS BEHIND FIRST SOLID-BODY ROTOR (Φ_2)

(Flow coefficient, $\bar{\phi}' = 0.499$. Solid line represents measured values. Dash-dot line represents calculated values.)

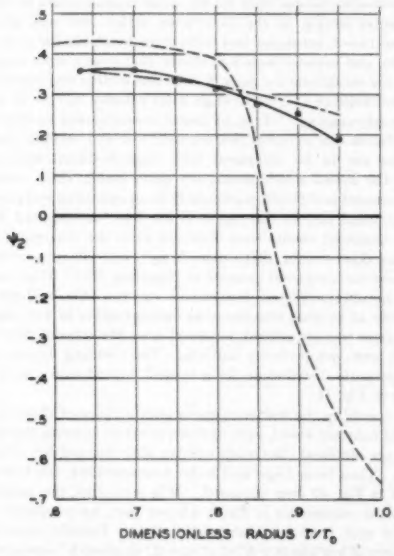

FIG. 8 TOTAL PRESSURE COEFFICIENT ψ, BEHIND FIRST ROTOR OF SOLID-BODY BLADING

(Flow coefficient, $\bar{\phi}' = 0.499$. Solid line represents measured values. Dash-dot line calculated by theory of this paper. Broken line calculated by two-dimensional theory.)

em of blade design as well as the problem of predicting the performance of a given blading, at least in a certain range about the design point. The necessary computations are sufficiently rapid to allow extensive surveys of blade types, so that the most suitable one may be selected for each application. The accuracy which can be obtained is believed to be sufficient for most engineering needs. If greater accuracy should be required, or if predictions are to be made for a very wide range of flow rates, the effects of viscosity must be taken into account in addition to refining the theory.

EFFECTS OF FLUID VISCOSITY

In examining the over-all performance of the test compressor, it was observed that compressor losses, stalling, and effective area contraction due to internal boundary layers are all effects which are induced by the fluid viscosity. It will be of interest to correlate these external effects with flow measurements in the compressor air stream.

Fig. 9 shows a map of constant total-pressure contours measured downstream of a stator-blade row (free vortex). For this case, the contours also represent very nearly lines of constant velocity. Thus it is seen that due to friction on the outer and inner bounding walls, total pressure and velocity are reduced over perhaps 20 per cent of the blade height. These regions may be referred to as the wall boundary layers. Because of reduction of the axial-velocity component in the boundary layers, in those regions the flow-incidence conditions relative to a rotating-blade row are quite different from those predicted by perfect-fluid theory. It is therefore desirable for compressor designers to be able to predict the wall boundary-layer thickness in successive stages of a compressor.

The region of total-pressure and velocity defect which occurs downstream of the stator-blade trailing edge is clearly seen in Fig. 9. At a sufficiently great distance downstream, this blade-wake region disappears due to mixing with the surrounding fluid. Thus, in discussing blade wakes, it is important to specify the measuring-plane location. Conditions downstream of a rotating blade appear quite similar, providing measurements are made relative to the rotor (8). With ordinary fixed instrumentation, the flow is actually unsteady, and the wake regions are not detected. It is significant to note that with close axial spacing of alternately fixed and rotating-blade rows, all blade rows except the first actually operate in an unsteady flow, because of wakes from the blades upstream. Friction on the blade surfaces accounts for a substantial portion of the compressor loss. Individual compressor cascades exhibit stalling characteristics which probably account for over-all compressor stalling. Hence it is of interest to know the loss and stalling characteristics of two-dimensional cascades and to have means of utilizing such knowledge for the prediction of compressor performance.

It is clear from Fig. 9 that both wall and blade-surface boundary layers contribute to the effective area contraction. Thus knowledge of boundary-layer extent and growth throughout successive stages allows the prediction of this effect.

CASCADE LOSSES

Flow conditions through a section of a compressor-blade row are quite similar to those in a corresponding two-dimensional cascade. Test data in two-dimensional cascade tunnels have been secured by many investigators, for example, references (4) and (9). Typical loss data from such tests are shown in Fig. 10 for a cascade which is essentially identical to the section $r = 14.40$ in. of the test compressor free-vortex stator blading. The air turning angle, $\theta°$, and mean total pressure-loss coefficient, Ω_p, are shown as functions of the flow incidence angle $i°$. Flow angles are defined in Fig. 1. The mean loss is conveniently calculated from total-pressure and velocity surveys upstream and downstream of the cascade. Then

$$\Omega_p = \frac{\bar{\Delta}p_t}{\frac{1}{2}\rho C_1^2} = \frac{2}{\rho C_1^2}\left\{\frac{\int_{s_i} p_{t_1}\rho C_{a_1}dy}{\int_{s_i}\rho C_{a_1}dy} - \frac{\int_{s_o} p_{t_2}\rho C_{a_2}dy}{\int_{s_o}\rho C_{a_2}dy}\right\} \quad [15]$$

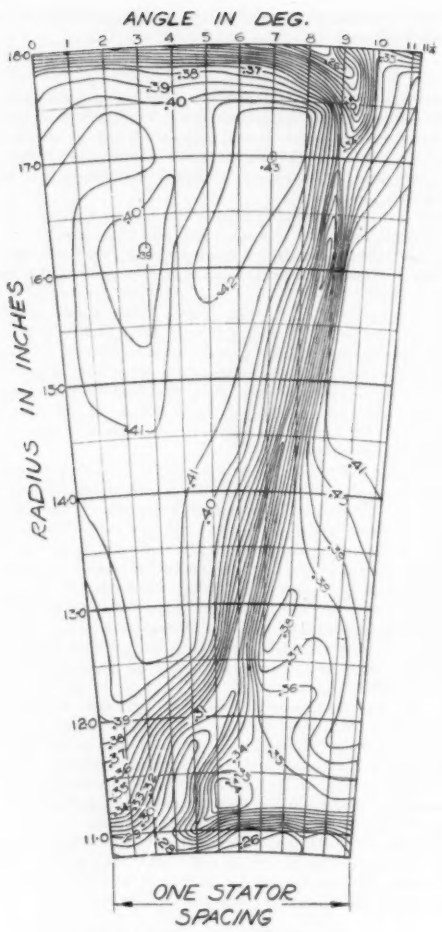

FIG. 9 TOTAL-PRESSURE CONTOUR MAP
(Contours are lines of $p_t/\frac{1}{2}\rho w_2^2$ = const, measured downstream of first free-vortex stator.)

where the integration paths extend over one blade spacing, and the downstream integration path is sufficiently near the cascade so that no appreciable mixing loss is included in Ω. The data show that the air turning angle increases linearly with increasing incidence angle over most of the range but approaches a limiting value near the stall condition. The total pressure loss is nearly constant for $-8° < i^* < +7°$ being about 1.3 per cent of the entrance-velocity pressure. However, at extreme positive or negative incidence angles, the loss becomes much greater as a result of flow separation on the convex or concave profile surfaces. Clearly, for high over-all compressor efficiency, it is necessary that most blade sections operate at incidence angles which result in low loss.

Perhaps the most satisfactory source of performance data for two-dimensional cascades is wind-tunnel test results. However, air turning angles can be calculated accurately by the methods of potential theory (e.g., references 10 and 11). If the calculated or measured pressure distribution on a cascade profile is known, it is possible to calculate the profile boundary layers and hence the total pressure loss, at least if flow separation does not occur. An alternate method of calculating cascade loss from diffuser data has also been proposed (4).

Boundary-layer and loss calculations were performed for the free-vortex stator cascade (r = 14.40 in.) whose properties are summarized in Table 1. Surface pressures measured in the operating test compressor formed the basis of the calculations. The Kármán boundary-layer momentum equation was used in a manner similar to that of reference (12). No attempt was made to predict flow separation, hence the calculations are valid only for small incidence angles. The results are shown in Fig. 10. It is seen that the calculated minimum loss is slightly greater than that from cascade-tunnel tests, probably because an attempt was made in the calculations to duplicate conditions in the compressor rather than those of a test tunnel. However, the agreement is sufficiently good to support the validity of both the test data and the calculation method.

Since a cascade tunnel cannot exactly reproduce conditions in an operating compressor, a series of tests were initiated with the purpose of determining cascade loss in the test compressor for a particular section so that comparison with measured and calculated two-dimensional data for the same cascade could be made. The center section of the free-vortex stator row was selected because two-dimensional test data were available for a similar cascade, and because tests had shown that over a wide range of operating conditions the mean flow at this section was practically two-dimensional, i.e., the average axial velocity at r = 14.40 in. was nearly constant. It is, of course, essential that no appreciable diffusion due to radial flow occurs if loss and stalling characteristics are to be compared with cascade-tunnel test data. Since the losses which occur are quite small, their accurate measurement is difficult, particularly in an operating compressor. It was found that in the region of low loss (unseparated flow), more consistent results were obtained when the maximum total pressure downstream of the cascade p_{t2}^*, was taken to represent the mean entering total pressure in Equation [15]. Thus results could be obtained from downstream surveys only, without the necessity of making simultaneous measurements in two planes. Some error was introduced, however, since the entering flow conditions were not perfectly uniform. The resulting velocity and total pressure distribution for a typical downstream survey are shown in Fig. 11.

By operating the test compressor over a range of throttle settings at constant speed, various flow directions entering the stator row were obtained (Reynolds number also changed by ±15 per cent). Then from angle and wake measurements, the loss data shown in Fig. 10 were obtained. It is seen that the minimum loss in the compressor is about 4.0 per cent, as compared with 1.3 per cent from two-dimensional tests. Equally important, the range of low loss is $-8° < i^* < -2°$ or about 6° compared to 15° for the two-dimensional case.

Before the comparison is further discussed some additional remarks on the experimental conditions should be made. The effects of wake mixing, measuring probe interference, and airfoil-contour accuracy are believed to be insufficient to account for the observed differences. In reference (4) it is shown that permissible air turning by a compressor cascade is affected by the flow Reynolds number (based upon chord length and entering velocity). Below an effective Reynolds number of 100,000, the maximum turning angle is severely reduced; above 300,000 optimum turning capacity is attained. It is stated that due to turbulent fluctuations, the effective Reynolds number in a cascade tunnel is increased by a factor as large as 3, and that the factor is

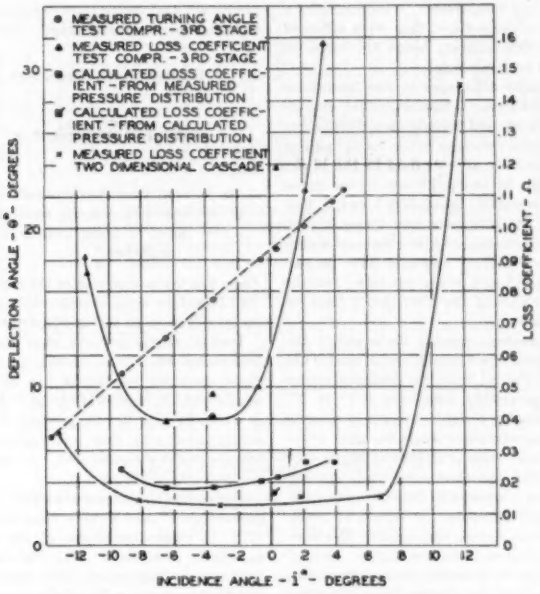

FIG. 10 CASCADE-LOSS DATA FOR FREE-VORTEX STATOR AT r = 14.40 IN.; (C/S = 0.92, θ = 30°)

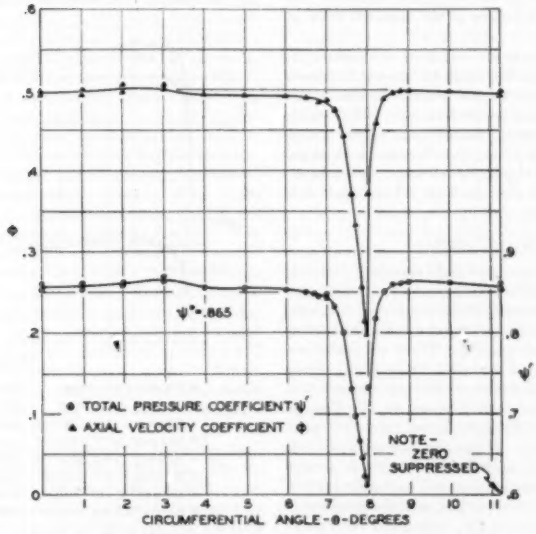

FIG. 11 WAKE-SURVEY DATA FOR FREE-VORTEX STATOR CASCADE AT r = 14.40 IN.; (i^* = —6.5°, SURVEY PLANE 0.05 IN. DOWNSTREAM)

as large or larger for an operating compressor. Assuming such a factor, both the tunnel and compressor test data were obtained near the upper critical Reynolds number, hence the effect of Reynolds number variation is probably small.

There are, however, two major differences in flow conditions between compressor and tunnel tests. These are radial, secondary flow along the blade surfaces, and periodic-flow fluctuation. It is clear that even though radial velocities in the main, "perfect fluid" flow may be small or totally absent, fluid in the blade-surface boundary layers cannot be in equilibrium in the radial static-pressure field. Thus so-called "secondary" radial flow must exist near the surfaces of both rotor and stator blades. Direct measurements (8) have demonstrated the existence of such flows. Precisely what effect secondary flow may have on cascade boundary-layer development and loss is not clear, but the phenomenon may account for part of the discrepancy between two and three-dimensional losses.

Due to the persistence of upstream-moving blade wakes, the flow entering a compressor cascade is not steady, but in reality has a strong periodic component. For example, the design incidence angle for the stator cascade previously considered is $i^* = 0°$. However, if the relative exit velocity from the preceding rotor is reduced 25 per cent, the stator incidence angle becomes $i^* = +13.2°$. The test data show that velocity defects of 25 per cent or more are to be expected with the close axial-blade spacing commonly used in compressors; hence the incident velocities fluctuate both in magnitude and direction. It should be noted that for both rotor and stator-blade rows, the incident flow contains components with larger, positive incidence angles. It may be that such fluctuations increase surface friction and thus promote rapid boundary-layer growth and greater loss. Further, the angle fluctuation may induce early cascade stalling. There is insufficient evidence to permit definite conclusions; however, it is suggested that both secondary flow and nonsteady incidence flow deserve further investigation as causes of the observed discrepancies.

It is interesting to note that the investigation of reference (8) also revealed a considerably smaller range of low-loss incidence angles than would be anticipated from two-dimensional data. British compressor designers have proposed a rule, based apparently upon over-all compressor-performance data, which corrects two-dimensional cascade drag (or loss) data for use in an actual compressor (13). Applied to the stator cascade, this rule increases the two-dimensional loss by about 60 per cent, which is less than the measured difference.

Wall Boundary Layers

The general nature of the case and hub boundary layers is illustrated by Fig. 9. In the test compressor, both axial and circumferential velocities must vanish at the outer wall; the axial velocity vanishes at the inner wall, but the circumferential velocity approaches the hub surface velocity. These conditions are typical of a compressor with unshrouded blade rows. Some measurements in multistage axial-flow compressors indicate that the thickness of wall boundary layers increases rapidly through successive stages, indeed so rapidly that the two layers join after perhaps three or four stages (13). It has also been proposed (14) that such rapid boundary-layer growth is inevitable in a compressor because of the rapid static-pressure rise in the direction of flow, since, for example, a similar effect is commonly observed in diffusers. However, it was believed that because of the importance of knowing the effective passage-area contraction for multistage compressor design, this question should be investigated more thoroughly.

It is convenient to specify the wall boundary-region extent at a particular point in the compressor by the boundary-layer displacement and momentum thickness which are computed from the axial-velocity distribution. These parameters are

$$\text{Displacement thickness, } \delta^* = \int_0^\delta \left(1 - \frac{\phi}{\phi^*}\right) dr \ldots [16]$$

$$\text{Momentum thickness, } \vartheta = \int_0^\delta \left(1 - \frac{\phi}{\phi^*}\right) \frac{\phi}{\phi^*}\, dr \ldots [17]$$

where

ϕ = local axial-velocity coefficient
ϕ^* = local axial-velocity coefficient at boundary-layer limit
r = radial distance from wall (effect of wall curvature is neglected)

From Fig. 9 it is seen that in the region between blade wakes, the wall boundary layer is sufficiently uniform in thickness to allow its specification by a single parameter without appreciable error.

Radial-velocity surveys were made before and behind each free-vortex blade row of the three-stage test compressor for three operating conditions. In all cases the test probes were located outside blade-wake areas. A typical set of radial surveys is shown in Fig. 12. As a check on the accuracy of the radial surveys, the total flow was computed and compared with the entrance-duct measurement. In all cases, agreement within 6 per cent was obtained.

For each of the measured profiles, the boundary-layer thickness parameters δ^* and ϑ were computed from Equations [16] and [17]. A reasonable choice of the free-stream velocity ϕ^* was possible in most cases. The boundary-layer shape parameter H (12) was also computed. The measured boundary-layer characteristics are shown in Fig. 13 for one operating condition.

Examination of the axial-velocity profiles in Fig. 12 reveals that, in general, the flow pattern is closely repeated throughout the three stages. At other flow rates, the axial velocity (as pre-

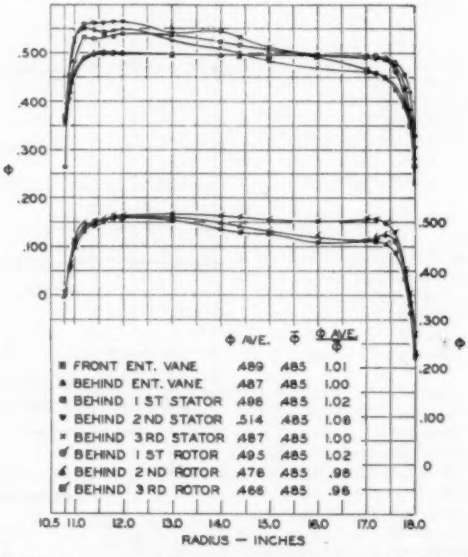

Fig. 12 Dimensionless Axial-Velocity Components for Three Stages of Free-Vortex Blading
(Flow coefficient, $\bar{\phi} = 0.485$.)

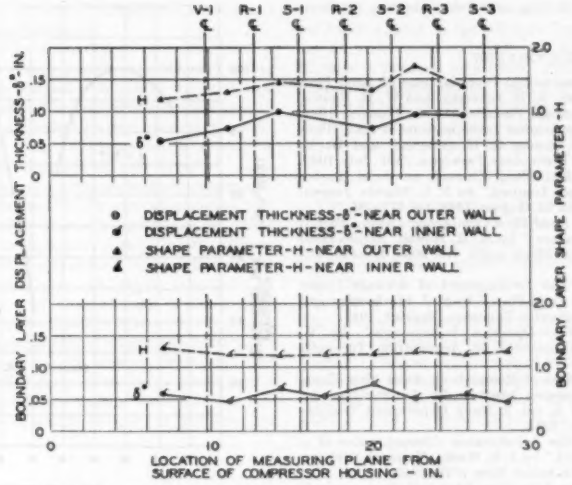

FIG. 13 WALL BOUNDARY-LAYER DATA FOR THREE STAGES OF FREE-VORTEX BLADING

(Flow coefficient, $\bar{\phi} = 0.485$, 750 rpm.)

dicted by the perfect-fluid theory) is no longer uniform over the cross section, but the profiles behind successive rotors and behind successive stators also repeat well except when extreme cascade stalling occurs. From the axial velocity at the annulus center, a general tendency for boundary-layer growth is detectable, but the tendency is by no means extreme. Indeed, an approximately equivalent rate of growth would be expected in an annular duct if no blades were present. The outer-wall profiles are generally similar to that of a flat-plate, turbulent boundary layer. However, the inner-wall profiles show some deviations which result from the more complex boundary condition. Again, if extreme cascade stalling occurs, the shapes may be considerably altered.

From Fig. 13 it is seen that the boundary-layer displacement thickness increases slightly through the compressor, which confirms the result of examining the velocity profiles. Most of the increase seems to occur through the entrance vanes; within the blade rows the thickness varies more or less at random. The boundary-layer shape parameter H, varies between 1.2 and 1.7 with an average value of perhaps 1.3. The value for the commonly used 1/7 root turbulent profile is 1.29. This parameter is helpful for indicating a general similarity of boundary-layer shape, but its significance should not be overrated for the complex three-dimensional profiles in question. Using the measured wall and blade-surface displacement thicknesses, an over-all effective area reduction of $4^1/_2$–5 per cent can be computed. This checks with the value of $4^1/_2$ per cent shown by compressor-performance curves.

No major effects which seemed chargeable to blade-tip clearance were observed in the wall boundary-layer data. The tip clearance at which the compressor was operated was 0.029 in. or about $^1/_2$ per cent of the blade height. Empirical volumetric efficiency formulas (e.g., reference 15) indicate that the resulting flow distortion should be slight in this case.

From the test data it is concluded that while, for some blade designs, hub ratios, and initial thicknesses, the wall boundary layers may grow rapidly, there is no a priori reason to assume that this must always be the case. It is believed that the diffuser analogy has been shown to be inapplicable, probably because diffuser flow is usually of constant energy whereas the rotor blades do considerable work on the compressor wall boundary layers.

INTERACTION OF WALL AND CASCADE BOUNDARY LAYERS

A number of flow-direction and velocity measurements were made near the boundary walls, from which the actual cascade velocity diagrams could be constructed. These diagrams were compared with the perfect-fluid blade-design diagrams for the same sections. In many cases it was found that blade sections within the boundary layers were operating at flow incidence angles as great as $i^* = +20°$. In a two-dimensional flow, the blade sections would experience flow separation (stalling) and high losses under such extreme incidence conditions. Similar phenomena may also occur in the wall boundary layers. Nevertheless, it was observed that considerable air turning was achieved near the walls, i.e., work was done on the boundary-layer air by the rotor blades. Measurements of cascade loss in the manner previously outlined confirmed that work was done on the boundary layer only at relatively great expense. In general, the loss coefficients were found to be between $\Omega = 0.050$ and 0.150 in these regions. A large proportion of compressor loss can be charged to this effect.

It seems reasonable to expect that cascades would operate at considerably lower loss in the boundary-layer region if the sections were designed to accommodate the actual flow rather than a hypothetical, perfect-fluid flow. Cascade stagger and airfoil camber could be selected from the probable velocity diagrams. Perhaps thick sections and high solidities would be used to obtain insensitivity to inlet conditions.

ACKNOWLEDGMENTS

The authors wish to express their gratitude to the Office of Naval Research for providing the financial support which made the experimental program possible. Special thanks are due Mr. L. J. Downs, Mr. F. T. Linton, and Mr. T. Taniguchi whose aid

in equipment construction, testing, and data reduction has been invaluable.

BIBLIOGRAPHY

1 "Theoretical and Experimental Investigations of Axial Flow Compressors," by J. T. Bowen, R. H. Sabersky, and W. D. Rannie, California Institute of Technology, Pasadena, Calif., January, 1949.

2 "Theoretical and Experimental Investigations of Axial Flow Compressors—II," by J. T. Bowen, R. H. Sabersky, and W. D. Rannie, California Institute of Technology, Pasadena, Calif., July, 1949.

3 "The Flow of a Perfect Fluid Through an Axial Turbo-Machine With Prescribed Blade Loading," by F. E. Marble, *Journal of the Aeronautical Sciences*, vol. 15, August, 1948, pp. 473–485.

4 "The Present Basis of Axial Flow Compressor Design, Part 1, Cascade Theory and Performance," by A. R. Howell, Aeronautical Research Council Reports and Memoranda, No. 2095, London, England, June, 1942.

5 "Instrumentation for the Development of Aircraft Power Plant Components Involving Fluid Flow," by S. J. Markowsky and F. M. Moffat, Society of Automotive Engineers, Reprint, 1947.

6 "Experiences With Flow-Direction Instruments," by B. Eckert, National Advisory Committee for Aeronautics, Technical Memorandum No. 969, 1941.

7 "Summary of the Results of Research on Axial Flow Compressors at the Stuttgart Research Institute for Automobiles and Engines," by B. Eckert, part A, vol. 3, Navy Department Translations, Bushipe Code 338, May, 1946.

8 "An Investigation of the Aerodynamic Characteristics of a Rotating Axial-Flow Blade Grid," by J. R. Weske, National Advisory Committee for Aeronautics, Technical Note 1128, 1947.

9 "Blade Design Data for Axial-Flow Fans and Compressors," by S. M. Bogdonoff and H. E. Bogdonoff, National Advisory Committee for Aeronautics, Wartime Report L-635, July, 1945.

10 "A Solution of the Direct and Inverse Potential Problems for Arbitrary Cascades of Airfoils," by W. Mutterperl, National Advisory Committee for Aeronautics, Wartime Report L-81.

11 "Interference Method for Obtaining the Potential Flow Past an Arbitrary Cascade of Airfoils," by S. Katsoff, R. S. Finn, and J. Lawrence, National Advisory Committee for Aeronautics, Technical Note 1252, 1947.

12 "Determination of General Relations for the Behavior of Turbulent Boundary Layers," by A. E. von Doenhoff and N. Tetervin, National Advisory Committee for Aeronautics, Report 772, 1943.

13 "Fluid Dynamics of Axial Compressors," by A. R. Howell, in British Gas Turbine Jet Unit, The Institution of Mechanical Engineers, War Emergency Issue No. 12, London, England.

14 "Research on Aircraft Propulsion Systems," by A. Silverstein, *Journal of the Aeronautical Sciences*, vol. 16, April, 1949, pp. 197–226.

15 "The Influence of the Radial Clearance of the Rotor on the Compressor Efficiency," by Fickert, part C, vol. 3, Navy Department Translations, Bushipe Code 338, May, 1946.

Discussion

J. L. KOETTING.[6] The minimum loss coefficient curve (Fig. 10 of the paper) measured at the third stage of the test compressor, shows the optimum range of operation for this specific geometry to be from —2 to —8 deg of incidence. This is in good agreement with tests run by the writer's company. These tests have also shown, as the camber angle is decreased, the range of maximum efficiency shifts in the direction of positive incidence, Fig. 14 of this discussion. The reason for this variation is for a highly cambered blade in cascade operating at positive incidence angles, the required turning is excessive, and flow separation takes place along the low-pressure surface of the blade near the trailing edge.

For the case of a cascade operating at relatively high subsonic Mach numbers (0.7–0.8) the range of efficient operation is substantially limited. Recent tests have indicated the maximum inlet relative critical Mach number (defined as the maximum Mach number before serious losses occur due to high local velocities along the blade surfaces) occurs at zero incidence. Departure from operation at zero incidence at a constant-inlet

[6] Design Engineer, Aviation Gas Turbine Division, Westinghouse Electric Corp., Lester, Pa. Jun. ASME.

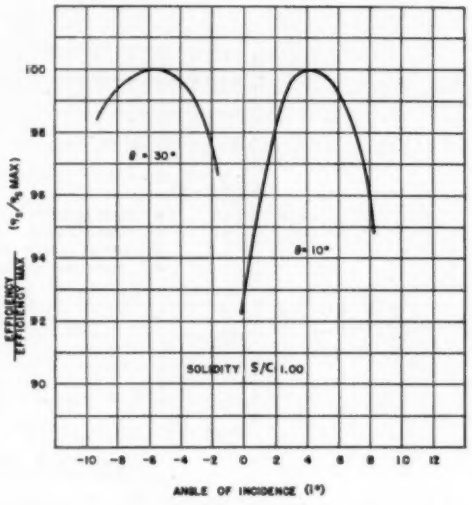

FIG. 14

relative Mach number results in high local velocities on the low and high-pressure sides of the blade leading edge with resultant large losses in cascade efficiency.

The statement in the paper, "there is no prior reason to assume that wall boundary layers must always grow rapidly," in all probability is correct for low Mach number, low flow per unit area compressors with a small number of stages. In aircraft gas-turbine compressors with ten or more stages, high flow per unit areas, and high internal relative Mach numbers, current tests have shown conclusively that the wall boundary layers grow rapidly, attaining displacement thicknesses several times the values shown in the paper.

The writer wishes to take this opportunity to advance several suggestions for a future program if not already considered. The first is to conduct a similar investigation of boundary-layer thickening in a high flow per unit area, high Mach number machine with ten or more stages. Additional test information from this type of machine is required to aid in formulating a boundary-layer theory for rotating machinery. Another suggestion entails a test similar to the first to investigate the effects of multistaging on flow deviation from blade trailing-edge angle, with particular emphasis in the region of the wall boundary layers.

J. R. WESKE.[7] The authors have developed a very effective method for design computations of axial-flow compressor stages which, while derived by ingenious use of mathematical analysis, in its application requires no more time and special skill than would reasonably be allowed in design projects. This has been achieved by introducing approximations valid for normal flow conditions of axial-flow stages. Proof has been furnished by test that the results are sufficiently accurate over a considerable range of operating conditions on both sides of the design point.

The method is regarded as having special merits because:

(*a*) When applied to the calculation of the performance of a stage of a given design ("direct" problem), it furnishes the span-

[7] Professor of Engineering, Engineering Department, Brown University, Providence, R. I. Mem. ASME.

wise load distribution as one of the results, making it unnecessary to start with an assumed distribution.

(*b*) When applied to the determination of blade shapes of a stage for a specified performance ("indirect problem"), many types of stages may now be handled with almost the same ease on the basis of the approximate "three-dimensional" theory with which the vortex stage was handled on the basis of the two-dimensional theory. This is an advantage which should be especially helpful in the development of new types of stages representing optimum solutions for given operating requirements.

Experimental results presented by the authors, showing that real fluid effects are of the same order of magnitude as the effects of the three-dimensional perfect-fluid theory, might offhand appear to belittle the practical significance of the latter. That this is not the case, however, is borne out both by theory and by test data which show that even minor changes of the perfect-fluid flow pattern, influencing the stability of real flow, may have decisive influence upon such quantities as range and efficiency.

In the discussion of test results the authors recommend that the actual rate of volume flow for a given design pressure of a compressor may be predicted by decreasing the theoretical rate by 4½ per cent. It would be well to reiterate at this point the statement made earlier in the paper to the effect that this empirical factor applies to operation at low Mach numbers only. It has been shown (viz., by Dr. M. Schilhansl of the USAF Air Materiel Command in a recent unpublished report) that compressibility effects of the magnitude encountered at operating Mach numbers of high-performance compressor stages tending to increase the rate of flow for a given pressure ratio, may reduce or even change the sign of the quantity in question.

Authors' Closure

The authors wish to thank Mr. Koetting and Professor Weske for their discussions. The findings concerning the boundary-layer growth were unexpected, and it should be understood that they may not have general significance. Different Mach numbers, Reynolds numbers, blade-aspect ratios, or blade designs may affect the ratio of boundary-layer growth appreciably. The experimental program in the future will be concerned principally with precise measurements of losses and effects of multi-staging. The loss data presented in this paper are of preliminary nature and are subject to revision. The installation described is designed for low-speed operation and cannot be used for the investigation of compressibility effects.

Experience With Machinability Repeat-Ability

By E. J. R. HUDEC,[1] CLEVELAND, OHIO

This paper describes experiences with certain phases of the machinability problem, and suggests a means by which repeat test runs can be made to give more consistent results.

Introduction

THE experimental work undertaken in the present study was a lathe-turning operation in which the effect of various kinds of cutting fluids on tool life was observed. The method of controlled experiment was used in which the factors involved were held constant while one was varied (in this case the cutting fluid), so that its effect upon the process could be observed.

To establish tool-life values that would be considered reliable, it was desired to check each value by making several repeat runs. With a close agreement between repeat runs, it was felt a reliable tool-life value was obtained. A difficulty encountered, however, was that a large variation occurred between repeat runs (as much as 145 per cent when based on the average) even after great care had been taken to make the repeat cutting conditions as nearly identical as possible.

The procedure described relates many experiences that had to be learned the "hard way," and the discussion suggests a means by which it is felt machinability repeat-ability can be obtained.

Description of Apparatus

For this work, a new 20-in. × 67-in. heavy-duty engine lathe was used. The original constant-speed a-c drive motor was replaced with a $7^1/_2$-hp variable-speed d-c motor, giving a stepless speed range from 3 rpm to 413 rpm when both the variable-speed range of the d-c motor and the various speed ratios of the geared head were used.

A cutting-fluid tank of 50 gal capacity was equipped with thermostatically controlled electric heating elements and agitator to keep the cutting fluid at a uniform temperature. The cutting fluid was discharged from a specially made nozzle which had a built-in thermometer.

A tangential-type toolholder, as shown in Fig. 1, was made to hold $^1/_2$-in. square tool bits in such a manner that one longitudinal corner formed the nose radius, while the adjacent surfaces formed the front and side clearance angles. One end of the tool bit formed the side and back rake angles (top surface) when mounted in this toolholder. A height gage attached to the toolholder could be swung quickly into place to facilitate rapid adjustment of the cutting edge to the height of the center line of the work.

The tailstock of the lathe was equipped with a ball-bearing rotating center. The standard faceplate was replaced with a specially made plate which had two spring-loaded driving pins, of about $^1/_{16}$ in. diam, which engaged holes in the end of the work to enable driving it.

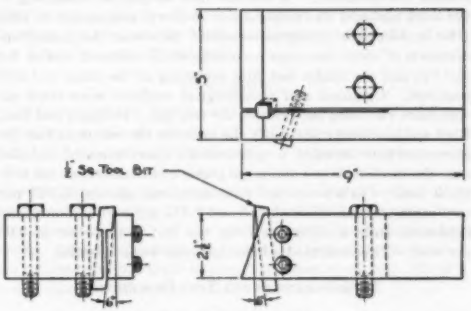

Fig. 1 Toolholder

Work Material

For work material, two pieces of $7^1/_2$-in-diam SAE 1045 steel, 5 ft long, were obtained. The two pieces were originally one bar. They were both given a high-temperature anneal, allowing $7^1/_2$ hr soaking time at 1600 F. This was followed by a furnace cool.

Earliest Procedure

To measure the cutting speed, an electric hand-type tachometer, with scale graduations in increments of 25 fpm, was mounted on the lathe so that its contact wheel would ride on the work just ahead of the cutting tool.

A batch of one hundred tool bits, all made in the same heat, were checked for homogeneity by taking Rockwell superficial hardness readings. On the 45 N scale, all the readings ranged between 73.2 and 75.8. After this, they were prepared by grinding a longitudinal corner to a $^3/_{32}$ in. radius and finish-grinding the two adjacent sides. Then one end of the tool bit was ground at a compound angle to form the side and back-rake angles. This latter was done on a pedestal-type tool grinder using a cup wheel and a holding fixture which was reciprocated by hand across the wheel face.

To set the depth of cut, the cutting edge of the tool was touched to the work, moved beyond the end of the work, and fed in a distance of 0.020 in. The motor rheostat was adjusted continuously throughout a test run to maintain the proper cutting speed as indicated on the meter. At the instant the tool started cutting, a stop watch was started to measure tool life in minutes. The point of tool failure was easily discernible since the chip flow suddenly decreased to a very light thread, and a step of about 0.015 in. occurred on the work. Tool-life values were determined in both the length of cut in inches along the work and in minutes of cutting time. With the diameter of the work and the cutting speed known, the time of the cut could be computed as a check on the stop watch time-of-cut.

After a considerable number of test runs, the results obtained with this procedure were not considered satisfactory because a wide variation occurred between repeat runs such that overlapping occurred in tool-life values for cutting fluids known to be

[1] Assistant Professor, Case Institute of Technology. Jun. ASME.

Contributed by the Research Committees on Cutting Fluids and Metal Cutting Data and Bibliography and presented at the Spring Meeting, Washington, D. C., April 12–14, 1950, of The American Society of Mechanical Engineers.

Note: Statements and opinions advanced in papers are to be understood as individual expressions of their authors and not those of the Society. Paper No. 50—S-2.

considerably different. In one particular test, 23 repeat runs were made, and a variation of 145 per cent was obtained from the lowest to the highest value when based on the average of the group.

An analysis of the position of each successive test run on the work material revealed that the short runs were obtained at the tailstock end of the test bar, and the longer test runs were obtained when started in the middle of the test bar and continued toward the headstock. It was felt that an unequal annealing of the work material was responsible; so it was reannealed at 1600 F for an 8-hr soak and furnace-cooled. However, the same characteristic of short test runs occurring at the tailstock end of the test bar and the longer test runs occurring at the other end still persisted. Chemical and metallurgical analyses were made on specimens cut from each end of the test bar. It was found that Rockwell hardness was exactly the same for the two ends, but the microstructure revealed a spheroidized distribution of carbides near the headstock end and large grains of carbides near the tailstock end. Carbon-content determinations showed 0.542 per cent carbon at the tailstock end and 0.452 per cent carbon at the headstock end; a difference from one end to the other of 0.09 per cent. This indicated a heterogeneous work material.

Improvement in the Test Procedure

An attempt was made to secure some homogeneous work material. An ingot from the middle of an open-hearth heat was selected and rolled into billets. The middle billet was then selected and hot-rolled into $3^1/_2$-in-diam bars. By this means, it was felt a steel homogeneous in chemical composition and metallurgical structure should be obtained. The stock was cut to 30-in. lengths and given a high-temperature anneal—$3^1/_2$-hr soak at 1600 F—and furnace-cooled.

The hand tachometer used to measure the cutting speed was replaced with a more sensitive generator-type tachometer with scale graduations in increments of 5 fpm.

Improvement was made in the tool-bit grinding procedure in that a circular grinding fixture was used to grind a batch of 26 tool bits at one time on a rotary surface-grinding machine. The abrasive wheel used, the speeds of both wheel and fixture, the quantity and quality of coolant used, and the rate of feed were all closely duplicated between successive batches so that the quality of the cutting edge on each tool bit was fairly uniform.

The test results obtained are given in Table 1, and graphically in Fig. 2, and show a definite difference in tool life between cutting fluids that are known to vary in their chemical compositions. It will be noted that variation still exists in the repeat runs, but there is no overlapping. The percentage variation is much less than previously—the greatest now being 48 per cent for cutting fluid B, compared to 145 per cent encountered with cutting fluid E in earlier repeat runs. Cutting fluid E in this set of tests varied 42 per cent.

The aim of this research was to be able to make repeat runs within a small degree of variation. The foregoing work indicates progress toward that aim, but it is not yet fulfilled. To achieve this aim it is felt that still greater control over the procedure is required.

Following is a résumé of the variables thought to be present in this machinability problem that would have to be controlled to get reliable and consistent test results. It is felt that each can be dealt with in one of three different ways:

1 By eliminating it completely from the test procedure.

2 By standardizing it so that it will always be the same to a degree of accuracy beyond that necessary for the present work.

3 By studying the effect of each variable which cannot be remedied by (1) or (2) and establishing correction factors for it so that a test result can be adjusted for its particular variables to reduce it to basic test conditions. There undoubtedly will be more than one variable to study at the same time so that a large number of test runs will have to be made to enable a statistical analysis of the data to determine the effect of each variable.

TABLE 1 SUMMARY OF TEST RESULTS MADE ON SPECIALLY PROCESSED WORK MATERIAL

Cutting Conditions:

Nominal cutting speed	250 fpm		
Depth of cut	0.020 in.		
Rate of feed	0.015 ipr		
Work material	SAE 1045 steel		
Cutting fluid	100 F, 5 gpm		
Tool bit:			
Material	Mo-Max HSS		
Angles:			
Front clearance	6°	Side cutting edge	10°
Side clearance	6°	Back rake	8°
End cutting edge	10°	Side rake	10°
Nose radius			$^3/_{32}$ in.

Cutting fluid	No. of test runs	Tool life, min — Lowest value	Tool life, min — Highest value	Per cent variation based on average
A	10	15.6	21.4	29
B	10	25.1	40.8	48
C	5	49.4	61.8	23
D	3	63.	67.7	6
E	4	68.8	103.3	42

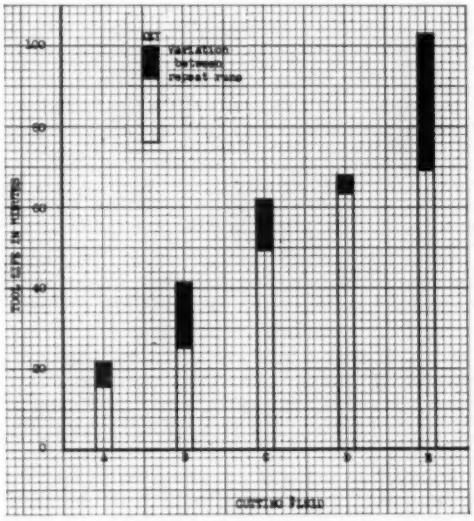

Fig. 2 Tool-Life Values for Various Cutting Fluids (Cutting data are given in Table 1.)

Variable Factors of Machinability Problem

The Lathe. The mechanical condition of the lathe should be good—with close-fitting bearings, straight, accurate ways, etc., and it should be mounted on a solid foundation so that it can be maintained perfectly level. In operating the lathe, a warm-up time should be allowed before conducting test runs to warm up and distribute the lubricating oil.

The Rate of Feed. The rate of feed of the tool, that is, inches of advance of the carriage per revolution of the work, during a test cut is fixed by gearing between the spindle and the feed shaft. A clutch arrangement is usually employed between the feed shaft and the carriage of the lathe. With a well-built machine, properly adjusted, there should be no slippage of this clutch

during a test run so that the rate of feed should be constant.

Depth of Cut. This is a variable. It varies between different test runs and throughout a single test run. The best indication of the actual average depth of cut can be obtained by making a large number of measurements of the diameter of the workpiece before and after each test cut. This is a variable that should be studied to establish a correction factor.

Cutting Speed. This has a great influence on resultant tool life and therefore should be measured as accurately as possible. A very small change in cutting speed causes a large change in tool life. Many devices are available to control or measure the cutting speed such as combination revolution counters and timers, tachometers of a large variety, highly sensitive variable-speed drives, and electronic controls for variable-speed drives. It would be desirable to measure and control the cutting speed accurately to $^1/_{10}$ ft per min.

Composition of Work Material. It is practically impossible to hold this factor exactly constant. There will be a variation in the carbon content and other elements throughout a piece of steel, and the metallurgical structure will also probably vary. Here, again, a correction factor should be determined for the chemical and metallurgical variations and be employed to correct test results to a standard material being cut. This entails analysing samples of the chip produced to determine the average composition of metal cut during one test run. Another factor is the temperature of the work material. Repeated tests on one piece of material cause it to heat up and may have an effect on the resultant tool life. This factor could be eliminated by standardizing the starting temperature of each test run, or again, by determining a correction factor to apply to the results if the temperature is allowed to vary.

Diameter of Work Material. This is a variable factor in tool life in that the curvature of the work above the chip, the circumference, and the diameter-to-length ratio all change as the diameter decreases. The force vectors acting on the tool bit and the rigidity of the work are subsequently changed, which introduces another variable in the test procedure. This variable can be eliminated by making test runs at a constant diameter which would not be very practical, or the variable could be studied and correction factors determined.

Surface Roughness of Previous Surface. This may have an effect on resultant tool life since it might affect the ease with which a chip would form and curl away from the tool bit. It is generally felt that this effect is exceedingly small and cannot be detected within the degree of accuracy usually obtained on these tests. If it were suspected of being significant, the roughness could be measured before each test run and a correction factor added to the results; or a standardizing procedure could be used, such as a cleanup cut to make the test surface always nearly the same in its surface finish.

Time of Cut. This must be determined accurately and may be obtained by direct measurement such as with a stop watch or some electrical timing device, or it may be computed, if the average cutting speed, diameter of the work, the rate of feed, and the axial length of cut are known.

Tool Bits. These present another variable in that the material in them may vary in chemical composition and metallurgical structure. The angles of the cutting edge and curvature of the nose radius as well as the surface roughness may vary. In this particular experiment it was felt this variation was held to a small degree in that all the tool bits used were produced in the same batch, the hardness readings varied only 3.5 per cent, the angles of the cutting edge were within 8 min of 1 deg of each other, the nose radii were all within 0.0005 in. of the true radius, and great care was employed to keep the surface finish as constant as possible, by duplicating the grinding procedure between batches of tool bits by using the same grinding wheel, speeds, feed, coolant, etc.

Cutting Fluid. In this case the cutting fluid is the deliberate variable. The effect of different cutting fluids on the resultant tool life is the object of this particular investigation. However, any one particular cutting fluid may have variations, such as temperature, rate of flow, and chemical composition. The physical properties must be controlled closely and duplicated between the different cutting fluids; this is accomplished rather easily by using sensitive thermostat controls on heating elements, thorough agitation of the fluid, and accurate calibration of the rate of flow for each different fluid.

Conclusion

Hitherto assumed "constant" factors, such as work material and others previously mentioned, which are involved in a machinability test, are actually variables over a certain range. In order to repeat machinability test data accurately, extremely accurate measurements are required of all the variable factors involved, to know the exact conditions of each particular test. Through careful study of the effect of each factor on the test results, correction factors may then be applied to individual test results to reduce them to some basic test condition. By this means, machinability repeat-ability may be obtained.

Discussion

H. A. Hartung.[3] The work described in this paper is a valuable contribution in the field of metal-cutting studies. In calling attention to some of the pitfalls that exist in the estimation of machinability, the author has rendered a real service to engineers engaged in this work.

Of the author's listing of variables involved in machinability studies, the fourth, cutting speed, merits some amplification. It is unquestionably true that cutting speed influences tool life, and speed, therefore, must be controlled quite accurately. At the same time, it should be pointed out that the level at which cutting speed is maintained has some influence on the reproducibility obtained. In general, higher cutting speeds lead to somewhat greater scattering; lower speeds tend to improve repeat-ability, at the price of a longer test. The explanation of this phenomenon probably lies in the greater effect at higher speeds of small changes in the other variables, due to the higher tool temperature. Thus some local variation in hardness or structure of the work might cause tool failure at 300 fpm, while at 200 fpm it would not.

E. J. Krabacher.[3] "Repeat-ability" must be considered the key word when conducting any type of machinability test. In the case of tool-life tests repeat-ability is of primary importance. In this paper the author has manifested a similar belief in the elimination, from the tests, of all variables except the one controlled factor which is to be evaluated, in this case cutting fluid.

The author is to be congratulated for the effective methods by which the undesirable variables either were eliminated or rigidly controlled. Therefore it was disturbing to find that under test conditions such as these, where all apparent variables had been eliminated to a high degree, a variation in repeat-ability as high as 48 per cent should have to be tolerated. Experience obtained in the tool-life testing that is constantly going on in the writer's laboratory has shown that a considerably more accurate degree of repeat-ability is obtainable in tool-life testing. What then is the reason for the large degree of variation obtained in these tests reported by the author?

[3] The Atlantic Refining Company, Philadelphia, Pa.

[3] Research Engineer, Cincinnati Milling Machine Company, Cincinnati, Ohio.

It has been found that a ball-bearing rotating center such as used in these tests does not give the rigidity that is obtained from a sturdy dead tailstock center. A large sturdy carbide center has been found to be very heat and wear-resistant and much more satisfactory from the standpoint of rigidity. The trouble, encountered by the author, of shorter tool life occurring when cutting near the tailstock end might have been due in part to less rigid support at that end of the test log. Instability and resultant chatter have a surprisingly significant effect on tool life. Turning the log end for end would have given a quick check on this point. This of course may have been done; however, mention is not made of the fact.

It is the opinion of this writer that an unfortunate choice was made in the selection of the depth of cut and nose radius used throughout these tests. A depth of cut of 0.020 in. was used in conjunction with a 0.015-in. feed per revolution, throughout these tests, resulting in a chip cross section for which the chip thickness was very nearly equal to its width. This type of chip results in poor chip formation and poor chip flow. It has been found that if the depth of cut is kept approximately 5 times the feed per revolution, the chip formation and flow are good. The selection of a $^3/_{32}$-in. nose radius used with a 0.020-in. depth of cut resulted in a condition where the cutting action took place entirely on the rounded portion of the tool formed by the nose radius. This resulted in chip crowding since the tool forces tend to act normal to the cutting edge, crowding the chip toward the focal point, or center, of the nose radius. This results in a wedge-shaped chip which would prevent chip curling, making it adhere to the tool face, thus increasing the friction between the chip and tool, increasing tool forces, temperature, and abrasion.

It has been found much better to keep the nose radius as small as possible, allowing most of the cutting to be done by the side cutting edge, the only purpose of the nose radius being to prevent burning and chipping of the tool, such as might occur due to high specific pressures if the tool were left with a sharp corner. It is easy to see how the foregoing conditions might seriously affect the stability, and thus repeat-ability, of the metal-cutting process.

Author's Closure

It has been our experience to have better repeat-ability at high cutting speeds (up to 500 fpm) than at lower cutting speeds such as 200 fpm. The explanation of this phenomena was that variables had more time in which to act and thus result in a greater difference (percentage wise) between repeat runs.

In all likelihood, each particular experimental setup is more susceptible to some variables than to other variables. Since Mr. Hartung has experienced greater scattering of data at high speeds, his experimental setup is more susceptible to those variables that are most affected by high speed, high temperatures, and short time. Our particular setup is apparently more susceptible to those variables most affected by low speeds, lower temperature, and longer time.

It is quite true that a large sturdy carbide center is more rigid than a ball-bearing rotating center. However, it seems unlikely that this could be the cause of variation in our repeat runs since chatter, when it was encountered, would always first occur in the middle of the test log; and secondly, the test log was placed end for end in the lathe and the same phenomenon of shorter tool life was observed on the same part of the test log.

The selection of depth of cut and nose radius was made not from the standpoint of chip formation and chip flow, but rather as a tool representative of light cuts made in industrial practice. The nose radius, giving a wedge-shaped chip and thus increasing friction between the chip and tool, increasing tool forces, temperature, and abrasion was desirable since these tests were accelerated tests when compared to industrial practice, and an objective of the test was to make direct comparisons between various cutting fluids. Since the purpose of a cutting fluid is to remove heat and reduce friction in a metal-cutting operation, an acceleration in the frictional forces and temperatures was desirable in these tests.

The author believes that the chip formation in a cutting action is dependent upon the geometry of the cutting tool; as long as this remains constant, the chip formation is stable. If the geometry of the cutting tool is accurately reproduced on each successive tool bit, the chip formation should be faithfully duplicated and thus not be the cause for variation in repeat runs.

It has been a pleasure to present this paper and the interest shown, as well as the comments by Messrs. Hartung and Krabacher, are deeply appreciated.

A Study of Heat Developed in Cylindrical Grinding

By R. E. McKEE,[1] R. S. MOORE,[2] AND O. W. BOSTON[3]

This paper, the fourth in a series on cylindrical grinding,[4,5,6] presents some of the results of an investigation of the grinding process with particular reference to the influence of the grain size of a grinding wheel and type of grinding compound used on certain criteria; such as volume of metal removed per unit of wheel wear, unit net horsepower, surface finish, grinding rating, temperature increase in the workpiece surface, temperature increase in the grinding compound, and possible injury to the structure of the metal.

Testing Conditions

THE machine used in this investigation was a standard Cincinnati No. 2 cylindrical grinder powered with direct-current motors on the wheel spindle, work spindle, and table-traverse mechanism. Details of the machine operating conditions and motor controls were given in an earlier paper.[4]

Specifications and Heat-Treatment of Material. The results given in this paper were obtained when grinding SAE 52100 steel in the form of cylindrical bars. These bars of approximately 1.2 to 1.5 per cent chromium, and 0.95 to 1.10 per cent carbon, were obtained in a spheroidized-annealed condition and machined to standard specifications of 2 in. diam and 12 3/4 in. length, with a driving shank of 1 1/8 in. diam × 2 3/4 in. length. This left a cylindrical surface 2 in. diam × 10 in. long to be exposed to a traverse cut against the grinding wheel.

The heat-treatment of the SAE 52100 steel specimens was accomplished by heating for 2 hr at 1600 F (50 deg above the critical for this material), quenching in oil to 100 F, and tempering or stress-relieving to 300 F in oil for a period of 2 hr.

Preparation of Photomicrographic Specimens. Photomicrographic specimens were cut from the ground cylindrical bars with an abrasive cutoff saw (Allison, A54V8R) operating at a peripheral velocity of 14,400 fpm. The disks, 3/8 in. thick, were then cut into small sections, carefully ground on the surfaces adjacent to the path of the saw, chromium-plated to a depth of approximately 0.005 in., and mounted in bakelite prior to the metallographic polishing operations, consisting of the use of the following: 80-grain wheel, numbers 1, 0, 00, 000 emery papers, tripoli, and gamal wheels. The specimens were then etched with a 4 per cent nital etchant, of 4 per cent by volume, concentrated nitric acid in alcohol, mounted in a Bausch and Lomb metallographic camera and photographed at 1000 magnifications.

Tukon Hardness Tests. A new Tukon hardness tester, made by the Wilson Instrument Company, was used in obtaining Knoop hardness values on the metallographic specimens. Values of Knoop hardness may be obtained by applying a light load to a diamond indenter with an elongated axis and measuring the length of the indentations with a filar microscopic lens calibrated in microns per filar unit. The diamond indenter used in this examination was shaped to an included longitudinal angle of 172°30′ and an included transverse angle of 130°.

The load applied was 100 grams for an interval of 15 sec. Measurements were made diagonally across the metal adjacent to the ground surface, so the hardness values would be representative of measurements made in a line perpendicular to the ground surface or radial in the cylindrical workpiece. The amount of traverse between indentations was kept at a ratio of 8 longitudinal to 1 transverse, in order that proper spacing of indentations might be obtained.

Grinding Wheels. The four grinding wheels used in this investigation were of the following grain size: 46, 60, 80, and 150. All were Al_2O_3 abrasive (A), J-grade, 6-structure, and vitrified bond. The specifications of the wheels are the same except for difference in grain size. They were produced under laboratory supervision at the Carborundum Company.

Grinding Compounds. The compounds used in this study are indicated by letters, A, B, C, and D and are designated as follows:

Compound A—a water-emulsifiable, low-molecular-weight, hydrocarbon mixture of high detergency.

Compound B—a water-emulsifiable, high-molecular-weight, hydrocarbon mixture of low detergency. It is a conventional soluble oil.

Compound C—a water-emulsifiable, high-molecular-weight, hydrocarbon mixture of high detergency.

Oil D—a nonaqueous, hydrocarbon solution of sulphurized fatty compounds. It consists of 80 per cent by volume of 80-viscosity SSU at 100 F paraffine oil and 20 per cent of a fatty-oil base containing 10 per cent of active sulphur.

These terms are approximate only and are used for purposes of comparison, in order to explain in part some of the effects obtained. The use of the word "detergency" is with deliberate license, but can be excused in view of the difficulty of explaining in any other word the cleaning action on the grinding wheel.

Results of Tests

Effect of Grain Size on Volume Ratio. An indication is given in Fig. 1 of the effect of grain size on the volume ratio, the volume of metal removed per unit of wheel wear, when grinding the hardened steel. Volume ratio is plotted as the ordinate, and grain size is used as the abscissa.

The 80-grain wheel gives the best performance with all four

[1] Assistant Professor of Metal Processing, University of Michigan, Ann Arbor, Mich.

[2] Manager, Detroit Branch, Quaker Chemical Products Corporation, Conshohocken, Pa.

[3] Professor of Metal Processing and Chairman of the Department of Metal Processing, University of Michigan. Fellow ASME.

[4] "An Evaluation of Cylindrical-Grinding Performance," by R. E. McKee, R. S. Moore, and O. W. Boston, Trans. ASME, vol. 71, 1949, pp. 893–901.

[5] "Experimental Study of Cylindrical Grinding," by R. E. McKee, R. S. Moore, and O. W. Boston, Trans. ASME, vol. 69, 1947, pp. 891–896.

[6] "An Investigation of the Removal of Metal by the Process of Grinding," by R. E. McKee, R. S. Moore, and O. W. Boston, Trans. ASME, vol. 69, 1947, pp. 125–129.

Contributed by the Research Committee on Cutting Fluids and Metal Cutting Data and Bibliography and presented at the Spring Meeting, Washington, D. C., April 12–14, 1950, of THE AMERICAN SOCIETY OF MECHANICAL ENGINEERS.

NOTE: Statements and opinions advanced in papers are to be understood as individual expressions of their authors and not those of the Society. Manuscript received at ASME Headquarters, January 11, 1950. Paper No. 50—S-11.

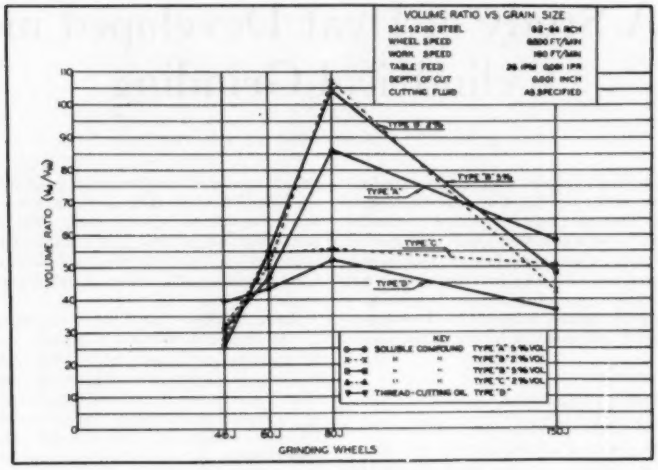

FIG. 1 VOLUME RATIO VERSUS GRAIN SIZE

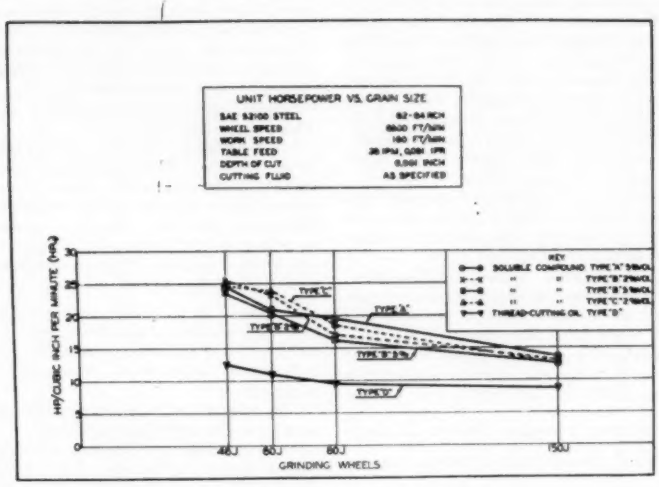

FIG. 2 UNIT HORSEPOWER VERSUS GRAIN SIZE

types of cutting fluids. The performance of the 46-J wheel is highest when used with the thread-cutting oil, type D.

Soluble compounds, types A and B, produce similar patterns in the curves with the highest values of volume ratio for the 80-J wheel. The volume ratios produced by the 150-J wheel are about equal to those for the 60-J wheel.

Effect of Grain Size on Unit Horsepower. Net horsepower per cubic inch of metal removed per minute, as determined by a wattmeter, is plotted versus abrasive grain size in Fig. 2. The water-soluble compounds produce values nearly equal but from 100 to 60 per cent higher than those for the oil. Compound type B at 5 per cent gives values lower than those of the other water compounds on all four wheels. All liquids give the lowest unit power for the finer grained wheels, ranging from about 24 for the 46-J wheel to 13 for the 150-J wheel.

Effect of Wheel Grain Size on Surface Finish. Fig. shows the effect of grain size on the resultant surface finish, allowing for no spark-out at the end of the test. The 80-J and 150-J wheels give surface finishes which are nearly equal, and in most cases they are lower than those obtained with the 46-J and 60-J wheels. The exception is for the type D oil which produces the best surface quality with the coarse-grain wheels.

The surface-finish values in microinches, rms, obtained with a profilometer are the averages of three readings taken transversely across the feed marks, on the periphery of the workpiece.

Effect of Grain Size on Grinding Rating. Fig. 4 shows a sum-

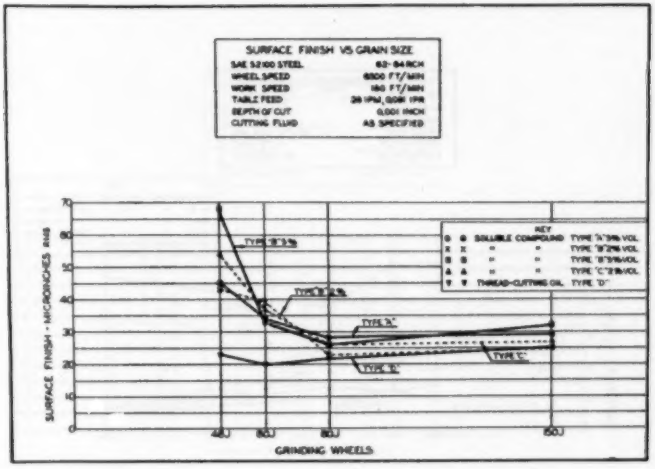

FIG. 3 SURFACE FINISH VERSUS GRAIN SIZE

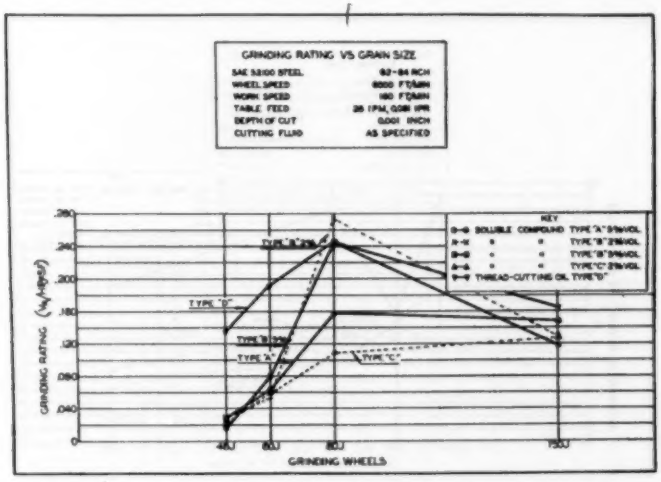

FIG. 4 GRINDING RATING VERSUS GRAIN SIZE

mary of the values given in Figs. 1, 2, and 3. "Grinding-rating" values are plotted as ordinates against the grain size of the wheels as abscissa, for each of the four grinding compounds.

Grinding rating represents the quotient of metal removed per unit of wheel wear, divided by product of unit net horsepower and the surface finish. Grinding rating = $(Vr)/(hp_n \times SF)$. This formula was prepared to show a general value of any condition to involve all three factors which are of equal importance. The highest value of grinding rating indicates the best performance in terms of the factors involved. The 80-J wheel may be considered to be the best wheel on this basis.

The 46-J and 60-J wheels show poor ratings with the soluble compounds as compared to those of the 80-J and 150-J wheels. Type D oil shows relatively high values owing to the low unit net power and the excellent surface finishes obtained as shown in the foregoing figures.

Temperature Increase of Work Surface. The temperature increase, as measured with an Alnor Pyrocon thermocouple on the surface of the workpiece, is shown in Fig. 5. Results from all of the soluble compounds are nearly equal for all wheels, and much lower in all cases than for the oil. The low temperature increase for the water compounds indicates the importance of their higher thermal conductivity, as compared to that of the oil. Values of thermal conductivity in "cal per cm sec deg C $\times$ 10^{3}" from Lange's Handbook of Chemistry are 0.34 to 0.36 for refined mineral oil and 1.40 for water, both at 20 C. Thus the amount

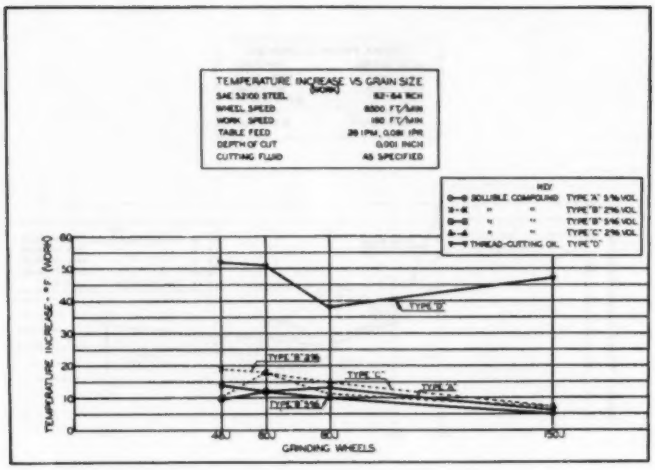

FIG. 5 TEMPERATURE INCREASE VERSUS GRAIN SIZE; WORK

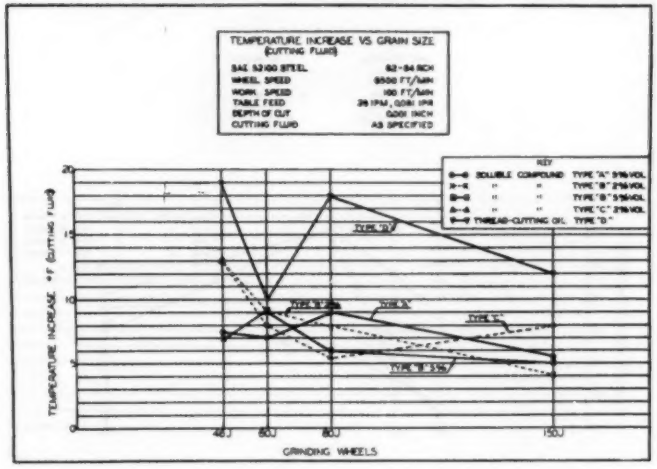

FIG. 6 TEMPERATURE INCREASE VERSUS GRAIN SIZE; CUTTING FLUID

of temperature increase on the work surface, as shown for each of the compounds, is consistent with known values of conductivity of water and oil.

Temperature Increase of Cutting Fluid. The temperature increases of the 20 gal of each of the grinding compounds used are shown in Fig. 6. There is an indication that the percentage by volume concentration of the soluble compounds may define a general trend as shown by either the solid lines for types A and B at 5 per cent, which reduce the temperature as the grain size is increased, or by the dashed lines for types B and C at 2 per cent, which give practically equal values for all grain sizes. The type D oil produces a greater increase in cutting-fluid temperature in all tests but gives the lowest value for the 60-J wheel.

Tukon Hardness Test. The influence of the several grinding compounds on the hardness of the subsurface of the bars is shown in Figs. 7 to 10, inclusive, when using the 46-J and 60-J wheels with each of the compounds, type B at 2 per cent and type C at 2 per cent. Fig. 7 shows the values of hardness tests taken radially across the hardened SAE 52100 steel adjacent to the ground surface obtained with a 46-J grinding wheel and the type B, 2 per cent, compound. The heavy vertical line at zero depth represents the intersection of the base metal and the chromium layer used in supporting the sharp edge during metallographic polishing.

The curve indicates values averaged from two complete traverses from 0.0003 in. inside the chromium layer to 0.0021 in. inside

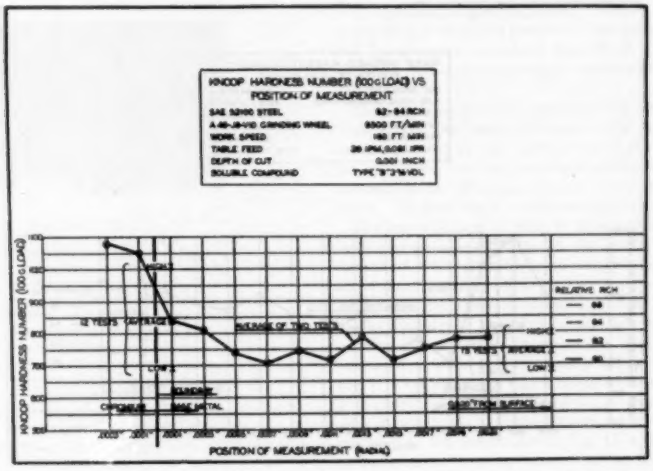

FIG. 7 KNOOP HARDNESS NUMBER (100 G LOAD) VERSUS POSITION OF MEASUREMENT

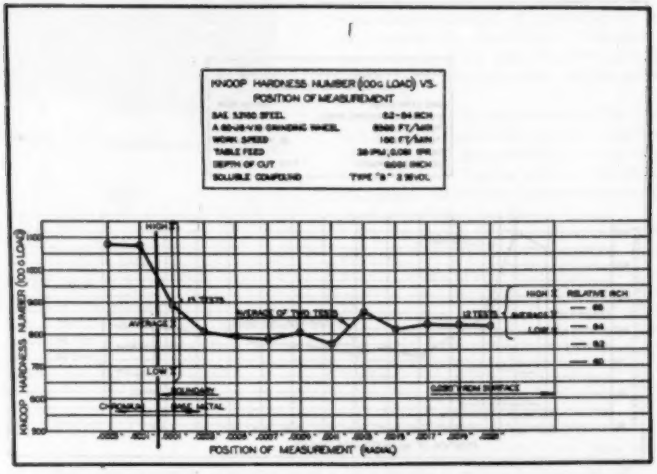

FIG. 8 KNOOP HARDNESS NUMBER (100 G LOAD) VERSUS POSITION OF MEASUREMENT

the base metal. Twelve additional tests were made in an area approximately 0.0001 in. in the base metal from the boundary.

The average of these twelve tests gives a Knoop hardness (Khn) value of 840 which is higher than the average value of 740 obtained from 15 similar hardness tests in the base metal, 0.020 in. from the surface. The highest and lowest individual test values are represented by an X. The values of Knoop hardness observed in the chromium layer are in the range of 1050 to 1080.

Both values of hardness observed at 0.0001 and 0.0003 in. from the boundary in the base metal are about 75 Khn higher than the remainder of the points shown in the base metal.

Similar hardness tests made on the steel ground with the 60-J wheel and the type B, 2 per cent, compound are shown in Fig. 8. The average value of 15 Knoop hardness tests made in the base metal approximately 0.0001 in. from the boundary is 835. This is about 45 Khn above the values for the next five locations from 0.0003 to 0.0011 in. The last five points on the right side of the curve are slightly higher. The twelve tests made at 0.020 in. from the surface give an average of 860.

The hardness values shown in Fig. 9 indicate a slight softening effect in the base metal just below the ground surface. The Type C, 2 per cent, water compound was used with the 46-J wheel. The average of twelve readings at 0.0001 in. from the boundary is 815 Khn, while the averages shown in the next three readings at depths of 0.0003, 0.0005, and 0.0007 in. are lower in

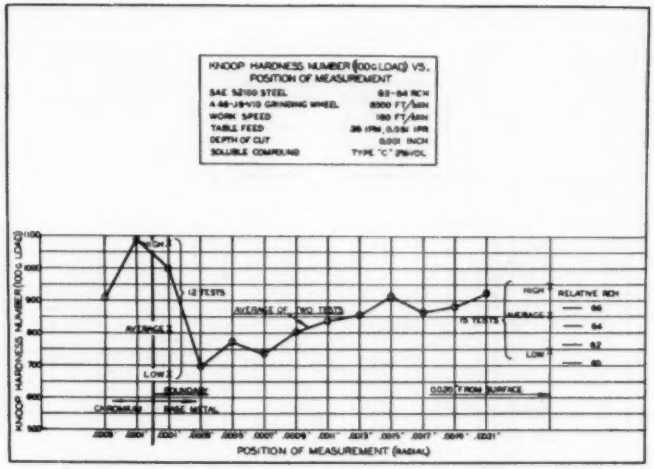

FIG. 9 KNOOP HARDNESS NUMBER (100 G LOAD) VERSUS POSITION OF MEASUREMENT

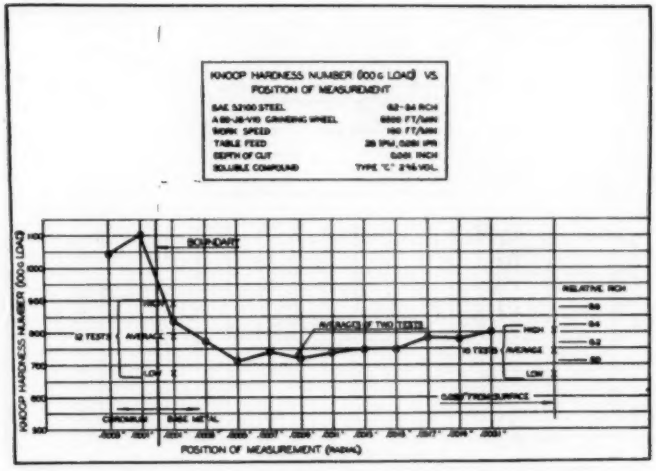

FIG. 10 KNOOP HARDNESS NUMBER (100 G LOAD) VERSUS POSITION OF MEASUREMENT

value. The average of 15 tests made at 0.020 in. from the surface is 855.

Fig. 10 shows an average hardness of 790 Khn for twelve tests made at approximately 0.0001 in. under the ground surface in the base metal, while an average value 745 is shown for ten tests located 0.020 in. under the surface, when a 60-J wheel was used with type C, 2 per cent, compound. The results indicate a condition of hardness near the surface in excess of that shown for the base metal.

The indentations were applied and measured on the metallographic specimens in a gamal polished condition, so they would appear as black in contrast to the white metallic surface. The pattern made by the diamond indentations is illustrated in the top view in Fig. 11. The bottom view of this figure shows the pattern after a 4 per cent nital etchant was applied to the structure. The proximity of the black indentations are discernible near the boundary of the base metal and the white layer of chromium.

PHOTOMICROGRAPHIC EXAMINATION

Figs. 12 to 16, inclusive, show the effects of cylindrical grinding on the structure of the SAE 52100 steel as heat-treated to a 62–64 Rockwell C hardness and ground under the conditions listed in Figs. 1 to 10, inclusive.

The SAE 52100 steel, heat-treated by oil-quenching from 1600 F to 100 F, followed by tempering or stress-relieving at 300 F, produces a tempered martensite represented by a needle-

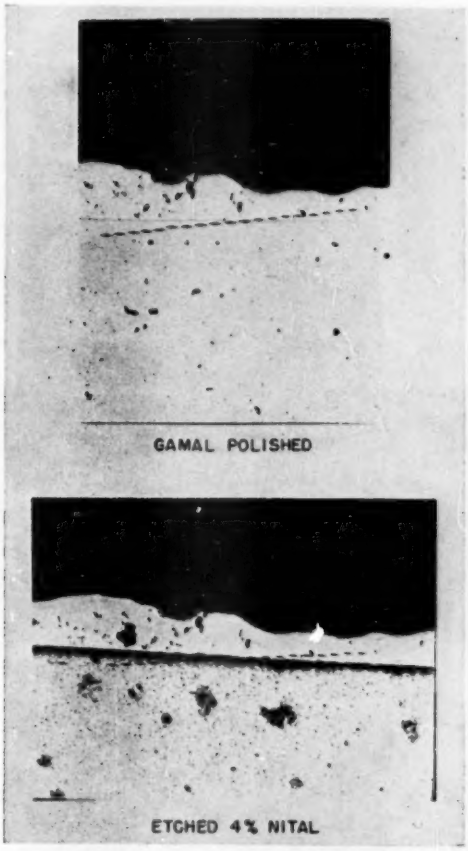

SAE 52100 steel (62–64 RCH), Chromium plated
Grinding wheel, A 60-J6-V10
Grinding compound, Type B, 2 per cent volume
Radial traverse between indentations, 0.0002 in.
Magnification, ×100

FIG. 11 PATTERN OF INDENTATION MADE BY TUKON HARDNESS TESTER 100-GRAM LOAD

like crystal structure in angular arrangements. Heating to a temperature above that of formation of the martensite but below the temperature at which the martensite will be softened, will result in discoloration in the martensitic structure and will affect the Rockwell C hardness only slightly up to certain limits. Discoloration of the martensitic structure indicates a condition of reheat. Conditions of excessive reheating (beyond the critical or austenitizing temperature), followed by quenching on the surface subjected to the heat, results in a surface structure consisting of white, untempered martensite, and tempered martensite, producing variable hardness values. This is termed a "skin" condition, indicating that a transition has occurred.

Various dark areas in the metal structure below the surface in some of the illustrations may indicate different degrees of etching.

The photomicrographs in Fig. 12 show the results obtained by grinding SAE 52100 steel with four different grinding wheels, and the grinding compound type A at 5 per cent volume in water (a low-molecular-weight hydrocarbon mixture of high detergency).

The effects of heat are indicated by skin in the upper-left, "temper" in the upper-right and in the lower-left views. The compound type A, 5 per cent, is one of the two used in this and the remaining four figures which produces any noticeable disturbance in the structure, as a result of grinding with the 80-J wheel. No heat effect is indicated in the view at the lower right.

The magnification of 1000 × indicates that 1 in. in the illustration represents 0.001 in. in the actual specimen. Further, the size of a 150 abrasive grain would be equal to the length of one of the photomicrographs.

The photomicrographs presented in Fig. 13 show disturbances in the structure of the material ground with the 46-J and 60-J wheels. The specimen shown in the upper left is the same as that used in obtaining the Knoop hardness values recorded in Fig. 7. The reason for values of higher hardness in the boundary of the base metal is indicated by the presence of the light etching skin shown in the specimen ground with the 46-J wheel. The specimen in the upper right in Fig. 13 is the same as that used in the hardness tests represented in Fig. 8, and the indication of lower values of Knoop hardness in the first 0.001 in. depth is due to the condition of temper, as shown in the photomicrograph. The 80-J and 150-J ground specimens show no evidence of structural change as a result of grinding under the conditions of operation maintained in these tests. This figure represents results obtained by using the type B compound at 2 per cent volume in water (high-molecular-weight hydrocarbon mixture of low detergency).

Fig. 14 shows the results obtained by the same compound used in Fig. 13, but at a 5 per cent by volume concentration instead of 2 per cent. The skin effect is not as severe with the 46-J wheel, and the temper effect is considerably modified by the 60-J wheel. No effects of change in structure are discernible with the 80-J and 150-J wheels.

Fig. 15 represents the condition of the structure produced by grinding with the type C compound at 2 per cent volume in water (high-molecular-weight hydrocarbon mixture of high detergency). Resultant skin effects produced by both the 46-J and 60-J wheels are shown. The actual hardness values of the specimens ground by these two wheels are shown in Figs. 9 and 10. This compound, like type A, produced an effect of temper resulting from grinding with the 80-J wheel. An outstanding similarity between the type A and C compounds that show this effect is "high detergency."

It is of interest that the compounds types A and C causing metallurgical disturbance when used with the 80-J wheel in Figs. 12 and 15 give the lowest values of "grinding rating" for the 80-J wheel in Fig. 4, indicating a possible correlation between the mechanical and metallurgical aspects of these results.

The results obtained by grinding with the type D oil (mineral oil with sulphurized fatty base) are shown in Fig. 16.

In spite of the fact that temperature increases on the work surface and in the cutting fluid, Figs. 5 and 6, were of higher values than those obtained with the water-soluble compounds, this cutting fluid aids materially in reducing the amount of disturbance, as shown by the absence of "skin effect" and the reduction in so-called temper. This oil gave evidence of low unit net horsepower in Fig. 2, and the most satisfactory surface finishes in Fig. 3. However, the use of this oil would not be practical under most circumstances because of the great heat generated.

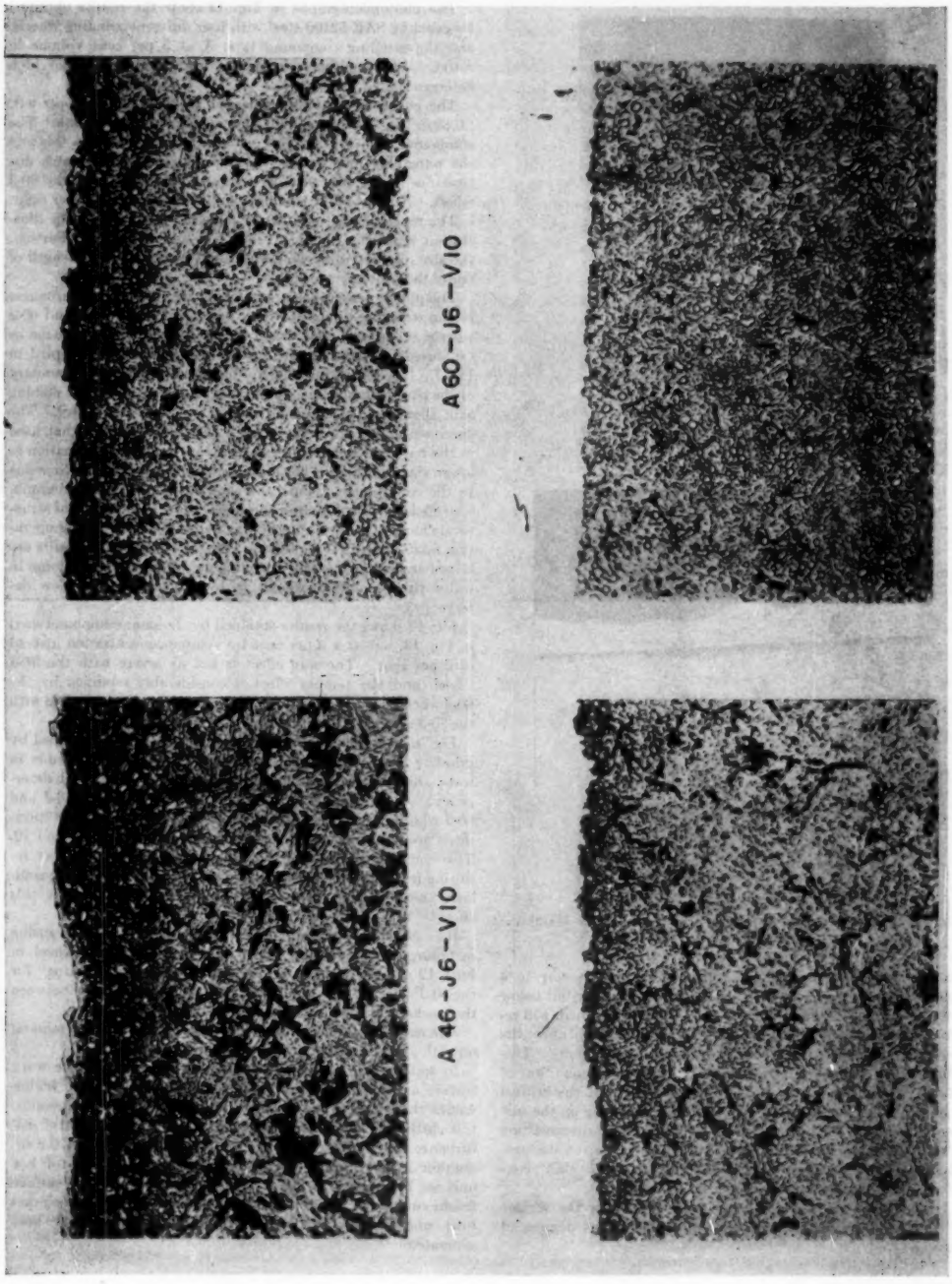

Grinding compound, Type A, 5 per cent volume, SAE 52100 steel; 62–64 RCH; ×1000

FIG. 12 PHOTOMICROGRAPHIC VIEWS OF METAL STRUCTURE ADJACENT TO GROUND SURFACES

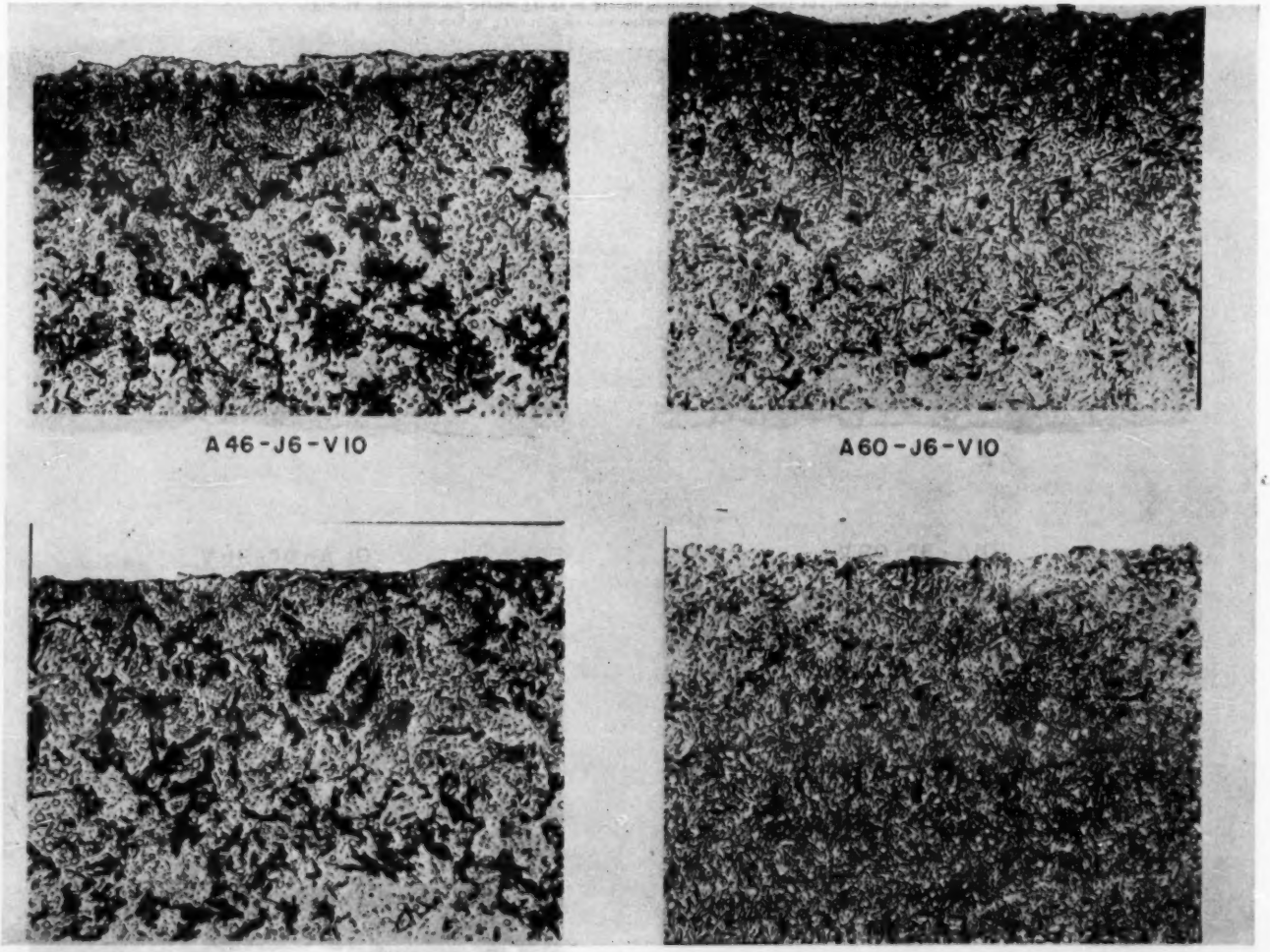

Grinding compound, Type B, 2 per cent volume, SAE 52100 steel; 62-64 RCH; ×1000

FIG. 13 PHOTOMICROGRAPHIC VIEWS OF METAL STRUCTURE ADJACENT TO GROUND SURFACES

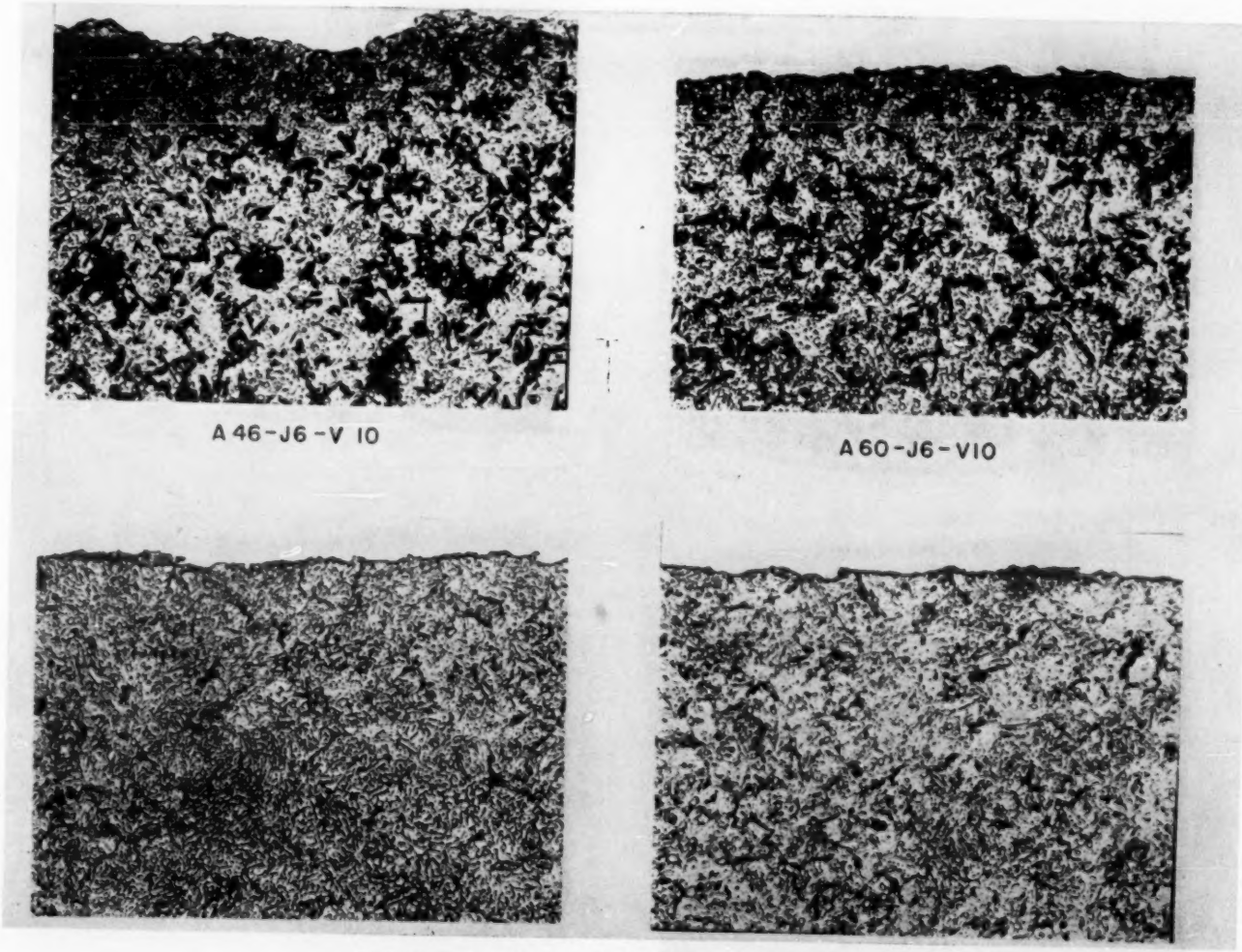

Grinding compound, Type B, 5 per cent volume, SAE 52100 steel; 62–64 RCH; ×1000

FIG. 14 PHOTOMICROGRAPHIC VIEWS OF METAL STRUCTURE ADJACENT TO GROUND SURFACES

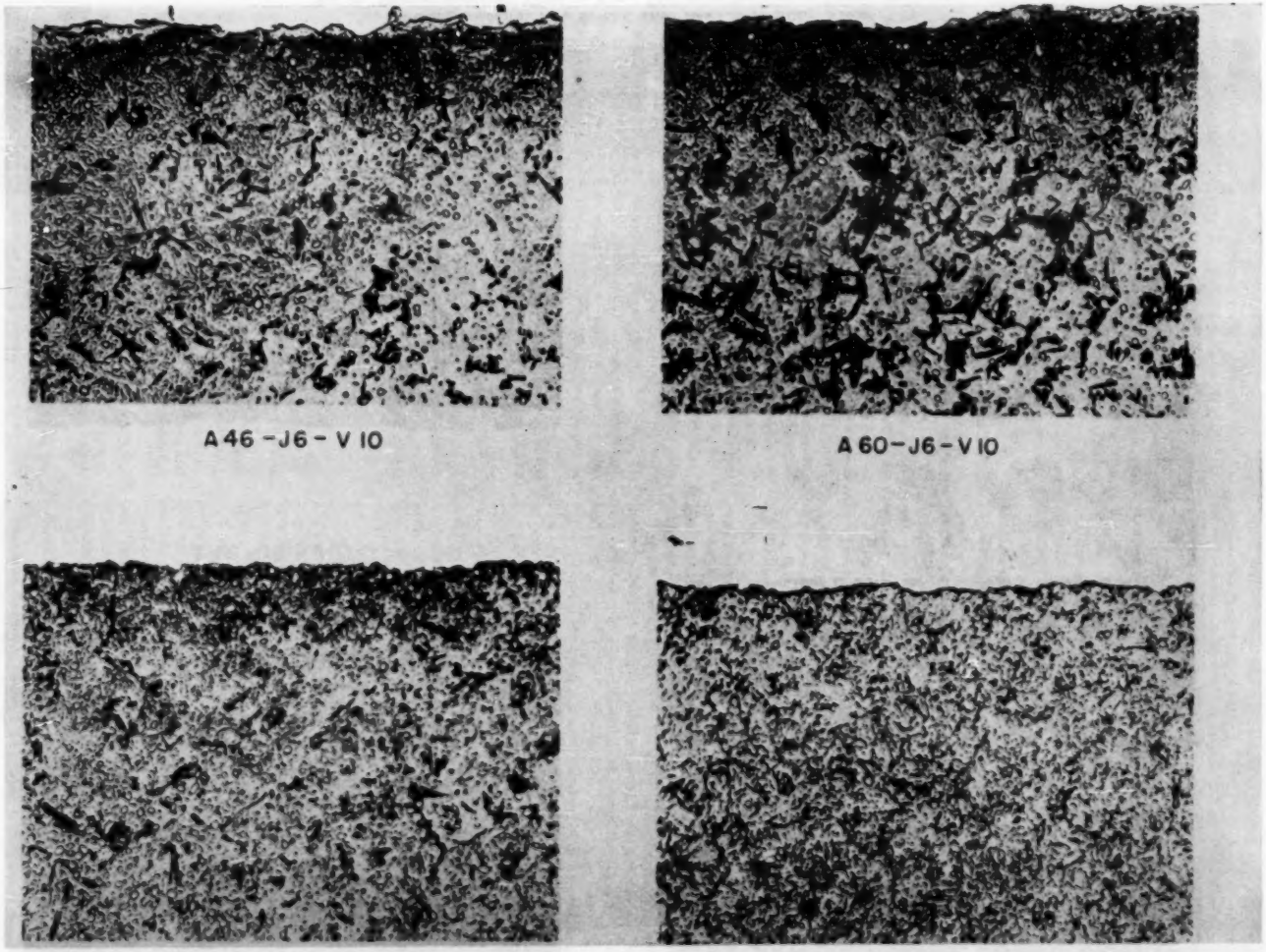

Grinding compound, Type C, 2 per cent volume, SAE 52100 steel; 62-64 RCH; ×1000

FIG. 15 PHOTOMICROGRAPHIC VIEWS OF METAL STRUCTURE ADJACENT TO GROUND SURFACES

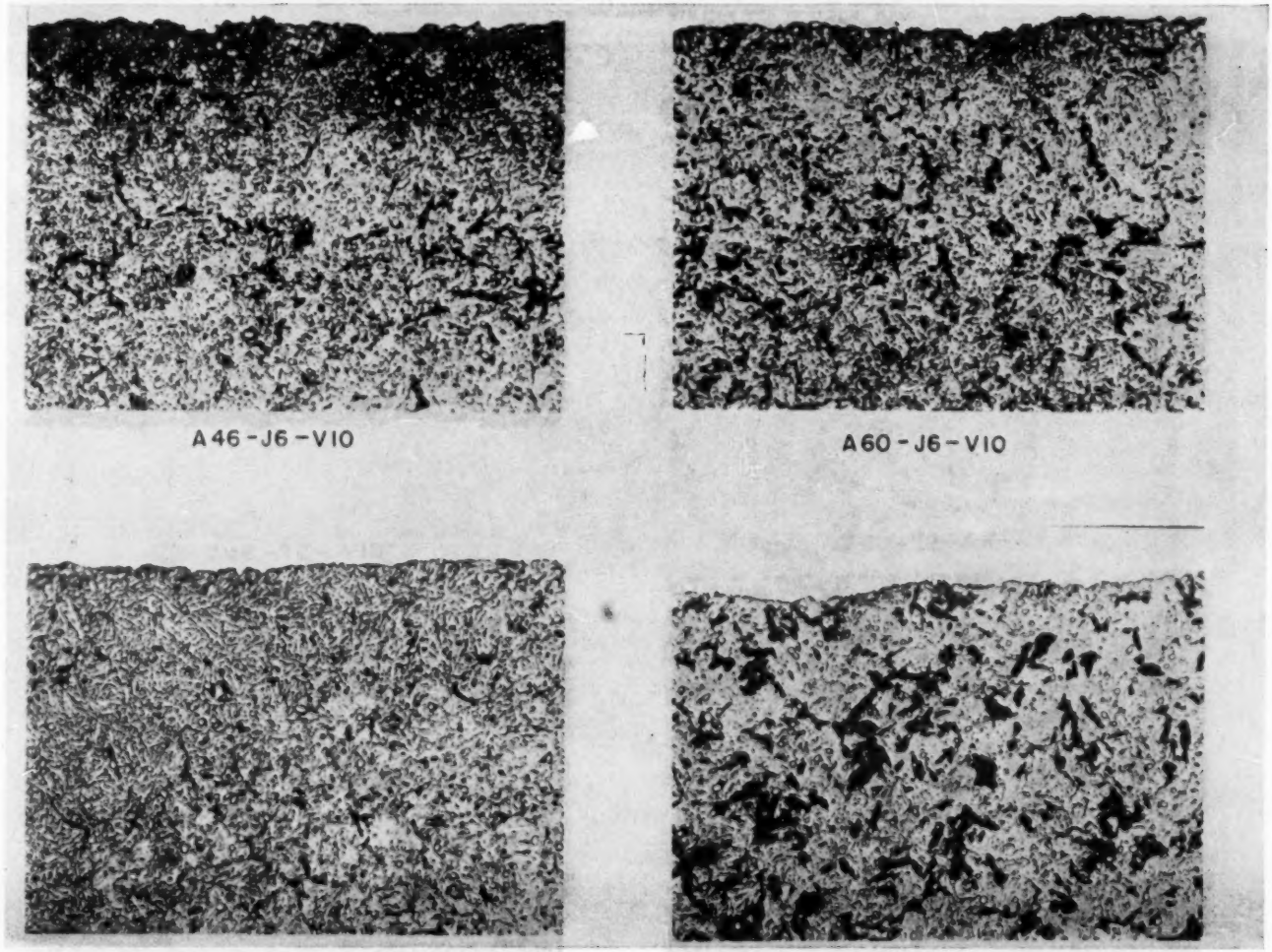

Grinding compound, Type D, SAE 52100 steel; 62-64 RCH; ×1000

FIG. 16 PHOTOMICROGRAPHIC VIEWS OF METAL STRUCTURE ADJACENT TO GROUND SURFACES

Summary and Conclusions

1 The highest values of "volume ratio" shown in these results were obtained with type B, water-emulsifiable, high-molecular-weight hydrocarbon mixture of low detergency when used with an A 80-J 6-V10 grinding wheel, Fig. 1.

2 The lowest values of "unit net horsepower" were obtained with the type B compound mentioned in (1) and the type D oil, consisting of a mineral oil mixed with a sulphurized fatty base. The oil gave much lower values than the water compound, however, Fig. 2.

3 The most satisfactory "surface finishes" were obtained with the type D, oil, when used with the coarse-grain wheels. Comparable results were also obtained with the type B compound when used with the 80-J wheel, Fig. 3.

4 The highest "grinding ratings" were obtained with types B compound and D oil when used with the 80-J wheel. Type A compound was quite satisfactory if limited to use with the 80-J and 150-J wheels, Fig. 4.

5 Temperature increases measured on the surfaces of the work specimens are approximately inversely proportional to the thermal conductivities of plain mineral oil and water, Fig. 5.

6 Tukon hardness tests give reasonable support to the evidence shown in the photomicrographs as to variation in structure as a result of the introduction of heat from a grinding wheel.

7 Obvious differences in microstructure, due to differences in the temperature to which the skin metal was heated, are doubtlessly controlled to some extent by both detergency and molecular weight of the dispersed phase, i.e., the hydrocarbons in emulsion.

8 Two out of three cases, in which hardness tests were made in areas showing skin or quench effect, indicate that the boundary layer of untempered martensite is of an average higher Knoop hardness value than the base metal.

9 Only two of the five cutting fluids (those of high detergency) show any effect of temper as a result of grinding with the 80-J wheel. These same fluids give the lowest values of grinding rating obtained with this wheel.

10 External cylindrical grinding of hardened SAE 52100 steel may affect, under certain conditions, the structure of the material adjacent to the surface.

Acknowledgment

This work was done as an Engineering Research Project in the Department of Metal Processing, University of Michigan. The program was initiated and sponsored by the Quaker Chemical Products Corporation of Conshohocken, Pa.

Discussion

W. H. Oldacre.[7] This paper seems to cover rather exhaustively the grinding of one steel with four different grinding fluids and wheels of four different grits.

In our experience, cylindrical grinding of 52100, a hard bearing steel, normally favors the use of a water-mixed grinding fluid, excepting where very fine finish or intricate contours are involved. It is on the softer tougher steels with sharp corners and other complex forms that oil grinding has clearly demonstrated its definite superiority.

As pointed out in the paper, damage to the surface of the workpiece is far from insignificant, and the benefits from the use of proper grinding fluid important. Oil, according to the paper, would seem to merit further attention on this basis.

It is, of course, difficult to define fluids in the terms of the paper, namely, high and low-molecular-weight and detergency, and, in the case of oil—"active sulphur." How was the activity of the sulphur measured? Such determination is difficult in the presence of fat.

The authors explain their "license" in the use of the term "detergency," but we feel that the mechanisms of chip formation and metallic behavior offer so many possible explanations for the "clean wheel" that the oversimplification is perhaps unfortunate.

The statement is made: "The use of this oil would not be practical under most circumstances because of the great heat generated." This generalization neglects the possibilities of heat control through redesign of the oil-handling system or a different selection of the grinding oil. It is generally recognized that high-sulphur oils give high temperatures under some grinding conditions, but frequently these high temperatures can be definitely lowered through the use of oils balanced to the conditions.

Only careful study over a wide range of conditions can answer satisfactorily the perennial question of water or oil, but the authors have made a significant contribution.

H. W. Wagner.[8] Findings for the conditions employed are clearly presented in the paper. Control of conditions, accuracy of measurements, and correlation of factors and results constitute an excellent example of fundamental research. It is hoped that the authors will continue their investigations with the object of making the findings more directly applicable in industry. Men responsible for the engineering of grinding in the country's production plants are hungry for knowledge of fundamental relationships between speeds, feeds, and wheel specifications, and production rates.

The discussion which follows is mainly a comparison of material in the paper with grinding practice and an attempt to point out how research might be of additional value to the grinding industry.

Conditions of the operation are classed as being closer to rough-grinding (stock removal) than to typical finish-grinding, and as approaching "corner grinding" because of the short lead (0.081 in.) per revolution of work. If these conditions represent some field job, it might be well to name that job. The volumetric rate of feed is calculated to be about 0.11 cu in. per min per in. of width of wheel face.

The wisdom of combining stock removal and finish characteristics in the same grinding rating for a comparison of wheel specifications is questioned when that rating is calculated from one set of grinding conditions. Conditions are usually altered when going from stock removal to finish-grinding.

It is suggested that rate of production be given more weight in a grinding-rating formula for stock removal. This is because time cost is larger than wheel cost, per unit of product, in commercial grinding. To arrive at the suggested rating, it may be necessary to use different rates of volumetric feed and perhaps harder (more durable) grades of wheels.

When wheels or grinding fluids are compared for maximum permissible rate of production, a convenient basis of comparison is equal power consumption. Fig. 2 of the paper and other data indicate that with Type D grinding fluid (oil), a more durable wheel and a faster rate of cut could be applied without drawing more power than with the water mixtures. Thus a higher rate of production could be attained with oil without more tax on the machine capacity and without more danger of heat injury to the work.

The high grinding benefit from oil in practice is well recognized.

[7] President and General Manager, D. A. Stuart Oil Company, Chicago, Ill. Mem. ASME.

[8] Research Engineer, Research Laboratories, Mechanical Section, Norton Company, Worcester, Mass.

It is not used more than it is because of the nuisances which accompany it. For example, it has something like only 10 to 20 per cent of the capacity of water to extract heat from the work and can leave the latter "too hot to handle." For support of this statement, see Fig. 5 of the paper.

Among the emulsifiable compounds, Type B appears to merit the highest rating mainly because power is generally lowest with it, especially at 5 per cent concentration.

It would seem worth while to seek a reason for the relatively low volume ratio shown for oil (Type D) in Fig. 1, in view of the low power shown for oil in Fig. 2. One might expect that when oil reduces the cutting effort (less power) it would at the same time reduce wheel wear and thereby increase volume ratio. However, much more practical significance is attached to the showing of Fig. 2 (see preceding discussion) than to the showing of Fig. 1. Differences of ratio, large in Fig. 1, correspond to small differences of rates of cut and of wheel wear in terms of thousandths of an inch. For example, when ratio drops from 100 to 50, the stock removal is calculated to drop only about 1 per cent.

One of the factors of ratio is wheel wear, which occurs while grinding. The latter factor may or may not be useful as an index of workpieces ground per truing of the wheel. The wheel is retrued because its working face "breaks down" or because it becomes too dull, in rough-grinding. Workpieces per truing are of more practical importance than ratio, because retruing detracts from production rate and also is likely to account for most of the wheel consumption in cylindrical grinding.

It is interesting to note that the present paper gives an 80-grit wheel the highest rating among those compared. This is considered to be in closer agreement with practical experience than is the high rating given a 150-grit wheel in the second paper (1946) of this same series.

Turning to surface finish, it should not be taken for granted that the same relative Profilometer readings would be obtained under both rough- and finish-grinding conditions, with the different grit sizes of wheels. The finish can be refined with any of the wheels by a fine truing lighter feed and "die-out" passes.

In this paper, metallurgical burn of the steel is indicated, to depths not exceeding about 0.0007 in. Such burn need not be serious, as it can be reduced by die-out passes at the end of rough-grinding or eliminated by light feed in finish-grinding.

Authors' Closure

The authors very much appreciate the informative discussions of Messrs. W. H. Oldacre and H. W. Wagner, both of whom are recognized as authorities in their respective fields. Mr. Oldacre asked the question concerning method of determination of activity of the sulphur. We must agree that an analytical approach to determination of active sulphur in a fatty base is difficult and likely to be quite misleading. The only dependable approach is to determine the functional efficiency of the material, fully realizing that all components of the product work together. Specifically, by our use of the term "active sulphur," we do not mean activity in the sense of a reaction in the cold to form copper sulphide.

It is recognized that detergency used as a single term is simplicity in itself and yet it is felt that the word does explain what is meant by the physicochemical action of the coolant in helping to keep the wheel clean without reference to the important mechanical and metallurgical factors involved.

Mr. Oldacre further suggests the design of an oil-handling system to control the temperatures of grinding oils. This is recognized as a standard commercial practice. However, in our tests it was found that the oil would permit excessive heating and the comments were based entirely on that observation. Admittedly, a thorough study of various grinding oils could well lead to a more efficient one than that particular blend used in the present work, even though this grinding problem is certainly not one we would normally expect to solve with an oil.

Mr. Wagner's comments are also very much appreciated. The question of rating for any grinding combination, which involves the material cut, the wheel, the cutting conditions and the cutting compound, by having in the same formula the subject of finish characteristic and stock removal, is purely a matter of judgment. Each of these items was determined separately and so reported but as explained in a previous paper, in order to have one single rating involving all of these factors the so-called rating formula was developed. A variation in any one of the factors of volume, ratio, finish characteristic or unit net horsepower would change this rating but naturally an analysis must be made to determine which element causes the change to the greatest extent and why. In our rating, each of the terms was given an equal weight, although it is recognized that any one of them could be given greater or less weight depending on the interest in that factor.

It is true that in this paper the 80-grit wheel gave the highest rating of those compared, while in a second paper, 1946, a 150-grit wheel was given a high rating because of the lower unit power developed in those tests in which a different grinding compound was used. The 80-grit and the 150-grit wheels as tested and reported in several papers have been found to be very close together in their performance in terms of surface on the work and volume ratio. However, the difference in performance in these two wheels has been in unit net horsepower. In our tests we did not use the spark-out or die-out passes as we were interested primarily in the surface quality of the work as developed under the actual grinding conditions of the tests.

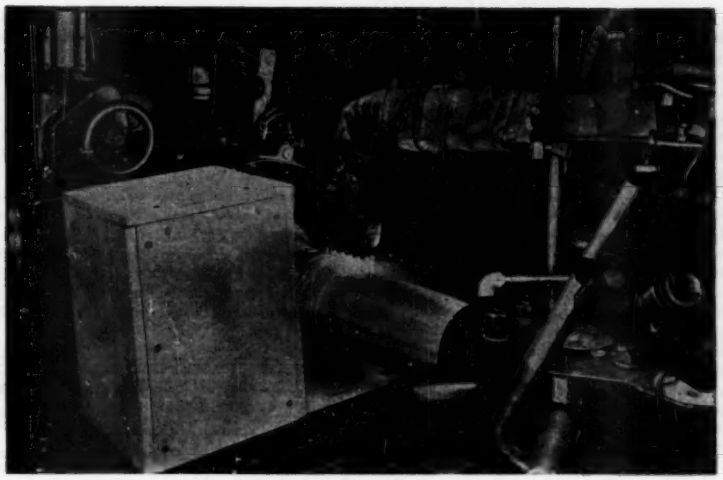

FIG. 1 FLAME-HEATING SETUP FOR HOT MACHINING

Machining of Heated Metals

BY E. T. ARMSTRONG,[1] A. S. COSLER, JR.,[2] AND E. F. KATZ,[2] COLUMBUS, OHIO

Studies are reported of the machinability of several materials at elevated temperatures. It was found that tool life, cutting austenitic stainless steel, was increased tenfold by heating to 400 F. High-temperature alloys, including vitallium, machined freely at temperatures from 700 F to 2000 F. Long curling chips and a smooth cleanly cut surface were produced in hot-machining. The same materials cut at room temperature developed a glazed uneven surface, and the chips were powdery. Austenitic manganese steel machined easily at 1200 F, as did fully hardened high-speed steel. An arc heating method was developed which permitted continuous heating while machining, without heating the work throughout.

INTRODUCTION

NEARLY 6 years ago, it was suggested by a member of the Battelle staff that the machining of materials might be facilitated by heating the workpiece. The advantages of such a course might be expected to result from either of two effects, the softening and weakening of materials at high temperatures, or avoiding the transformation of metastable materials such as austenitic manganese steel, in which the transformation is normally induced by the work of machining.

Several crude machining tests were made, using material heated by a welding torch, to determine qualitatively the effects of heating on machining. It was found that machining was invariably improved, spectacularly in some cases, and that there appeared to be no insuperable obstacles to hot machining.

These initial tests were so encouraging that the Warner and Swasey Company decided to sponsor the work, and full-scale research was begun. One phase of this research was an appraisal of the capabilities of hot machining, including definition of the suitable range of temperature for hot-machining several materials. The other phase was the development of suitable means for heating materials in turning operations. Since this work was completed, references have appeared in the literature concerning hot machining.[3]

EFFECT OF TEMPERATURE ON MACHINABILITY

The method used to obtain data on the effect of temperature on machinability consisted of heating the workpiece with a large flame-hardening torch while the work rotated in a lathe. The apparatus is shown in Fig. 1. Owing to the relatively low power input from this torch, it was necessary to heat the workpiece throughout, rather than to heat the surface only, as would be desirable.

The effects of heating were appraised by tool-life tests, when sufficiently large samples of material were available. When

[1] Research Engineer, Battelle Memorial Institute. Jun. ASME.
[2] Research Engineer, Battelle Memorial Institute.

Contributed by the Research Committee on Metal Cutting Data and Bibliography and Research Committee on Cutting Fluids and presented at the Spring Meeting, Washington, D. C., April 12–14, 1950, of THE AMERICAN SOCIETY OF MECHANICAL ENGINEERS.

NOTE: Statements and opinions advanced in papers are to be understood as individual expressions of their authors and not those of the Society. Manuscript received at ASME Headquarters, July 29, 1949. Paper No. 50—S-5.

[3] "Hot Milling," by A. O. Schmidt, *Iron Age*, vol. 163, 1949, p. 66.
"Metals Handbook," American Society for Metals, Cleveland, Ohio, 1948, p. 724.
"Hot Spot Machining," by Sam Tour and L. S. Fletcher, *Iron Age*, vol. 164, 1948, p. 78.

sufficient material was not available, qualitative studies were made of surface finish, types of chips formed, or some other characteristic of the machining operation.

With the torch heating method, it was possible to obtain the basic information on the temperatures required for machining various materials, the effect of these temperatures on machinability, the influence of the temperatures on tools, and a background of experience in machining at high temperatures, while a concurrent development program on practical heating methods was in progress.

Type 304 Stainless Steel. An austenitic, 20 per cent chromium and 9.5 per cent nickel, stainless steel was selected for initial study of the effect of temperature on machining. This material is strong and tough and exhibits marked work-hardening when it is deformed as in machining. In addition, the selected stainless steel machines without great difficulty at room temperature, thereby yielding a convenient reference machinability. Many of the other materials studied in this investigation are essentially unmachinable at room temperature.

In Fig. 2, which presents the tool-life data for stainless steel, it is shown that at a cutting speed of 500 surface ft per min (sfm), and at a billet temperature of 400 F, the tool life is 3 to 7 times that obtained at the other test temperatures. It is also apparent that an optimum temperature range exists for which, at given machining conditions, the tool life will be a maximum. The nature of the optimum temperature range is indicated more clearly in Fig. 3, using data derived from the preceding figure. Note, for these machining conditions, that the optimum temperature is approximately 400 F for this stainless steel and tool material. The best temperature for machining is, of course, a function of the material machined, the cutting conditions, and the tool material.

It is apparent that heating improves the machinability of stainless steel markedly. Such a result seems reasonable, since optimum machinability would be expected when a balance between the properties of the tool and the workpiece has been achieved, and it would be remarkable if this optimum were always achieved at room temperature.

However, the results on stainless steel, while significant, reflect a change largely in the degree of machinability. More startling results were obtained on other essentially unmachinable materials. In these the machinability was greatly changed in character owing to heating the work.

Vitallium. Vitallium is a useful alloy, at high temperatures, which is widely used in gas-turbine blades. The material machines with such difficulty that these intricate and precise elements are cast to size to eliminate all possible machining. The material is usually ground, when finishing is necessary, in preference to turning at very slow speeds. From the standpoint of convenience and economy, it would often be advantageous to fabricate such parts by machining. For this reason, vitallium was included among the materials to be investigated for hot machinability.

Large changes were observed in the machinability of vitallium at elevated temperatures. When machining was done cold, the chips were powdery, the surface finish glazed and uneven, and tool life short. At high temperatures, about 2000 F, the material machined freely, with long curling chips; the cut surface was smooth and even, and the tool life was satisfactory.

The pronounced improvement in machinability resulting from

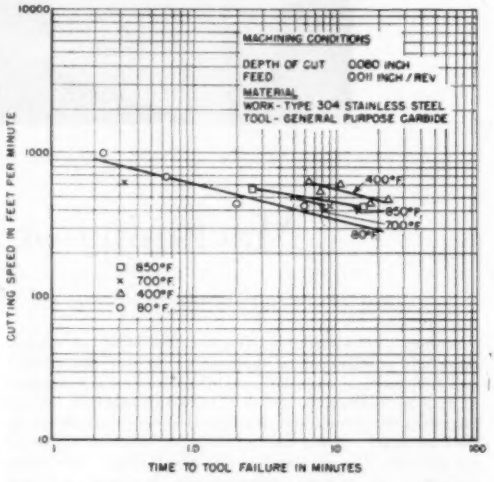

FIG. 2 EFFECT OF TEMPERATURE ON TOOL LIFE - CUTTING SPEED RELATION

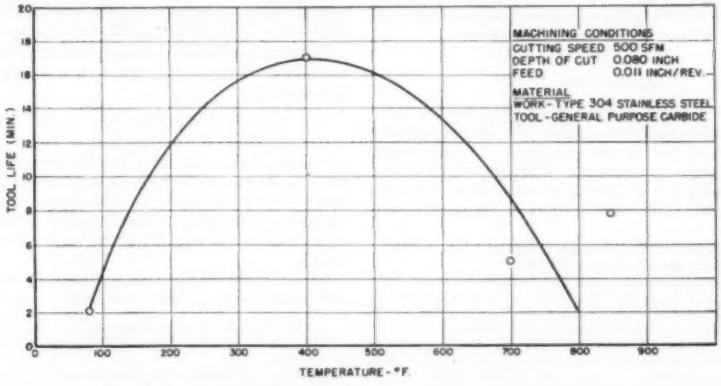

FIG. 3 RELATION BETWEEN TOOL LIFE AND WORKPIECE TEMPERATURE

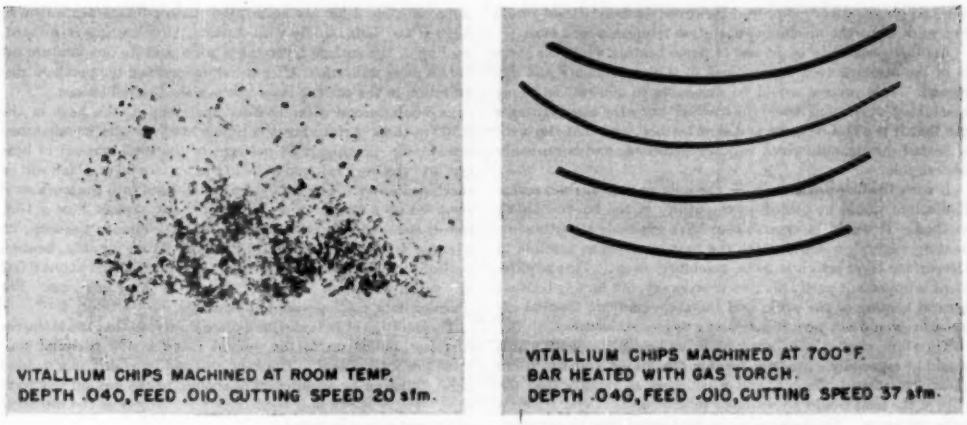

FIG. 4 EFFECT OF MACHINING TEMPERATURE ON VITALLIUM-CHIP STRUCTURE

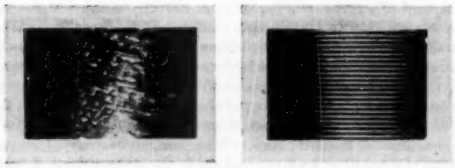

FIG. 5 EFFECT OF MACHINING TEMPERATURE ON VITALLIUM SURFACE FINISH

(*Left*) Machined at room temperature, feed 0.011 in. per revolution, depth 0.040 in., V = 20 sfm.

(*Right*) Machined at 700 deg F, flame-heated, feed 0.011 in. per revolution, depth 0.040 in., V = 40 sfm.

TABLE 1 TOOL MATERIALS[a] FOR USE IN HOT MACHINING

Manufacturer and designation		Conventional application	Composition— WC	TiC	Co	Vickers hardness	Tool life,[b] min
I	A	General finishing	84	10	6	1890	13.5
	B	High-speed finishing	76	16	8	1670	17.1
	C	Low-shock finishing	67	25	8	1690	22.0
II	D	General purpose	..	..	..	1470	9.0
	E	Roughing	..	..	..	1480	4.4
	F	Light roughing	..	..	..	1560	6.6
III	G	Finishing	..	..	..	1720	11.5

[a] Tool geometry is listed in the Appendix.

[b] Tests run at 700 F workpiece temperature at 400 sfm cutting Type 304 stainless steel with zero rake-angle tools.

heating vitallium is strikingly demonstrated by the chip photographs in Fig. 4 and by the surface photographs in Fig. 5.

Austenitic Manganese Steel. Austenitic manganese steel is a material which, at room temperature, consists of metastable austenite, and is soft and ductile. However, when the material is worked, as by machining, the austenite transforms to stable martensite which is hard and brittle.[4] For this reason, it is impractical to machine this material at room temperature.

The transformation temperature for this material, under equilibrium conditions, is 1250 F. If machining were done at higher temperatures than this, martensite would not form, and easy machining would be expected. This anticipated result has been confirmed in turning and drilling tests. The chip appearance, surface appearance, and the other machining characteristics were similar to those for the machining of vitallium.

Tool Materials. As might be expected, the tool material exerts a marked influence on the life which may be attained in hot-machining under given cutting conditions. The foregoing results are representative of general-purpose carbide tools. Table 1 presents data on various tool compositions which were investigated for use in hot machining. As shown in this table for the first series of compositions, at essentially the same hardness and cobalt content, tool life improves with increasing TiC content. As noted in Table 1, it was found that finishing tools lasted as much as twice as long as general-purpose tools, while roughing tools were definitely inferior. In a particular series (I), optimum results were obtained for a low-shock-resistance finishing tool containing about 25 per cent TiC. This tool gave a life more than twice that of general-purpose carbides.

The general superiority of the harder grades of carbide, as compared to roughing grades, is attributed to the fact that they contain smaller amounts of cobalt binder, which would soften markedly when the tool temperature is high, reducing the tool strength. In spite of the brittleness of these harder carbide tools, heavy cuts could be taken owing to the softness and weakness of the work at these elevated temperatures.

Other Metals. As will be described later, other materials were hot-machined, including two high-temperature alloys, and a low-alloy, deep-hardening, nickel-chromium-molybdenum steel with high manganese content, NE 8949. In each case, machinability was improved by heating the work. As the advantages and generality of application of hot machining were revealed, the requirements of the practical heating means were established. This permitted concurrent development of the heating method, culminating in the combination of the two phases of the study.

DEVELOPMENT OF HEATING METHODS

General Requirements. For certain types of machining operations, simple methods of heating will suffice. For example, when milling bucket teeth made of manganese steel, the simplest method would be to heat the teeth in a furnace and remove and drill them quickly. The advantages of hot machining would

[4] "Metals Handbook," American Society for Metals, Cleveland, Ohio, 1948, p. 527.

then be obtained very simply. However, such a method would not work when the machining operation requires a long time.

Another possibility is the use of flame heating while the piece is in the machine tool, as was used in the experiments just discussed. This process would be amenable to control, and long machining operations could be carried on. Its disadvantages are that it is a cumbersome and slow method, and that the work is heated throughout, which is quite inefficient, and is generally undesirable.

If such heating processes were the only ones available, severe limitations would be placed on the utility of the hot-machining method. It would be desirable to have available a continuous-heating method, which confines the heat as much as possible to the surface layer which is to be machined away. This requirement is important partly because of economy, but largely because general heating of the work, and the accompanying thermal expansion, would not permit machining to close tolerances.

Therefore, studies were begun to devise heating methods which would be especially suited for turning operations, and which are cheap, convenient, flexible, and which heat so rapidly that the bulk of the heat would be confined to the surface layer which is to be cut away. The balance of the heat could then be removed, if desirable, by a coolant stream directed at the cut surface.

Theoretical Analysis of Heating Problem. Before beginning an experimental study, it was desirable to conduct a simplified theoretical study in order to estimate the requirements which a practical method of heating would have to meet. It should be emphasized that the results of this theoretical study cannot be interpreted strictly, owing to the simplification made in the analysis as compared to the actual situation. Within this limitation, the results of the analysis have proved valuable as a guide for experimental work.

The assumptions which were made to facilitate the theoretical analysis were quite broad. It was considered that the heat was added to the surface of an infinite flat plate. Conduction to the interior of the metal was the only mechanism for heat transfer which was taken into account in the actual computations made on the basis of this analysis. It was considered that the surface layer was heated at a constant rate of power input for a certain length of time and then cooled for varying time intervals. A typical history of the heating and cooling cycles for steel is given in Fig. 6, for a particular set of conditions.

In this case the desired result was a surface temperature of 980 F, and a temperature of 755 F at a depth of 0.100 in. (the intended depth of machining in this case). The top curve shows that after heating for about $1^1/_2$ sec at a specific power input of

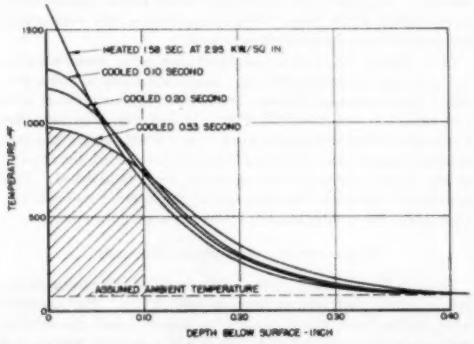

FIG. 6 WORKPIECE TEMPERATURE PROFILES FOR A PARTICULAR HEATING-COOLING CYCLE

approximately 3 kw per sq in., the surface temperature rises to 1640 F and falls rapidly with depth. After heating is stopped, cooling of the surface layer takes place and its temperature becomes more uniform. After a half-second the temperature distribution in the surface layer reaches the desired values.

One-half second after heating has stopped, the heat in the 0.100-in-thick surface layer is represented by the crosshatched area in Fig. 6. About 54 per cent of the total amount of heat put into the work is found to be in this surface layer which will be machined away. The balance either diffuses into the work or is removed by a stream of coolant. If the workpiece were a 4-in. bar of steel, and no attempt were made to remove the heat, its average temperature would be raised 85 F by the heating cycle described. This would cause the bar to expand about 0.002 in., which is not an excessive amount for roughing cuts. For finishing cuts, cooling would be desirable.

The addition of heat can take place slowly, so that the temperature just builds up to the desired value as the material contacts the cutting tool. The heat also can be added as a sudden burst, followed by an interval of cooling to the desired temperature. Fig. 7 shows how conditions are changed as the intensity of the heat source is varied.

From Fig 7, it is seen that the lowest rate of heat input which will achieve the conditions of a 900 F surface-temperature rise, and 675 F rise at a depth of 0.100 in., is 0.6 kw per sq in. It is seen that considerably more total heat input is required at this low rate of heat input than at higher ones. The most suitable rate of power input is shown to be at least 3 kw per sq in. Any value in excess of this would, on the basis of our restricted assumptions, appear to be quite satisfactory.

As the specific power input is increased the maximum surface temperature of the work rises. When the rate reaches 10 kw per sq in., this temperature is approximately the melting point of steel.

This information is presented in more generalized form, in terms of the dimensionless parameters of the system, in the Appendix. This information will enable estimates to be made of the conditions required for other depths of cut, or workpiece materials.

The theoretical analysis was useful in showing the general requirements of a satisfactory heating method. These were rapid heating, with a specific power input in excess of 2–3 kw per sq in., and a brief cooling period. These estimates sufficed to permit the development of a suitable heating means.

Heating Methods. Two heating methods appeared to hold promise for heating at the required rate. These were induction heating and arc heating, both of which were investigated.

Induction heating has the advantages of cleanliness and convenience to a high degree. In this application, however, it has the disadvantages of high equipment cost and poor efficiency. The special requirements of hot machining were such that induction heating did not prove to be suitable for this application. As the analysis has shown, it is necessary that heat be put into an exceedingly small area, at a fairly high power density. With induction heating, a very high total power could be put into the work, but it was quite difficult to obtain an adequate power density. When it was obtained, the area heated, while small by ordinary standards, was still too large. In the usual applications of induction heating, where a fairly sizable area is being heated, the efficiency of the process is good. Here, however, where a very small area must be heated, the conversion of power in the line to heat in the work is poor. Another factor militating against the use of induction heating as a flexible production process is that materials of widely different electrical and magnetic characteristics may have to be machined, and hence heated in the same piece of equipment.

The best heating method which has been found is arc heating,

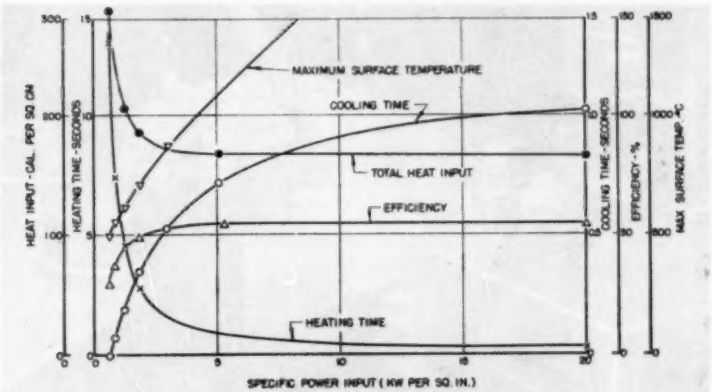

FIG. 7 EFFECT OF POWER INPUT ON HEATING CONDITIONS

with the arc struck between the work and a carbon electrode. Since the surface to which the arc is struck is one surface of the chip that is to be removed, roughening or pitting of that surface is of no moment. The method, as finally developed, has proved to be convenient, reasonably efficient, and capable of supplying high specific power inputs to the work material. Therefore, most of the work has been done with arc heating. It is regarded as the method which undoubtedly will be preferred for the great majority of commercial applications of this machining technique. It is possible to use either an a-c or a d-c arc for this process.

The most troublesome feature of arc heating proved to be the nonuniformity of heating. This nonuniformity was caused by the motion of the work, bringing cold metal under the arc continually, and thus tending to extinguish the arc. Two important improvements had to be made to achieve satisfactory uniformity of heating. The first of these was the use of a high-frequency high-voltage spark. This was superimposed on the arc in the manner common to many welding machines. If the arc tended to go out at any time, the spark would maintain a core of ionized air and the arc would strike again immediately. The second improvement effected in the arc heating apparatus was magnetic stabilization of the arc position. These improvements, together, resulted in an increased and satisfactory uniformity of heating and cured the previous troubles caused by wandering of the arc.

These steps were responsible for a significant improvement in uniformity of heating. This was demonstrated by testing the uniformity of drawing of the surface of bars of hardened steel which had been arc-heated.

The device adopted for a qualitative measurement of uniformity of heating was to heat a fully hardened steel bar and determine uniformity of heating from measurements of the final hardness. For this purpose a bar of SAE 4140 was heat-treated to maximum hardness. The bar surface was then ground off until a region of uniform hardness was reached. A part of the surface of the bar was then arc-heated. The electrode was fastened to the carriage and the feed drive was engaged, so that the arc progressed along the surface of the bar.

Two areas, each $^1/_2$ in. square, were laid out on the surface of the bar. One of these was chosen several inches removed from the heated area so that it would not be affected by the heating. This was the control area. The other area was chosen to lie approximately in the center of the heated portion of the surface and was the test area. Hardness readings were taken at points seperated by $^1/_8$ in. in the control area, for a total of 25 points in this area. In the test area the separation of points was $^1/_{16}$ in., for a total of 81 points.

Sets of hardness readings were made in both areas before heating. After heating, the bar was ground enough to clean it up so that hardness readings could be taken in the heated, or test, area. A removal of 0.0035 in. from the radius was found sufficient. Then, sets of hardness readings were made in both the control and test areas, at depths of 0.0035, 0.010, 0.030, 0.050, and 0.100 in. below the surface. Wet surface-grinding was used to remove the metal from the bar between successive sets of hardness readings. During this grinding, care was taken to have the amount of metal removed by a single pass of the grinding wheel very small, and the supply of coolant quite large. This was done to avoid any appreciable change in hardness of the bar due to overheating caused by grinding.

As an example of the results of this type of test, the hardness readings obtained from bars heated with stabilized and unstabilized arcs will be considered. When an SAE 4140 [illegible] bar, fully hardened, was heated with an unstabilized arc, the readings in the control area, at depth of 0.010 in. below the original surface, covered a range from 59–61 RC. The readings in the test area, at the same depth, covered a range of 45–56 RC. This shows clearly that the heating was quite nonuniform.

When a high-voltage high-frequency spark and magnetic stabilization were used with the arc, the following was found: The hardness readings in the control area covered a range of 54–57 RC. Those in the test area covered a range of 48–51 RC. Both these sets of readings were for a depth of 0.010 in. below the surface. The lower hardness readings in the control area in this latter case are due to the fact that the bar had not hardened up as much as the one used in the unstabilized heating runs, although in both cases it was supposed to have been fully hardened. The improvement in uniformity of heating brought about by these modifications of the arc was, of course, quite apparent in the work. These tests simply put on a semiquantitative basis what was immediately apparent to one working with the apparatus.

Views of the equipment which was developed are shown in Figs. 8 and 9.

The over-all efficiency of the arc-heating process was found to be between 50 and 60 per cent. Approximately one half of the heat supplied will be contained in the chip, and this is a far larger amount than for any other method investigated. This fact, plus the high attainable power densities, makes the arc-heating method pre-eminent.

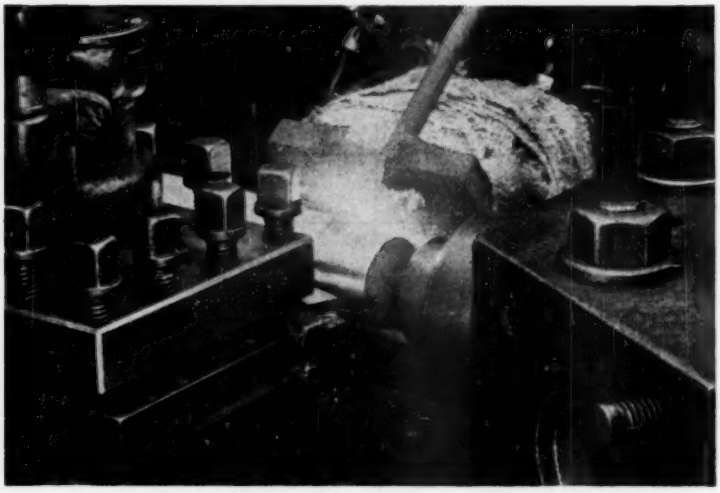

FIG. 8 ARC HEATING FOR HOT-TURNING

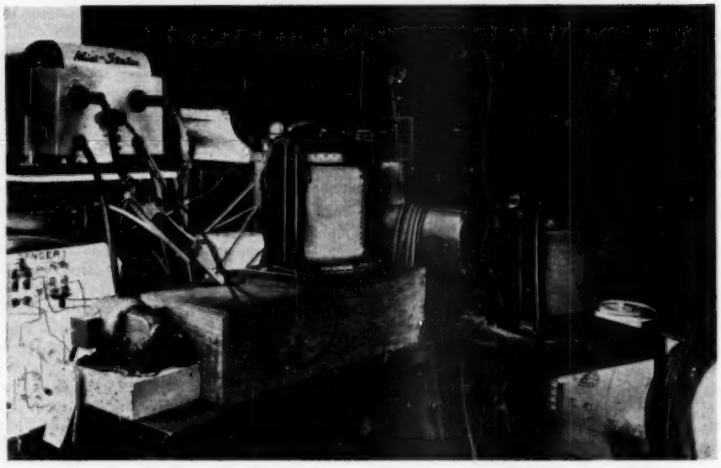

FIG. 9 EXPERIMENTAL ARC-HEATING POWER-SUPPLY SETUP

These heating efficiencies were determined by simple calorimetric measurements. For determining the over-all efficiency of the heating process, the bar was heated for a definite length of time, during which a known amount of power was drawn from the line. Heating was then stopped and the bar quickly removed from the lathe and immersed in a known weight of water. From the temperature rise of the water, the amount of heat which had actually been put into the bar was easily found.

Calculations of the total power requirements for the hot and cold machining of stainless steel were made. These calculations were based upon the efficiency information given previously and experimental work on machining. They showed that, for hot-machining, the sum of the power required for the machine tool and for heating was about the same as the power required for the machine tool alone in cold machining. Thus the total power requirements are about the same in the two cases.

The utility of the hot-machining process must therefore be based on other considerations than power requirements. One such consideration is the amount of work which can be done on a given machine tool. In the case of stainless steel, since cutting force is reduced to one third of its value cold, this would mean that the capacity of the machine tool would be tripled.

For other, less-machinable materials, the decision is weighted heavily in favor of hot machining, since the alternative is more expensive finishing methods, particularly grinding.

Hot Machining With Arc-Heating

Tool Life - Cutting Speed - Power Density Relation. At the completion of the development of an arc-heating method, machining tests were run on a variety of materials, using this heating method. The apparatus used was that shown in Figs. 1 and 8. Workpiece composition is given in Table 2. The tool-material composition is that designated I C in Table 1.

Of general interest is the effect of hot-machining on workpiece structure and hardness. Photomicrographs were made before and after hot-machining studies and little change in structure was evident except for slight grain growth in the NR-74. Hardness data taken before and after hot-machining with arc heating also indicate that tempering may be minimized for hot machining. These hardness data are shown in Table 3.

The same figure also shows that NE 8949, hardened to 42 Rockwell C, may be machined at 200 sfm to yield a tool life of about 20 min. It has been estimated[6] that conventional machining under these conditions would result in a tool life of about 13 min, assuming that general-purpose carbide tools were used. For the low-shock finishing carbides used in the arc-heated machining studies, limited experience with the machining of NE 8949 at room temperature suggests that even shorter tool life is likely under these conditions.

Further indications of the data in Fig. 10 include the essential equivalence of machinability of vitallium and NR-76, two gas-turbine-blading alloys which were included in this study after extreme difficulty had been experienced in fabricating creep specimens of these materials. The other turbine-blading alloy, NR-74, machines with comparable difficulty by conventional methods; however, with NR-74, hot-machining improves cutting even more than for vitallium and NR-76.

TABLE 2 CHEMICAL COMPOSITION OF MACHINING-TEST MATERIALS

Material	Composition, per cent C	Mn	Ni	Cr	Mo	Si	P	S	Co	W	Cb	Fe	Va
Stainless steel (Type 304)	0.08	0.29	9.50	20.0	..	0.33	0.019	0.009	..	..	..	Bal.	..
NE 8949	0.48	1.20	0.50	0.50	0.35	0.27	0.04	0.04	..	..	..	Bal.	..
Clarite	0.72	0.25	..	4.0	..	..	..	..	..	18.0	..	Bal.	1.25
Vitallium	.22–.25	..	..	25.0	5.5–6.0	..	..	..	Bal.	..	..	..	..
NR-76	0.40	..	20.0	20.0	4.0	..	..	..	45.0	4.0	4.0	6.0	..
NR-74	.45	..	20.0	20.0	4.0	..	..	..	20.0	4.0	4.0	Bal.	..

TABLE 3 HARDNESS CHANGE WITH HOT MACHINING, ARC HEATING

Material	Hardness, Initial Rockwell C	Final Rockwell C
NE 8949	42	40
Vitallium	42	39
High-speed tool steel	60	58
NR-76	26	23
NR-74	96[a]	85[a]

[a] Rockwell B.

The results of the tool life - cutting speed tests are shown in Fig. 10. In this figure, the data for stainless steel indicate that at power densities as low as 5 kw per sq in., the tool life at a cutting speed of 600 sfm is 10 min. It is approximately 1 min for conventional machining at this speed. In this case, hot-machining enables an increase in tool life by 10 times, and arc heating is demonstrated to be even better than torch heating.

Still referring to the stainless-steel data, there are some indications that for the arc-heated test, the tool life will be a maximum under these conditions at a cutting speed near 300 sfm. The effect is also apparent in the data for NE 8949, in the same figure. This may be the same effect as has been observed by Field and Stansbury,[5] for the conventional machining of cast iron. More probably, it is an overheating effect resulting from the low speeds of turning. At low speeds, reduced arc-power inputs would be expected to be better.

In Fig. 10 the data for fully hardened high-speed tool steel are of interest in illustrating the marked effect of variations in arc-heating power density on machining performance. Recalling that this material is essentially unmachinable by conventional means at the test-hardness level of 60 Rockwell C, it is seen that a power density of 5 kw per sq in. barely permits turning. However, increasing the power density to 20 kw per sq in. enables turning at 100 sfm with a tool life of over 3 min. While extrapolation is hazardous, it might be possible to achieve a tool life of about 20 min cutting at 50 sfm.

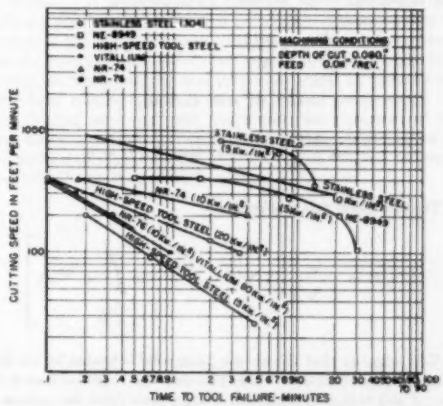

Fig. 10 Effect of Power Density on Tool Life - Cutting Speed Relation

(Data for hot-turning several materials with carbide finishing tools. Depth of cut 0.080 in.; feed 0.011 in. per revolution.)

Conclusions

For specified machining conditions and given work and tool materials, an optimum temperature for machining exists at which tool life will be a maximum. For several materials, machinable at room temperature only with difficulty, this optimum temperature range is well above room temperature and may be in excess of 1200 F.

An arc-heating method has been devised which may be applied in practice to exploit the advantages of machining at elevated temperatures. Through the use of this method, surprising improvement in machinability may be achieved. Many materials

[5] "Effect of Microstructure on Machinability of Cast Irons—I," by M. Field and E. E. Stansbury, Trans. ASME, vol. 69, 1947, p. 665.

[6] "Metal-Cutting Nomograph," by W. W. Gilbert and W. C. Truckenmiller, *Mechanical Engineering*, vol. 65, 1943, p. 895.

which are unmachinable by usual methods have been found to machine with ease at elevated temperatures.

Acknowledgment

The suggestions of hot-machining, and of using an arc-heating method, were made by Dr. H. W. Gillett of Battelle. This and further assistance from Dr. Gillett during the course of the research is gratefully acknowledged. The work was done under the direct supervision of Dr. H. W. Russell and Dr. R. W. Dayton, and their assistance throughout this work has been very helpful. The mathematical analysis was made by Dr. J. C. Bell, mathematician at Battelle.

The research was sponsored by the Warner and Swasey Company. Their encouragement throughout this work and their permission to publish these results are greatly appreciated.

Appendix

Theoretical Analysis of Hot-Machining Heating Problem

Consider a semi-infinite solid, bounded by the plane $x = 0$. It is initially at temperature zero and is then supplied at its surface with a constant flux of heat φ per unit area. The determination of the temperature $U(x, t)$ at depth x after time t involves solution of the boundary value problem

$$\frac{\partial U}{\partial t} = k \frac{\partial^2 U}{\partial x^2}; \quad (x > 0; \quad t > 0)$$

$$U(x, 0) = 0; \quad (x > 0);$$

$$-K \frac{\partial U(0, t)}{\partial x} = \varphi; \quad \lim_{x \to \infty} U(x, t) = 0$$

The solution of this problem[7] is

$$U(x, t) = \frac{\varphi}{K \sqrt{\pi}} \left[2 \sqrt{kt}\, e^{-\frac{x^2}{4kt}} - 2x \int_{\frac{x}{2\sqrt{kt}}}^{\infty} e^{-\lambda^2} d\lambda \right]$$

Now, suppose that this semi-infinite solid is heated by the flux φ for a period of time t_1. After this time the source of heat is removed and radiation is allowed to take place from the surface of the solid into a medium at temperature zero. If t denotes the time elapsed after radiation began (i.e., cooling time), the temperature $T(x, t)$, at depth x, after time t, is the solution of the problem

$$\frac{\partial T}{\partial t} = k \frac{\partial^2 T}{\partial x^2}; \quad (x > 0, t > 0)$$

$$T(x, 0) = U(x, t_1); \quad (x > 0)$$

$$\frac{\partial T(0, t)}{\partial x} = hT(0, t); \quad \lim_{x \to 0} T(x, t) = 0; \quad (t > 0)$$

where h is the surface-transfer coefficient. The solution to this problem[8] is

$$T(x, t) = \int_0^{\infty} \left[e^{-\frac{(x-x')^2}{4kt}} + e^{-\frac{(x+x')^2}{4kt}} - 2h \int_0^{\infty} e^{-h\xi - \frac{(x+x'+\xi)^2}{4kt}} d\xi \right] \frac{U(x', t_1) dx'}{2\sqrt{\pi kt}}$$

Actually, calculations were made only for $h = 0$. This corresponds to the practical circumstance in which heat losses across the surface can be ignored. In this case

$$T(x, t) = \frac{\varphi}{K\pi} \sqrt{\frac{t_1}{t}} \int_0^{\infty} \left[e^{-\frac{(x-x')^2}{4kt}} + e^{-\frac{(x+x')^2}{4kt}} \right] \times \left[e^{-\frac{x'^2}{4kt_1}} - \frac{x'}{\sqrt{kt_1}} \int_{\frac{x'}{2\sqrt{kt_1}}}^{\infty} e^{-\lambda^2} d\lambda \right] dx'$$

This function can be expressed in terms of tabulated functions by a process involving principally integration by parts and appropriate grouping of terms. The result is

$$T(x, t) = \frac{2\varphi \sqrt{kt_1}}{K \sqrt{\pi}} \left\{ \left[\frac{1}{\sqrt{\frac{\rho}{1+\rho}}} e^{-\frac{\rho y^2}{1+\rho}} - 2y \int_{y\sqrt{\frac{\rho}{1+\rho}}}^{\infty} e^{-\lambda^2} d\lambda \right] - \left[\frac{1}{\sqrt{\rho}} e^{-\rho y^2} - 2y \int_{y\sqrt{\rho}}^{\infty} e^{-\lambda^2} d\lambda \right] \right\}$$

where

- φ = heat flux per unit area; i.e., power per unit area
- k = thermal diffusivity
- t_1 = time of heating
- t = time of cooling
- K = thermal conductivity
- $\rho = t_1/t$
- $y = x/(2\sqrt{kt_1})$
- x = depth below surface of solid
- h = surface heat-transfer coefficient

The foregoing is an abbreviated account of the theoretical work on the heating problem. All the essential equations are given, and from them the data for a particular metal or depth of cut may be obtained. In general, curves of the same type as those presented in Figs. 6 and 7 will be needed for any survey of this type.

Discussion

E. J. Krabacher.[9] Machining at elevated temperatures seems to be a logical solution to the problem of machining high-

[7] "Modern Operational Mathematics in Engineering," by R. V. Churchill, McGraw-Hill Book Company, Inc., New York, N. Y., 1944, pp. 107–108.

[8] "Introduction to the Mathematical Theory of the Conduction of Heat in Solids," by H. S. Carslaw, completely revised by The Macmillan Company, London, England, 1921, pp. 176–177.

"Conduction of Heat in Solids," by H. S. Carslaw and J. C. Jaeger, Clarendon Press, Oxford, England; Oxford University Press, New York, N. Y., 1947.

[9] Research Engineer, Cincinnati Milling Machine Company, Cincinnati, Ohio.

temperature high-strength alloys which heretofore have been found practically unmachinable at room temperature. The authors are to be congratulated for their early realization of this possibility, and for the excellent work done in preparation of their paper.

Tool-life studies made by the authors show conclusively that for certain materials the machinability may be improved greatly by machining at high temperatures. It has been found from investigations of hot machining, which are now and have been going on for some time in this writer's laboratory, that there is, as the authors state in their paper, an optimum temperature for which the tool life will be a maximum. A striking example of this is in the case of an ordinary material such as 3145 steel (as received). This material gave a tool life, when machined at room temperature, which was 5 times as great as that obtained when machining at 1500 F. When this same material was heat-treated to give it a Brinell hardness of 350, the opposite was true. In this case the tool life at 1500 F was 5 times that obtained at room temperature, while the hardness of the material was affected only very slightly. The question now arises, what are the factors which control this optimum temperature. Tool dynamometer tests are being conducted to determine the effect on basic quantities due to machining at elevated temperatures. Table 4 of this discussion shows a comparison of results obtained when machining a typical steel at room temperature and at an elevated temperature. It can be seen that the greatest change occurred in the value of shear strength which was greatly reduced at the elevated temperature, lowering the tool forces, and thus the abrasive action between the tool and work. Investigations such as this should lead to a better understanding of the underlying principles involved.

TABLE 4 HOT MACHINING: TYPICAL EFFECT ON BASIC QUANTITIES

Cutting speed, fpm	Work temp, deg F	Cutting force, F_c, lb	Thrust force, F_t, lb	Coefficient of friction, μ	Mean shear strength, S_s, psi	Machining constant, C, deg
92	75	298	136	0.68	121,000[a]	73[a]
	1550	110	50	0.68	38,000	62
605	75	331	177	0.78	104,000	62
	1550	145	78	0.78	55,000	76

[a] Type 3 chip, values approximate only.

It has been established that materials which heretofore have been considered unmachinable can be machined freely at elevated temperatures. It now remains for us to investigate further the underlying factors involved so that a more complete understanding in this field may be acquired.

Authors' Closure

Mr. Krabacher's comments are appreciated and we are pleased to know that hot-machining studies are continuing in his laboratory. The data he reports showing the effects of workpiece heating on tool forces are interesting and offer further evidence of the advantages of hot machining. Possibly the difference in behavior between as-received and partially hardened steel, noted by Mr. Krabacher, may be explained in part by characteristics of the tool materials. Apparently in the tool-life tests described, the tool material could be used at room temperature. However, the preliminary data reported in this paper suggest that tool materials which retain much of their strength at high temperatures are needed to fully exploit the advantages of hot machining. Such tools cannot ordinarily be used at room temperature since they are extremely brittle.

The data for machining SAE-AISI 3145 steel at 1500 F are also of interest. It is indicated that only a very slight change in hardness was noted after the test procedure. Possibly this indicates that Mr. Krabacher used local heating at fairly high-power density, to confine the heating to the work surface. Under these conditions, workpiece physical properties might be retained despite brief surface heating above the critical temperature. If such heating were not used, the initial heat-treatment of the steel would be expected to have little effect on its properties at the machining temperature. This is so since the test temperature exceeds the critical temperature for this steel.

The Effect of the Cutting Fluid Upon Chip-Tool Interface Temperature

By M. C. SHAW,[1] J. D. PIGOTT,[2] and L. P. RICHARDSON[3]

An analysis is presented of the short-circuiting effect of a cutting fluid in conjunction with chip-tool interface temperature measurements by the tool-work thermocouple technique. An experimental arrangement based upon the results of this analysis and capable of giving reliable cutting temperatures in the presence of fluids is described. The temperature-reducing characteristics of a representative group of water-base cutting fluids are studied, and these experiments reveal that the fluids become less effective in reducing the cutting temperature as the volume of metal removed per unit time is increased. The water-base fluids considered are found to reduce the tool-tip temperature by a cooling action to a greater extent than by a reduction of the friction force on the face of the tool.

Introduction

WHEN metal is cut by a single-point tool, essentially all of the work expended is converted into heat. The heat thus developed gives rise to a complex temperature distribution at the tool point, the temperature at the interface between the chip and the tool having the highest and most significant value. The temperature pertaining at this interface is related closely to tool life, surface finish, the residual stress produced in the finished surface, and the power required, and hence is a significant variable to study experimentally when investigating the performance of a cutting tool.

Fig. 1 is a photomicrograph of the region of the workpiece in the vicinity of the tool point and was obtained by suddenly stopping the workpiece while a cut was being made using water as the cutting fluid. It has been definitely established that metal is cut by a plastic shearing action, and plane AB clearly separates the zone in which plastic deformation has occurred from that in which the stress pattern is essentially elastic. The tool and work were in contact from point A to a point in the vicinity of C while the cut was in process. It is the mean temperature at the interface extending from A to C with which this paper is concerned.

While the surface AC appears essentially smooth, greater magnification reveals that actually the chip and tool make contact at a finite number of distinct points rather than at all points of the surface. The extent of the plastic deformation which has taken place is evident by comparing the depth of cut (vertical distance between points A and B) with the chip thickness. The ratio of these two distances for the two-dimensional case considered here is what is sometimes called the "chip-length ratio" or cutting ratio. If there were no plastic deformation, the depth of cut and the thickness of the chip would be the same and hence the chip-length ratio would have a value of 1. From the standpoint of cutting efficiency, it is desirable that the chip-length ratio be as large as possible.

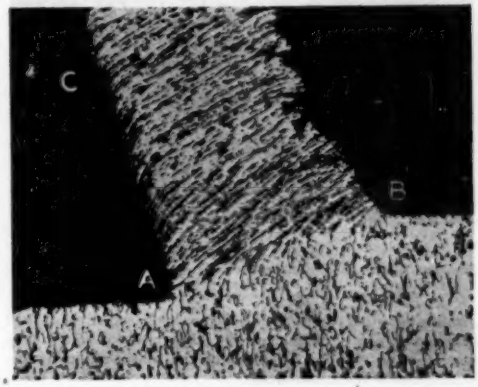

Fig. 1 Photomicrograph of Partially Formed Chip at Point of Cutting Tool

(Material, annealed SAE 1015 steel; cutting speed, 24 sfpm; cutting fluid water plus 0.1 per cent sodium nitrite; ×100.)

It is believed that the friction force which acts along plane AC and tends to retard the motion of the chip is due to the periodic welding and weld rupture which occurs at the tool-chip interface. When an effective cutting fluid is used, the welds that are thus momentarily established fail at the points at which the surfaces went together. The chip thus passes continuously up the face of the tool as shown in Fig. 1, and the photomicrograph is independent of time. Under less favorable cutting conditions the strength of the weld may exceed the plastic shear strength of the chip material and an appendage frequently referred to as a "built-up edge" may develop along the tool face. A representative built-up edge is shown in Fig. 2. Such a picture is not independent of time, the built-up edge periodically changing its size and shape. The built-up edge is undesirable from the standpoint of tool life, surface finish, dimensional accuracy, and the power required, but unfortunately is present in varying degrees in most of our metal-cutting operations.

The heat developed at the point of a cutting tool has two principal sources, i.e., (*a*) the work of plastic deformation which is developed primarily along plane AB, and (*b*) the frictional work that is generated along plane AC. These sources of heat make the resulting average temperature along the interface AC much higher than that at B or the mean bulk temperature of chip, tool, or workpiece. While a wide variety of methods have been used to estimate the chip-tool interface temperature, including complicated radiation pyrometers, embedded thermocouples, tem-

[1] Associate Professor, Department of Mechanical Engineering, Massachusetts Institute of Technology, Cambridge, Mass. Mem. ASME.

[2] Research Engineer, The Draper Corporation, Hopedale, Mass. Jun. ASME.

[3] Research Engineer, Shell Development Company, Emeryville, Calif. Jun. ASME.

Contributed by the Research Committees on Metal Cutting Data and Bibliography, and Cutting Fluids, and the Production Engineering Division and presented at the Semi-Annual Meeting, St. Louis, Mo., June 19–23, 1950, of The American Society of Mechanical Engineers.

Note: Statements and opinions advanced in papers are to be understood as individual expressions of their authors and not those of the Society. Manuscript received at ASME Headquarters, August 1, 1949. Paper No. 50—SA-19.

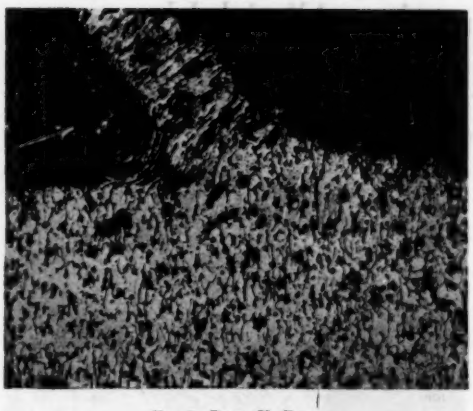

FIG. 2 BUILT-UP EDGE
(Material, annealed SAE 1015 steel; cutting speed, 24 sfpm; cutting fluid, dry tool; ×100.)

perature-sensitive paints, the development of temper colors, and indirect calorimetric techniques, all of these methods suffer from a slow speed of response, adverse geometric considerations, or the indirectness of the measurement.

The most successful approach to this problem has been the tool-work thermocouple, apparently first used by Shore (1)[4] in 1924, and since developed by many other investigators (2 to 9) to study not only cutting problems but also abstract studies of friction phenomena. In this method the tool-work contact area serves as the hot junction in a thermoelectric circuit and the emf generated is proportional to its temperature. Actually the maximum tool-tip temperature is not measured, but rather the average temperature over the area of contact. Since the tool face on a microscopic scale is not a plane surface but rather a series of peaks and valleys, the hot junction is essentially a series of small thermocouples in parallel, all of which contribute to the observed emf Holm (10) analytically estimates the maximum temperature at the points of contact to be approximately 1.27 times the observed mean surface temperature. Another point of interest in connection with chip-tool interface-temperature measurements is that a steady-state condition is not established when a built-up edge is present. The cutting forces, power consumed, chip thickness, and even the depth of cut vary appreciably with time as will the temperature at the tool tip. The values of tool-tip temperature that are given in this paper when a built-up edge is present are thus necessarily average values.

According to thermoelectric theory, if two dissimilar metals are joined to form a closed loop and the two resulting junctions are maintained at temperatures T_1 and T_2, respectively, an emf will be generated which is proportional to the quantity $T_2 - T_1$. Some important features of thermoelectric circuits include the following:

1 If a junction of two metals is at a uniform temperature, the emf generated is not affected by the introduction of a third metal (solder, weld metal, etc.).

2 The emf generated is independent of temperature gradients along the wire constituting the circuit, but depends upon the difference between the hot and cold junctions $T_2 - T_1$.

3 The emf generated is independent of the size or resistance of the conductors.

Very little work is to be found in the literature concerning the use of the chip-tool thermocouple technique to measure machining temperatures in the presence of a cutting fluid. In his original paper in 1925, Herbert (2) described certain experiments in which fluids were employed but mentions difficulty due to a spurious galvanic action. Herbert's experience apparently has discouraged others from investigating the influence of cutting fluids upon the chip-tool interface temperature.

There are two principal functions of a fluid in a metal-cutting operation. An effective fluid should reduce the heat that is generated in the cutting operation; (*a*) directly, by reducing the friction along plane AC in Fig. 1, and (*b*) indirectly, by reducing the flow stress along plane AB. At the same time, it should also carry away an important part of the heat that is generated. Each of these functions gives rise to a reduction of tool-tip temperature. The reduction in friction along AC depends primarily upon the formation of a solid lubricant by a chemical reaction involving the cutting fluid and the chip material. Such a rate of chemical reaction is influenced by the pressure and temperature obtaining, the state of stress in the chip surface, and the concentration of the fluid. In order that a cutting fluid be effective in reducing friction, it is necessary that the reaction rate be sufficient to develop the required quantity of solid lubricant in the time available at a given cutting speed. Furthermore, the cutting fluid must find its way to the tool point if it is to lower the temperature at the tool face. It is thus evident that the ability of a cutting fluid to lower the chip-tool interface temperature at different cutting speeds is a complex problem which must be investigated experimentally. The chip-tool thermocouple technique offers an interesting and useful approach to this problem.

APPARATUS

The test arrangement employed in this investigation is shown in Fig. 3. All experiments were performed upon a lathe providing a range of spindle speeds from 21 to 900 rpm, and a range of feeds from 0.0023 to 0.0104 inches per revolution (ipr). The workpieces were obtained from the same bar of SAE 1015 plug-pierced seamless tubing. This tubing had an outside diameter of 2 in. and a wall thickness of $^3/_{16}$ in. The material was cut in the annealed condition, the microstructure being as shown in Fig. 4. The hardness of this material was Bhn 105.

The tools employed were all obtained from the same $^3/_8$-in. square bar of 18-4-1 high-speed steel, and the shape of the tools used is shown in Fig. 5. This particular tool shape was chosen because of its simplicity, thus eliminating the distracting complications introduced by the nose radius, side-rake angle, etc., that are found on conventional lathe tools. In order to use the two-dimensional tool shown in Fig. 5, it was necessary to cut the workpiece from the end, which accounts for the choice of seamless tubing for the work material. While all of the data presented in this paper are for a cutting arrangement of such simple geometry and hence are not specifically applicable to any particular complex commercial lathe tool, the general picture presented should be the same for all single-point cutting tools operating in the range of speed and depth of cut of the tests discussed herein.

The thermoelectric circuit employed is shown in Fig. 3. One cold junction is at A, where a copper lead joins the tool, and the other is at B. These points are far enough removed from the hot junction H, so that they remain at constant temperature throughout a test. The emf generated is thus a function of the temperature at H only and was measured by means of the manually operated potentiometer P.

The particular materials constituting the tool and workpiece

[4] Numbers in parentheses refer to the Bibliography at the end of the paper.

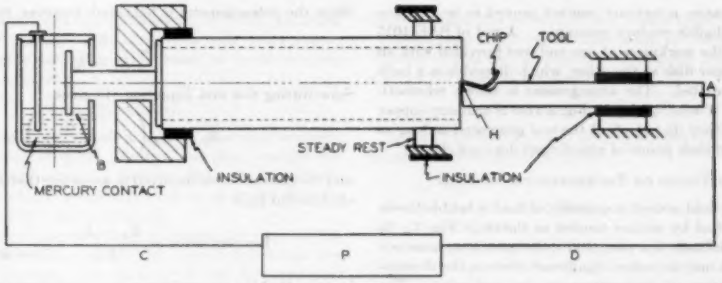

FIG. 3 TEST APPARATUS

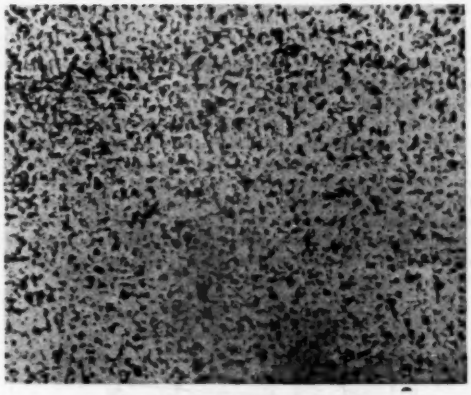

FIG. 4 PHOTOMICROGRAPH OF WORK MATERIAL
(Etch, 1 per cent nital; ×100.)

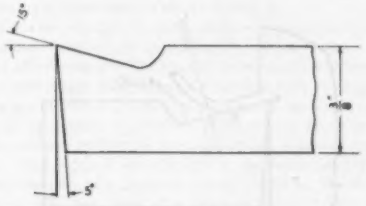

FIG. 5 TOOL DETAIL

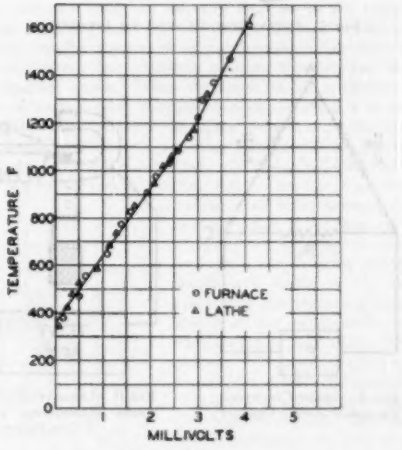

FIG. 6 CALIBRATION CURVE

were calibrated in two ways: (a) By clamping a bar of tool steel against the work material so as to give a limited area of contact and heating this junction in a nonoxidizing atmosphere furnace. A standard chromel-alumel couple was embedded in the workpiece near the juncture for the purpose of calibration. The controlled atmosphere was important inasmuch as the potentiometer used was a low-internal-resistance instrument which had poor response if the resistance of the circuit increased appreciably as by an increase in contact resistance. As explained later, such a low-resistance instrument is advantageous when used in conjunction with cutting-fluid studies. (b) By employing a cutting tool in contact with a partially severed chip. The lathe was suddenly stopped when a cut was being taken, and the chip and tool point allowed to remain in contact under pressure. A chromel-alumel thermocouple was mounted in the workpiece within $^1/_{16}$ in. of the chip, and the entire unit was thermally shielded with dry asbestos fiber held in place by asbestos string. When heat was applied to the end of the workpiece the chip-tool interface was heated by conduction, and the tool-interface couple was calibrated. The calibration data obtained by both of these methods are presented in Fig. 6 and it is evident that each of the methods yields essentially the same result. This experiment shows conclusively that the state of stress and the degree of cold work of the specimen cut have a negligible effect upon its thermoelectric characteristics, a fact which has caused some concern among workers in the past.

In preliminary tests it was found necessary to isolate the entire thermoelectric circuit from the machine. In the past many tests have been made in which only the tool or workpiece was insulated. In the present investigation it was found necessary to avoid such parallel circuits through the machine if consistent data were to be obtained. The desirability of a low-resistance circuit in conjunction with tests involving cutting fluids has already been mentioned. In this connection the method of attaching a lead wire to the moving workpiece with a minimum of contact resistance was given special attention. Previous investigators have used some sort of brush with its attendant contact resistance. In

the present apparatus, a mercury contact proved to be effective and provided negligible contact resistance. A rod of SAE 1015 steel attached to the workpiece at one end was provided with an amalgamated-copper disk at the other, which dipped into a bath of mercury as it rotated. The arrangement is shown schematically in Fig. 3. Wires *C* and *D* in Fig. 3 were of ordinary copper wire inasmuch as they do not affect the emf generated as long as the temperature of their points of attachment does not change.

Effect of Fluids on Thermoelectric Circuit

When a cutting fluid is used, a quantity of fluid is held between the chip and the tool by surface tension as shown in Fig. 7. If the fluid offers relatively low electrical resistance, it represents a short circuit which may introduce significant errors in the thermoelectric determination of temperature at the tool point. The electrical circuit shown in Fig. 8 represents the situation in which

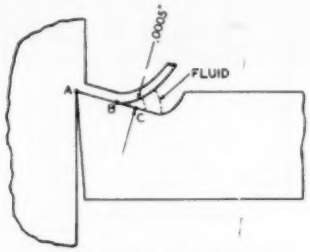

Fig. 7 Fluid Film at Chip-Tool Interface

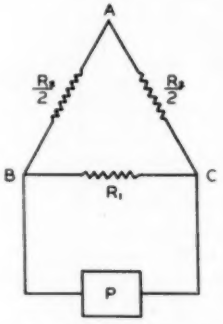

Fig. 8 Short-Circuited Thermoelectric Circuit

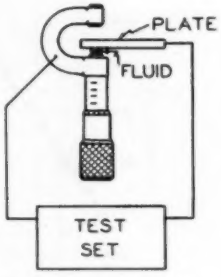

Fig. 9 Apparatus for Measuring Resistance of Thin Fluid Films

a conducting layer of fluid is present. Here point *A* represents the region of metallic contact between chip and tool, R_1 the resistance of the conducting layer of fluid, and R_2 the resistance of the thermoelectric circuit when no fluid is present. If no fluid is used, conductor *BC* is not present, and the potentiometer will measure the thermoelectric emf that is generated at point *A*. However, when resistance R_1 is introduced, a parasitic current i will flow in the loop *ABC* even when the potentiometer is balanced to give no current flow through *BPC*. In this case, the emf measured by the potentiometer (E_P) is not that generated thermoelectrically at *A* (E_A) but is rather

$$E_P = E_A - i R_2 \quad [1]$$

Since the potentiometer is balanced, however, the current is

$$i = \frac{E_A}{R_1 + R_2} \quad [2]$$

Substituting this into Equation [1] gives

$$E_P = E_A \left(1 - \frac{R_2}{R_1 + R_2}\right) \quad [3]$$

and the per cent error involved in assuming that E_P is the thermoelectric emf E_A is

$$\text{Per cent error} = \frac{E_A - E_P}{E_A} = \frac{1}{1 + R_1/R_2} \quad [4]$$

In order that the per cent error due to the short-circuiting effect of a fluid be less than 1 per cent it is then necessary that

$$\frac{R_1}{R_2} > 99$$

It is thus evident that it is advantageous to have the resistance of the entire thermoelectric circuit (R_2) as small as possible when conducting fluids are employed.

In order to investigate the resistance to current flow that is offered by representative water-base cutting fluids, the apparatus shown in Fig. 9 was used. The frame of the micrometer was fixed to a wooden table as was the plane steel surface *A*. The plate and micrometer were then electrically connected to a resistance-measuring test set as shown, so that the resistance of a thin film of fluid held between the micrometer anvil and the plate by capillary action could be determined. The results of tests of this sort with the following fluids are given in Fig. 10:

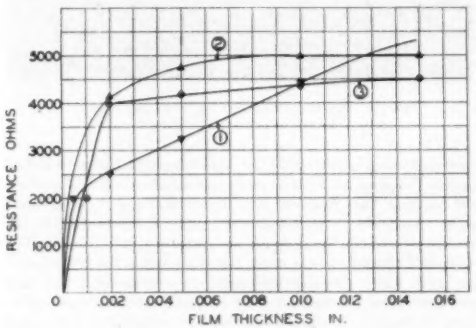

Fig. 10 Fluid Resistance—Film-Thickness Curves

Fluid 1, water plus 0.1 per cent sodium nitrite
Fluid 2, a commercial cutting emulsion
Fluid 3, a commercial water-base cutting solution

From these data it is evident that the resistance of a water-base fluid will be of the order of 1000 ohms or more for a film thickness greater than 0.0005 in. Since the resistance of the thermoelectric circuit used in all tests was but 2.2 ohms, the presence of a short-circuiting film of 0.0005 in. or greater will give rise to an error of 0.22 per cent or less in the determination of the true thermoelectric emf.

Conditions at the point of a cutting tool with fluid present are shown to a large scale in Fig. 7. In a dry test the tool-work thermocouple actually gives the average temperature over the area *AB*. Since the short-circuiting effect of the fluid will be negli-

gible beyond point C, and the distance BC is small compared with AB, the emf readings obtained in tests with fluids present should give a reliable indication of the mean temperature along the chip-tool interface AB.

Test Procedure

In order to assure that all tools used were of similar keenness, an arbitrary reference speed of 160 sfpm was used, and the emf for each new tool was noted. A given tool was also periodically checked at the reference speed and, when it no longer gave the standard emf, a new tool was substituted.

In all tests a pair of pliers was used to remove the chips as they left the work to prevent a possible short circuit due to the chip curling back on the tool. The duration of each test was sufficient to insure that the equilibrium temperature was reached.

In the tests involving cutting fluids, the stream of fluid was directed toward the gap between the chip and the tool and a constant rate of flow was maintained.

Results and Discussion

Series of tests were made at several speeds and depths of cut using the following cutting fluids:

1 Dry tool.
2 Commercial emulsifiable water-base cutting fluid in concentration of 40 to 1.
3 Commercial soluble water-base cutting fluid in concentration of 40 to 1.
4 Water plus 0.1 per cent sodium nitrite (rust inhibitor).
5 Water plus 0.1 per cent sodium nitrite plus wetting agent.

The results of these tests are shown in Fig. 11.

The fluids are seen to be most effective in lowering the chip-tool interface temperature at the smaller depth of cut. In all cases the effectiveness of the fluid in lowering the tool temperature on a percentage basis is seen to decrease with cutting speed. At the larger depths of cut and cutting speeds, the fluids are seen to become completely ineffective. The cutting speed at which the fluid becomes ineffective decreases as the depth of cut is increased. At a depth of cut of 0.0023 in. the fluid was effective at all speeds tested; at a depth of cut of 0.0052 in. the fluid was effective to 400 sfpm, and, at a depth of cut of 0.0104 in., the fluid became ineffective at 200 sfpm.

These observations might be explained in several ways: (*a*) The fluid may not reach the chip-tool interface at the higher speeds and depths of cut. In such a case the fluid would be carried away by the outward flowing chip more rapidly than it was drawn between the interstices between the chip and the tool by capillary forces. When the depth of cut is increased the force on the tool point likewise increases, resulting in an increase of the real area of contact along the tool face and a decrease in the intersticial volume, thus making it more difficult for the fluid to find its way to the tool point. (*b*) If the fluid does reach the interface the rate of the reaction may be too low to provide sufficient low shear-strength reaction product in the short time available at increased cutting speeds. (*c*) At higher cutting speeds and depths of cut, the rate of heat generation is greater, and there may not be sufficient time for this excess heat to flow out of the chip and the tool to be picked up by the cutting fluid.

It is evident in Fig. 11(*b*) that the chip-tool interface temperature is essentially the same at a cutting speed of 400 sfpm for the several fluids tested. In Fig. 12 photomicrographs are shown of chip-tool interfaces for a cutting speed of 400 sfpm, and a depth of cut of 0.0052 in., both (*a*) with a dry tool, and (*b*) using water as the cutting fluid. The similarity of these photomicrographs and the presence of the built-up edge in each case attest the ineffectiveness of the fluid under these conditions.

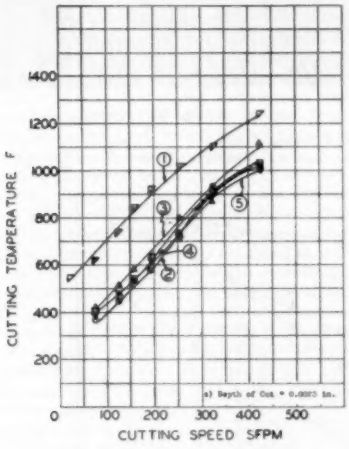

(*a*) Depth of cut = 0.0023 in.

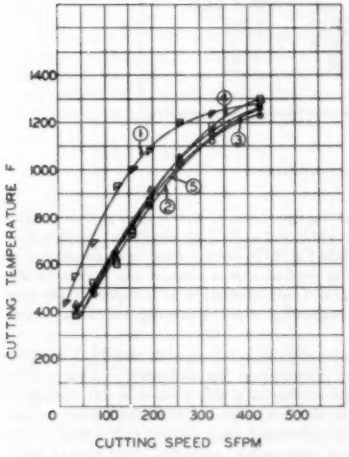

(*b*) Depth of cut = 0.0052 in.

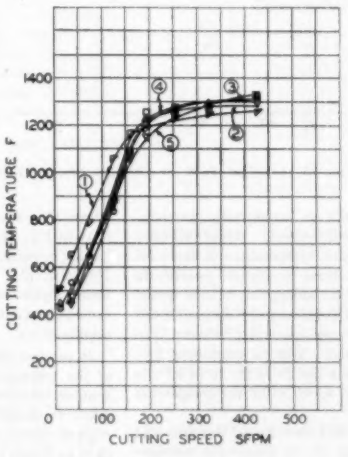

(*c*) Depth of cut = 0.0104 in.

Fig. 11 Cutting Speed–Temperature Curves

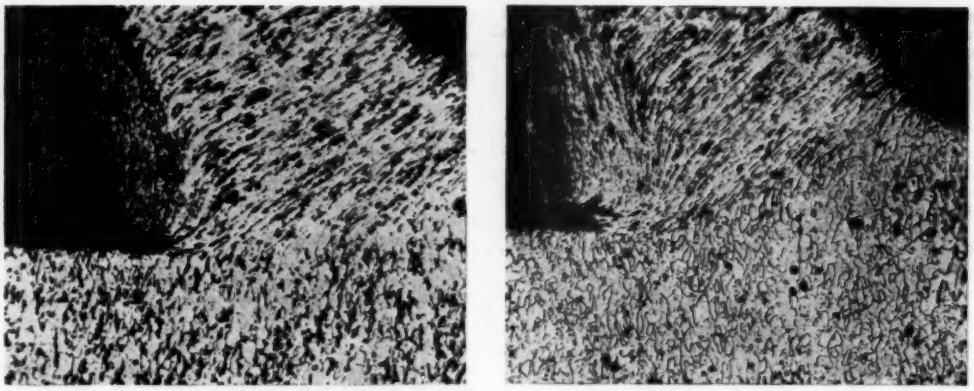

(*a*) Dry tool (*b*) Cutting fluid—water

FIG. 12 PHOTOMICROGRAPHS OF PARTIALLY FORMED CHIPS
(Material, annealed SAE 1015 steel; cutting speed, 400 sfpm; depth of cut, 0.0052 in.; ×100.)

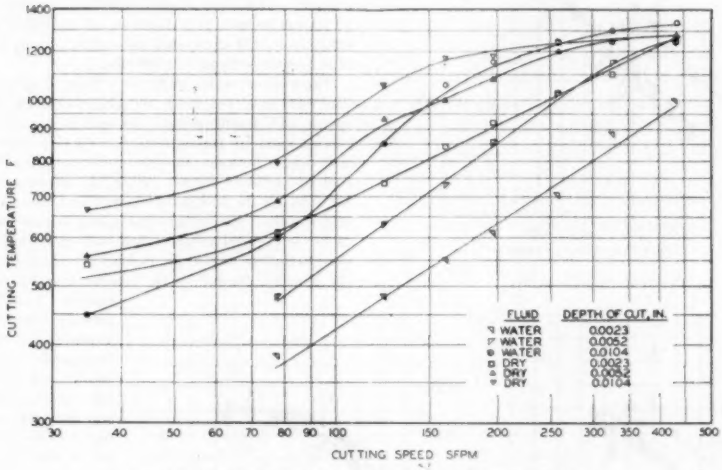

FIG. 13 LOG-LOG PLOT OF CUTTING SPEED–TEMPERATURE DATA

In Fig. 11(*c*) all curves approach an asymptotic temperature of about 1350 F as the speed is increased. While this temperature is close to the transformation temperature of the steel cut (1330 F), and a transformation from ferrite and pearlite to ferrite and austenite with its attendant absorption of heat would account for the asymptotic value, it is not certain that sufficient time is available during the short duration contact between chip and tool for a transformation to occur. Due to insufficient tool life, tests could not be made at higher speeds to try to observe a further increase in temperature with speed after the completion of the transformation.

Previous workers (4, 7, 8) in this field have found the chip-tool interface temperature for lathe tools (T) to follow the relationship

$$T = C V^n \quad \ldots\ldots [5]$$

where V is the cutting speed and C and n are constants. The data in Fig. 11 for water and a dry tool are shown replotted on log-log co-ordinates in Fig. 13 in order to test the applicability of Equation [5]. It is evident that a straight line results for the lower depths of cut but this correlation with Equation [5] does not exist over the entire range of speeds investigated for the higher depths of cut.

In practice the color of the chip is frequently noted as a measure of the temperature obtaining at the tool point. Thus a blue temper color on the surface of a chip formed in dry cutting is taken to mean that the tool point is hotter than when an uncolored silvery chip is obtained when cutting with a fluid. The data in Table 1 show that such a conclusion is not always justified and that temper colors must be interpreted carefully.

In Table 1 it is seen that several different temper colors can be

TABLE 1 TEMPER-COLOR DATA

Fluid	Cutting speed, sfpm	Chip color	Temper color temp, deg F	Chip-tool interface temp deg F
Dry.....	332	Dark straw	490	1250
Dry.....	436	Deep blue	520	1250
Water.....	332	Uncolored	Under 400	1250
Water.....	436	Uncolored	Under 400	1250

obtained with the same chip-tool interface temperature. Temper colors are produced by interference colors developed when light passes through a thin oxide layer on the surface of the metal, the thicker the layer the nearer the interference color will be to the blue end of the spectrum. Since the oxide layer is produced as the result of a time, temperature, and concentration sensitive reaction, the temper color is really a measure of the temperature at the "surface" of the chip, how long the chip remains at this temperature (which is influenced by cutting speed), and the oxygen concentration at the surface. Thus, as shown by the foregoing data, different temper colors may be obtained at different cutting speeds, even though the chip-tool interface temperature is the same. The absence of any temper color when a fluid is used simply means that oxygen was excluded from the chip surface by the fluid during the time it was hot and not necessarily that the chip-tool interface temperature was low.

All of the fluids tested had approximately the same cooling characteristics. Since these fluids are not the same chemically, this would indicate that the reduction in chip-tool temperature was due to the cooling effect of the water-base lubricants rather than to a reduction in the coefficient of friction at the tool face. In order to check this point the friction characteristics of the fluids tested were obtained using the apparatus of Burwell and Strang (11), which employs crossed steel cylinders one of which is rotated while the other is held elastically to enable the friction force to be measured. The specimens employed were of SAE 1117 case carbonized steel hardened to Rockwell 15N and superfinished to a roughness of 1 to 2 microinches rms. The resulting friction curves are given in Fig. 14. A curve for dry cylinders could not be obtained due to the resulting instability of the measuring system under such conditions. The difference in the friction characteristics of water and the other fluids tested and the lack of significant differences in the temperature data for the several fluids tested indicate that the chief function of the fluids here considered is one of cooling rather than a reduction of friction.

Further evidence of the fact that the chief function of the cutting fluid in the speed range considered here (generally above 100 sfpm) is due to cooling action rather than to a reduction in friction is offered by tests using carbon tetrachloride and benzene as the

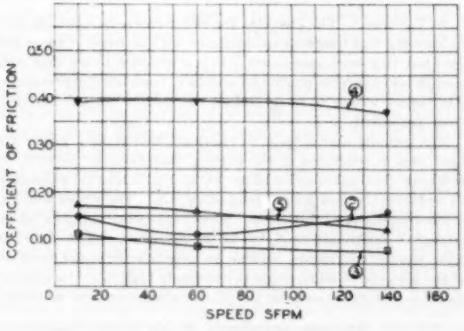

FIG. 14 FRICTION DATA

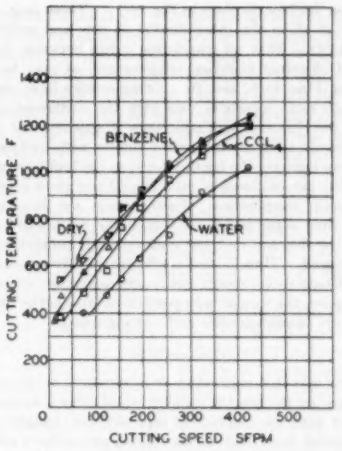

FIG. 15 CUTTING SPEED—TEMPERATURE CURVES
(Depth of cut = 0.0023 in.)

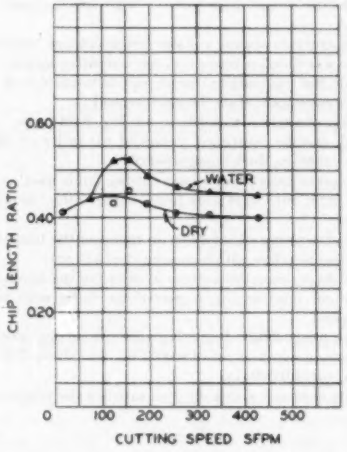

FIG. 16 CHIP-LENGTH RATIO–CUTTING SPEED CURVES

cutting fluids. Temperature data for these two materials are given in Fig. 15, together with the curves for water and a dry tool for reference. It may be seen that carbon tetrachloride, which is known to be very effective in reducing the friction force on the face of a tool when machining steel at slow speed, is little more effective than the generally poor fluid benzene in reducing the chip-tool interface temperature. The further observation that both of these materials are inferior to water (which has the greatest specific heat of all liquids) in lowering the tool temperature, further substantiates the observation that the major role of the cutting fluid in reducing temperature, in this speed range, is one of cooling.

The previously mentioned chip-length ratio is shown plotted against cutting speed in Fig. 16, for a dry tool, and with water as

the cutting fluid for the tests in Fig. 11(*b*). These data are representative of all of the other depths of cuts and cutting fluids. It is significant that no correlation exists between chip-length ratio and chip-tool interface temperature, as may be seen by comparing Figs. 11(*b*) and 16. Other studies have shown that chip-length ratio correlates well with the coefficient of friction between the chip and tool and, since it appears that the fluids in the present tests are concerned mainly with cooling the tool rather than lowering the friction force on the tool face, it appears logical that the chip-length ratio should not show a correlation with tool-tip temperature. Furthermore, the heat generated per unit time depends not only upon the coefficient of friction between the chip and tool, but is also directly proportional to the cutting speed. Thus if the coefficient of friction (and hence the chip-length ratio) should remain approximately constant with cutting speed, the rate of heat generation (and hence the tool-tip temperature) would increase with cutting speed.

Conclusions

1 The fact that calibration data obtained in the usual way in a furnace are the same as those obtained using a stationary chip in contact with the tool reveals that physical changes which the work material undergoes during cutting are without effect upon its thermoelectric properties.

2 An analysis of the short-circuiting effect of a cutting fluid at the tool point shows that this effect is negligible if a low-resistance thermoelectric circuit and fluids of high specific resistance are employed.

3 In order to obtain a stable low-resistance thermoelectric circuit, it was found necessary to use a positive mercury contact instead of the conventional brush and to insulate both tool and workpiece electrically from the machine tool.

4 Representative water-base cutting fluids were found to have high specific resistance, values of the order of 1000 ohms for a film 0.0005 in. thick being observed.

5 Representative water-base cutting fluids used to machine annealed SAE 1015 steel were found to have the following characteristics:

(*a*) A decreasing effectiveness in reducing the temperature at the chip-tool interface with increasing depth of cut.

(*b*) A decreasing effectiveness in reducing the temperature at the chip-tool interface on a percentage basis with increasing cutting speed.

(*c*) No temperature-decreasing effect at cutting speeds above 400 sfpm for a depth of cut of 0.0052 in., and above 200 sfpm for a depth of cut of 0.0104 in.

6 Data obtained with a dry tool satisfied the relation

$$T = CV^n$$

where

T = chip-tool interface temperature
V = cutting speed
C and n = const

for lower depths of cut, but did not hold over the entire range of speed investigated for the higher depths of cut.

7 A comparison of chip temper-color temperatures with chip-tool interface temperatures showed that different temper colors may be obtained readily by varying the cutting conditions, even though the chip-tool interface temperature remains the same.

8 No correlation was observed between the coefficient of sliding friction in the presence of the fluids tested and their ability to reduce the chip-tool interface temperature.

9 No correlation was observed between chip-length ratio and chip-tool interface temperature data.

10 Tests employing carbon tetrachloride and benzene as cutting fluids showed that these materials, which have widely different cutting-force reducing ability at relatively low cutting speeds, were ineffective in reducing the chip-tool interface temperature. In fact, these materials were inferior to water in lowering the tool temperature.

11 Collectively the data presented indicate that the temperature-reducing action of the water-base cutting fluids considered in this investigation is due more to the cooling action of the fluids than to their reduction of the friction force on the face of the tool.

Acknowledgment

The authors wish to express their gratitude for valuable discussions with Prof. G. B. Wilkes of the Heat Measurements Laboratory at the Massachusetts Institute of Technology, and to thank Mr. Sylvester F. Murray of the Lubrication Laboratory at the Institute, for determining the coefficients of sliding friction.

BIBLIOGRAPHY

1 "Tool and Chip Temperatures in Machine Shop Practice" by H. Shore, thesis, Massachusetts Institute of Technology, 1924.
"Thermoelectric Measurements of Cutting Tool Temperatures," by H. Shore, *Journal of Washington Academy of Science*, vol. 15, 1925, p. 85.

2 "The Measurement of Cutting Temperatures," by E. G. Herbert, *Proceedings of The Institution of Mechanical Engineers*, London, England, vol. 1, 1926, p. 289.

3 "Die Messung der Schneidentemperatur biem Abdrehen von Flueseisen," by K. Gottwein, *Maschinenbau*, vol. 4, 1925, p. 1129.

4 "Cutting Temperatures Developed by Single-Point Turning Tools," by O. W. Boston and W. W. Gilbert, Trans. American Society for Metals, vol. 23, 1935, p. 703.

5 "Measurement of Temperatures in Metal Cutting," by A. O. Schmidt, O. W. Boston, and W. W. Gilbert, Trans. ASME, vol. 68, 1946, p. 47.

6 "A Method for Measuring Tool Tip Temperature," by B. A. Crowder, Technical Paper no. 55, Engineering Experiment Station, University of Minnesota, Minneapolis, Minn., 1946.

7 "Progress Report No. 1 on Tool-Chip Interface Temperatures," by K. J. Trigger, Trans. ASME, vol. 70, 1948, p. 91.

8 "Progress Report No. 2 on Tool-Chip Interface Temperatures," by K. J. Trigger, Trans. ASME, vol. 71, 1949, p. 163.

9 "A Note on the Surface Temperature of Sliding Metals," by F. P. Bowden and K. E. W. Ridler, Proceedings of the Cambridge Philosophical Society of London, England, vol. 31, 1935, pp. 431–432.

10 "Calculation of the Temperature Development in a Contact Heated in the Contact Surface and Application to the Problem of the Temperature Rise in a Sliding Contact," by R. Holm, *Journal of Applied Physics*, vol. 19, 1948, p. 361.

11 "The Incremental Friction Coefficient—A Non-Hydrodynamic Component of Boundary Lubrication," by J. T. Burwell and C. D. Strang, *Journal of Applied Physics*, vol. 20, 1949, p. 79.

Discussion

B. T. Chao.[5] The fact that the effectiveness of a cutting fluid in lowering tool temperature decreases with increase of speed and feed has long been speculated. It is a pleasure to see that such speculation has been proved by carefully conducted experiments. The writer wishes to congratulate the authors on the excellent work presented.

The authors stated that an effective fluid should reduce the heat that is generated in the cutting operation (*a*) directly, by reducing the friction along plane AC in Fig. 1, and (*b*) indirectly, by reducing the flow stress along plane AB. The writer wonders if this terminology "flow stress" refers to the same thing as "shear strength" designated as S_s by M. E. Merchant. This dynamic shear strength (dynamic, because we have to refer to the property of the material in its response to extremely high rate of straining) depends essentially only on the plastic property of the work ma-

[5] Research Associate, Department of Mechanical Engineering, University of Illinois, Urbana, Ill.

terials. When a cutting fluid is present and if it is effective, the heat generated as a consequence of the shearing deformation of the metal along AB is reduced mainly because a lowering of the coefficient of friction at the interface results in an increase of the shear angle. A greater shear angle means a shorter plane of shear; thereby the material undergoes less deformation and so less heat is produced. Cooling action of the cutting fluid of course plays an important role in reducing cutting temperature as indicated by the authors. But this is another matter.

The second point which the writer would like to discuss is the analysis made by the authors on the effect of cutting fluids on the thermoelectric circuit. The writer fails to see how Fig. 8 can represent the true situation. Since R_2 is designated by the authors as the resistance of the *entire* thermoelectric circuit when no fluid is present, the equivalent circuit depicting the short-circuiting effect of the cutting fluid (if galvanic action between work and tool material does not occur) should be as shown in Fig. 17.

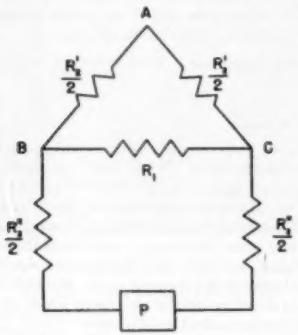

FIG. 17 CORRECTED SHORT-CIRCUIT THERMOELECTRIC CIRCUIT (Without galvanic action.)

In Fig. 17 R_2' represents the combined resistance offered by tool, chip, and workpiece in the *neighborhood* of the tool tip, while R''_2 represents the resistance of the remaining thermoelectric circuit including that of the potentiometer. In the usual case of toolwork thermocouple arrangement, R_2' will have a very low value, say, in the order of few ohms or even less and is, therefore, negligible as compared to R_1 (in the order of 1000 ohms as reported by the authors). In other words, Equations [1], [2], [3], and [4] should be rewritten with R_2 replaced by R_2' which is only a very small fraction of the resistance of the entire thermoelectric circuit. Therefore the use of a special low-resistance potentiometer might not be necessary.

The incremental friction coefficient as determined by Burwell and Strang's apparatus may not be directly applicable to cutting operations because conditions existing at actual contact in the two cases are vastly different. The friction specimens used in their investigation consist of case carburized and hardened SAE 1117 steel cylinders, while in cutting operations we are dealing with friction between the heated chip (the surface of which is believed to be chemically clean as the chip comes off the shear zone and makes contact with the tool) and the tool tip which is also at high temperature. Any attempt to correlate their results without taking into consideration the effect of temperature is liable to be misleading. Perhaps the most reliable and simple way to determine tool-chip interface friction is by means of tool-force dynamometer and chip-thickness measurements employing orthogonal cutting conditions.

M. EUGENE MERCHANT.[6] The authors are to be congratulated on their accomplishments in the carrying out of the useful investigation described in this informative paper. They have made at least three quite important contributions to the field of cutting-temperature studies. First, they have, for the first time, worked out successful techniques for making cutting-temperature measurements in the presence of cutting fluids having appreciable electrical conductivity. Secondly, they have demonstrated that it is unlikely that the thermoelectric emf of the severely deformed chip metal which is in contact with the tool during cutting is significantly different from the emf of the undeformed work material when in contact with the tool (which emf is normally used for calibration). Lastly, they have shown that the cooling ability of a cutting fluid can have an important effect on the temperature at the chip-tool interface.

The main importance of an understanding of temperatures at the chip-tool interface lies in the considerable effect which this temperature has on the tool life. Schallbrock, Schaumann and Wallichs[7] have shown that, in the case of dry cutting, tool life varies as approximately the 20th power of the temperature at the chip-tool interface. Whether or not tool temperature has quite as drastic an effect on tool life when cutting fluids are used is not yet known. It is unfortunate, therefore, that in the present study, no tool-life tests were made for correlation with the tool-temperature measurements. We hope that the authors may find it possible to run such comparative tests in the future to round out their contributions.

It is evident from the authors' tests, however, that within the present limits of experimental error, at least, tool-temperature tests do not distinguish clearly between the relative effectiveness of various different cutting fluids in lowering tool temperatures. The action of a cutting fluid in lowering tool temperatures is two-fold, namely, the direct cooling action of the fluid and, in addition, the reducing of the amount of heat generated in cutting by reducing the rubbing friction between chip and tool. Thus, in the writer's laboratory, it has been found that the differences in the effectiveness of different cutting fluids can be more readily and accurately determined by independent measurements of these two functions (cooling ability and friction-reducing ability) than by direct measurement of tool temperatures. Further improvement in the experimental accuracy of chip-tool interface temperature measurements in the presence of various types of cutting fluids is needed before this method can be anything other than a useful supplement to these two types of measurements.

R. G. MOYER.[8] It is probably true that lubrication under the conditions of metal cutting is in part due to the "formation of a solid lubricant by a chemical reaction involving the cutting fluid and the chip material." However, it is also possible that the active chemicals of the cutting fluid require a vehicle to carry them to the tool-chip interface. If the vehicle is too volatile, it is conceivable that it could vaporize before reaching the interface losing the aid of the important forces of capillarity and failing to carry the chemicals into the reaction zone in sufficient quantity. The cutting fluids selected by the authors all have low boiling points and some have no chemicals which could feasibly combine with the metal to form a "solid lubricant." All test fluids present the possibility of "vapor blanketing" rather than lubrication.

[6] Research Physicist, The Cincinnati Milling Machine Co., Cincinnati, Ohio. Mem. ASME.

[7] "Testing for Machinability by Measuring Cutting Temperature and Tool Wear," by H. Schallbrock, H. Schaumann, and R. Wallichs, Vortrage der Hauptversammlung, 1938, der Deutsche Gesellschaft für Metallkunde, Verein deutscher Ingenieure Verlag, 1938, pp. 34–38.

[8] Research Engineer, Research and Development Department, The Pure Oil Company, Winnetka, Ill. Jun. ASME.

Most practical cutting fluids which contain sulphur and chlorine for the purpose of supplying solid lubrication are mineral-oil-base or mineral-oil fat-base materials. It is unfortunate that one of these oil-base fluids was not included for comparison with the low-boiling-point fluids.

Water is known to be of little value for increasing tool life under the more severe conditions of cutting and it is possible that the combinations of speeds and feeds used for the higher temperature values are in the critical range. It is believed that tool-life data under the test conditions used for the paper would help to complete the picture and perhaps reveal the range of conditions requiring lubrication rather than cooling.

W. H. Oldacre.[9] Mr. Shaw and his co-authors, Mr. Pigott and Mr. Richardson, are to be congratulated on a carefully conducted and painstaking investigation. Seemingly, they establish the fact that it is possible to secure useful temperature data with the toolwork thermocouple even in the presence of water-mix cutting fluids.

The assumption, however, that the "hot spot" in the cutting orbit lies along plane *AC*, Fig. 1, and is a governing factor in the mechanism of cutting is hardly justified by the facts.

Temperature variations shown in Fig. 11 (*a*), (*b*), (*c*) between different water mixtures are small in contrast to the wide variations in performance observed in actual machining practice.

If the authors have run tests of this type with straight oils it would be interesting to have the results to compare with those from the water mixtures.

We feel that the temperature of the workpiece metal in the cutting orbit governs the characteristics of the metal which, in turn, determine chip geometry; and that it is in the regulation of these temperatures rather than tool-chip interface temperatures that cutting fluids play a most important part.

However, much remains to be done in this field and the authors have made an interesting start.

K. J. Trigger.[10] The writer has reviewed the subject paper with a great deal of interest and wishes to compliment the authors for this timely contribution to the metal-cutting literature.

The authors have demonstrated clearly the negligible effect of chip deformation upon the thermoelectric characteristics of the work material. Using a less direct method, the writer found a negligible effect with a steel-cemented-carbide couple as reported in a previous paper (7). The confirming evidence presented by the authors should remove all doubts about the effect of chip deformation.

There are a number of points in this paper with which the writer is in full accord. There are also some pertinent items which should be discussed or supplemented. The writer's comments are offered in the hope of enhancing the value of this paper.

The first of these concerns the wet cutting arrangement. The setup is interesting but, from appearances, the possibility of a galvanic action at the tool and chip is still present. The writer has done some exploratory work with cutting fluids using cemented-carbide tools on steel at speeds higher than 100 sfpm, a depth of cut of about 0.100 in. and feed of about 0.01 ipr. The tool and brush of the toolwork thermocouple were both insulated from the lathe. Certain cutting fluids caused no difficulty in the thermocouple circuit whereas one activated water-soluble coolant caused a sharp galvanic action which indicated a greatly increased emf—quite contrary to the effect of a short circuit.

It is probable that the galvanic effect between steel and cemented-carbide tools is considerably higher than that between high-speed steel tools and low-carbon steels, and that the effect observed by the writer was much more severe than that which would arise under similar conditions with the authors' tool and workpiece materials and setup. It is not clear how the authors' setup eliminates troubles due to such galvanic effects.

A further point of discussion pertains to the heat-treatment applied to the high-speed steel tools used in this investigation. Commercially treated high-speed steel tools are generally tempered at 1050 to 1100 F, and, properly treated, they are structurally stable at all cutting temperatures below the maximum tempering temperature. However, when the cutting temperatures exceed the maximum tempering temperature, structural changes alter the calibration and therefore affect the indicated cutting temperature.

This factor was illustrated in a paper (8) by the writer. The cemented-carbide member of the thermocouple was the *constant* factor and the structure of the 9445 steel was varied by adjustment of the tempering temperature after oil-quenching. The following table indicates the role of tempering temperature upon the thermoelectric effect of such a thermocouple.

Tempering temperature deg F	Temperature corresponding to 10 mv, approximately, deg F
850	949
950	955
1050	985
Annealed	1015

These data illustrate the effect of structural changes in the steel upon the calibration curve. If one were to apply the calibration curve for the steel quenched and tempered at 850 F to an emf obtained when cutting the annealed steel the indicated temperature would be some 75 F below the actual temperature.

Since the tool is the "stationary" member of the thermocouple (the chip moves away rapidly and changes are insignificant during the very brief contact of a segment of the chip with the tool) any changes in its structure beyond that upon which the calibration curve is based are apt to lead to difficulties.

If, then, the cutting temperature exceeded the tempering temperature of the steel tool the structural change would invalidate the calibration. It is the writer's opinion that any cutting temperatures in excess of the tempering temperature of the tool are subject to error. However, since the temperature-emf relationship of the authors' combination of materials was low (3 mv at about 1200 F) the changes may have had comparatively little effect.

Boston and Gilbert in their paper (4) observed that the calibration curve changed when the temperature exceeded 1100 F (the tempering temperature of the tools they used). They state: "This seemed to indicate definitely that to obtain reliable and reproducible results, the tool temperature must remain below 1100 F."

It seems desirable, therefore, that cutting-temperature studies using high-speed steel should be confined to interface temperatures of approximately 1100 F maximum and probably lower since tool life at corresponding speeds will be very short anyway. The writer has observed no change on the calibration curve of cemented carbides when heated to as high as 1850 F. This structural stability was one of the reasons for the use of cemented carbides in cutting temperature studies.

The writer questions the authors' use of the cutting temperature equation $T = CV^n$ when applied to high-speed steels or other tools in which a significant built-up edge is present. Boston and Gilbert (4) report an equation of the form $T = CV + K$ in the range of 550 to 1100 F. Similarly, Crowder (6) finds the same sort of relationship for high-speed steels cutting cold-rolled SAE 1020 steel.

It is to be expected that suitable cemented-carbide tools would

[9] President, D. A. Stuart Oil Co., Chicago, Ill. Mem. ASME.

[10] Professor, Department of Mechanical Engineering, University of Illinois, Urbana, Ill. Mem. ASME.

have a different relationship since tool forces, friction, and the tendency to adhesion are different than obtain with high-speed steel. The cutting-temperature equation as proposed in 1947 (7) was within the scope of cutting conditions resulting in a type 2 chip, and under such conditions, it has applied for various combinations of feed, speed, and depth of cut, both with steel and aluminum alloys.

The presence of a built-up edge has the well-known effect of lowering the indicated emf and therefore the indicated cutting temperature. The effect may be illustrated by Fig. 18 of this discussion. A decrease in the magnitude of the built-up edge

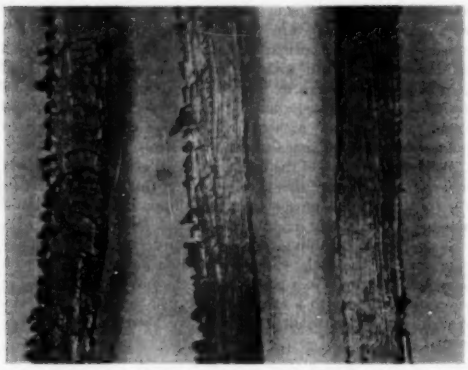

13.42 mv 955 F | 13.88 mv 987 F | 14.18 mv 1004 F

FIG. 18 CHIPS FROM 118 SFPM TEST

Steel: [illegible] 9445 annealed, 183 Bhn
Tool: tungsten carbide.
Depth of cut: 0.100 in.
Feed: 0.01 in. per rev.
Mag: × 3½

(though a small one was still present) increased the indicated emf from 13.42 to 14.18 mv without any other changes occurring. A severe built-up edge may lower the indicated tool-chip interface temperature nearly 100 F below that given by the cutting-temperature equation for the same speed (7, 8).

In view of this profound effect the writer believes that a significant built-up edge virtually eliminates the tool-work thermocouple as a useful tool for study under such conditions. Inasmuch as a "steady state" does not obtain, the results are too erratic to be of much value.

Fig. 11(*c*), and to a lesser extent 11(*b*) of the authors' paper, serves to illustrate the effect of an excessive built-up edge which, according to the authors, was present under the cutting conditions used.

The writer can see no reason why the "true" cutting temperatures have an asymptotic relationship to speed. Certainly, the rate of heat "generation" increases with speed and the cutting temperature should also increase with speed, as the authors state just prior to their conclusions. The asymptotic trend in Fig. 11(*c*) is then due to two factors: First, it is noted that the temperatures are above 1200 F or approximately 100 F above the probable maximum tempering temperatures of the tool. This will cause the calibration curve to be altered although as stated previously, the effect may not be very great. More probably the major factor is the built-up edge—the more severe it is, the greater is the divergence of indicated temperature from the true temperature.

Boston and Kraus[11] observed a decrease of about 100 F in indicated cutting temperature as the cutting speed was increased from 210 to 320 sfpm. This they attributed to the pronounced built-up edge. A similar effect apparently has given rise to Fig. 11(*c*).

The writer believes that any possible heat absorption due to an allotropic change in the 1015 steel is nil. First, there is not much to transform (at about 1350 F) and second, the time of contact of the chip and the tool is of the order of 1/400 sec which is insufficient for transformation to occur.

In the opinion of the writer the toolwork thermocouple is really valid only in so far as the cutting temperature is below the so-called "temperature of stability" of the tool and as long as little or no built-up edge is present on the tool.

AUTHORS' CLOSURE

The authors wish to express their gratitude to the several discussers for the many helpful suggestions and comments presented.

The "flow stress" referred to in the paper is the mean stress developed on the shear plane in producing the observed strain in a chip. It should not be called a shear strength inasmuch as this conveys the idea that rupture has occurred and further that the mean stress found on the shear plane is a material constant. Actually the mean stress depends upon the strain that the chip experiences, as given by the stress-strain curve at the rate of strain pertaining. Since experiment shows that metals exhibit an even greater tendency to strain harden at high rates of strain than at low rates of strain, it is evident that the mean stress on the shear plane in metal cutting is not a material constant. If, as Dr. Chao infers, metals did behave as ideal plastics (such as celluloid) at the high strain rates obtaining in metal cutting, then it would be proper to speak of a shear strength and to regard this quantity as a material constant.

The authors agree that the resistance R_2 in Fig. 8 is but a small part of the total resistance of the circuit. In the absence of exact knowledge regarding the distribution of resistance as shown in Dr. Chao's Fig. 17, the authors assumed the entire resistance of the circuit to act from A to B since this leads to a conservative result with regard to the importance of the short-circuiting effect of the cutting fluid.

As Dr. Chao correctly indicates, caution must be exercised in comparing ordinary sliding-friction data with that found in cutting. Some results we have recently obtained show that the friction along the face of a cutting tool is of a distinctly different type from that in ordinary sliding. This observation also has direct bearing upon Dr. Merchant's contention that the real way to study friction and cooling characteristics is separately in the laboratory. Aside from the fact that the friction in metal cutting is different from that in sliding, it is evident that the cooling characteristics of a fluid in bulk under atmospheric pressure may be entirely different from those for a thin film of the fluid under the extreme pressure found in cutting. There is also the problem of getting the fluid to the tool point fast enough to be effective, which is absent in the bulk cooling tests of the laboratory.

Several of the discussers have suggested the desirability of an extension of the work to include tool-life data and tests upon the so-called straight oils and oils containing additions of sulphur and chlorine-bearing molecules. Work is currently being continued along these lines.

Mr. Oldacre appears to doubt the importance of the mean temperature along the tool face and contends that the tempera-

[11] "A Study of the Turning of Steel Employing a New Type Three Component Dynamometer," by O. W. Boston and C. E. Kraus, Trans., ASME, vol. 58, 1936, pp. 47–53.

ture in the "cutting orbit" is the one of importance. In order to reply to this statement it is necessary to known the criterion of importance considered. If this criterion were the magnitude of the flow stress (mean shear stress) in producing a chip, then the foregoing observation is correct. However, tool life is an over-all criterion of far more practical importance and in this connection the mean temperature on the tool face is very important. This is demonstrated by the high degree of correlation which is shown to exist between tool life and chip-tool interface temperature in the reference cited by Dr. Merchant (footnote 7).

No galvanic action was observed with any of the fluids used in this investigation. It is the opinion of the authors that in the past some of the difficulty attributed to this cause has been due to the failure to insulate the workpiece completely from the lathe. Spurious effects were frequently observed by the authors when this precaution was not taken.

Professor Trigger's remarks regarding the failure of a toolwork thermocouple to give reliable data above a certain tempering temperature are based upon observations for metals in bulk. In the case of a cutting tool operating at an indicated mean chip-tool temperature of 1200 F, there is such an extremely high-temperature gradient extending from the tool surface that a layer of but a few ten thousandths of an inch is actually near the indicated temperature. Inasmuch as the strength, toughness, and other mechanical and chemical properties of thin layers are entirely different from the same metal in bulk, it does not appear justified to assume that the time-temperature transformation characteristics of a very thin layer of metal are the same as those for the metal in bulk. It is well known that high-speed-steel tools will operate successfully for long periods at chip-tool interface temperatures high enough to cause sufficient softening of the metal in bulk to produce a tool that is useless.

While the importance of tool transformations are questionable for a toolwork thermocouple in use, due to the thinness of the layer that is subjected to the indicated temperature, Professor Trigger's remarks are directly applicable to the calibration of a toolwork thermocouple. In this case the metals are heated in bulk and a transformation with attendant change in calibration may occur for the workpiece or more probably for the heat-treated tool. However, the magnitude of this effect may be determined by successive calibrations, the same specimens being reheated to the maximum temperature more than once. If successive calibrations are the same then the influence of a possible phase transformation is negligible. Alternatively a calibration carried out with the temperature increasing should give an identical curve to that obtained with the temperature decreasing if the transformation effect is negligible. This was found to be the case with the combination used in this paper (high-speed steel and annealed SAE 1015 steel).

While the presence of the built-up-edge in general gives a lower tool-chip temperature this does not mean that the temperature observed is any less precise than that obtained without a built-up-edge. Due to the characteristic shape, the presence of a built-up edge invariably gives rise to an increase in the effective rake angle of the tool. Since the cutting force decreases with increased rake angle it is possible that the observed decrease in temperature is due to a change in the real tool geometry even though at first glance all variables have been maintained constant.

An Analytical Evaluation of Metal-Cutting Temperatures

By K. J. TRIGGER[1] and B. T. CHAO,[2] URBANA, ILL.

This paper presents an analytical method for the determination of metal-cutting temperatures. The average tool-chip interface temperature is calculated by considering the mechanism of heat generation during metal-cutting operations in which a type 2 chip is formed. The analytical results agree well with those obtained by test methods, and the theoretical analysis has also yielded some important physical quantities and measurements which affect cutting temperatures.

Introduction

CUTTING temperatures have been investigated experimentally by many previous investigators in metal cutting. Gottwein (1)[3] and Herbert (2) are among the pioneers. Much useful information has since been contributed by Schwerd (3), Boston (4), and others. Quite comprehensive summaries of test results can be found both in the paper (5) presented by Schallbroch, Schaumann, and Wallichs at the 1938 Convention of the German Institute of Metals, and in two recent progress reports (6, 7) on the interface temperatures by one of the authors. However, published work on the "mechanism" of heat generation during cutting is very limited, and the lack of an analytical study of the heating of the chip and the tool has limited the scope of many engaged in metal-cutting research.

Woxen (8) appears to be the first to attempt the development of the tool-life equation from a theoretical study of the heat balance in lathe turning. However, some of his assumptions are quite removed from actual cutting conditions. On the other hand, Merchant's development of the basic mechanics of metal-cutting operations (9), has, in effect, shed a great deal of light on the temperature problem in cutting. His excellent analysis is very useful in the evaluation of cutting temperatures, and it enables a better approach than heretofore has been possible.

The Cutting-Temperature Equation

Main Source of Heat in Metal-Cutting Operations—Orthogonal Cutting and Type 2 Chip. The analysis presented in this paper is limited in theory to the case of orthogonal cutting which is the simplest and most suitable for mathematical analysis. If, however, in conventional turning operations with a single-point tool, the primary cutting edge is not oblique by more than a few degrees to the direction of relative motion of tool and workpiece and if the depth of cut is large compared with the feed and nose radius of the tool, the approximation to orthogonality is good. The analysis is also limited to the case of type 2 chips, since the basic mechanism of this type of chip formation is better known.

The first law of thermodynamics states, in effect: "When work is transformed into heat, the quantity of work is equivalent to the heat produced." This heat will be generated when the conversion of energy in the form of mechanical work takes place. In metal-machining operations where a type 2 chip is produced, the heat is generated in two distinct regions, as follows:

1 The shear zone *OW*, where the main plastic deformation takes place.

2 The tool-chip interface *OT*, where pronounced rubbing occurs. This is shown in Fig. 1.

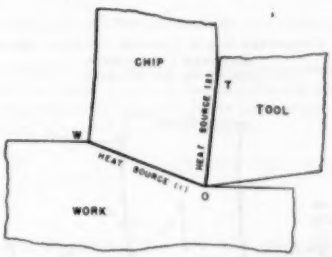

Fig. 1 Sources of Heat in Metal Cutting, Type 2 Chip

The convection and radiation losses are neglected since they will be small during the short interval when the chip is formed at the shear zone and passes the region in contact with the tool.

However, the latent energy stored in the deformed chip is another matter, and it must be taken into consideration. In two papers (10, 11) Taylor and Quinney have reported on the latent energy remaining in various metals after cold-working. By one method (10), that of the difference between the work done on the specimen and the heat given off, they found that about 11 per cent of the energy of deformation remained in the cold-worked mild steel. A later method (11), the emission of energy when the deformed metal was reheated above recrystallization temperature, revealed that 15 per cent of the energy remained in pure (carbonyl) iron.

Where the same materials were tested by both methods the second one generally gave higher results. Therefore it appears plausible that from 10 to 15 per cent of the energy of deformation is stored as latent energy in the deformed chip material. The annealed steel used in this investigation was in the spheroidized condition and quite analogous to that used by Taylor and Quinney. It is reasonable to assume that about 12½ per cent (the mean of the 10 to 15 per cent range) of the energy of deformation at the shear zone is stored as latent heat in the chip material, and this assumption is used in the subsequent analysis.

---

[1] Professor, Department of Mechanical Engineering, University of Illinois. Mem. ASME.

[2] Research Assistant, Department of Mechanical Engineering, University of Illinois.

[3] Numbers in parentheses refer to the Bibliography at the end of the paper.

Contributed by the Research Committees on Metal Cutting Data and Bibliography and Cutting Fluids, and Production Engineering Division, and presented at the Semi-Annual Meeting, St. Louis, Mo., June 19–23, 1950, of The American Society of Mechanical Engineers.

Note: Statements and opinions advanced in papers are to be understood as individual expressions of their authors and not those of the Society. Manuscript received at ASME Headquarters, January 6, 1950. Paper No. 50—SA-1.

The remainder of the heat energy from the two sources will be shared between the work, the chip, and the tool as sensible heat.

Determination of Average Chip Temperature as It Leaves the Shear Zone. In accord with the previous discussion, an expression for the average chip temperature due to heating at the shear zone may be derived. This is achieved by using the force and velocity relationships developed by Ernst and Merchant (12), as shown in Figs. 2(*a*) and 2(*b*). The mechanical-energy input at the shear zone per unit time can be expressed as $F_s V_s$, while the total energy consumed by cutting per unit time is $F_c V_c$.

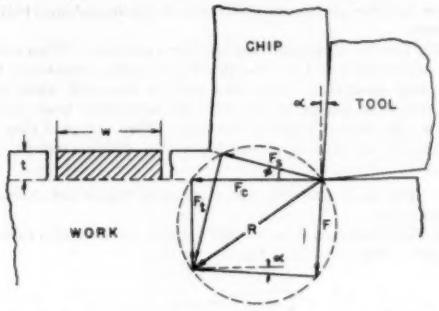

FIG. 2(*a*) CONDENSED FORCE DIAGRAM SHOWING RELATIONSHIPS BETWEEN COMPONENTS
(After Ernst and Merchant)

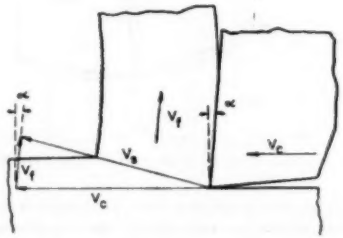

FIG. 2(*b*) VELOCITY RELATIONSHIP IN ORTHOGONAL CUTTING
(After Merchant.)

As has been shown elsewhere (9), the following relationships can be derived readily from the chip geometry and from the law of conservation of energy

$$F_s V_s = F_s V_s + F V_f, \text{ or } F_s V_s = F_c V_c - F V_f \quad [1]$$

$$F = F_c \cos \alpha + F_c \sin \alpha \quad [2]$$

$$V_f = V_c r_t \quad [3]$$

r_t being the chip-thickness ratio.

Not all of the heat energy developed at the shear zone will go into the chip as sensible heat. A part of it will be transferred back into the workpiece by conduction. The relative distribution will vary with cutting speed, feed, ratio of size of chip to workpiece, etc.; the higher the cutting speed and the thicker the chip, the greater will be the proportion of heat in the chip. Exact analysis is extremely difficult, owing to an additional complicating fact that a part of the heat which flows into the workpiece by conduction will be present in the chip which is removed in the succeeding revolution. Schmidt and Roubik (13) have reported that in the case of drilling operations performed on a tubular workpiece, the heat going into the workpiece constitutes about 10 per cent of the total heat generated in cutting at speeds higher than 100 sfpm and at a feed of 0.0091 in. per revolution (ipr). In the absence of further data in this respect the results of Schmidt and Roubik for drilling shall be used in the subsequent calculations for single-point turning. It will become evident later that this approximation will not introduce serious errors in so far as the calculated interface temperatures are concerned, and it does not affect the method at all.

From the preceding discussion it follows that the temperature rise due to chip deformation at the shear zone can be expressed as follows

$$(\theta_t - \theta_0)_{avg} = \frac{A\{F_c V_c (1 - B_1) - F V_f\}}{J C \rho (V_c \times 12) tw} \quad [4]$$

in which

θ_t is average temperature, deg F of chip as it leaves the shear zone, and θ_0 is ambient temperature, deg F.

A is proportion of energy of deformation which appears as sensible heat in chip, to be taken as 0.875 for annealed steel (Taylor and Quinney).

B_1 is proportion of total heat left in workpiece; 0.1 for present conditions (Schmidt and Roubik).

J is mechanical equivalent of heat, 778 ft-lb/Btu.

C is specific heat of heated chip, Btu/(lb)(deg F).

ρ is density of chip material, lb per cu in.

t is feed, ipr, and w, depth of cut, in.

Forces F and F_c, lb.

Velocities V_c and V_f, fpm.

The heating of the chip at the shear zone as a result of the mechanical deformation is considered to take place on the atomic scale, and the temperature rise is, therefore, virtually instantaneous.

Since both the specific heat and thermal conductivity vary with temperature, there arises the question as to the appropriate values to be used in Equations [4] and [14], or [16].

Data on the specific heat and thermal conductivity of NE 9445 steel are lacking, and recourse must be made to existing information on similar low-alloy steels. The ASM Metals Handbook, 1948 edition (14), lists mean specific heats and thermal conductivities for a number of low-alloy steels, one of which is reasonably similar in chemistry to the steel used. The effect of temperature upon the mean specific heat and thermal conductivity of this reference steel is shown in Figs. 3 and 4, respectively. The probable effect of deformation is to raise the specific heat and lower the conductivity, but since these effects are of small magnitude, they may be neglected.

According to Austin (15), the change in thermal conductivity of ferrous metals due to deformation is generally insignificant. Apparently, the data for the selected steel provide a first approximation to the specific heat and conductivity of the steel used in this investigation. Inasmuch as the temperature rise at the shear zone is practically instantaneous, and, on the basis that the specific heat may vary instantaneously with temperature, it is concluded that the best approximation is secured by use of the mean specific heat at the average temperature of the range involved. This specific heat, for Equation [4], may be obtained from Fig. 3.

The solution of Equation [4] involves the estimation of the chip temperature as it leaves the shear zone in order to obtain

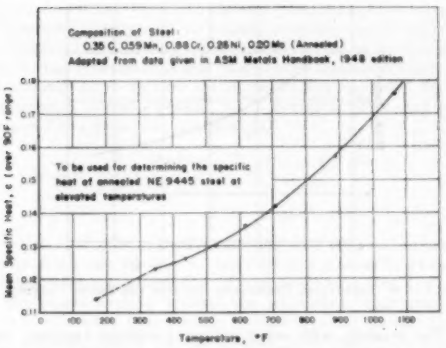

FIG. 3 EFFECT OF TEMPERATURE ON THE SPECIFIC HEAT OF AN ALLOY STEEL

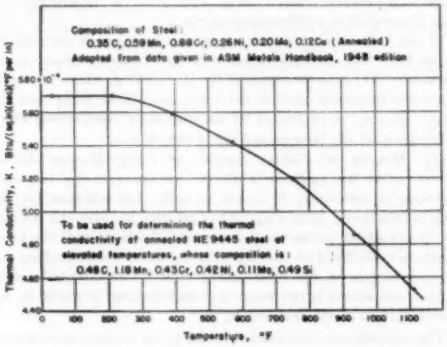

FIG. 4 EFFECT OF TEMPERATURE ON THE THERMAL CONDUCTIVITY OF AN ALLOY STEEL

the specific heat at the average temperature. This procedure constitutes the common cut-and-try method.

Temperature does have an effect on the density of the chip material, but the change is of small magnitude, i.e., 0.283 lb per cu in. at room temperature, as compared to 0.281 at about 700 F, a reasonable estimate of the average chip temperature. The latter figure is used in temperature calculations although the slight variation could be neglected.

Distribution of Heat at Tool-Chip Interface. A study of the generation of heat at the tool tip suggests that this problem bears a striking resemblance to those involving moving sources of heat, as, for example, the calculation of temperature at sliding contacts. As it leaves the shear zone the heated chip rubs on the top surface of the tool at a high velocity. Under the conditions of very clean contact which exist in a cut, the coefficient of friction is usually large, varying from about 0.5 to 1.5 or more, depending on the work and tool materials as well as the cutting variables. The quantity of heat liberated at the interface per unit time may be expressed as FV_c/J, and it will be shared between the chip and the tool.

This type of heating problem, particularly that of heating by sliding contacts, has been investigated by Blok (16), Jaeger (17), and others. Some of their results will be used in the following analysis.

(a) *Heating at Tool Tip—Stationary Source (Tool).* For simplicity, consider first the case where cutting is being done at one edge of a rectangular tool, the dimensions of which are large compared with that of the contact area. In Fig. 5, m denotes the average length of contact of the sliding chip on the tool surface, and l denotes the average width of contact which is essentially the same as the chip width. The x-, y-, and z-axes are chosen as shown.

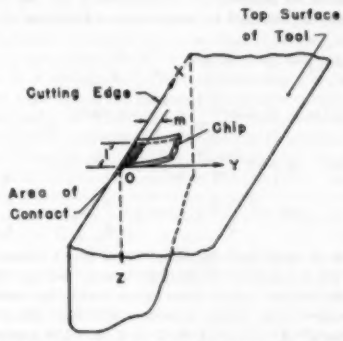

FIG. 5 IDEALIZED HEAT SOURCE AT THE TOOL-CHIP INTERFACE

In an "infinite" solid initially at zero temperature, the temperature at the point (x, y, z) at the time t due to a quantity of heat Q instantaneously liberated at the point source (x', y', z') at zero time, is, according to Carslaw (18)

$$\theta = \frac{Qk'}{8K_t(\pi k't)^{3/2}} \exp\left[-\frac{(x-x')^2 + (y-y')^2 + (z-z')^2}{4k't}\right] \quad \ldots\ldots\ldots\ldots [5]$$

k', K_t being the thermal diffusivity and conductivity, respectively, of the tool material.

Since the isothermal surfaces are symmetrically situated with respect to the point source (x', y', z'), the temperature at any point (x, y, z) in the first quadrant of an infinite solid with a source of the same intensity located at one edge of the quadrant will be 4 times the foregoing value, while it will be 8 times as much if the same source were situated at the corner of an octant.

This simplified conception of considering the tool to extend infinitely along x-, y-, and z-axes (see Fig. 5), is permissible, in so far as temperature in the neighborhood of the heat source is concerned. The error will be small if the temperature of the free surfaces of the tool does not rise much above ambient temperature. In this analysis the effect of clearance angles is neglected, and the rake angles of the tool are assumed to be zero degrees.

Thus the temperature above zero at time t, at point (x, y, z) in the body of the tool due to a heat source supplied at the rate q_1 per unit time per unit area over the small contact rectangle $(0 < x' < l, 0 < y' < m, z' = 0)$ commencing at zero time when the tool is at zero temperature, is

$$\theta = \frac{q_1 k'}{2K_t(\pi k')^{3/2}} \int_0^l dx' \int_0^m dy' \int_0^t \frac{dt'}{(t-t')^{3/2}} \exp\left[-\frac{(x-x')^2 + (y-y')^2 + z^2}{4k'(t-t')}\right] \quad \ldots\ldots [6]$$

The evaluation of the last integral may be made more com-

venient by introducing a new variable such as $T^2 = 1/(t - t')$. In order to find the steady-state temperature,[4] let $t \to \infty$ and thus obtain

$$\theta = \frac{q_1}{\pi K_t} \int_0^l dx' \int_0^m \frac{dy'}{[(x - x')^2 + (y - y')^2 + z^2]^{1/2}} \quad [7]$$

If, initially, the tool is at room temperature θ_0, and since only the temperature in the plane $z = 0$ is of interest, the following expression for temperature distribution in the top surface of the tool may be obtained by integration of Equation [7]

$$\frac{\pi K_t}{q_1}(\theta - \theta_0)_{x,y} = (l - x) \operatorname{csch}^{-1} \frac{l - x}{m - y} + (m - y) \sinh^{-1} \frac{l - x}{m - y} - x \operatorname{csch}^{-1} \frac{x}{m - y} + (m - y) \sinh^{-1} \frac{x}{m - y} + (l - x) \operatorname{csch}^{-1} \frac{l - x}{y} + y \sinh^{-1} \frac{l - x}{y} - x \operatorname{csch}^{-1} \frac{x}{y} + y \sinh^{-1} \frac{x}{y} \quad [8]$$

It is thus obvious that the temperature is not uniformly distributed over the area of the sliding contact, and that the temperature distribution can be determined readily by substituting assigned values of (x, y) into Equation [8] within the boundary of the rectangle $0 < x' < l$, $0 < y' < m$. The average temperature over the area of sliding contact, may be calculated thus

$$(\theta - \theta_0)_{avg} = \frac{1}{lm} \int_0^l \int_0^m (\theta - \theta_0)_{x,y} \, dx \, dy$$

which has been found to be

$$(\theta - \theta_0)_{avg} = \frac{4q_1 l}{\pi K_t} \left\{ \frac{1}{3}\left(\frac{m}{l}\right)^2 + \frac{1}{6} \frac{[(m/l)^2 + 1]^{3/2}}{(m/l)} + \frac{1}{2}\left(\frac{m}{l}\right) \sinh^{-1}\left(\frac{l}{m}\right) - \frac{1}{6}\left(\frac{l}{m}\right) - \frac{1}{2}\left(\frac{m}{l}\right)\left[1 + \left(\frac{m}{l}\right)^2\right]^{1/2} \right\} \quad [9]$$

The quantity in the braces depends only upon the ratio (l/m), i.e., the shape of the "rectangular" area of contact. This quantity is called the "shape factor," and its graphical representation is shown in Fig. 6.

Equation [9] may then be written

$$(\theta - \theta_0)_{avg} = \frac{4q_1 l}{\pi K_t} \text{ (shape factor)} \quad [10]$$

where K_t denotes the thermal conductivity of the tool as distinguished from that of the chip or workpiece.

If the cutting is being done at one corner of the tool, i.e., only on a small nose radius, Equation [10] becomes

$$(\theta - \theta_0)_{avg} = \frac{8q_1' l}{\pi K_t} \text{ (shape factor)} \quad [11]$$

This does not mean, however, that the cutting temperature will be twice as high since the relative distribution of heat between the chip and the tool is altered (i.e., $q_1 > q_1'$), as are also the forces and tool-chip contact area.

[4] From actual tests on cutting temperature, it is observed that a steady state is approached in a short time, at least within the conventional speed range for carbide tools (6).

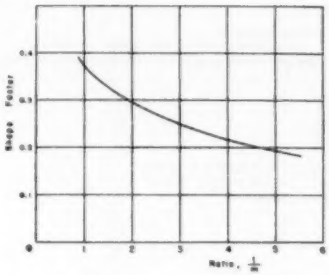

FIG. 6 GRAPHICAL REPRESENTATION OF THE SHAPE FACTOR

For example, with other cutting conditions constant, the cutting temperature will be some 10 per cent higher when the cut is taken entirely at the nose radius of the tool than it will be when the cut is confined to the middle of the side cutting edge of a relatively large tool. This point is further clarified and illustrated in a subsequent section.

If the rate of heat liberation at the interface is denoted by q per unit time per unit area over the contact surface, q_1' in Equation [11] may be replaced by $(1 - B_2)\, q$, where B_2 represents the fractional part of the "interface" heat going into the chip. B_2 may be evaluated by an analysis of the heating which takes place at the bottom surface of the chip.

(*b*) *Heating at Contact Surface of Chip—Moving Source.* In so far as the analysis of the temperature at the tool-chip interface is concerned, it makes no difference whether (*a*) the chip is considered as moving with a velocity V_f over the stationary (tool) source at the area of contact, or whether (*b*) the same source is considered as moving with the same velocity along the contact surface of the (stationary) chip. The relative motion of the heat source is the same, and this concept is useful in the determination of the fraction B_2.

The temperature distribution in the plane of the source as well as the penetration perpendicular to the plane of the source have been discussed quite comprehensively by Jaeger (17). He found that both depend upon the dimensionless quantity $V_f m/k$, where V_f is the chip flow velocity, m the average length of the path of contact of the chip on the tool surface, and k the thermal diffusivity of the heated chip material. With the usual cutting velocities and feeds encountered in practice using cemented carbide tools, the heat penetration, while a segment of the chip is in contact with the tool, is extremely shallow.

Considering the case of the moving source on the stationary chip, the average temperature rise, under steady-state conditions, over the area of the band source of width w, moving with a velocity V_f on the surface of a semi-infinite solid, due to a heat source of intensity $B_2 q$ per unit time per unit area, has been found by Jaeger (17) to be

$$\Delta\theta_{avg} = \frac{8}{3(2\pi)^{1/2}} \frac{B_2 q}{K} \left[\frac{km}{2V_f}\right]^{1/2} = \frac{4}{3(\pi)^{1/2}} \frac{B_2 q}{K} \left[\frac{km}{V_f}\right]^{1/2} \quad [12]$$

provided $(V_f m)/(4k) > 5$. The body of the chip which slides on the tool surface has already been heated to a temperature depicted by Equation [4] due to the main chip shear. Thus, at the interface, the average temperature rise above ambient is the sum of the two, that is

$$(\theta_i - \theta_0)_{avg} = (\theta_s - \theta_0)_{avg} + \frac{4}{3(\pi)^{1/2}} \frac{B_2 q}{K} \left[\frac{km}{V_f}\right]^{1/2} \quad [13]$$

In accord with a previously stated interpretation, the average temperature (steady-state conditions) over the area of contact as calculated for a moving source of intensity B_2q on the bottom chip surface is the same as that calculated for a stationary source of intensity $(1 - B_2)q$ on the top surface of the tool. As a consequence of this argument, the following equality may be written (from Equations [11] and [13])

$$(\theta_s - \theta_0)_{src} + \frac{4}{3(\pi)^{1/2}} \frac{B_2 q}{K} \left[\frac{km}{V_f}\right]^{1/2} = \frac{C(1 - B_2)\, ql}{\pi K_t}$$

(shape factor) ..... [14]

in which $C = 8$, when cutting is being done only on the nose radius of the tool, and $C = 4$ when cutting is confined to a small portion of the side cutting edge of a relatively large tool.

The Jaeger analysis involves the conductivity and specific heat of the entire sliding mass; in this case the heated chip. The necessary values may be obtained from Figs. 3 and 4, at the temperature of the chip as it leaves the shear zone.

The fraction B_2, may be evaluated by means of Equation [14], exercising care to use a consistent system of units for the quantities involved.

The cutting temperature, degrees F (above zero), is given by

$$\theta_t = \theta_s + \frac{4}{3(\pi)^{1/2}} \frac{B_2 q}{K} \left[\frac{km}{V_f}\right]^{1/2} \quad \ldots\ldots [15]$$

which can be reduced further to

$$\theta_t = \theta_s + \frac{B_2}{9(5\pi)^{1/2}} \frac{F}{KJl} \left[\frac{kV_f}{m}\right]^{1/2} \quad \ldots\ldots [16]$$

in which

θ_t is average tool-chip interface temperature, deg F.

θ_s is temperature of chip body, deg F, as it comes off the shear zone. This is calculated from Equation [4].

B_2 is fraction, determined by means of Equation [14].

F is friction force, lb.

K is thermal conductivity of heated chip body Btu/(in.^{2})(sec)(deg F/in.).

J is mechanical equivalent of heat, 778 ft-lb/Btu.

l is average width of tool-chip contact, in., which can be taken as measured width of chip.

m is average length of tool-chip contact, in.

V_f is chip sliding velocity, fpm.

Experimental Equipment and Methods

Cutting-Temperature Measurements. The cutting-temperature equation derived in the foregoing sections of this paper may be verified by comparison with the observed cutting temperature incurred in a specific cut. The experimental determinations have been made previously by one of the authors, using a Herbert-Gottwein toolwork thermocouple. The temperatures so obtained represent the average temperature of all points of contact of the tool and the chip. They, therefore, may be compared directly with temperatures calculated by Equation [16]. Some of the results presented in a previous paper (7) are included in this paper along with one series of tests in which the side cutting edge was the only active portion of the tool. The latter series of tests is denoted as "orthogonal cutting" in Fig. 14.

Cutting-Force Measurements. The solution of the cutting-temperature equation requires an accurate determination of the cutting forces, both components of which were measured by a dynamometer designed and constructed in the department of mechanical engineering at the University of Illinois.

The cutting tool was mounted in a holder at the end of a short, stiff, cantilever arm of rectangular cross section having approximately 0.0008-in. deflection at the tool tip under a vertical load of 600 lb. The minute deflections caused by the various forces were measured by two master electrolimit gage heads,[5] one each mounted to act in the vertical and horizontal directions. The toolholder was designed so that both components of the cutting forces acted approximately through the centroidal axis of the cantilever. Therefore the dynamometer responded independently to vertical and horizontal forces, and it was unnecessary to consider any cross-readings.

The discrepancies between the meter readings during loading and unloading were negligible. Several check calibrations revealed no drift in the dynamometer nor was there any difference between the original calibration and that made after several months of operation. The instrument, illustrated in Fig. 7, was found to be dependable and sturdy, yet highly sensitive.

The principle of operation of the electric gage head may be found elsewhere. Briefly, it involves the unbalancing of a reactance bridge circuit by changes produced in the air gap of one reactor arm when the cantilever is deflected. In order to get a better reading accuracy within a relatively wide range of forces, a system of series and parallel resistors connected in conjunction

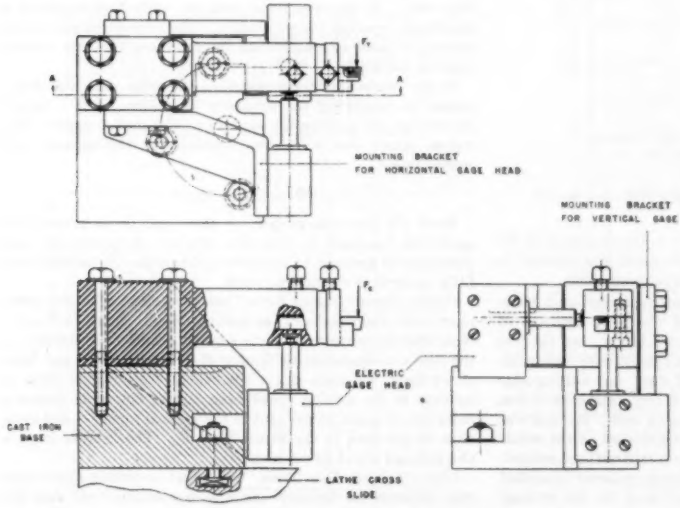

Fig. 7 Cutting Force Dynamometer

[5] General Electric Co., Schenectady, N. Y.

with the microammeter has been introduced into the circuit. Fig. 8 is a diagrammatic representation of this modified circuit. Simple shunting of the resistance to the microammeter was not deemed advisable since it changes the combined load on the copper-oxide rectifier, and thereby changes the selected operating point. Calibration was done by dead weights. A typical set of calibration curves, which are essentially straight lines, is shown in Fig. 9.

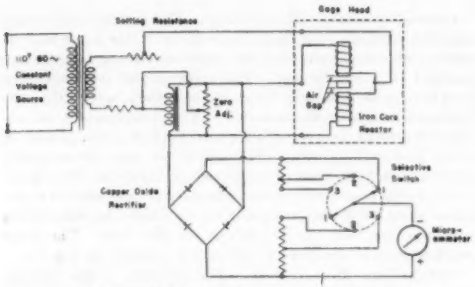

FIG. 8 BRIDGE CIRCUIT WITH SELECTIVE SENSITIVITY

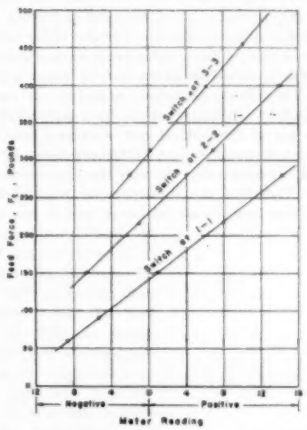

FIG. 9 TYPICAL CALIBRATION CURVE FOR DYNAMOMETER

Since temperature has a decided effect on the resistance of the windings in the bridge circuit, the instrument was allowed to warm up for at least 1 hr before it was used or adjusted.

Test Procedure. The cutting tests were conducted on a 16-in. × 54-in. heavy-duty lathe. The feed was kept constant at 0.0098 ipr; the nominal depth of cut was 0.100 in., and the tool shape for all tests was as follows: Back rake, 0 deg; side rake, 4 deg; end relief, 7 deg; side relief, 7 deg; end cutting-edge angle, 8 deg; side cutting-edge angle, 0 deg; and nose radius $^{3}/_{64}$ in. The setting angle was 90 deg in all tests; the tool was finished with a 400-grit diamond hone and was set on the center line of the workpiece. All tests were conducted without coolant. The tool used was a standard steel-cutting grade of cemented carbide of the same composition as that used for the cutting-temperature determinations reported in a previous paper (7). The cutting forces and cutting temperatures are thus based on the same carbide composition.

Simultaneous readings of vertical and horizontal tool forces were obtained for tests of short duration (10 to 15 sec). During such brief tests the dynamometer was not affected by any heating of the tool. In each test, the cutting speed was the independent variable, and force measurements were taken at each speed increment from minimum to maximum, and each decrement back to the minimum used. Such duplicate tests served both as check runs and also to detect possible tool wear. In the event of significant tool wear the test was repeated at reduced maximum speed.

Surface speeds were measured with a calibrated indicator during cutting. The test stock consisted of a 5-in-diam bar of NE 9445 steel mill-annealed to 183 Bhn. During the tests, chips were collected from each run, and measurements of chip thickness were obtained.

The tool-chip interface area of contact was determined by a series of separate tests of about 30 sec duration each, and using several identical tools. After each cut the tool was dipped into a dilute (3 per cent) solution of nitric acid in alcohol for about 2 min, then immersed in alcohol and dried. This treatment removed the discoloration usually observed on the surface of the tool, and thereby revealed, distinctly, the true area of contact. The tool surface is discolored in the vicinity of the cutting edge due to the thin oxide formed as a result of heating. Such discoloration frequently results in an erroneous impression of the contact area.

The contact areas were photographed at low magnification after adjusting the illumination to reveal the contour most favorably. Fig. 10(*a*) is reproduced from one of the several photographs so obtained. The various areas of contact were measured by a planimeter for not less than ten trials, the average of which is reported as the area of contact.

It is apparent from Fig. 10(*a*) that the contact areas are not rectangles as assumed in the theoretical derivation. The nose radius of the tool is largely responsible for the discrepancy. In the subsequent calculations the width of contact l, is obtained by measuring the distance between parallel lines as illustrated in Fig. 10(*b*). It has been found that the width thus measured is practically equal to the chip width. The average length of contact m, is obtained by dividing the measured tool-chip contact area by the width l.

In the course of the investigation, the areas were also determined by measuring the necessary dimensions with a Brinell microscope and plotting the outline on cross-section paper. The values agreed well with those obtained by photography and measurement.

RESULTS OF TESTS

Since the principal purpose of this paper is to present the analytical approach to tool-chip interface temperatures, only those results germane to the present discussion are included and little analysis is attempted herein.

Cutting Speed—Cutting Force Tests. The effect of cutting speed upon both components of the cutting force is shown in Fig. 11. Note that an increase in cutting speed results in a decrease in the forces, a characteristic feature observed by Ernst and Merchant nearly a decade ago. It is evident from Fig. 11 that an increase in the cutting speed from 100 to 600 sfpm causes a reduction of about 25 per cent in the vertical force Fc, and more than 50 per cent in the thrust force F_t. The friction force is also reduced about 50 per cent.

Chip-Thickness-Ratio Tests. The effect of cutting speed upon chip thickness for annealed and heat-treated NE 9445 steel has been reported in a previous paper (7). The cutting-temperature

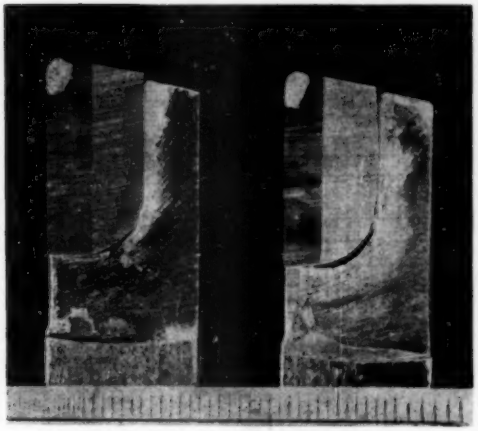

Steel: NE 9445—mill annealed, 183 Bhn
Tool: Triple carbide
Depth of cut: 0.102 in.
Feed: 0.0098 ipr.
Magnification: × 2.2

FIG. 10(a) TOOL-CHIP CONTACT AREAS

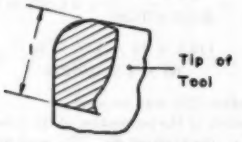

FIG. 10(b) AVERAGE WIDTH OF CHIP CONTACT

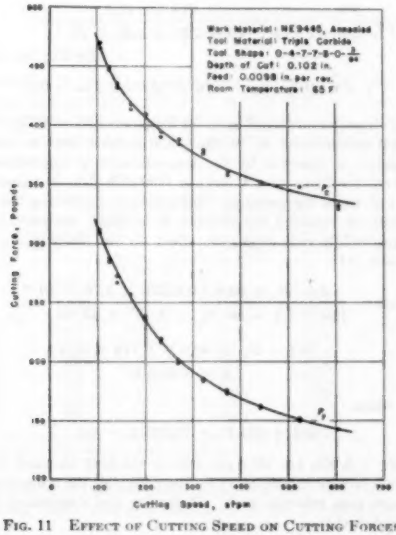

FIG. 11 EFFECT OF CUTTING SPEED ON CUTTING FORCES

calculation presented herein requires the chip-thickness-ratio r_t, at various speeds. This ratio is defined by Merchant (9) is the ratio of the thickness of the "uncut" chip (feed) to the mean chip thickness after removal. The mean chip thickness has been obtained by multiplying the measured (maximum) chip thickness by the ratio of mean to maximum chip thickness. This ratio is determined readily from a longitudinal section of the chip by means of a microscope and filar-micrometer eyepiece. The ratio of mean to maximum chip thickness varies with steel hardness, being 91 per cent for the annealed steel tested.

The effect of cutting speed upon the chip-thickness ratio of the annealed steel tested is shown in Fig. 12. It is evident that an increase in cutting speed results in a higher chip-thickness ratio, i.e., a decrease in the chip thickness.

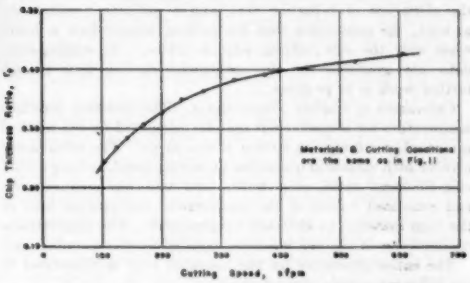

FIG. 12 EFFECT OF CUTTING SPEED ON CHIP THICKNESS RATIO

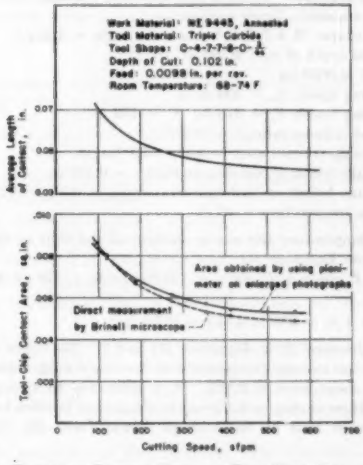

FIG. 13 EFFECT OF CUTTING SPEED ON TOOL-CHIP CONTACT AREA

Tool-Chip Contact-Area Tests. With constant workpiece material, the cutting speed has a profound effect on the size and shape of the tool-chip contact area. For any given tool, the contact area decreases with an increase in speed, other factors remaining constant. For the annealed steel, this is illustrated in Fig. 13. Note that the areas as obtained by planimetric measurement agree well with those derived from a plot using the Brinell microscope. The upper curve in Fig. 13 shows

how the average length of contact of the chip and tool m, is affected by cutting speed.

The decrease in contact area at increased cutting speeds is a significant factor in the higher cutting temperatures experienced at greater cutting speeds.

Cutting Speed—Cutting Temperature Tests. The effect of cutting speed upon cutting temperature is shown in Fig. 14. The upper line labeled "conventional turning" is from a previous paper (7) by one of the authors, and represents the relationship experienced when both the side cutting edge and nose radius are the active cutting portions of the tool. The lower curve portrays the same type of relationship, i.e., $T = CV^n$, when the side cutting edge is the only active part of the tool. Note that the observed cutting temperatures are some 80 to 95 F lower in "orthogonal" cutting with other conditions constant. This decrease is in accord with the discussion of Equation [11], and it confirms, qualitatively at least, the contention that the cutting temperature is lower when only the side cutting edge is active. No cutting-force data are available for the orthogonal cutting tests though further work is in progress.

Calculation of Cutting Temperatures. The tool-chip interface temperature for a specific cut may be calculated by the method presented in a foregoing section of this paper. The calculations involve such measured quantities as cutting speed, cutting forces, chip-thickness ratio, chip width, and tool-chip contact area, and estimated values of the conductivity and specific heat of the chip material at elevated temperatures. The approximate conductivity of the tool has been supplied by the manufacturer.

The entire procedure for the annealed steel is illustrated in the following sample computation:

Sample Computation. Data are as follows:

Work material: NE 9445 mill-annealed, 183 Bhn
Tool material: Triple carbide
Tool shape: 0–4–7–7–8–0–$\frac{3}{64}$ (rake angle = 4 deg.)
Actual depth of cut: 0.102 in.
Feed: 0.0098 ipr
Cutting speed, V_c = 300 sfpm
Cutting forces, F_c = 378 lb; F_t = 192 lb
Chip-thickness ratio, r_t = 0.375
Tool-chip contact area = 5.66×10^{-3} sq in.
Average width of tool-chip contact l = 0.119 in.
Average length of tool-chip contact $m = 4.76 \times 10^{-2}$ in.
Room temperature = 65 F

1 Temperature rise above ambient of the chip at the shear zone from Equation [4]

$$F = F_t \cos \alpha + F_c \sin \alpha = 192 \cos 4 \text{ deg} + 378 \sin 4 \text{ deg} = 218 \text{ lb}$$

$$V_f = V_c r_t = 300 \times 0.375 = 112.5 \text{ fpm}$$

The fraction B_1 in Equation [4] is 0.1. The mean specific heat at the average temperature of the chip during deformation at the shear zone is 0.125. It is necessary to estimate the temperature of chip as it leaves the shear zone in order to obtain the specific heat at the average temperature. By Equation [4]

$$(\theta_s - \theta_0)_{avg} = \frac{0.875\,[378 \times 300(1 - 0.1) - 218 \times 112.5]}{778 \times 0.125 \times 0.281 \times 300 \times 12 \times 0.0098 \times 0.102} = 683 \text{ F}$$

and the temperature of the chip as it leaves the shear zone θ_s, is

$$683 + 65 = 748 \text{ F (above zero)}$$

2 Criterion for the applicability of Equation [12]. The quantity

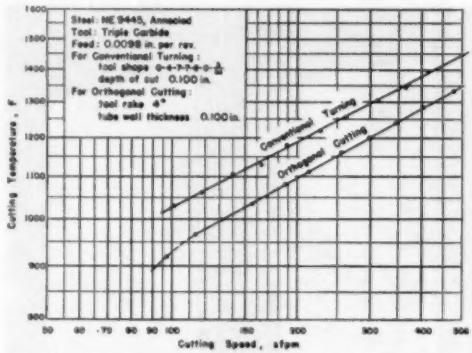

FIG. 14 EFFECT OF CUTTING SPEED ON TOOL-CHIP INTERFACE TEMPERATURE

$$\frac{V_f m}{4k} > 5.$$

At 748 F the specific heat of the chip, c = 0.145 Btu/(lb)(deg F) and the conductivity, $K = 5.2 \times 10^{-4}$ Btu/(in.²)(sec)(deg F/in.). The density of the chip, ρ = 0.281 lb per cu in. The thermal diffusivity

$$k = \frac{K}{c\rho} = \frac{5.2 \times 10^{-4}}{0.145 \times 0.281} = 0.01276 \text{ in.}^2 \text{ per sec}$$

$$\frac{V_f m}{4k} = \frac{112.5 \times 12 \times 4.76 \times 10^{-2}}{60 \times 4 \times 0.01276} = 21.0$$

Therefore Equation [12] may be used.

3 Determination of the proportion of the interface heat going into the chip, i.e., the fraction B_2. The heat liberated per unit time per unit area at the interface

$$q = \frac{FV_f}{J \times \text{contact area}} = \frac{218 \times 112.5}{60 \times 778 \times 5.66 \times 10^{-3}} = 92.8 \text{ Btu/(in.}^2\text{)(sec)}$$

$$l = 0.119 \text{ in.}, m = 4.76 \times 10^{-2} \text{ in.}, l/m = 2.5$$

The shape factor from Fig. 6, (or Equation [9]) = 0.272. The thermal conductivity K_t of the triple carbide used in this investigation is reported by the manufacturer as approximately 0.100 cal/(cm²)(sec)(deg C/cm) or 0.000559 Btu/(in.²)(sec)(deg F/in.) at room temperature. Information concerning the conductivity at elevated temperature is lacking; however, slight changes will have a negligible effect on the fraction B_2. By Equation [14]

$$683 + \frac{4}{3(\pi)^{1/2}} \frac{B_2 \times 92.8}{5.2 \times 10^{-4}} \left[\frac{0.01276 \times 4.76 \times 10^{-2}}{112.5 \times 12/60}\right]^{1/2} = \frac{8(1 - B_2) \times 92.8 \times 0.119 \times 0.272}{\pi \times 0.000559}$$

from which

$$683 + 694\,B_2 = 13{,}685(1 - B_2)$$

and B_2 = 0.904, i.e., 90.4 per cent of the heat liberated at the interface will be carried away by the chip, and the remaining 9.6 per cent goes into the tool. (Radiation and convection losses are neglected.)

4 The final tool-chip interface temperature by Equation [16]

$$\theta_t = 748 + \frac{0.904}{9(5\pi)^{1/3}} \frac{218}{778 \times 5.2 \times 10^{-4} \times 0.119} \left[\frac{0.01276 \times 112.5}{4.76 \times 10^{-2}}\right]^{1/3}$$

from which

$$\theta_t = 748 + 626 = 1374 \text{ F}$$

For the same cutting conditions the temperature as determined by the toolwork thermocouple was 1300 F (Fig. 15), or approximately 5.7 per cent lower.

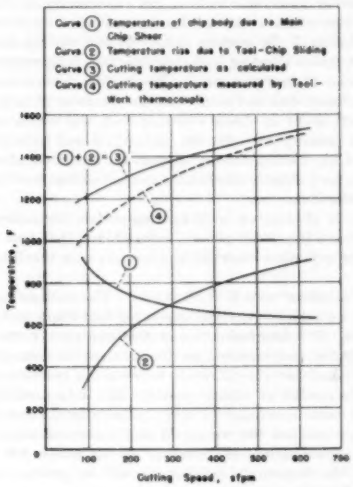

FIG. 15 COMPARISON OF CALCULATED AND MEASURED TOOL-CHIP INTERFACE TEMPERATURES

Tabulation of Cutting-Temperature Results. The tool-chip interface temperatures have been calculated for a number of cutting speeds on the mill-annealed NE 9445 steel. The calculated and measured interface temperatures are summarized in Table 1.

TABLE 1 SUMMARY OF CALCULATED AND MEASURED INTERFACE TEMPERATURES

Actual depth of cut: 0.102 in. Tool: Triple carbide
Feed: 0.0098 ipr Tool shape: 0-4-7-7-8-0-$^1/_{32}$
Room temperature: 65 F

Cutting speed sfpm	Temp of chips leaving shear zone, deg F, (θ_s)	Temp rise at contact surface of chips due to rubbing on tool, deg F	Calculated tool-chip interface temp, deg F	Measured tool-chip interface temp, deg F[a]	Difference per cent
100	940	269	1209	1030	17.4
200	800	507	1307	1190	9.8
300	748	626	1374	1300	5.7
400	719	713	1432	1380	3.8
500	703	781	1484	1445	2.7
600	696	827	1523	1502[b]	1.4

[a] From reference (7), reproduced as the upper curve in Fig. 15.
[b] Extrapolated from experimental results.

The results are shown graphically in Fig. 15. Note the effect of cutting speed upon each component of the tool-chip interface temperature. At low speeds the principal factor is chip deformation at the shear zone, the temperature rise due to rubbing of the chip on the tool being relatively small. At high speeds the distribution is reversed and the increase in temperature due to chip-tool rubbing is greater than that caused by chip shear. Obviously, at some speed (approximately 300 sfpm in the present case), the two components of the tool-chip interface temperature are equal. The fact that the two components have opposite trends with increasing speed accounts for the relatively small (approximately 0.2) exponent in the cutting speed - cutting temperature equation, $T = CV^n$.

The effect of cutting speeds upon the temperature due to chip shear closely parallels the relationship of cutting speed to chip hardness and to chip thickness, as reported in a previous paper (7). The decrease in the temperature due to chip shear as well as the drop in chip hardness and chip thickness as the speed is increased is due to the lesser degree of shearing deformation at the shear zone, which results from the decrease in tool-chip friction.

A comparison of the upper curves in Fig. 15 reveals that the measured and calculated tool-chip interface temperatures are quite divergent at low speeds but that the difference becomes very small at speeds of 500 to 600 sfpm. The difference is due largely to the fact that convection and radiation losses were neglected and since the proportionate heat loss is higher at low speeds, the difference should be correspondingly greater.

Considering that several approximations, of necessity, were employed in the theoretical analysis, it appears that the calculated and measured tool-chip interface temperatures are in excellent agreement. Further refinements undoubtedly are possible, particularly with reference to the proportion of heat left in the workpiece in turning, and to the latent energy left in the chip due to deformation. These factors, however, do not affect the validity of the method employed in this investigation.

CONCLUSIONS

The following conclusions are based on conditions within the limits of this investigation:

1 The cutting forces decrease with an increase in cutting speed.

2 The contact area at the tool-chip interface decreases with an increase in cutting speed.

3 The tool-chip interface temperature is composed of two components: (*a*) that due to chip deformation at the shear zone, and (*b*) that due to friction on the tool face.

4 At low cutting speeds the principal factor affecting tool-chip interface temperature is the deformation at the shear zone.

5 At higher cutting speeds the tool-chip friction is an important factor in the interface temperature.

6 An increase in cutting speed lessens the temperature rise at the shear zone, and increases the temperature rise due to the tool-chip friction.

7 The proportion of the "interface" heat (the fraction, B_3) going to the chip increases with an increase in cutting speed. The variation is from about 68 per cent at 100 sfpm to 94.5 per cent at 600 sfpm.

8 Lower tool-chip interface temperatures are encountered in orthogonal cutting than obtain with conventional turning in which the nose radius is an active part of the tool.

9 Tool-chip interface temperatures may be calculated with reasonable accuracy by the methods developed in this investigation.

ACKNOWLEDGMENT

The authors herewith express their appreciation to Dr. Frederick Seitz, Professor of Physics at the University of Illinois, for the valuable advice so kindly given during the preparation of this manuscript.

BIBLIOGRAPHY

1 "Die Messung der Schneidentemperatur beim Abdrehen von Flusseisen," by K. Gottwein, *Maschinenbau*, vol. 4, 1925, pp. 1129–1135.

2 "The Measurement of Cutting Temperatures," by E. G. Herbert, Proceedings of The Institution of Mechanical Engineers, London, England, vol. 1, 1926, pp. 289–329.

3 "Über die Bestimmung des Temperaturfeldes beim Spanablauf," by F. Schwerd, *Zeitschrift des Vereines deutscher Ingenieure*, vol. 77, 1933, pp. 211–216.

4 "Cutting Temperatures Developed by Single-Point Turning Tools," by O. W. Boston and W. W. Gilbert, Transactions ASM, vol. 23, 1935, pp. 703–726.

5 "Testing for Machinability by Measuring Cutting Temperature and Tool Wear," by H. Schallbroch, H. Schaumann, and R. Wallichs, Vorträge der Hauptversammlung 1938 der Deutschen Gesellschaft für Metallkunde, VDI Verlag, 1938, pp. 34–38. Translation by Henry Brutcher, Altadena, Calif.

6 "Progress Report No. 1 on Tool-Chip Interface Temperatures," by K. J. Trigger, Trans. ASME, vol. 70, 1948, pp. 91–98.

7 "Progress Report No. 2 on Tool-Chip Interface Temperatures," by K. J. Trigger, Trans. ASME, vol. 71, 1949, pp. 163–174.

8 "Tool-Life and Balance of Heat in Lathe Work," by R. Woxen, Proceedings of the Royal Swedish Institute for Engineering Research, No. 142, 1937. (Handlingar Nr. 142, Ingeniörs Vetenskaps Akademien, Stockholm, Sweden.)

9 "Basic Mechanics of the Metal-Cutting Process," by M. E. Merchant, *Journal of Applied Mechanics*, Trans. ASME, vol. 66, 1944, p. A-168.

10 "The Latent Energy Remaining in a Metal After Cold Working," by G. I. Taylor and H. Quinney, Proceedings, of the Royal Society of London, series A, vol. 143, 1934, pp. 307–326.

11 "The Emission of the Latent Energy Due to Previous Cold Working When a Metal is Heated," by H. Quinney and G. I. Taylor, Proceedings of the Royal Society of London, series A, vol. 163, 1937, pp. 157–181.

12 "Chip Formation, Friction, and Finish," by H. Ernst and M. E. Merchant, The Cincinnati Milling Machine Company, Cincinnati, Ohio, 1940, p. 5.

13 "Distribution of Heat Generated in Drilling," by A. O. Schmidt and J. R. Roubik, Trans. ASME, vol. 71, 1949, pp. 245–252.

14 Metals Handbook, 1948, American Society for Metals, Cleveland, Ohio, pp. 313–314.

15 "Flow of Heat in Metals," by J. B. Austin, published by The American Society for Metals, Cleveland, Ohio, pp. 62–69.

16 "Theoretical Study of Temperature Rise at Surfaces of Actual Contact Under Oiliness Lubricating Conditions," by H. Blok, Proceedings of the General Discussion on Lubrication and Lubricants, The Institution of Mechanical Engineers, London, England, 1938, pp. 222–235.

17 "Moving Sources of Heat and the Temperature at Sliding Contacts," by J. C. Jaeger, Proceedings of the Royal Society, NSW, vol. 76, 1942, pp. 203–224.

18 "Introduction to the Mathematical Theory of the Conduction of Heat in Solids," by H. S. Caralaw, Macmillan and Company, London, England, 1921, p. 150.

Discussion

M. EUGENE MERCHANT.[6] This paper is an important and useful contribution to the literature on metal cutting and marks a real advance in the knowledge and science connected with the machining process. The authors are to be heartily congratulated on the fine piece of work reported here. The great importance of this work resides not only in the genuine scientific contribution which it makes, but also in the fact that the field of knowledge to which it contributes relates to the temperature at the chip-tool interface, which is one of the most important factors controlling tool life in practice. Thus this analytical evaluation holds forth the promise of bringing much closer the possibility of directly estimating cutting-speed tool-life relationships from simple calculations involving only the simple physical and mechanical properties of the work material and tool material being used.

The fact that the analysis still involves several uncertainties and assumptions on which further clarification is desirable does not lessen its importance. The analysis as it stands can be *used*—it can be used to estimate cutting temperatures in many types of machining operations where direct temperature measurement is not practical. By so doing it can provide important information related to observed tool-life behavior. Thus this analysis can and will, we are sure, be put to immediate use in machinability investigations.

The writer would like to take this opportunity to clarify the implications of one of the conclusions arrived at by the authors. In conclusion 4, the authors state "At low cutting speeds the principal factor affecting tool-chip interface temperature is the deformation at the shear zone." We would like to point out that this conclusion does not mean that the control of chip friction at low speeds, as by an effective cutting fluid, will have a negligible effect on temperature. On the contrary, it will have a marked effect! Chip friction directly controls the size of the shear angle which, in turn, directly controls the amount of deformation taking place at the shear zone.

Again, in closing, we wish to congratulate the authors on a very fine and important piece of research and shall look forward to further important contributions from them in this field.

A. O. SCHMIDT[7] AND J. R. ROUBIK.[8] The authors have contributed a good mathematical analysis of tool-chip interface temperatures. It is interesting to note that at a given cutting speed the computed temperatures are greater than the measured temperatures and that the difference between the two becomes progressively smaller at higher speeds. The data presented here could be more informative if they would extend far enough to determine whether the computed and measured temperatures will be approximately the same at speeds above 600 fpm or whether the measured temperatures will be greater than the computed temperatures.

Taylor and Quinney (1)[9] report that 10 to 15 per cent of the energy of deformation does not appear as sensible heat but remains as latent energy in metals which have been cold-worked to an excessive degree. They also indicate, however, that the percentage of latent energy in cold-worked metals depends on the material and the type and amount or degree of cold work applied. Observations of work and power required to cut metals by drilling, obtained with a calorimeter mounted on a dynamometer registering torque and thrust, indicate that all of the work done in a machining operation (within 1 to 2 per cent) appears as sensible heat (2). Some experiments of Joule (3) and also Favre (4) and Hirn (5), in determining the value for the mechanical equivalent of heat, which is accepted universally, involved deformation or cold-working of metal. The degree of cold-work in the chips or workpiece is not sufficiently great to justify the assumption that 10 to 15 per cent of the total work does not appear as sensible heat even assuming that Taylor and Quinney are correct. The proportion of the energy of deformation which appears as heat in a machining operation is very close to 100 per cent.

Below a cutting speed of approximately 250 fpm the proportion

[6] Research Physicist, The Cincinnati Milling Machine Co., Cincinnati, Ohio. Mem. ASME.

[7] Research Engineer, in charge of Metal-Cutting Research, Kearney and Trecker Corporation, Milwaukee, Wis. Mem. ASME.

[8] Research Department, Kearney and Trecker Corporation, Milwaukee, Wis. Jun. ASME.

[9] Numbers in parentheses refer to the References at the end of this discussion.

of the total heat which appears in the chip will increase with an increase in speed and chip thickness (6). Beyond 250 fpm the proportion of heat in the chips remains almost constant with increasing speed but will increase with increasing chip thickness.

The graph in Fig. 11 showing cutting forces decreasing with increasing cutting speeds, especially the 25 per cent reduction in tangential cutting force from 100 to 600 fpm, is very misleading. Similar statements have appeared in the metal-cutting literature for the last twenty years but it has not been possible to verify these reports with other measurements or to gain the apparent advantage in practice, namely, to remove a larger amount of metal with less horsepower. Higher cutting speeds in machine tools often have produced much better finishes, less objectionable vibrations and chatter, and have made the operation, as such, appear much smoother. But nowhere have we been able to attribute a substantial reduction in power consumption to lower cutting forces at higher speeds. Usually it has been a more efficient gear train, motor loading, and better lubrication as well as operating temperature to which any horsepower reduction or saving could be ascribed. Considering these factors it is possible to remove 70 to 100 per cent more material at 50 per cent above rated capacity than at the rated capacity of a machine tool.

There have been other investigations which did not show any such reduction in tool forces at higher cutting speeds (7). In our previous investigation of high-speed milling a calorimeter was used to measure power requirements (8). Although it was found that the rake angles would affect the magnitude of the tool forces, no such influence, to any considerable degree, due to variation of cutting speed could be detected. In the evaluation of several thousand calorimetric power measurements from 200 to 1200 fpm cutting speed, the variations were within ±5 per cent without exhibiting a marked tendency to be lower at higher cutting speeds.

In order to simulate as closely as possible the conditions of the test data plotted in Fig. 11, a number of test bars of NE 9445, 196-207 Bhn, were machined in a milling calorimeter at various cutting speeds, and, as long as the feed per tooth remained constant, no remarkable variations in the cutting forces could be observed at cutting speeds between 300 and 1200 fpm.

However, this entire question of the influence of cutting speed on tool forces is so important that it might be worth while to have a special ASME committee make an independent investigation.

Our experience agrees with the conclusion that the contact area at the tool-chip interface decreases with an increase in cutting speed, at least when milling steel, up to cutting speeds of about 600 fpm. At higher speeds the area of contact will soon increase because of more rapid tool wear.

REFERENCES

1 "The Latent Energy Remaining in a Metal After Cold Working," by G. I. Taylor and H. Quinney, Proceedings of the Royal Society of London, series A, vol. 143, 1934, pp. 307–326.

"The Emission of the Latent Energy Due to Previous Cold Working When a Metal Is Heated," by H. Quinney and G. I. Taylor, Proceedings of the Royal Society of London, series A, vol. 163, 1937, pp. 157–181.

2 "A Thermal-Balance Method and Mechanical Investigation for Evaluating Machinability," by A. O. Schmidt, W. W. Gilbert, and O. W. Boston, Trans. ASME, vol. 67, 1945, pp. 225–232.

3 "On the Mechanical Equivalent of Heat," by J. P. Joule, Philosophical Transactions of the Royal Society of London, 1850, pp. 61–82.

4 "Recherches sur l'equivalent mechanique de la chaleur," by P. A. Favre, Comptes Rendu de l'Academie des Sciences, Paris, France, vol. 46, 1858, pp. 337–340.

5 "Theorie Mechanique de la Chaleur," by G. A. Hirn, vol. 1, third edition, Gauthier-Villar, Paris, France, 1875, pp. 91–118.

6 "Distribution of Heat Generated in Drilling," by A. O. Schmidt and J. R. Roubik, Trans. ASME, vol. 71, 1949, pp. 245–252; *The Tool Engineer*, vol. 21, 1948, pp. 20–23.

7 "Determining Tool Efficiency in High-Speed Milling," by W. E. Brainard, *Mechanical Engineering*, vol. 66, 1944, pp. 301–302.

8 "Radial Rake Angle in Face Milling," by J. B. Armitage and A. O. Schmidt, *Mechanical Engineering*, vol. 67, 1945, pp. 403–406; vol. 67, 1945, pp. 453–456; vol. 67, 1945, pp. 507–510. *Canadian Machinery and Manufacturing News*, vol. 56, 1945, pp. 114–116 and 227; vol. 56, 1945, pp. 81–84 and 156; vol. 56, 1945, pp. 90–93.

AUTHORS' CLOSURE

The authors are grateful to Dr. Merchant for his kind and most encouraging remarks, and to Dr. Schmidt and Mr. Roubik for their pertinent discussion on the subject matter of this paper.

As a result of this study of the mechanism of heat generation during metal-cutting operations, the tool-chip interface temperature has been found to be made up of two components, namely, (*a*) that due to chip deformation at the shear zone and (*b*) that due to friction at the interface. In conclusion 4 of the paper, by stating that at low cutting speeds the principal factor affecting tool-chip interface temperature is the deformation at shear zone, the authors meant that, under the stated conditions, a *relatively* smaller proportion of the final interface temperature is contributed by tool-face friction as compared with a much greater proportion at high cutting speeds. By no means, should this be confused with the fact that the change of chip friction will have an appreciable effect on cutting temperature at low speeds. Any condition which reduces tool-chip friction will increase the shear angle which, in turn, lessens the amount of shearing deformation at the shear zone. This is in agreement with Dr. Merchant that at low cutting speeds an effective cutting fluid will have a marked effect in reducing cutting temperature.

Dr. Merchant's comment on the possibility of correlating the two important practical questions of tool life and machinability with cutting temperature is certainly a very pertinent one. As a matter of fact, this is one of the objectives of the present theoretical study.

Dr. Schmidt and Mr. Roubik have raised some interesting points, each of which will be considered in subsequent discussion.

With respect to the agreement between measured and calculated temperature above 600 sfpm—no test was conducted above that approximate limit. The succeeding step would have resulted in a cutting speed of about 700 sfpm or a chip velocity of about 300 fpm. A hot chip moving at this rate presents obvious difficulties of manual manipulation.

The comments concerning the proportion of the energy of deformation which remains latent in the deformed metal are, in fact, not germane to the case in so far as the method is concerned.

Reliable data on the proportion of latent energy under the conditions of these tests are actually nonexistent. The data by Taylor and Quinney are cited by such authorities as Barrett[10] and Seitz[11] as being the most acceptable information available. Whether the numerical values of Taylor and Quinney may be applied rigidly in the present case is, as stated in the paper, subject to further scrutiny. The same may well be said regarding the proportion of total heat going into the workpiece. The authors used the data by Schmidt and Roubik obtained while drilling a magnesium alloy (of low work-hardening capacity), for the proportion of heat going into the workpiece when turning steel with a single-point tool. In the latter, the range of speeds was considerably higher than that employed in drilling, and the work material was of entirely different strain-hardening properties. Thus the data of Schmidt and Roubik may not apply very well, but it represented the best information available. If one assumption is acceptable, the other should be also. The authors

[10] "Structure of Metals," by C. S. Barrett, McGraw-Hill Book Company, Inc., New York, N. Y., 1943.

[11] "Physics of Metals," by F. Seitz, McGraw-Hill Book Company, Inc., New York, N. Y., 1943.

chose to alter neither until further information is available. They reiterate that these approximations will not introduce serious errors in so far as the calculated temperatures are concerned, and they do not affect the method at all.

However, the problem of latent energy in deformed metal is a pertinent one, and the authors wish to discuss it further.

When a metal is deformed plastically and the crystal structure distorted (either according to the block concept of slip or the more recent theory of dislocations), a part of the energy of deformation is retained within the crystal structure, and this latent energy is associated with the increased strength and hardness of the deformed metal. Comparison of a cold-rolled steel strip to the same metal in the annealed state is a familiar example. When the deformed metal is heated, the latent energy is released prior to the recrystallization of the distorted crystal structure. Such recrystallization (which may be very fast at sufficiently high temperatures) restores the distorted metal to its original undeformed state.

In order that the crystal structure of a metal be distorted it must be plastically deformed at a temperature below that at which recrystallization takes place. This is referred to as "cold-working." If the plastic deformation is imposed at such a temperature that recrystallization may occur simultaneously with the deformation, the metal is "hot-worked," and no crystal deformation or latent energy remains in the metal, i.e., hot-working does not harden or strengthen the metal. The distinction between hot and cold-working comes then not at some arbitrary temperature *but only in relation to the recrystallization temperature of the particular metal concerned*. The recrystallization temperature of a chosen metal is dependent upon a number of factors, the more important being the amount of deformation, the temperature at which it is recrystallized, and the time at that temperature. Steels may be hot-worked in the general vicinity of 1400 F. Tungsten is cold-worked at 1800 F whereas lead is hot-worked at room temperature. The creep of lead at room temperature is a manifestation of this hot-working. It does not work-harden at room temperature; otherwise, the plastic deformation would cease.

Hirn's experiment to evaluate the mechanical equivalent of heat (not very accurately) by deforming lead could be based on nearly 100 per cent conversion since the lead was hot-worked. Joule's figures on the interconversion of heat energy and mechanical energy have as their basis the agitation of water by paddles. Taylor and Quinney conducted their experiments by twisting various metals. The magnitude of shearing strain imposed was less than that encountered at the shear zone during cutting. On the other hand, the rate of straining is much higher in the latter case, and this may have some effect on the amount of latent energy. Any release of stored energy is prefaced by recovery which, with recrystallization, is a time-dependent phenomenon. The time in the shear zone is of the general order of 10^{-6} sec and inconsequential from the standpoint of any recovery or recrystallization during deformation. Furthermore, the maximum temperature at the shear zone in this series of tests was about 940 F or too low for any recrystallization of the steel, except possibly over extended periods of time.

The proportion of latent energy stored in the deformed chip is a moot point. A recent publication[12] describes methods to determine the proportion of total work of cutting absorbed by the deformed chip as latent heat. An average value of approximately 3 per cent is reported in the case of drilling annealed aluminum. No data on steel were given, and it is questionable that the data on aluminum can be applied to steel since the recrystallization temperature of the former is reported to be about 300 F, or less than one third that of steel. It is not unreasonable that the deformed aluminum chip could attain such a temperature that recovery and perhaps partial recrystallization would ensue. Such a change would result in the low percentage of latent energy.

According to Barrett,[10] Koehler in his studies of the latent energy of deformation reports figures in close agreement with those of Taylor and Quinney. Other investigators as discussed by Barrett report higher proportions of latent energy.

Because of the high degree of strain at the shear zone, the phenomena of saturation may be involved. If so, the 10 to 15 per cent, as reported by Taylor and Quinney, would be reduced somewhat. On the other hand, the extremely high rate of straining may possibly increase the energy retained. Dr. Merchant in his discussion of a paper[13] by one of the authors shows that the per cent increase in hardness of the chip bears a linear relationship to the shearing strain undergone by the chip at the shear zone. Such a relationship does not indicate saturation. At low cutting speeds (where the shearing strain is greatest) the hardness of the chip may be some 300 per cent of the hardness of the annealed steel workpiece.

If it is held that practically 100 per cent of the energy of deformation appears as heat, then it must with equal vigor be held that the chip is no harder than the workpiece. Observations on steel, with which this report is concerned, reveal such is not the case.

The actual value of the proportion of energy of deformation which remains latent in the deformed chip can be determined only by further carefully conducted experiments on material deformed under conditions encountered at the shear zone. When such information is available, it can be incorporated into Equation [4] of the paper without difficulty. Similarly, when data for the proportion of total heat conducted back into the workpiece under the conditions of these tests are available, that, too, can be incorporated into Equation [4].

With reference to the comment by Schmidt and Roubik on the trend of cutting forces with speed as shown in Fig. 11 of the paper, the authors fail to see where the curves are misleading. Nothing is said about removing the metal at higher speeds with less horsepower. The combination of tool and work material used in these tests revealed a decrease (approximately 29 per cent) in the cutting force with increase in cutting speed from 100 to 600 sfpm. The work, inch pounds per cubic inch, decreased, owing to less tool-chip friction and, consequently, a thinner chip as shown in Fig. 12. The thinner chip is associated with a shorter length of the shear zone which reduction shows up in lower forces and less work per unit volume of metal removed. The power required is an entirely different matter. Here, one is concerned with the time rate of doing work. At 600 sfpm, the power required is some $4\frac{1}{4}$ times that at 100 sfpm, according to the data in Fig. 11. The confusion lies in the failure to differentiate between work and power.

With respect to the effect of cutting speed upon cutting forces, let it be repeated that Fig. 11, and its counterpart Fig. 12, represent the results obtained under the test conditions of this investigation. Not all combinations of tool and workpiece reveal the trend shown in Fig. 11. When steel is machined with high-speed-steel tools, the forces will increase with an increase in cutting speed (within limits). The same is true of certain cemented carbide-workpiece combinations. The forces may first decrease, then increase, and then decrease again with further increase in speed. This phenomenon is further discussed in a forthcoming paper by the authors.

[12] "Energy Balance of the Metal Cutting Process," by G. I Epifanov and P. A. Rebinder, *Doklady Akademii Nauk SSSR*, vol. 66, 1949, pp. 653–656. Translation by Henry Brutcher, Altadena, Calif.

[13] "Progress Report No. 2 on Tool-Chip Interface Temperatures," by K. J. Trigger, Trans. ASME, vol. 71, 1949, pp. 163–174.

Residual Stresses in Machined Surfaces

By E. K. HENRIKSEN,[1] ITHACA, N. Y.

Experiments on measuring stresses in castings for precision equipment in the early 1930's, led to an investigation of stresses formed by the cutting action. The stress-inducing effect of single-point tools working in steels with varying carbon content has been studied, and methods for computing the stresses induced have been developed. Highly concentrated stresses (up to 100,000 psi) are produced. In ductile materials, such as carbon steel, the stresses are, generally, tensile, in cast iron they are compressive. Methods of investigation are described and data are given for stresses produced in various materials, by various tools, and under various cutting conditions. The possible detrimental effects of the existence of these stresses are discussed.

A RESEARCH project on residual stresses in castings, undertaken by the author in 1933 (1)[2] involved the method of stress determination by removing a layer of metal by a cutting tool (on a planer) and computing the stresses from the subsequent deformation (2); this generally adopted method usually takes the measured deformations at their face values, assuming by implication that no "new" stresses are generated by the cutting action [though some investigators are aware of this possible source of error but hope to eliminate it by using carefully sharpened tools and taking fine cuts only, (2, 3)].

No experimental results, and no data were available on this subject back in the early 1930's, only some vague remarks and mostly to the effect that stresses may be produced by the action of heavy roughing cuts and dull tools (4, 5, 6, 7). This complete lack of information is so much more surprising in view of the knowledge, already present at that time, of the deformation and distortion of grain and structure in and immediately below a machined surface (8, 9, 10).

Under the pressure of this entirely unsatisfactory state of affairs, the author made some preliminary investigations, primarily with the view of establishing a correction to Staeblein's formula (2) for any new stresses that might be generated by the cutting action, but feeling the need for a more complete investigation of this subject, he took it up as an independent project. Reports of earlier work with details of experimental methods have been published before (12, 13, 14). The present paper deals with work done in 1937–1948, and previous results are included here only to the extent necessary for giving a well-rounded picture.

Mechanics of Stress Formation

When metal of the ductile type is cut by a cutting tool the surface layer undergoes heavy distortion. Further, the cutting process is accompanied by heating of the chip and the tool and to a certain extent by local heating of the material under the cutting edge. Consequently a state of stress is induced with maximum stress in the surface.

A prismatic specimen being machined lengthwise by planing or shaping on one side only will bend slightly, the machined side being concave (provided that no "old" residual stresses due to rolling, heat-treatment, bending, straightening, or the like are present to disturb the metal). This observation has been made in numerous experiments with ductile materials, i.e., on various grades of steel (except austenitic manganese steel), and under cutting conditions ranging from very coarse to the finest values of feed and depth of cut. Consequently, the primary residual stress produced under these circumstances is a tension.

The numerical value of the tension is different in the various directions relative to the direction of travel of the tool and has its maximum in a direction parallel to the tool movement (see Figs. 1 and 2). This seems to indicate that the tension to a great extent must depend on the mechanical action of the tool and not,

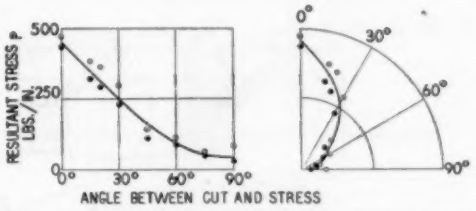

Figs. 1 and 2 The Resultant Stress p Under Various Angles to the Direction of Cut

(Material, 0.35 carbon steel; cutting speed, 52 fpm; depth of cut, 0.02 in.; feed, 0.04 in.; side-cutting tool, $\gamma = 16$ deg; $r = 0.084$ in.)

or only to a less extent, on the thermal effect of the cutting process, because the initial effect of local heating in a certain point would be expected to be approximately equal in all directions which is not the case with the mechanical effect (distortion). A few experiments were made with cooling, the test specimen being totally submerged in cold water, but there was no sign of difference. Further, it was found that higher speeds and higher carbon contents, in general, tend to produce lower tension values, while the scattered and not too consistent evidence available from other sources seems to indicate a rising temperature in the cutting zone, although more and more concentrated, as speed and carbon content increase. This seems further to eliminate the possibility that the tension should be due mainly to local heating, and leaves the distortion as the principal or exclusive source of the tension. In fact, all evidence available until now points in the same direction.

The picture of the distortion of the material is well known from numerous micrographs and publications. The grains near the surface are pulled out parallel to the surface (see Figs. 3 and 4), and appear in the micrographs as thin strings or bands. A little further down in the material the grains take on a pear-shaped form with their thin upper ends bending gradually toward parallelism with the surface.

Incidentally, this gives an explanation of the mechanism of the

---

[1] Head of Materials Processing Department, College of Engineering, Cornell University.

[2] Numbers in parentheses refer to the Bibliography at the end of the paper.

Contributed by the Research Committees on Metal Cutting and Bibliography, and Cutting Fluids, and Production Engineering Division and presented at the Semi-Annual Meeting, St. Louis, Mo., June 19–23, 1950, of The American Society of Mechanical Engineers.

Note: Statements and opinions advanced in papers are to be understood as individual expressions of their authors and not those of the Society. Manuscript received at ASME Headquarters, April 24, 1950. Paper No. 50—SA-27.

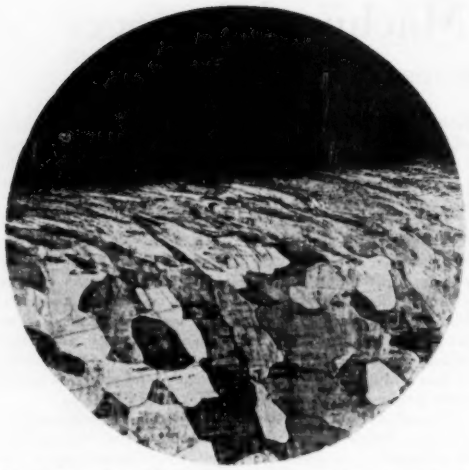

FIG. 3 MICROGRAPH SHOWING DISTORTION OF MATERIAL UNDER A MACHINED SURFACE; MILD STEEL 0.1 PER CENT C; ×120

FIG. 4 MICROGRAPH OF SECTION THROUGH MACHINED SURFACE, SHOWING FRAGMENT OF BUILT-UP EDGE CUT OFF BY TOOL AND EMBEDDED IN SURFACE; MILD STEEL 0.1 PER CENT C; ×65

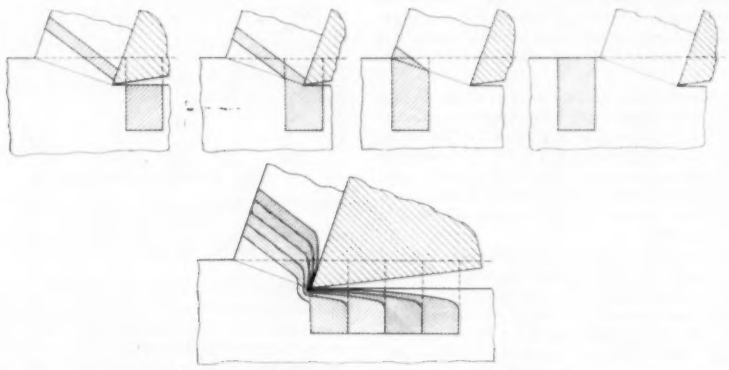

FIG. 5 DIAGRAMMATIC VIEWS OF CHIP FORMATION
(Top, conventional representation of chip formation as a shearing process. Bottom, chip formation by combined shear and additional bending action over cutting edge.)

formation of the built-up edge, Fig. 5. A grain of the metal situated in the path of the cutting edge is captured by the tool and the projecting part of the grain is being carried away embedded in the chip while still in connection with the remaining part of the grain which undergoes the characteristic deformation just described.

The middle portion of the grain is being pulled out to a thin band or string and is finally torn off, not only from the part of the grain that remains in the surface layer, but also from the portion that is carried away in the chip. That middle portion adheres to the front side of the tool, other similar elements are added in the same manner, all together forming the built-up edge.

Although this explanation of built-up-edge formation is somewhat different from those given by Hans Ernst (15), and Hans Ernst and M. Eugene Merchant (16), it is not necessarily in conflict with them; the separation of the thin layers from the rest of the chip material, and their adhesion to the face of the tool in a stationary position embedded between the tool face and the continuously flowing chip would not be possible unless there is a stress distribution with a high sheer stress in a direction forming an acute angle with the tool face (16).

The top part of the portion remaining in the surface has been subjected to a pull while still in solid connection with the rest of the material. This pull has given effect not only to the distortion, but also to a tensile stress, and, when relieved from the pull, the strained part will try to contract, but being prevented from this by the connection with the underlying material it must retain its tension partially.

In order to get a preliminary idea of what happens, let us assume an infinitely large elastic plate with a straight-line boundary, loaded at a point O of the boundary by a tangential force F, Fig. 6. Without going into a detailed stress analysis, it

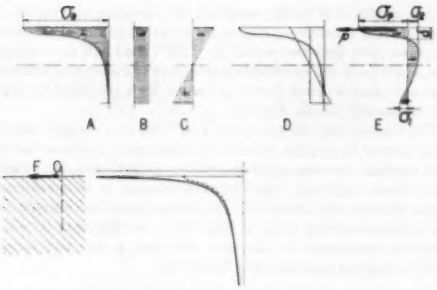

FIG. 6 (*below*) STRESS DISTRIBUTION IN AN ELASTIC PLATE

FIG. 7 (*above*) RESULTING STRESS DISTRIBUTION DURING AND AFTER MACHINING

can be said that tensile (and shearing) stresses will dominate to the right of O, decreasing in value as the horizontal distance from O increases, and also rapidly decreasing in value at increasing distances from the boundary, following a hyperbola.

In cutting metal, the action of the tool is represented by the force F. The workpiece is clamped so that it cannot move (bend) to any appreciable extent during the machining operation, and, therefore, the stress distribution below the surface may be of a similar nature as that in an infinitely large elastic body, except that the material will be subject to plastic flow and the stress rise will be limited by properties inherent in the material. Therefore the stress distribution under the tool edge may be expected something like that shown by the dotted line in Fig. 6.

As the tool moves away the stresses will decrease, but owing to permanent deformations in the material, Fig. 5, some stresses will remain, see Fig. 7(A) (any effect of rise of temperature being ignored). When unclamped, an "elastic" deformation will take place, accompanied by a rearrangement of stresses. The residual tensile stress will act as an eccentric axial-compressive load and cause an axial compression and a lateral bending. These phases are shown in Fig. 7(B), (C), and (D), and the resultant stresses are shown in Fig. 7(E).

These stress curves are not to scale and represent only the principal pattern of the stress distribution. In most cases, such as when machining carbon steel, it will be found that the stress σ_p is dominating, while σ_1 and σ_2 and the depth δ are negligible. Consequently the stress σ_p after unclamping is almost equal to the stress σ_0 induced directly by the cutting.

The exact form of the curve for the stress distribution is not known. We know, however, that the area below the curve represents the resultant p of all stresses σ acting on the layer of thickness δ, taken over a width of 1 in. of material. The resultant p will have the dimension pounds per inch (not square inch), when the stress σ is expressed in pounds per square inch, and p can be considered as located in the surface of the metal, when the thickness δ is negligible, which is usually the case. This is of course an approximation, but it is justified by the results of numerous experiments, as will be explained later.

The stress p is described as *resultant stress*. It constitutes a simple measure of the total stress-inducing effect of the cutting action. In order to avoid any misunderstanding, it must be borne in mind that it is not a surface stress in the common physical sense, but its dimension of pounds per inch (not square inch) is simply a consequence of the fact that it is the resultant of some stresses located within a negligible distance from the surface.

METHOD OF STRESS COMPUTATION

As described, we consider the residual stress as a surface tension p lb per in. width acting as an axial load on a specimen B in. wide, H in. high, and $2L$ in. long (see Fig. 8). The load on the total width B of the specimen amounts to pB lb.

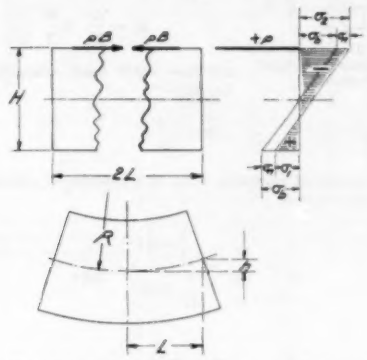

FIG. 8 DIAGRAM OF FORCES AND STRESSES IN SPECIMEN AFTER LENGTHWISE MACHINING OPERATION

This load now induces over the cross-section area BH, an evenly distributed normal compression stress

$$\sigma_n = -\frac{pB}{BH} = -\frac{p}{H} \text{ psi}$$

and then a set of bending stresses to be calculated as follows:

The bending moment is

$$M = {}^1/_4 HpB \text{ in-lb}$$

the moment of inertia of the cross section is

$$I = {}^1/_{12} BH^3 \text{ in.}^4$$

and the section modulus is

$$Z = {}^1/_6 BH^2 \text{ in.}^3$$

Thus the stresses from the bending moment are

$$\sigma_b = \pm \frac{M}{Z} = \pm \frac{\frac{1}{4}HpB}{\frac{1}{6}BH^2} = \pm \frac{3p}{H} \text{ psi}$$

and the combined elastic stresses induced by the contraction and bending at the lower and upper extreme fibers are

$$\left.\begin{matrix}\sigma_1 \\ \sigma_2\end{matrix}\right\} = \sigma_n + \sigma_b = \begin{cases} \dfrac{2p}{H} \\ -\dfrac{4p}{H} \end{cases} \text{ psi}$$

These combined stresses are altogether small in comparison with the stress σ_p induced directly by the cutting, and the latter compression stress σ_2 which should appear at the upper side of the specimen (machined surface) is completely overwhelmed by σ_p.

The curvature of the specimen is constant throughout its length. This has been ascertained by repeated measurements at an early stage of the experiments.[3] The bent form is part of a

[3] Bibliography (12), pp. 13–16.

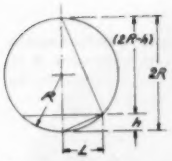

FIG. 9 DIAGRAM OF DEFLECTION AND CURVATURE

circle, consequently the curvature is defined completely by measuring the deflection h in the middle of a length $2L$ (see Fig. 9). We then have

$$L^2 = (2R - h)h$$

$$R = \frac{L^2}{2h} + \frac{h}{2}$$

and since $h/2$ is small compared with $L^2/(2h)$

$$R = \frac{L^2}{2h}$$

With radius of curvature R in. and modulus of elasticity E psi, we have further

$$\frac{1}{R} = \frac{M}{EI} = \frac{\frac{1}{2}HpB}{\frac{1}{12}EBH^3} = \frac{6p}{EH^2}$$

and

$$\frac{2h}{L^2} = \frac{6p}{E_R{}^2}$$

Now this equation is written

$$h = \frac{3L^2}{E} p \frac{1}{H^2}$$

and it is clear that if p is constant, the deflection h should give a straight line when plotted against $1/H^2$.

If a specimen is being machined by repeated cuts under the same cutting conditions, it is to be expected that p shall remain constant, and that the points $(h, 1/H^2)$ shall fall in a straight line, apart from the inevitable scatter due to measuring inaccuracies, etc., and we have hereby a means for a graphical fairing of the measuring results, Fig. 15.

The feature that the points $(h, 1/H^2)$ fall in a straight line has been proved in a great number of cases and confirms the fact that constant cutting conditions give constant value for p (apart from those materials where work-hardening to a considerable depth changes the situation). It also supports the opinion that the tension-carrying layer is very thin; so thin that it will be removed completely by the next cut, and a new one formed.

The foregoing equation may be written

$$p = \frac{E}{3L^2} \frac{h}{\frac{1}{H^2}}$$

Hence it is seen that a mean value for p from a number of measurements can be calculated from the slope $h \Big/ \frac{1}{H^2}$ of the straight line.

EXPERIMENTS ON PLAIN CARBON STEELS

Experiments on Planing and Shaping. The carbon steels used during these experiments are, in short, termed 0.1 carbon steel, etc. In Table 1 is given a specification of their analysis and mechanical properties. Experiments were carried out with square-end and side-cutting tools. The cutting was done on a planer and a shaper.

The square-end tool, Fig. 10, has the great advantage that it involves orthogonal cutting, this being the simplest possible for experimental and scientific purposes.

TABLE 1 ANALYSIS AND MECHANICAL PROPERTIES OF CARBON STEELS USED IN PLANING EXPERIMENTS

Designation used	Analysis					Mechanical properties as delivered					
	C	Si	Mn	P	S	Ultimate stress		Yield point		Elongation	Contraction
	%	%	%	%	%	kg/mm^2	psi x 10^{-3}	kg/mm^2	psi x 10^{-3}	%	%
0.10 Carbon steel						32 - 38	45 - 52	22	31	28 10x dia.	60
0.35 Carbon steel	approx. 0.35	approx. 0.25	approx. 1.00	max. 0.040	approx. 0.070	approx. 60	approx. 85	approx. 35	approx. 49	16 10x dia.	
0.50 Carbon steel	approx. 0.50	approx. 0.25	approx. 1.00	max. 0.040	approx. 0.070	approx. 70	approx. 98	approx. 40	approx. 90	13	
0.70 Carbon steel	0.70	approx. 0.27	approx. 0.40	max. 0.020	max. 0.015	85	120	approx. 45	approx. 65	approx. 10	

Designation used	Annealing for experimental purpose
0.10 Carbon steel	Heated to 915° C. (1679° F.) in 1/2 hour, cooled slowly
0.35 Carbon steel	Heated to 850° C.(1562° F.) in 1/2 hour, cooled slowly
0.50 Carbon steel	Heated to 820° C.(1508° F.) in 1/2 hour, cooled slowly
0.70 Carbon steel	Heated to 760° C.(1400° F.) in 1/2 hour, cooled slowly

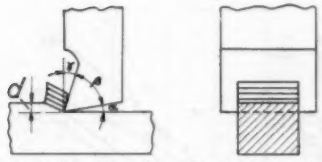

FIG. 10 SQUARE-END TOOL WITH NOTATIONS OF ANGLES AND DEPTH OF CUT

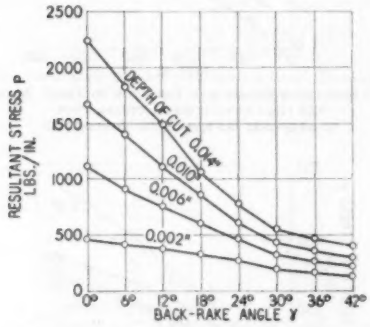

FIG. 11 VARIATION OF RESULTANT STRESS p IN RELATION TO BACK-RAKE ANGLE OF TOOL AND DEPTH OF CUT

(Square-end tool. Material, 0.10 carbon steel; depth of cut, 0.014 in., 0.01 in., 0.006 in., and 0.002 in.)

Some series of experiments were made in order to determine the effect on the resultant stress p of varying back-rake angle γ and depth of cut, and also the effect of varying carbon content in the material. In Fig. 11 is shown a summary of the results of these experiments on 0.10 carbon steel. The resultant stress values are gradually increasing with depth of cut and decreasing back-rake angle, thoroughly in accordance with the opinion set forth that the tension has a direct relation to grain distortion.

A further series of experiments were made on a number of different carbon steels varying from 0.1 to 0.7 per cent C. The depth of cut was chosen as 0.008 in., the back-rake angles γ were nearly the same as before, only with a slight variation due to grinding, and a tool with a —2-deg back-rake angle was added. The results are shown in Fig. 12. As before, the resultant stress increases with decreasing back-rake angle and with decreasing carbon content in the material, all in accordance with increase in grain distortion, but not in accordance with cutting temperature, the latter being higher in the case of higher carbon content.

When leaving the square-end tool and changing to tools of other forms, such as the ordinary round-nosed side-cutting tool, some more variables are introduced in the problem. Before going to an extended series of experiments with the side-cutting tools, therefore, experiments were made to investigate the influence of some of the elements constituting the geometric form of such a tool.

The contour of a round-nosed side-cutting tool in action is shown in Fig. 13. It was shown by numerous tests in the earlier experiments that normally in this case depth of cut d had no effect on the resultant stress values apart from those materials (other than plain-carbon steels), where a work-hardening took place to a considerable depth.

This result is only what might be expected from the fact that the conditions in the finished surface are controlled by the cutting action at the nose of the tool (point c), and not by the location

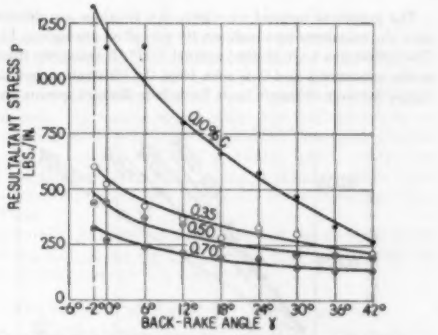

FIG. 12 VARIATION OF RESULTANT STRESS p IN RELATION TO BACK-RAKE ANGLE OF TOOL IN VARIOUS CARBON STEELS

(Square-end tool. Cutting speed 15.7 fpm; depth of cut 0.008 in.)

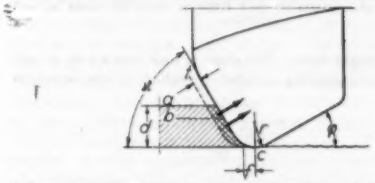

FIG. 13 GEOMETRY OF CUTTING FOR A ROUND-NOSE SIDE-CUTTING TOOL

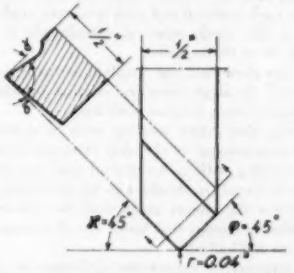

FIG. 14 DIMENSIONS AND DATA FOR EXPERIMENTAL SIDE-CUTTING TOOL

a or b of the unfinished surface. For the same reason no appreciable effect may be expected from variations (within normal limits) of the side-cutting-edge angle κ. The value of the nose radius had quite some effect, giving higher resultant stress values p at decreasing values of nose radius. For very small values of the nose radius a variation of the end cutting-edge angle φ also had some effect, the resultant stress values p being larger for larger values of φ. To sum up: the more "pointed" the tool is, the larger resultant stress values p are produced. Consequently, these elements of the design of the cutting tool would have to be standardized throughout the research program, and the values were chosen as shown on Fig. 14, side and end cutting-edge angles κ and φ being fixed at 45 deg, and nose radius $r = 0.04$ in., leaving as significant variables the feed (inches per stroke, in the following abbreviated to "inch") and the normal rake angle γ.

The graphical method by which the p-values are determined from the measurements is shown by way of an example in Fig. 15. The deflections h are plotted against $1/H^2$ (H being the thickness of the specimen), and it is seen from the illustration how the h-values for four different feeds form four distinct groups and determine four straight lines. The slope of each line serves in calculating the corresponding p-value according to the equation

$$p = \frac{E}{3L^2} \frac{h}{\frac{1}{H^2}}$$

as previously outlined in the general theory.

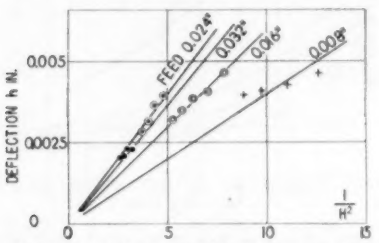

FIG. 15 METHOD OF GRAPHICAL TREATMENT OF DEFLECTION MEASUREMENTS
(Material, 0.35 carbon steel; side-cutting tool; $\gamma = 6$ deg; cutting speed, 28.9 fpm; depth of cut, 0.02 in; feed, 0.008 in., 0.016 in., 0.024 in., and 0.032 in.)

Through this graphical treatment, mean values of the tension p are obtained and these mean values are plotted against feed, separately for each material and each true rake angle, giving the total result of the whole series of experiments in the curves shown in Fig. 16 to 18, inclusive.

All the curves show that the resultant stress p increases with increasing feed. In some cases the relation between feed and resultant stress is linear, in other cases not.

Remembering that when working with a side-cutting tool the feed f is proportional to the chip thickness t (see Fig. 13), while when cutting with a square-end tool the depth of cut equals chip thickness, it should not be surprising to find an analogy between the curves given here for side-cutting tools and the results for square-end tools, the difference being that feed substitutes depth of cut.

There is, however, a remarkable difference in the effect of varying the back-rake angle of the square-end tools and the true rake angle of the side-cutting tools.

When cutting with the square-end tool, a steady decrease of resultant stress values was found when increasing the back-rake angle (see Fig. 11). This applies equally to the normal rake angles on the side-cutting tools in so far as the values 6, 12, and 24 deg are concerned but when the 30-deg tool was used, the resultant stress values rose again. This effect is shown clearly for 0.35 and 0.50 carbon steel (see Figs. 16 and 17), while not investigated for 0.70 carbon steel.

The results from these two materials have been treated graphically in another way. In Figs. 19 and 20 the resultant stress values p are plotted against normal rake-angle values, separately for each feed, and the curves thus obtained are in their origin fully analogous with the curves in Fig. 11.

A comparison between these two sets of curves is interesting. While there is a steady increase in resultant stress values along the axis in Fig. 11, the curves in Figs. 19 and 20 show a minimum somewhere in the middle and a rise on either side.

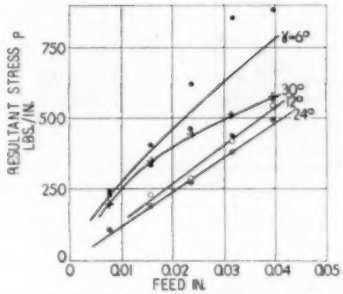

FIG. 16 RESULTANT STRESS p IN RELATION TO FEED; MATERIAL, 0.35 PER CENT C; SIDE-CUTTING TOOL
(Cutting speed 28.9 fpm; depth of cut 0.02 in.)

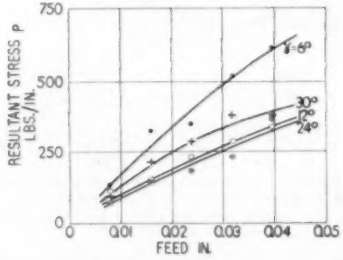

FIG. 17 RESULTANT STRESS p IN RELATION TO FEED; MATERIAL, 0.50 PER CENT C; SIDE-CUTTING TOOL
(Cutting speed 28.9 fpm; depth of cut 0.02 in.)

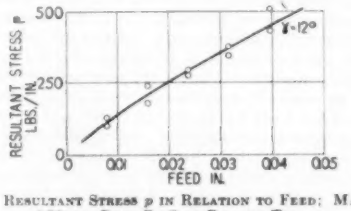

FIG. 18 RESULTANT STRESS p IN RELATION TO FEED; MATERIAL, 0.70 PER CENT C; SIDE-CUTTING TOOL
(Cutting speed 28.9 fpm; depth of cut 0.02 in.)

The significance of this is that a side-cutting tool has a certain value for its normal rake angle that will give the lowest tension values obtainable, all other conditions being kept equal. In both cases these optimum values seem to lie in the neighborhood of 18 deg.

Even with fine feeds this minimum is extremely pronounced. Only a 6-deg alteration of the normal rake angle will increase the resultant stress values by 75 to 100 per cent.

The practical consequence is, that in such cases where residual stresses should be kept low, finishing cuts should be taken with tools ground with a not-too-small nose radius and that a too-large rake angle is just as detrimental as a too-small rake angle.

EXPERIMENTS ON TURNING, EFFECT OF CUTTING SPEED

When cutting in a shaper, low cutting speeds only can be attained, and, in order to test higher speeds, the lathe must be resorted to.

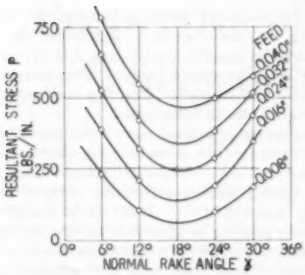

FIG. 19 RESULTANT STRESS p IN RELATION TO NORMAL RAKE ANGLES OF TOOL; MATERIAL, 0.35 PER CENT C; SIDE-CUTTING TOOL
(Cutting speed 28.9 fpm; depth of cut 0.02 in.)

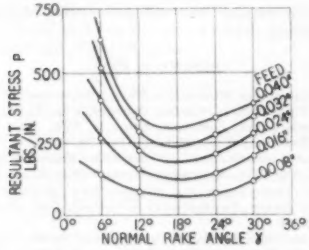

FIG. 20 RESULTANT STRESS p IN RELATION TO NORMAL RAKE ANGLES OF TOOL; MATERIAL, 0.50 PER CENT C; SIDE-CUTTING TOOL
(Cutting speed 28.9 fpm; depth of cut 0.02 in.)

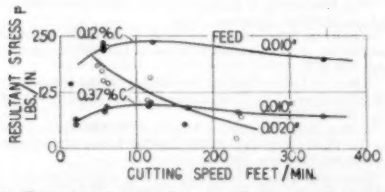

FIG. 21 EFFECT OF CUTTING SPEED ON RESULTANT STRESS VALUES p; SIDE-CUTTING TOOL
(Material, 0.12 per cent and 0.37 per cent carbon steel; depth of cut 0.03 in.; feed 0.01 in. and 0.02 in.)

In principle, the experimental technique is the same as before; it is necessary only to imagine the straight test specimen being bent to a circular ring so that the two ends meet without being joined together.

When using the straight specimen, the curvature was calculated from the deflection in the middle of the specimen. Now, with an annular specimen, the difference in curvature, due to the machining stresses in the outer surface, is calculated by measuring how much the two adjacent ends move axially from one another when a cut has been taken.

Rings were turned, cut across and stress-relieved, then placed in a special fixture, an experimental cut taken, and the deformation measured. The mathematical treatment is to some extent analogous with the one previously described, giving straight lines when the resultant stress is constant.

The main object of this series of experiments is to show whether there is any variation of stress due to variation of cutting speed. The results are shown in Fig. 21 and may be summarized thus: When using the coarser feed of 0.02 in. there is a marked variation; the resultant stress values decrease steadily as the cutting speed increases. At finer feeds, 0.01 in., the situation is a little more complicated. At cutting speeds above 130 fpm the fall in resultant stress values is clear, although small, compared with the curve for the coarser feed, but at cutting speeds below this speed the tendency is opposite, so that a fall in resultant stress values appears at decreasing speeds and the maximum is found at 130 fpm.

Incidentally, it might be mentioned that the resultant stress values for 0.12 carbon steel are a little more than double the corresponding values for 0.37 carbon steel.

ESTIMATING THE DEPTH OF WORK-HARDENING

Only a very few publications deal with the work-hardening of the material in a machined surface and make attempts to determine the depth of the work-hardened layer.

A comparison of such data with those obtained by the author shows, in general, good conformity when taking into consideration the rather heterogeneous material. The principal issues are that heavier cuts give larger depths of work-hardening (9, 10) and that feed seems to be considerably more effective than depth of cut (10), while (9) did not reveal any such difference. Decreasing values of nose radii and normal rake angles are found to produce deeper work-hardening in the case of nickel steels and 18/8 nickel-chromium steels (9), while this effect was not studied on other materials. Decreasing values of rake angles give increasing depths of work-hardening (9, 17).

The publications investigated give some details concerning the thickness of the work-hardened layer. Therefore it seems possible to combine this information with the resultant stress values p (force per unit of length) found by the author for the purpose of computing proper stress values σ (force per unit of area).

The resultant stress p, as determined by the author, is actually equal to the resultant of a proper tension σ distributed in some unknown manner over the depth δ, but if a uniform distribution (see Fig. 22) is assumed tentatively, it gives

$$p\left(\frac{\text{force}}{\text{length}}\right) = \sigma\left(\frac{\text{force}}{\text{length}^2}\right) \times \delta\,(\text{length})$$

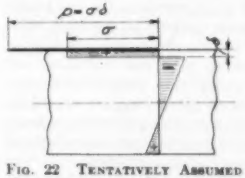

FIG. 22 TENTATIVELY ASSUMED UNIFORM STRESS DISTRIBUTION OVER DEFORMED LAYER

Materials (SAE 1020) and conditions of cutting almost equivalent to those used by the author are found in (17, 18). The stresses computed by these means were found to be 125,000 psi, using depth values from (17) and 89,000 psi with depth values from (18). These values compare fairly well with the value of approximately 100,000 psi for the real tensile strength at breaking for this material.

It must be remembered that the stress in the surface was produced when the cutting tool finally pulled the deformed and elongated grains apart (compare Figs. 3–7), so that the tension σ obtained may be expected to be in the vicinity of the real tensile stress at breaking.

When judging this result the possible presence of several sources of error must be borne in mind, and, consequently too, much accuracy cannot be expected in the values computed in the foregoing, yet they serve as an indicator of the magnitude of the stress involved.

Summary and Conclusions

1 The principal result of the experiments described here is that extremely high residual stresses are induced in the surface of a piece of metal by the action of a cutting tool even when light cuts are taken.

2 In ductile materials, such as carbon steels and the like, the stress induced is tensile.

3 The stresses are closely related to the work-hardening properties of the material and seem to be a function of the mechanical action of the tool and do not appear to depend much upon the thermal effect of the cutting; they increase with decreasing carbon content and—as has been shown for a few cases—with decreasing cutting speed.

4 The stresses are concentrated near the surface.

5 The resultant stress values p depend largely upon the shape and angles of the tool.

6 When carbon steel is cut with a square-end tool, the resultant stress values p decrease steadily with the increasing back-rake angle of the tool.

7 When carbon steel is cut with a side-cutting tool, the resultant stress values p show a definite minimum for a normal rake angle of approximately 18 deg and increase rapidly for smaller normal rake angles, and they also increase for larger normal rake angles, which is contrary to what might be expected.

8 For a low-carbon steel an attempt has been made to evaluate the actual stress value in terms of force per unit of area. The maximum stress seems to be in the vicinity of the real tensile strength at breaking, a result that is well in accordance with the explanation of the mechanism of the stress formation during cutting.

Stresses are invisible and their existence can be revealed only by the observation of their effects.

The concentration and the magnitude of the machining stresses are greatly in excess of all other known types of stresses of macroscopic order (László's "tessellated stresses" of microscopic order are not considered here), and the machining stresses, therefore, are of a considerable detrimental effect. Warping has been mentioned before, but a stress concentration in the surface almost of the same order of magnitude as the real tensile strength at breaking (approximately 100,000 psi for SAE 1020) cannot be without other serious adverse effects upon the finished article. It lowers its resistance to wear and corrosion, and constitutes the unseen cause of failure from fatigue or hairline cracks. Consequently, it should be given adequate consideration in calculation, design, and manufacturing methods, so much the more as it is located in the surface where also the calculated working stresses usually attain their maximum values.

In the experimental determination of residual stresses of thermal and related origin (other than cutting action) a stress-carrying section of the material is often separated from the bulk of the test piece by a cutting tool, and the value of the stress is then computed from measurement of the subsequent deformation. In the vast majority of investigations relating to residual stresses, the presence of machining stresses has not been considered. A knowledge of the stress values induced by cutting would, however, make it possible to compensate for this source of error in future experimental work on residual stresses in general.

The scope of the present paper is, of necessity, limited. It deals only with carbon steels, and the method of cutting has been restricted to dry-cutting with a single-point tool at low and medium cutting speeds.

Therefore, further work should be done on the effect of high-speed cutting, and the effect of cutting fluids; also on milling, broaching, drilling, reaming, and grinding, and on other materials such as alloy steels for aircraft, turbine components, and similar highly stressed machine parts. Cast iron and nonferrous metals and alloys should also be investigated.

When successfully completed, such investigations would make it possible to correlate the stress-inducing effects of various tool forms (square-end versus side-cutting-nosed tools, etc.), and methods of cutting (single-point cutting versus milling, broaching, drilling, grinding, etc.). They would contribute to our general knowledge of the mechanism of cutting, thereby throwing new light upon old problems the solutions of which still are far from complete. They would also give designers and manufacturers a deeper understanding of problems of stress and fatigue and enable them to make a better and safer choice of materials and methods than has hitherto been possible.

It is the hope of the author that he has contributed to the solution of a few of the problems, but he is also aware that he has, at the same time, disclosed the existence of many more which still remain unsolved.

BIBLIOGRAPHY

1 "Bestemmelse af Stoebespaendingers Stoerrelse" ("Determination of the Magnitude of Casting Stresses"), by E. K. Henriksen, *Stoeberiet*, Copenhagen, Denmark, Sept. 1, 1934; also in *Gjuteriet*, Stockholm, Sweden, vol. 24, 1934, pp. 121–124.

2 "Spannungsmessungen an einseitig abgeloeschter Knueppeln," by F. Staeblein, *Kruppsche Monatshefte*, vol. 12, 1931, p. 99.

3 "Über Spannungen in kaltgereckten Metallen," by E. Heyn and O. Bauer, *Internationale Zeitschrift fuer Metallographie*, vol. 1, 1911, p. 16.

4 "Taschenbuch fuer den Maschinenbau," by H. Dubbel, Julius Springer, Berlin, Germany, third edition, vol. 1, 1921, p. 538.

5 "Die Waermebehandlung der Werkzeugstaehle," by Brearley-Schaefer, Berlin, Germany, 1913, pp. 67–68.

6 "Rostfreie Staehle," by J. H. G. Monypenny and Rudolph Schaefer, Berlin, Germany, 1928, p. 177.

7 "The Machining of Stainless Steel," by Brown-Bayley's Steel Works, Ltd., Sheffield, England, 1934.

8 "Report on Machinability," by E. G. Herbert, Proceedings of The Institution of Mechanical Engineers, London, England, vol. 2, 1928, pp. 775–825.

9 "Effect of Lathe Cutting Conditions on the Hardness of Carbon and Alloy Steels," by T. G. Digges, Trans. ASME, vol. 54, 1932, paper no. MST—54-4.

10 "X-Ray Determination of Depth of Cold Working by Machining," by L. Thomassen and D. M. McCutcheon, *Mechanical Engineering*, vol. 56, 1934, pp. 155–157.

11 "Verformung und Regelung durch Oberflächenbearbeitung (Spanabhub) bei Eisen," by M. Renninger, *Metallwirtschaft*, vol. 13, 1934, pp. 889–892.

12 "Zerspanung und Eigenspannungen," by E. K. Henriksen, Ingenioervidenskabelige Skrifter, A, no. 43, Copenhagen, Denmark, 1937.

13 "Internal Stresses in Machined Surfaces," by E. K. Henriksen, International Congress for Testing Materials, London Congress 1937, Supplement to Group A, pp. 173–176.

14 "Residual Stresses in Machined Surfaces," by E. K. Henriksen, Transactions of the Danish Academy of Technical Sciences, no. 7, 1948 (Copenhagen).

15 "Physics of Metal Cutting," by H. Ernst, *Machining of Metals*, ASM, Cleveland, Ohio, 1938, pp. 16–20.

16 "Chip Formation, Friction and Finish," by H. Ernst and M. Eugene Merchant, Surface Treatment of Metals, ASM, Cleveland, Ohio, 1941, pp. 317–318.

17 "X-Ray Diffraction as a Gage for Measuring Cold Work Produced in Milling," by F. Zankl, A. G. Barkow, and A. O. Schmidt, Trans. ASME, vol. 69, 1947, pp. 307–318.

18 "The Distribution of Hardness in Chips and Machined Surfaces," by N. Zlatin and M. Eugene Merchant, Trans. ASME, vol. 69, 1947, pp. 5–14.

Properties of Thin-Walled Curved Tubes of Short-Bend Radius

By T. E. PARDUE[1] and IRWIN VIGNESS,[1] WASHINGTON, D. C.

Flexibility factors and stress-intensification factors have been measured for a group of thin-walled tube bends having a ratio of pipe radius to bend radius of 1/3. A theoretical analysis, which eliminates some of the simplifying assumptions of previous theoretical analyses, has been included for comparison with the experimental data. Reasonably good agreement between theory and experiment has been found for U-bends and 90-deg bends with straight sections of piping attached to the ends of the bend. Rigid constraints attached to the ends of the bend have been found to affect the measured quantities greatly. The effect of the end conditions has been studied experimentally but not theoretically.

Nomenclature

The following nomenclature is used in the paper:

E = Young's modulus (taken as 29×10^3 psi for steel)
I = area moment of inertia, in.^{4}
K_{ij} = flexibility factor associated with an applied load i and a measured deflection j
M, N, T = moments applied to end of pipe bend, in-lb
P, Q = forces applied to end of pipe bend, lb
R = bend radius, in.
r = tube radius, in.
t = tube wall thickness, in.
XYZ = co-ordinates
α = r/R = ratio of tube radius to bend radius
$\epsilon_\phi, \epsilon_\theta$ = strains in axial and circumferential directions in./inch.
λ = tR/r^2 = dimensionless parameter
ν = Poisson's ratio (0.3 for steel)
$\sigma_\phi, \sigma_\theta$ = surface stresses in axial and circumferential directions, psi
σ_m = stress at middle surface of pipe wall, psi
θ = angle giving position on pipe circumference
ϕ = angle giving position along axis of pipe bend.
Ψ, B, Θ = angular rotations of free end of pipe bend relative to fixed end

Introduction

Previous work on the elastic properties of curved tubes has consisted of theoretical analyses (1, 2, 3, 4)[2] based on the assumption that the radius of the bend is large compared with the tube radius, and of experimental tests (2, 3) made on pipes for which this assumption was valid. Recent piping practice has tended to make increased use of short-radius pipe bends, with bend radius only 2 or 3 times larger than the tube radius. Occasionally the tubes have very thin walls, as, for example, the low-pressure crossover pipes between high-pressure and low-pressure turbines. The case of short-radius bends of small wall thickness is of particular interest because the factors of stress intensification and of flexibility may be very high, often 10 or 20 times as large as the factors commonly encountered in tube bends of large radius and of greater wall thickness. Little information has been available previously as to the limitations of earlier theories, for either thin-walled or moderately thick-walled tubes when the radius of the bend is not large compared to the tube radius.

The present paper gives results of an investigation designed to extend present knowledge of the behavior of tube bends into the range of very thin-walled tubes of short-bend radius. Experimental work for a series of short-turn tubes typical of those used in high-pressure steam lines is near completion and will be reported at a later time. The work presented at this time consists of (*a*) tests made on a series of tube bends having a ratio of bend radius to tube radius equal to 3, and having relatively thin walls, the ratio of wall thickness to tube radius ranging from 0.015 to 0.044, and (*b*) an extension of the previous theory, contained in the Appendix of this paper, to take into account the small-bend radius.

The most important source of error in the consideration of these problems for short-turn tubes is caused by the neglect of end constraints. Because of the degree of complication involved, no mathematical treatment has been made taking into consideration either of the constraints at the ends of a bend, or of the constraining effects of sections of a bend subjected to a change of moment along its length. An experimental study of these problems has been made, however, by means of which corrections can be applied to the usual equations. Two main types of constraints are considered as follows:

1 The tube bend is joined to straight tubes (tangents) at its ends, without appreciable change of dimensions at the juncture. A partial constraint is exerted by the tangent pipes in this case, the wall deformations decreasing quite rapidly with distance away from the bend.

2 The tube bend is terminated by a heavy flange so that the end constraint approaches that of rigid clamping with all displacements prevented in the end plane.

Where the effects of these end constraints are important, it is evident that instead of having one flexibility factor depending only upon λ, where $\lambda = tR/r^2$, the proper factor applying to each section of a bend varies along the length of the bend, and depends not only on the constraints at the two ends but also on the total angle of the bend, the type of loading, and on the ratio r/R. This being the case, the apparent flexibility of a particular tube bend will depend on all of these variables, and, in addition, will be a function of the particular deflection considered, i.e., the direction of displacement or rotation measured. In addition to the error expected from the neglect of end constraints in the long-radius theory, it was expected that when the ratio r/R was not small it would have to appear in the analysis in addition to the parameter λ.

[1] Mechanics Division, Naval Research Laboratory, Washington, D. C.

[2] Numbers in parentheses refer to Bibliography at end of paper.

Contributed by the Power, Applied Mechanics, and Metal Engineering Divisions, and the Joint Committee on Effect of Temperature on Properties of Metals, and presented at, the Spring Meeting, Washington, D. C., April 12-14, 1950, of The American Society of Mechanical Engineers.

Note: Statements and opinions advanced in papers are to be understood as individual expressions of their authors and not those of the Society. Manuscript received at ASME Headquarters, December 27, 1949. Paper No. 50—S-21.

Therefore the previous analyses were repeated (see Appendix) but with terms proportional to r/R retained instead of being dropped as in the long-radius theory. Calculations of stress-intensification factors and flexibility factors were made for in-plane and transverse bending for the two cases $r/R = 1/2$ and $1/3$ and were compared with values obtained in the long-radius theory. It was found that the long-radius theory gave both stress and flexibility factors with surprisingly good accuracy (aside from the neglect of end effects) for pipes in the range of dimensions such that λ varied from 0.04 to 1.0.

Experimental Methods

Types of Experiments Performed. Two types of experimental measurements were made. One type consisted primarily of applying suitable forces or moments to one end of a bend and of measuring the resulting translations and rotations. In addition, changes of tube diameters were determined both for the curved section and for attached tangents when the latter existed. The other type of measurement consisted of determining the strains in the surface of the bend as caused by the forces or moments. Both longitudinal and transverse strains were measured, generally around a circumference where maximum values were expected.

Construction of Tube Bend. A series of tube bends, constructed from cold-rolled steel sheeting, with ratios of tube radius to bend radius of 1/3, and with ratios of wall thickness to tube radius ranging from 0.015 to 0.044, were selected to give data for piping installations such as the connections between high- and low-pressure turbines. Fig. 1 shows a typical pipe bend. The dimensions of the tubes used are given in Table 1.

Straight sections of tubing about 12 in. long were welded to each end of the bend, and square plates 7 in. on a side $\times$ $^1/_2$ in. thick were welded to the free ends for use in anchoring the bends to a base plate and for applying loads. For the flanged end conditions, flanges cut from $^1/_2$-in. steel plate were soldered to the ends of the bend as indicated by the dashed lines in Fig. 2. Wall thickness was normally correct to within 5 per cent, and the variations of the tube radius was generally less than 1 per cent.

Deflections and Wall Deformations. Measurements were made of the components of deflections for the various conditions of loading. The nomenclature and co-ordinates used for the loads and deflections are indicated in Fig. 2; forces P and Q are denoted by arrows, moment vectors M, T, and N by double-headed arrows, the rotation and displacement vectors are similarly oriented and are designated by Greek and English letters, respectively. Dead-weight loads, consisting of forces and moments, were applied to the flange at the free end of the pipe through long flexible cables. When no flanges were used at the ends of the bend, measurements were made of rotations and translations of end A relative to end D; the relative motions between the ends B and C of the bend were then obtained by subtracting the calculated contributions of the tangents. When flanges were used at the ends of the bend, rotation measurements were made directly on them.

Translatory deflections at the end of the free tangent were measured by means of a traveling microscope mounted on the base plate and focused on the center of the flange. Deflections for the bend alone were obtained by subtracting contributions, due to the tangents, from the measured values. The deflections were read and were reproducible to within 0.0002 in.

Rotations were measured by means of a pair of prisms attached to the two cross sections, between which relative rotations were desired. A Tuckerman auto-collimator was used to provide collimated light and a scale for reading deflections of the light beam. This method was suggested by the Tuckerman optical strain gage (5, 6).

TABLE 1 DIMENSIONS OF PIPE BEND

Pipe 180° bend	Number 90° bend	Outside diam, in.	Bend radius R, in.	Wall thickness t, in.	Mean pipe radius r, in.	$\lambda = \frac{tR}{r^2}$	Moment of inertia I, in.^{4}
82B	82	5.0	7.5	0.036	2.48	0.044	1.73
83B	83	5.0	7.5	0.050	2.48	0.061	2.38
84B	84	5.0	7.5	0.062	2.47	0.077	2.96
86B	86	5.0	7.5	0.078	2.46	0.097	3.65
85B	85	5.0	7.5	0.109	2.45	0.137	5.01

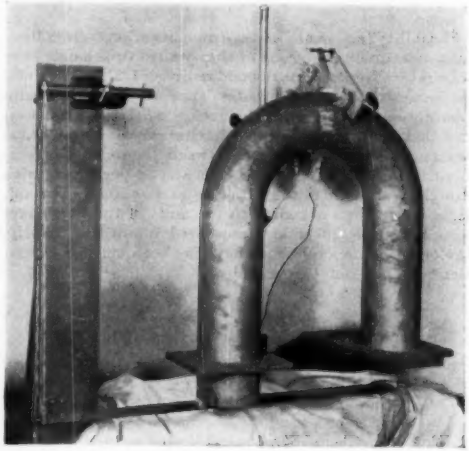

Fig. 1 Typical U-Bend

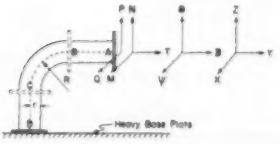

Fig. 2 Schematic Diagram of Tube Bend Showing Positions of Rigid Flanges at B and C and Notation Used for Loads and Deflections

Measurements were made of the cross-sectional deformation of the tubes by determining the changes of diameter resulting from the application of a load. These deformations originated, of course, in the curved section of the tube and were not local disturbances around the area of load application. Curves illustrating these types of deformation are shown in Figs. 3 and 4.

Strain Measurements. Strains were obtained from wire resistance strain gages, SR-4 type AX-10, cemented to the outside surface of the pipe wall. This gage has two mutually perpendicular elements of $^3/_4$ in. and $^3/_8$ in. gage length, respectively. They were mounted around a circumference of a pipe at intervals of about 10 deg, between $\theta = +90$ deg and $\theta = -90$ deg (Fig. 18), with the long gage placed along the axial direction and the short gage in the circumferential direction. The transverse strain varies directly as the distance from the center of the tube wall. Since the center of the gage was about 0.004 in. from the surface of the pipe, a small error in the transverse stress results. No correction was made for this error.

Discussion of Results

Flexibility Factors. The flexibility factor is defined as the

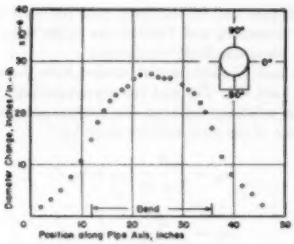

FIG. 3 DIAMETER CHANGE VERSUS POSITION ALONG PIPE AXIS, MEASURED AT $\theta = 0$ DEG FOR IN-PLANE BENDING
(θ defines position on pipe circumference as shown on inserted bend.)

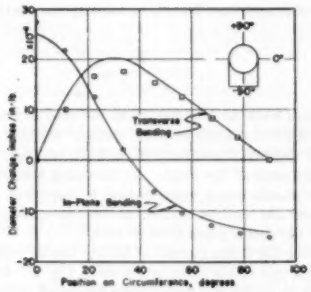

FIG. 4 DIAMETER CHANGES AROUND THE CIRCUMFERENCE OF A TUBE
(Solid curves represent theoretical data; circles and squares represent measured values. Position on circumference is defined by inserted bend.)

ratio of the actual deflection of a curved tube for a given load to that which is calculated for a similarly curved rod of equal cross-sectional moment of inertia and under the same condition of loadings and deflection measurement. There is assumed to be no shift of the neutral plane from the center of the rod. The increased flexibility of the tube over that for the rod exists only for bending moments. It has been checked experimentally for some of the bends used in this paper that the ratio of the torsional displacement for the tube to that for the rod is very nearly unity.

Initial measurements of deflections of short-turn tubes showed, as would be expected, that a different flexibility factor was required relating each component of load to each component of deflection, and that the flexibility factors were dependent upon the type of restraint at the end of the bend, as well as upon the bend length and dimensions of the tubing. In labeling this large number of factors, K_{ij} was used to designate the flexibility factor obtained when a load i was applied to the end of the tube bend, and the deflection j was measured. The number of different coefficients involved is too great for practical use, and it was expected to reduce the number by lumping together those of approximately equal values.

In order to determine the effects of usual types of end constraints on the experimental values of the flexibility factors, tests were made with the ends of the bends terminated by the following:

(*a*) Straight sections, or tangents, of the same diameter and wall thickness as the material in the curved tube.

(*b*) A straight section on one end and a rigid flange at the other (used only for right angle bends.)

(*c*) Rigid flanges at both ends of the bend.

Table 2 gives values of flexibility factors measured for 90-deg bends with straight tangents. It can be seen from symmetry that certain of the flexibility factors would be equal for a perfectly constructed right-angle bend. A bend with straight sections of piping or rigid flanges at both ends of the bend would give

$$K_{NB} = K_{TB} \quad \text{and} \quad K_{NB} = K_{TO}$$

Average values were used for experimental quantities that should be identical. Tables 3 and 4 show the effects of rigid flanges at the ends of the bend. The results in Table 3 were obtained with the flange at position *B*, Fig. 2. The data show that applied loads, such that the maximum bending moment is at *B*, give flexibility factors which are decreased to a greater extent than the factor arising from applied loads which give the maximum bending moment at *C*. Table 4 shows that all flexibility factors are greatly decreased when rigid flanges are attached to both ends of the bend.

The lack of complete data prohibits an assignment of values of K_{ij} for all the conditions of end constraints, loading, and types of measurement. Furthermore, in practical applications, the labor involved in selecting a flexibility factor for each combination of deflection and load would be enormous; therefore it is desirable to reduce the number of factors to a minimum. As the differences between many of the values for K_{ij}, obtained with identical end conditions, are not large compared to the variations to be expected in pipe constructions, all results for a given bend length and end conditions were averaged and presented in Figs. 5 and 6, except a few cases in which K_{ij} is radically different from the mean. The term "all values" used in these figures includes only experimental values of K_{ij}, measured under the specified end conditions, for both in-plane and transverse bending. The points represented by circles in Fig. 5 contain the flexibility fac-

TABLE 2 MEASURED FLEXIBILITY FACTORS FOR TRANSVERSE BENDING OF RIGHT-ANGLE BENDS WITH TANGENTS AT BOTH ENDS OF BEND

Flexibility factor	$\lambda = tR/r^2$ 0.044	0.061	0.077	0.097	0.137
K_{QO}	41.4	32.2	27.9	22.1	15.9
K_{QB}	33.2	23.1	22.5	17.8	13.2
$\frac{K_{NO} + K_{TB}}{2}$	32.2	21.9	19.7	14.5	10.4
$\frac{K_{NB} + K_{TO}}{2}$	36.9	27.0	24.0	17.3	12.7

TABLE 3 MEASURED FLEXIBILITY FACTORS FOR TRANSVERSE BENDING OF RIGHT-ANGLE BENDS WITH ONE TANGENT AND ONE RIGID FLANGE

Flexibility factor	$\lambda = tR/r^2$ 0.044	0.061	0.077	0.097	0.137
K_{QO}	18.1	17.7	16.0	14.2	10.1
K_{QB}	23.4	17.4	18.9	16.1	13.1
K_{NO}	8.3	8.9	7.6	7.0	5.6
K_{TB}	24.1	17.5	17.4	14.2	11.0
$\frac{K_{NB} + K_{TO}}{2}$	20.8	18.3	16.2	13.9	10.4

TABLE 4 MEASURED FLEXIBILITY FACTORS FOR TRANSVERSE BENDING OF RIGHT-ANGLE BENDS WITH RIGID FLANGE AT BOTH ENDS OF BEND

Flexibility factor	$\lambda = tR/r^2$ 0.044	0.061	0.077	0.097	0.137
K_{QO}	6.3	7.9	7.3	7.9	6.3
K_{QB}	6.6	8.1	10.1	9.2	9.1
$\frac{K_{NO} + K_{TB}}{2}$	5.5	5.8	6.2	5.8	5.3
$\frac{K_{NB} + K_{TO}}{2}$	7.6	8.2	7.8	7.6	6.8

tors obtained from (*a*) the rotations produced by the three moments, (*b*) the major translation produced by the in-plane moment, and (*c*) the rotation Θ produced by a load *Q* applied at the end of the free tangent (this factor is designated $K_{[QL]\Theta}$). Curve *A* gives an average of all the foregoing factors, except those noted on the figure, for flanges at both ends of the bend.

Data for right-angle bends are given in Fig. 6. The values for $K_{Q\Theta}$ were considerably larger than the other data and therefore were plotted separately. Curve *B* contains factors obtained from (*a*) rotations produced by moments *T* and *N*, (*b*) the rotation B produced by the force *Q*, applied at the end of the bend, and (*c*) the rotation Ψ, and the major translation produced by the force *P* applied at the end of the free tangent. Curve *C* gives values for bends with a rigid flange at end *B*, Fig. 2. This curve

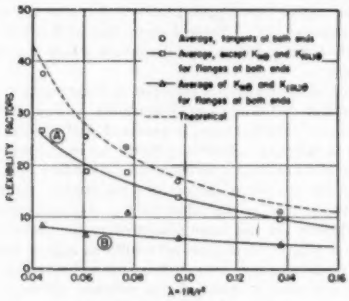

FIG. 5 FLEXIBILITY FACTORS FOR U-BENDS

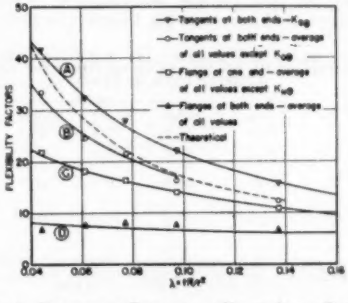

FIG. 6 FLEXIBILITY FACTORS FOR RIGHT-ANGLE BENDS

contains factors obtained from (*a*) rotations produced by moments *M* and *T*, (*b*) rotations produced by the force *Q*, and (*c*) the rotation B produced by the moment *N*. Curve *D* gives data which contain factors obtained from the rotations produced by the moments *M*, *N*, and *T*, and the force *Q*. In all the foregoing cases the force *Q* was applied at the ends of the bend.

In summary, the flexibility factors of short-turn tubes are greatly affected by constraints, such as flanges, at the ends of the bends. Many flexibility factors exist for a given bend, but, to keep their application within practical limits, average values have been given for factors not greatly different from the mean. For bends with flanges it is suggested that experimental values of flexibility factors be used. For bends with tangents the theoretical values are usually sufficiently accurate.

Stresses and Stress-Intensification Factors. Values of stresses have been obtained from the two principal strains at the outside surface of the pipe wall for the list of tube turns given in Table 1. Methods of mounting and loading the tubes were identical to that used for obtaining flexibility factors.

The axial and circumferential strains have been designated as ϵ_ϕ and ϵ_θ (see Fig. 18), and the corresponding stresses as σ_ϕ and σ_θ. The relations between the stresses and strains on the outside surface of the pipe wall are given by

$$\sigma_\phi = \frac{E}{1 - \mu^2}(\epsilon_\phi + \mu\epsilon_\theta)$$

$$\sigma_\theta = \frac{E}{1 - \mu^2}(\epsilon_\theta + \mu\epsilon_\phi)$$

The stress at the middle surface of the pipe wall σ_m, was obtained by assuming the longitudinal strain to be constant through the pipe wall, and the circumferential strain to be caused by bending of the pipe wall and therefore to be zero at the middle surface; thus

$$\sigma_m = \frac{E}{1 - \mu^2}\epsilon_\phi$$

The stresses were determined, as in the case of the flexibility factors, for the end conditions of (*a*) straight sections (tangents), (*b*) one rigid flange and one tangent, and (*c*), two rigid flanges attached to the ends of the bend. In obtaining the experimental curves on U-bends, loads were applied to the pipes which produced a maximum bending moment at the mid-section of the pipe bend where the strain gages were located.

In obtaining the stress curves for 90-deg bends, moments were applied to the end of the bend as shown in Fig. 2. For in-plane bending this gave the maximum cross-sectional deformation at a position 45 deg from the beginning of the bend. Strain gages were mounted around a circumference at this position which would be at a location of maximum stress amplification. However, for transverse bending, the maximum bending moment occurs at one end of the bend and reduces to zero at the other end. In order to determine the influence of this moment distribution on the stress factors, strains were measured at 22.5-deg, 45-deg and 67.5-deg positions along the axis for one 90-deg bend with straight tangents. Only small differences were found for the stress-intensification factors measured at these positions; therefore maximum stress factors were determined for the 45-deg position only.

Typical stress curves are shown in Figs. 7 through 9, for a U-bend with straight tangents. Following the usual practice, the nondimensional stress-intensification factor, $\sigma/(Mr/I)$, is plotted instead of the stress. Curves obtained from the theoretical considerations, given in the Appendix, are included. The qualitative agreement between the experimental and theoretical curves is generally good here, as was the case for all measurements on both U-bends and right-angle bends having straight sections at the ends of the bend. The magnitudes of stresses measured on U-bends were generally higher than the values predicted by the theory. An exception is noted in the circumferential stresses for transverse bending, given in Fig. 14. These low stress values are in agreement with wall-deformation measurements given in Fig. 4, which show diameter changes in the mid-section of the bend to be smaller than the calculated values. Additions of rigid flanges decreased the stress factors and caused shifting of the stress concentrations around the circumference of the pipe. This was especially true for right-angle bends.

In analyzing the stresses in a piping system the quantity of most interest is generally the maximum stress. To conserve space, only these intensification factors are presented here. They have been obtained by reading the peak values from the

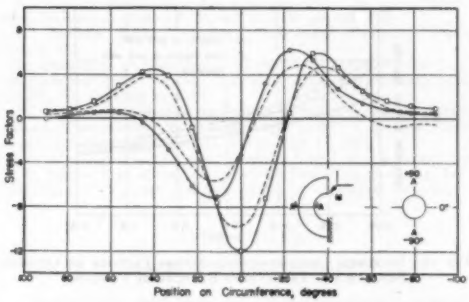

FIG. 7 STRESS-INTENSIFICATION FACTORS VERSUS POSITION ON PIPE CIRCUMFERENCE FOR IN-PLANE BENDING

(Circles and squares give longitudinal and transverse factors, respectively, for $\alpha = 1/3$ and $\lambda = 0.077$, measured at outside surface of pipe wall; broken curves give corresponding theoretical values for $\alpha = 1/3$ and $\lambda = 0.08$.)

stress curves and are given in Figs. 10 through 17. The values indicated by these curves should provide sufficient design information for the determination of stresses of these types. The location of the maximum stresses can be approximated from Figs. 7 through 9.

SUMMARY AND CONCLUSIONS

Flexibility and stress-intensification factors have been measured for a series of U-bends and right-angle bends having values of $\lambda = tR/r^2$ between 0.04 and 0.14, with $r/R = 1/3$. A theoretical analysis and a corresponding experimental study have been carried out to determine the importance of omitting terms containing the ratio of the tube radius to the bend radius. Experimental work has also been performed to determine the effects of constraints at the ends of the bends. This latter problem has not been studied theoretically. Measurements were made on the foregoing types of bends with (*a*) straight sections, (*b*) one rigid flange and one straight section (this condition used for right-angle bends only), and (*c*) two rigid flanges attached to the ends of the bend.

The following conclusions which apply to very thin-walled short-turn tubes have been reached:

1 Different flexibility and stress-concentration factors exist for each type of applied load and for each type of deflection, for bends with end constraints and for bends in which the moments vary along their lengths. Because of the impracticability of using such a large number of different flexibility factors, those of approximately the same amplitude have been averaged. A minimum number of values have been retained.

2 The theory as previously developed for tube turns of long-bend radius, which neglects the ratio r/R, gives the tube flexibility with good accuracy when the effects of end constraints are small. The results as given by von Kármán (1), Beskin (4), and the discussion of Beskin's paper by Symonds and Vigness (7), indicate the precision obtained when a sufficiently high order of approximation is used in the solution.

3 The addition of constraints such as flanges at the ends of the bend, greatly increases the bending rigidity. This is especially true if the angle of turn is 90 deg or smaller. If the flexibility of a bend is an appreciable part of the flexibility of a piping system, then under these conditions the flexibility factors should be taken from the experimental data.

4 The longitudinal stress factors at the middle surface are considered to be the most important for calculating stresses in piping systems (2). These measured quantities were consistently

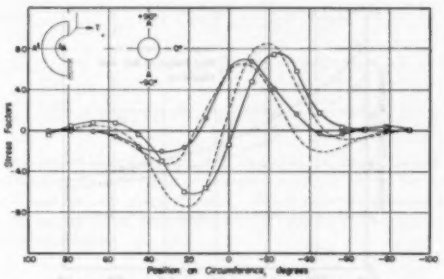

FIG. 8 STRESS-INTENSIFICATION FACTORS VERSUS POSITION ON PIPE CIRCUMFERENCE FOR TRANSVERSE BENDING

(Circles and squares give values of longitudinal and transverse factors, respectively, for $\alpha = 1/3$, and $\lambda = 0.077$, measured at outside surface of pipe wall; broken curves give corresponding theoretical values for $\alpha = 1/3$ and $\lambda = 0.08$.)

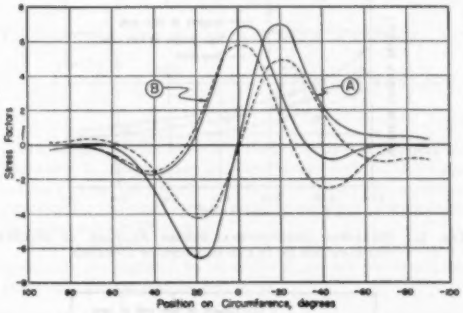

FIG. 9 STRESS-INTENSIFICATION FACTORS AT MIDDLE SURFACE VERSUS POSITION ON PIPE CIRCUMFERENCE

(Solid curves *A* and *B* give values for in-plane and transverse bending, respectively, with $\alpha = 1/3$ and $\lambda = 0.077$ obtained from strains measured at outside surfaces; broken curves give theoretical values for $\alpha = 1/3$ and $\lambda = 0.08$.)

higher than the calculated values for all bends with straight tangents attached and also for U-bends terminated by rigid flanges. The addition of rigid flanges to right-angle bends, reduced the stress factors by 50 to 75 per cent. It is believed that the experimental data are more accurate than theoretical work as limited by its present assumptions.

ACKNOWLEDGMENTS

The authors gratefully acknowledge the assistance given especially by Drs. Paul S. Symonds and Herman Jarrell, and to the other members and former members of the Mechanics Division of the Naval Research Laboratory who have given of their time in the performance of these problems.

BIBLIOGRAPHY

1 "Über die Formanderung Dunnwandiger Rohre, insbesonder federnder Ausgleichrohre," by Th. von Kármán, *Zeitschrift des Vereines deutscher Ingenieure*, vol. 55, 1911, p. 1889.

2 "The Elastic Deformation of Pipe Bends," by William Hovgaard, *Journal of Mathematical Physics*, M.I.T., vol. 6, 1926, pp. 69–118; vol. 7, 1927–1928, pp. 198–238; vol. 7, 1927–1928, pp. 239–297; vol. 8, 1929, pp. 293–344.

3 "Elastic Properties of Curved Tubes," by Irwin Vigness, Trans. ASME, vol. 65, 1943, pp. 105–120.

4 "Bending of Thin Curved Tubes," by Leon Beskin, *Journal of Applied Mechanics*, Trans. ASME, vol. 67, 1945, p. A-1.

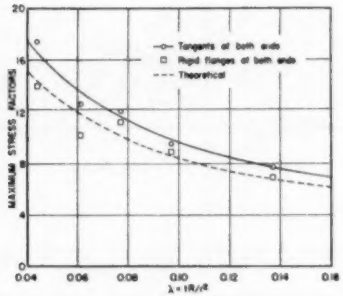

FIG. 10 MAXIMUM CIRCUMFERENTIAL-STRESS FACTORS AT THE OUTSIDE SURFACE FOR IN-PLANE BENDING OF U-BENDS

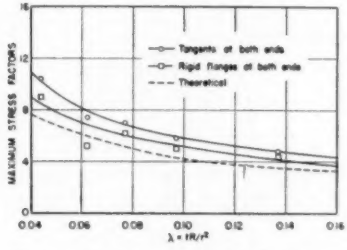

FIG. 11 MAXIMUM LONGITUDINAL-STRESS FACTORS AT MIDDLE SURFACE FOR IN-PLANE BENDING OF U-BENDS

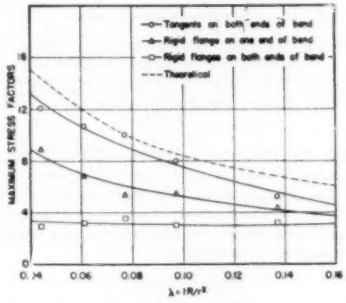

FIG. 12 MAXIMUM CIRCUMFERENTIAL-STRESS FACTORS AT OUTSIDE SURFACE FOR IN-PLANE BENDING OF RIGHT-ANGLE BENDS

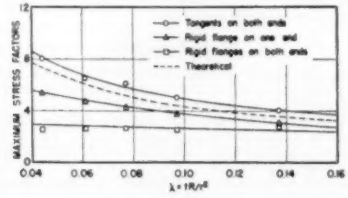

FIG. 13 MAXIMUM LONGITUDINAL-STRESS FACTORS AT MIDDLE SURFACE FOR IN-PLANE BENDING OF RIGHT-ANGLE BENDS

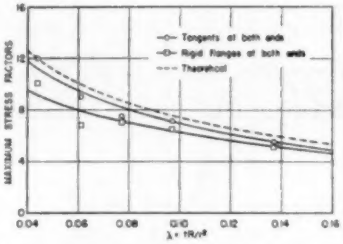

FIG. 14 MAXIMUM CIRCUMFERENTIAL-STRESS FACTORS AT OUTSIDE SURFACE FOR TRANSVERSE BENDING OF U-BENDS

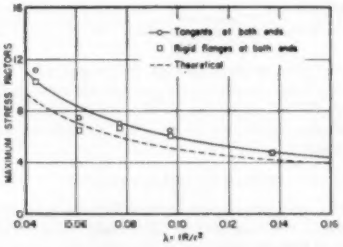

FIG. 15 MAXIMUM LONGITUDINAL-STRESS FACTORS AT MIDDLE SURFACE FOR TRANSVERSE BENDING OF U-BENDS

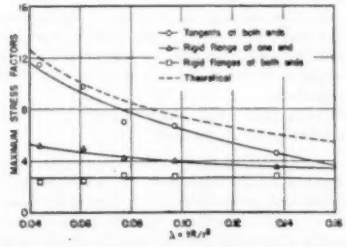

FIG. 16 MAXIMUM CIRCUMFERENTIAL-STRESS FACTORS AT OUTSIDE SURFACE FOR TRANSVERSE BENDING OF RIGHT-ANGLE BENDS

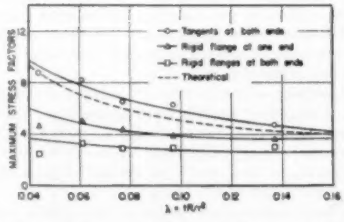

FIG. 17 MAXIMUM LONGITUDINAL-STRESS FACTORS AT MIDDLE SURFACE FOR TRANSVERSE BENDING OF RIGHT-ANGLE BENDS

5 "Optical Strain Gages and Extensometers," by L. B. Tuckerman, Proceedings of the ASTM, vol. 23, 1923, pp. 602–610.

6 "Bulletin 2084," American Instrument Company, Silver Spring, Md.

7 Discussion of "Bending of Thin Curved Tubes," by P. S. Symonds and Irwin Vigness, *Journal of Applied Mechanics*, Trans. ASME, vol. 68, 1946, p. A-66.

8 "Characteristics of Short Radius Tube Bends, Second Partial Report (Theoretical)," by P. S. Symonds and T. E. Pardue, Naval Research Laboratory Report no. 0-2761, Feb. 18, 1946.

9 "Mathematical Theory of Elasticity," by I. S. Sokolnikoff and A. D. Specht, first edition, McGraw-Hill Publishing Company, Inc., New York, N. Y., 1946 (See last chapter on variational methods.)

Appendix

Theoretical Considerations

The theoretical work presented in this Appendix is a condensation of a Naval Research Laboratory report by Symonds and Pardue (8). The theoretical work has been prepared primarily by Symonds.

Both the theories of von Kármán (1) for bending in the plane of the bend, and of Vigness (3) for bending out of the bend plane, made the simplifying assumption that R, the radius of the bend, was large compared to r, the radius of the tube, so that terms proportional to r/R were neglected in comparison to unity. When R is only 2 or 3 times larger than r, then it is questionable whether this assumption is sufficiently accurate. The errors to be expected because of the neglect of end constraints are not considered at this time. It is not difficult to develop the theory of in-plane and transverse bending without neglecting terms of the order r/R, although the numerical work is considerably increased.

In order to determine the relative importance of the neglect of r/R terms and that of the end constraints, the von Kármán theories were extended to take into account the finite r/R values, and calculations were made for the cases r/R equal to 1/3 and 1/2.

The assumptions underlying both the previous theories and the present ones are as follows:

1 Plane sections of the bend are assumed to remain plane.

2 The circumferential strains are assumed to be one of pure bending of the tube wall, and hence vanish at the middle surface of the wall.

3 The axial or longitudinal strains are assumed to be uniform throughout the wall thickness.

4 All strains and wall deformations in cross-sectional planes are assumed to be proportional to the bending moment at each section.

Under these assumptions the normal strains and stresses can be written as follows:

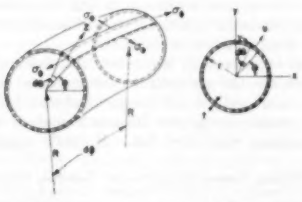

Fig. 18 Section of Curved Tube

("Middle" surface of tube wall is shown by dotted line midway between inner and outer surfaces. Co-ordinate z is a measure in radial direction, of distance from middle surface; u and v represent radial and tangential displacements of wall, respectively.)

$$\left.\begin{array}{lll} \epsilon_\phi = e & (a) & \sigma_\phi = \dfrac{E}{1-\nu^2}(e + \nu z\kappa) \quad (d) \\ \epsilon_\theta = z\kappa & (b) & \sigma_\theta = \dfrac{E}{1-\nu^2}(z\kappa + \nu e) \quad (e) \\ \epsilon_z = \dfrac{-\nu}{1-\nu}(e + z\kappa) & (c) & \sigma_z = 0 \qquad\qquad (f) \end{array}\right\} \quad \ldots [1]$$

The notation is explained in Fig. 18 and in the Nomenclature.

The longitudinal strain is assumed constant across the wall thickness for any given location. From these expressions the strain energy dV of an element of the tube wall of surface area dA is found to be

$$dV = \frac{Et}{2(1-\nu^2)}\left(e^2 + \frac{t^2\kappa^2}{12}\right) dA \quad \ldots\ldots [2]$$

Since the element included between planes at ϕ and $\phi + d\phi$ and between radii at θ and $\theta + d\theta$ has the area

$$dA = Rr\left(1 + \frac{r}{R}\sin\theta\right) d\phi d\theta \quad \ldots\ldots [3]$$

The total strain energy in a length of bend ϕ_1 is, therefore

$$V = \int_0^{\phi_1}\int_0^{2\pi} \frac{EtRr}{2(1-\nu^2)}\left(e^2 + \frac{t^2\kappa^2}{12}\right)\left(1 + \frac{r}{R}\sin\theta\right) d\phi d\theta \quad \ldots\ldots [4]$$

The foregoing expressions apply equally well to in-plane and transverse bending, under the assumptions listed. The longitudinal strains differ in the two cases, however, so that the expressions for the total strain energy in terms of cross-sectional displacements are different.

In the case of "in-plane" bending (in which the bending moment may be assumed to be uniform around the bend), the longitudinal strain may be written as

$$e_p = e(\theta) = \left[\frac{c(\delta + r\sin\theta) + \dfrac{1}{R}(u\sin\theta + v\cos\theta)}{\left(1 + \dfrac{r}{R}\sin\theta\right)}\right] \quad \ldots [5]$$

where u and v are displacements of an element of the tube wall in the radial and circumferential directions, respectively (see Fig. 18), c is the change of curvature of the bend, and δ is the displacement of the "neutral surface" of the bend.

In the case of transverse bending, the transverse curvature is variable with ϕ in all types of loading. The longitudinal strain may be written, under the stated assumptions, as

$$e_t = e(\phi, \theta) = \frac{\left[c_t(\phi) r\cos\theta + \dfrac{1}{R}(u\sin\theta + v\cos\theta)\right]}{\left(1 + \dfrac{r}{R}\sin\theta\right)} \quad \ldots [6]$$

In both in-plane and transverse bending, the change of curvature κ, of the cross section is as follows

$$\kappa = -\frac{1}{r^2}\left(u + \frac{\partial^2 u}{\partial\theta^2}\right) \quad \ldots\ldots [7]$$

In view of Assumption 2, the radial and circumferential displacements are related by the formula

$$u = -\frac{\partial v}{\partial\theta} \quad \ldots\ldots [8]$$

This allows the strain energy to be written in terms of one of the wall displacements; the circumferential displacement v seems to be the more convenient one.

Using these results, the strain energies in the two cases may be written in terms of the displacement v as follows

(*a*) *In-Plane Bending:*

$$V = \frac{EtR\phi_1}{2(1-\nu^2)} \int_0^{2\pi} \left\{ \frac{\left[c(\delta + r\sin\theta) + \frac{1}{R}\left(v\cos\theta - \frac{\partial v}{\partial\theta}\sin\theta\right)\right]^2}{1+\frac{r}{R}\sin\theta} + \frac{t^2}{12r^4}\left(\frac{\partial v}{\partial\theta} + \frac{\partial^3 v}{\partial\theta^3}\right)^2 \left(1+\frac{r}{R}\sin\theta\right) \right\} d\theta \quad [9]$$

(*b*) *Transverse Bending:*

$$V = \frac{EtRr}{2(1-\nu^2)} \int_0^{\phi_1}\int_0^{2\pi} \left\{ \frac{\left[c_t r\cos\vartheta + \frac{1}{R}\left(v\cos\theta - \frac{\partial v}{\partial\theta}\sin\theta\right)\right]^2}{1+\frac{r}{R}\sin\theta} + \frac{t^2}{12r^4}\left(\frac{\partial v}{\partial\theta} + \frac{\partial^3 v}{\partial\theta^3}\right)^2 \left(1+\frac{r}{R}\sin\theta\right) \right\} d\theta d\phi \quad [10]$$

The method used for determining u and v is based on the theorem of minimum potential energy with respect to variation of displacements, [see, for example, reference (9)]. In the present case only the displacements in cross-sectional planes are assumed to be varied, so that the "potential energy of the loads" is zero, and the potential energy is equal to the strain energy. Approximate solutions are obtained by writing v as a trigonometric series containing certain parameters. By the theorem of minimum potential energy the "best" values of these parameters are those which make the potential energy stationary, and hence make the strain energy stationary, in the present problem. The trigonometric series suitable for the two cases of in-plane and transverse bending are determined by considerations of symmetry. They are as follows

(*a*) *In-Plane Bending:*

$$v = -rRc\left(\sum_{2,4,6,\cdots} a_m \sin m\theta + \sum_{3,5,\cdots} b_m \cos n\theta\right) \quad [11]$$

(*b*) *Transverse Bending:*

$$v = -rRc_t(\phi)\left(\sum_{2,4,6,\cdots} a_m' \cos m\theta + \sum_{3,5,\cdots} b_n' \sin n\theta\right) \quad [12]$$

The dimensionless parameters a_m, b_n, a_m', b_n' are now determined by inserting the foregoing expressions into Equations [9] and [10], respectively, and solving simultaneously the sets of equations obtained by differentiating V with respect to each of the parameters used in the formal solutions given. In the case of in-plane bending, an additional equation, expressing the fact that the resultant axial force is zero, is required for the determination of the neutral-axis shift δ.

In the von Kármán and Vigness "first approximation" solutions the quantity $1 + (r/R)\sin\theta$ was replaced by unity, and all terms except the first in the series solutions were dropped; the neutral-axis shift was also neglected, in the case of in-plane bending. The parameters a_m and a_m' were then found to be equal to $3/(5+6\lambda^2)$ where $\lambda = tR/r^2$ as before.

The bending moments may be calculated by relations

(*a*) *In-Plane Bending:*

$$M_p = \frac{E}{1-\nu^2}\int_0^{2\pi} e_p\, t r^2 \sin\theta\, d\theta \quad [13]$$

(*b*) *Transverse Bending:*

$$M_t = \frac{E}{1-\nu^2}\int_0^{2\pi} e_t\, t r^2 \cos\theta\, d\theta \quad [14]$$

These may be put in the form

(*a*) *In-Plane Bending:*

$$M_p = \frac{EIc}{K_p} \quad [15]$$

(*b*) *Transverse Bending:*

$$M_t = \frac{EIc_t}{K_t} \quad [16]$$

Here the factors K_p and K_t are "flexibility factors" for in-plane and transverse bending, respectively. In the von Kármán and Vigness approximations, these are equal and given by

$$K_p = K_t = (1-\nu^2)\frac{10+12\lambda^2}{1+12\lambda^2} \quad [17]$$

The factor $(1-\nu^2)$, which appears in the result was not given by the previous investigators, although a consistent use of the assumptions listed (which were made or implied in the previous work) leads to the result just given. These assumptions are plausible, but in at least some cases cannot be strictly true. The difference of about 10 per cent due to the factor $(1-\nu^2)$ would not usually be appreciable compared to the uncertainties in pipe installations, and its omission provides a safety factor. Therefore it has been dropped in all calculations made in the present theory, in order that results may be in agreement with the familiar results of the long-radius theory, in the limiting case of small r/R and large λ.

Discussion

NICOL GROSS[2] AND HUGH FORD.[4] The authors are to be congratulated on making a further contribution to elucidating the problem of thin short-radius curved tubes. It is the first time that the importance of end constraints has been assessed and, though an extreme case, seldom occurring in practice, is dealt with, their experimental results are valuable as only pipe bends of large λ have been examined in the past.

Of greatest importance to students of the elastic properties of curved tubes are the theoretical considerations given in the Appendix. Berg[5] and his collaborators had stated in 1941, that it was not possible to use von Kármán's analysis for accurate stress calculations when $\lambda < 0.1$. It would appear to be a

[2] British Welding Research Association, London, England. Mem. ASME.

[4] Imperial College of Science and Technology, London, England.

[5] "Zur Frage der Elastisitat, der Beanspruchungen und der Festigkeit Warmbetriebener Rohrleitungen," by S. Berg, H. Bernhard, and H. Richter, *Forschung auf dem Gebiete des Ingenieurwesens*, July-August, 1941.

consequence of Symond's analysis that the error introduced by assuming symmetry not only with respect to the axis in the plane of the bend, but also with respect to that perpendicular to it is unimportant, and that the assumption $R + r \sin \phi \approx R$ also did not influence much the magnitude of the stresses, provided a sufficient number of terms of the von Kármán series for the displacements were considered.

In this experimental work, the authors have used resistance strain gages which were applied only to the outside surface of the bend. Presumably it was decided not to apply gages on the internal surface because von Kármán's second assumption was considered to be valid. If this assumption is valid, transverse stresses calculated on this basis would exhibit the following characteristics:

(*a*) The largest value of transverse stress inside would be equal in magnitude and opposed in sign to the largest transverse stress outside.

(*b*) At 0 deg the transverse stress at the middle layer (mean of outside and inside surface) would be 0.

Had the authors applied strain gages on the inside surface, they would have found that for in-plane bending (reducing the radius of curvature):

(*a*) The largest value of transverse stress inside (compression) is considerably larger than the largest transverse stress outside (tension).

(*b*) At 0 deg there is at the middle layer a transverse compression (for $\lambda \approx 0.3$ and $r/R \approx 1/3$ this was $1/4$ of the transverse stress measured outside).

These conclusions are drawn from recent tests carried out at the Engineering Laboratory, Cambridge University, the results of which have not as yet been published.[6]

If an element of the pipe wall is considered, it will be found that in addition to the stresses which cause the cross section to deform roughly to elliptical shape, it is necessary for equilibrium that a mean transverse stress should also exist. Since the value of this mean transverse stress is a function of the ratio r/R, this effect is not important in large-radius bends, the error introduced by von Kármán's assumption being insignificant for the types of bends considered by him.

Hovgaard,[7] who had suggested in one of his earlier papers the existence of what he called "the transverse compression," considered this effect also in large-radius bends only, since in his later papers he decided to neglect it when estimating the largest stresses occurring in curved tubes. From consideration of equilibrium, this mean transverse stress S'_w can be shown as being

$$S'_w = -\frac{r}{R} \cos \theta \int_{\theta}^{\pi/2} S_l \, d\theta$$

where S_l = longitudinal stress at middle layer.

It can be seen that this does not alter materially the transverse stress in large-radius bends ($r/R \ll 1$). In a short-radius bend, however, it is added to the transverse stress as obtained from von Kármán's theory, and having its maximum near $\theta = 0$ deg, it will reduce there the tensile transverse stress on the outside and increase the corresponding compressive stress at the inside surface. This may also explain the comparatively large discrepancy between measured and calculated values at 0 deg in Fig. 4 of the paper, where otherwise the agreement is very satisfactory.

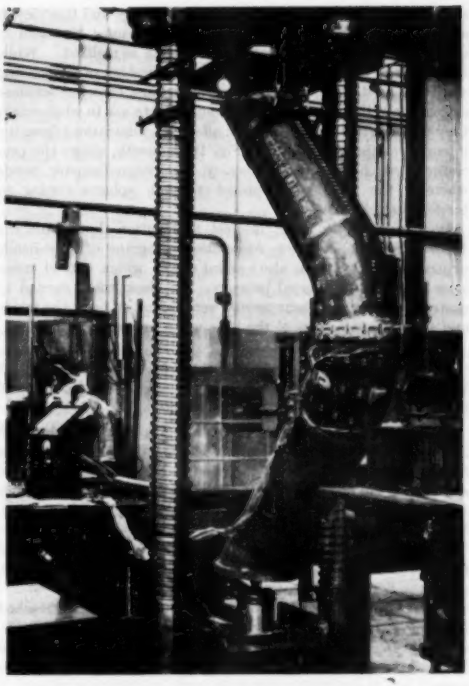

FIG. 19 GENERAL TEST ARRANGEMENT

Fig. 19, herewith, shows the general test arrangement used in our tests for applying forces reducing the radius of curvature for in-plane bending of a curved pipe having $\lambda \approx 0.09$. It was found that the difference between the largest transverse stress inside and outside was of the order of 40 per cent.

This fact is not entirely unimportant, as, in the case of the experiments of the authors, it affects the following points:

(*a*) The calculation of stress at the middle surface, dealt with under the heading Stresses and Stress-Intensification Factors.

(*b*) Fig. 9; curve A.

(*c*) The fourth point of the conclusions, which, in our view, would require revision.

It is perhaps worth mentioning that though Hovgaard had thought, as the authors mention in their fourth conclusion, the longitudinal stress at the middle layer was important for calculating stresses in pipe systems, he recognized later[8] that it was necessary to use as a strength criterion what he termed an "equivalent" stress, as determined by one of the theories of strength of materials under states of combined stress. The equivalent stress (obtained from measured longitudinal and transverse stresses) bears no relation whatsoever to the longitudinal stress at the middle layer.

The authors have investigated a number of different end constraints and rightly emphasize the importance of these constraints

[6] Earlier tests, however, carried out by N. Gross and reported in the discussion of J. R. Finniecombe's paper (see Proceedings of The Institution of Mechanical Engineers, vol. 158, 1948, p. 377) had already shown that the assumption was not valid for small λ and small R/r.

[7] "The Elastic Deformation of Pipe Bends," by W. Hovgaard, *Journal, Mathematics and Physics*, vol. 6, 1926, pp. 69–118.

[8] "Stresses in Three Dimensional Pipe-Bends," by W. Hovgaard, Trans. ASME, vol. 57, 1935, p. 413.

and of the method of loading. We have found—and this view is supported by others[9]—that the greatest care must be taken to insure that the intended method of loading is realized. While Fig. 1 of the paper does not give much indication of the loading appliance used, it is felt that the authors must have encountered difficulties in this respect, and we would like to ask to what extent they consider their results may be affected by deviations from the intended method of loading. Fig. 19, herewith, shows the precautions we have found necessary with large-diameter bends whereby the loading is applied through spheres resting on hardened steel plates.

It may, perhaps, be of interest to mention that within the British Welding Research Association program of pipe-bends experiments, tests were also carried out in which curved tubes were subjected to internal pressure. In these tests, carried to destruction, strain measurements were taken on both the inside and the outside surface of the tube up to pressures of 4000 psi.

A. R. C. MARKL.[10] This paper gives at least partial answers to the following questions, which have long been in the mind of those engaged in piping flexibility analysis:

1 Existing theories (von Kármán,[11] Vigness,[12] Beskin[13]) all have been based on the assumption that the pipe radius r is sufficiently small in terms of the bend radius R so that the ratio r/R can be ignored. Is this assumption reasonably satisfactory also for welding elbows of 1 and $1^1/_2$-diam bend radius, particularly those of thin wall?

2 Existing theories strictly apply to an endless toroidal section. To what extent do end effects, such as tangents or flanges, affect the flexibility and stress factors?

With regard to the first problem, the conclusion to be reached from the authors' investigation is that a reasonably precise theory, such as Beskin's,[13] predicts both the flexibility and stress-intensification factor with ample accuracy for engineering purposes.

To illustrate, Beskin's flexibility factor K in the range of low flexibility characteristics λ closely follows the formula

$$K = 1.65/\lambda$$

The authors' "theoretical" values, as taken from the curves in Fig. 5 and 6, are only about 4 per cent higher, and the test points plotted for the condition with tangents at both ends could be taken to equally confirm Beskin's and the authors' prediction.

In so far as stress-intensification factors are concerned, to judge from the theoretical curves plotted in Figs. 10 to 17 of the paper, these are substantially identical with those derived from Beskin, with the exception of the longitudinal factor for in-plane bending, which the authors show to be roughly 10 per cent higher than Beskin's. The experimentally determined values show a scatter of ±25 per cent, and in some cases more, about the theoretical values.

With respect to the second problem, it would be reasoned (1) that any form of end restraint, which does not induce higher stress intensifications of its own, would tend to lower both the flexibility and stress-intensification factors, and (2) that this lowering would be the more pronounced the shorter the arc of the bend, the lower the flexibility characteristic λ (or the higher the basic flexibility), and the stiffer the restraint.

Actually, the flexibility and stress-intensification factors obtained in the tests with tangents were of the order predicted by theories ignoring end effects, indicating that the restraint imposed by tangents is of a low order. On the other hand, rigid flanges produced a sizable lowering.

The expectation that the flexibility would differ with different arc lengths apparently was not borne out by the tests, although it is appreciated that experimental determination of flexibility factors is somewhat uncertain; the authors are to be congratulated on what may be considered a relatively small spread between different determinations, which is evidence of a very careful measurement procedure.

Stress-intensification factors of the specimens behaved as anticipated. Even where the restraint was produced by tangents only, the results for the right-angle bends were consistently lower than for the U-bends, values for the former apparently ranging from 70 to 95 per cent of those for the latter. The writer's company, in yet unpublished tests covering a wide range of arcs, has observed a similar trend.

For restraint by flanges, the end effect is obviously much more pronounced. It would appear from a study of Figs. 10 to 17, in conjunction with data of the writer's company on small arcs, that each flange canceled the influence of between, roughly, 25 and 35 deg of arc of the bend, i.e., bends flanged at both ends gave approximately the same stress-intensifications as bends of 50 to 70 deg shorter arc with end tangents. As expected, this effect was more pronounced for low values of λ, as is evident from the fact that the stress-intensification factors for 90-deg bends with flanges at both ends are about the same, despite a more than 2:1 ratio in theoretical stress-intensification factors for the limiting cases of $\lambda = 0.044$, and $\lambda = 0.137$. In order to make it possible for the average engineer who has not access to test data to follow the authors' recommendation that, under certain conditions stated in item 3 of the conclusions, "the flexibility factors should be taken from experimental data," it would appear necessary for the authors to devise some approximate rule for evaluating the effects of flanges, possibly of the type indicated in this discussion.

In final comment, the writer cannot subscribe to the authors' statement in item 4 of the conclusions that the longitudinal stress factor is the most important. Even the originator of the practice of using this criterion, Professor Hovgaard, in the writer's interpretation, never proposed this as more than the best correlation between theory and tests he could offer at the time. Tests made in the writer's laboratories and reported upon by the writer[14] clearly demonstrated that failure is caused by either longitudinal or circumferential stress intensification, whichever is the greater, but that the apparent stress-intensification factor (in relation to straight commercial pipe or butt welds between such) is only about one half that predicted by theory. It so happens that for in-plane bending, the condition explored by Hovgaard, one half the controlling circumferential stress factor approximately equals the longitudinal factor, so that the same result is obtained with Hovgaard's and the writer's approach. However, failure for in-plane bending definitely occurs in the form of a longitudinal crack connoting transverse stress, and for this reason it would seem more logical to apply the criterion suggested by the writer.

D. R. ZENO.[15] The writer agrees with the authors' foresight in cutting out some of the flexibility and stress-intensification factors.

In the description of the construction of tube bends there is no mention of having thoroughly annealed and descaled the tube bends before the tests were made.

---

[9] "Load-Deflection Relations for Large Plain, Corrugated, and Creased Pipe Bends," by E. T. Cope and E. A. Wert, Trans. ASME, vol. 54, 1932. Paper FSP-54-12; discussion by H. E. Jenks.

[10] Chief Research Engineer, Tube Turns, Inc., Louisville, Ky.

[11,12,13] Reference is to authors' Bibliography (1), (3), and (4), respectively.

[14] "Fatigue Tests of Welding Elbows and Comparable Double-Mitre Bends," by A.R.C. Markl, Trans. ASME, vol. 69, 1947, pp. 869–879.

[15] Engineer, Newport News Shipbuilding and Dry Dock Company, Newport News, Va. Mem. ASME.

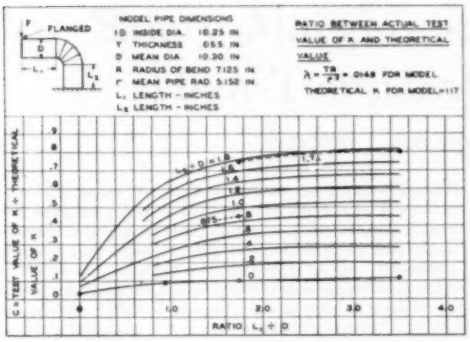

FIG. 20 RESULTS OF TESTS ON BUILT-UP ELBOW

The test results, in so far as the over-all flexibility is concerned, may change only slightly because of the lack of annealed tubing. On the other hand, in regard to the stress measured from strain, large errors may exist, since the stresses introduced from forming of the tube added to the stresses from the loading may have carried beyond the yield point before that due to the loading only. It would be interesting to know the actual measured stress for the more highly stressed specimens.

Information may be available from these tests to note the additional flexibility obtained for a straight tube over that for a straight bar. It also may be possible to include the effect of length of tangent on the flexibility and stress of the curved tube.

Fig. 20 of this discussion shows the results of some tests, on a built-up elbow with varying length of tangents, conducted by R. W. Nolan of the writer's company. These tests were made for a definite production job with the idea of obtaining a quick answer of the load versus deflection. The free end of the test specimen was welded to a $^1/_4$-in. plate, and the fixed end was welded to a 1-in. plate which was bolted to a 3-in. plate which was dogged to a steel slab. Other particulars of the elbow are shown in the illustration.

AUTHORS' CLOSURE

The work involved in calculating stresses and flexibilities of complex piping systems is already so great that one feels most hesitant about showing that the methods are still too simplified for proper accuracy.

Messrs. Gross and Ford have pointed out that there exists a component of transverse stress that is uniform across the thickness of the pipe wall. This stress is maximum at 0 deg (see Fig. 4) and vanishes at 90 deg for in-plane bending. The reason for the existence of this stress is shown clearly in Fig. 2(*a*) of reference 3, where it is shown that a bending moment decreasing the bend radius causes a transverse compressive stress which is maximum at the neutral plane. This stress always adds to the local transverse stress on the inside surface of the wall of the pipe and subtracts from the local stress on the outside surface. The local stresses are caused by bending of the pipe wall in the plane of the section. Gross and Ford have made measurements on both the inside and outside surfaces of the pipe wall and have found differences in transverse stresses in the order of 40 per cent. This would indicate that the general transverse stresses, which the authors have tacitly neglected, amount to about 20 per cent of the value of the local transverse bending stresses at the zero-degree axis for the type of pipe considered by the discussers. It would be well if later papers would further refine this type of work by a correction of this type.

It is interesting to note that no such general transverse stress is predicted for out-of-plane bending; however, in this case a torsional stress exists that has been neglected. The origin of this torsional stress is illustrated by Fig. 2(*b*) of reference 3, and its amplitude to first-order approximation is obtainable from Equation [11] of the same reference.

Their second point considered the method of loading. The pipes consisted of a curved section together with its tangents, as shown in Figs. 1 and 2. At or near the free end of each of these tangents was welded a flange which prevented any deformation of the tube cross section at that location. The flanges were several tube diameters distant from the end of the curved section so that they did not appreciably affect cross-sectional deformations there. Known forces and moments were applied to the tube so that the flanges were between the area of load application and the section of tubing studied. All deflections and rotations were made from one flange with respect to the opposite flange, hence the rigidity of the supports was not important. No deflection measurements were made from points on the pipe-wall surface as to do so would confuse the tube center-line deflections with displacements caused by deformations of the pipe cross section. When no flanges existed at the immediate ends of the curved section (see Fig. 2), measurements were made from the flanges at the ends of the straight sections; deflections contributed by the straight sections were calculated and subtracted from the total deflection to obtain that due to the curved section.

It was shown by Markl[14] that the transverse stresses were the principal cause of tube fracture when they were of greater amplitude than the maximum longitudinal stresses. The work by Markl involved failure by fatigue and there is no doubt but that if fatigue is important then no stress concentration can be neglected. There is also a possibility that the physical properties of metals may be such, at unusual operating temperatures, that the multiaxial stress conditions might be of great importance. Exclusive of these factors it is often considered in piping that hoop stresses due to internal pressures are most important as no amount of strain will relieve these stresses; next in importance are the longitudinal stresses due to expansion which require a considerable plastic strain for their relief; and finally, of least importance are the transverse stresses which because of their high stress gradient are relieved by a relatively small amount of plastic strain.

Because of restrictions as to the length of this paper most information relating to the details of accuracy and techniques were omitted. In regard to the comments by Zeno, the tube bends were not annealed after construction. They were, however, subjected to several cycles of load before measurements were made and all curves relating strain or deflection to load were linear. The maximum strains measured corresponded to stresses of less than 10,000 psi.

Very careful tests have been made to determine any difference in flexibility between a straight section of tubing and a straight section of rod having the same elastic modulus and cross-sectional moment of inertia. No differences have been discovered.

The authors express their appreciation to the discussers of this paper. The work reported by Messrs. Gross and Ford is of particular interest as it takes into account hitherto neglected factors and it brings to light the type of work being performed at their Laboratory.

Safety Margins and Stress Levels in High-Temperature Equipment

By ERNEST L. ROBINSON,[1] SCHENECTADY, N. Y.

In this paper the author reviews the factors of safety and working stress levels currently in use in high-temperature equipment and discusses their relationship to physical properties at high temperature, as determined by the various kinds of tests currently in use. Differences between various industrial applications are pointed out in comparison with the general rules at present used by the author's company. Any conclusions as regards advisable changes of practice are left to the judgment of the reader whose critical comments are invited.

Introduction

THE greatly increased use during the past decade of equipment operating at high temperatures makes it desirable to examine the factors of safety used in proportioning such apparatus and machines, and to review the working stresses used in their design. By continuous review of these procedures engineers can take advantage of extended knowledge of performance and design to better advantage using existing materials. By running a wide variety of tests on standard materials and the same tests on new materials with improved properties, engineers can add to their resources the new materials being steadily discovered, invented, and evaluated for useful application. There is much to be learned from comparisons, and it is only through divergencies of practice that progress can occur.

Factor of Safety and Elastic Analysis

For generations structures have been proportioned with a "factor of safety" relative to the tensile strength of the material which might be 3, 4, or 5 to 1. The tensile test is quite arbitrary. A standard specimen is pulled in a rather standard manner to fracture, and the maximum pull is divided by the original area of cross section. This simple procedure facilitates design. Assuming that the material is elastic up to more than one half its strength, a factor of safety of 4 would provide a 2 to 1 margin for uncertain or local overstresses, or increases of service loads with time, without permanent set or distortion.

With the development of complex elastic analysis and the perfection of analytical and mechanical means of determining local stress maxima, came also the stating of a so-called "factor of safety" relative to the elastic limit of the material. It is a moot point if a working stress set at 40 per cent of the elastic limit should be described as corresponding to a factor of safety of $2^1/_2$ on the elastic limit, because no question of safety is necessarily involved in exceeding the elastic limit. There is usually a sufficient margin of ductility to assure local yielding, if the overstress is only secondary, and a redistribution to a value which at the worst has a more representative safety factor equal to the ratio of tensile strength to the elastic limit. Very likely further distortion (which may not involve serious geometric changes of shape) may suffice completely to relieve the local stresses and show that there is really an excellent margin of safety relative to ultimate rupture.

In such a case the real margin of safety may lie between the elastic limit and the tensile strength rather than between the design stress level and the elastic limit. When this is the case the practice of specifying a high elastic limit actually may involve more hazard than safety. There is much to be said for such a rule as that to be found in the requirements of the American Bureau of Shipping (1),[2] limiting the mean tangential stress in a turbine rotor to $^1/_2$ the yield strength or $^1/_4$ the ultimate strength, whichever is lower. This places no premium on trying to increase the elastic properties by special heat-treatment beyond $^3/_4$ of the tensile strength.

The proportioning of a structure to avoid elastic overstress may lead to an excellent design, but its reserves of safety may be out of proportion to the comparison of the ratio of its elastic properties to its working stresses. In other words, elastic analysis is sometimes useful for proportioning but not so good as a criterion of safety. Thus bursting tests on disk wheels show a better correlation between average stress and tensile strength than between elastic stresses and tensile strength (2).

Elastic theory is so "teachable" in schools and opens so many beautiful vistas for the application of mathematics that there is danger of cultivating a degree of false security in the minds of students new to the complexities of material behavior. Certain theories of failure have been based on a definition of failure as the occurrence of a local strain in excess of a small fraction of 1 per cent, for instance, 0.002 in. per in. Actually this definition constitutes a good statement as to the limitations of elastic theory. To try to connect elastic analysis as such with the success or failure of equipment, may give a false notion as to the safety of a machine or structure which is simply undergoing normal adjustment to service (3).

When the author was studying the theory of least work in engineering school, it was pointed out to him that the architects of the great cathedrals of Europe knew nothing of modern elastic theory and used methods of stress analysis which would be deemed faulty according to its tenets, in spite of which the structures they built have endured the ages.

Consequences of Going to Higher Temperatures

It is always hard to read the complex motives that have influenced action in the past, and all too easy to oversimplify the reasoning used at the time. In the 1920's, when temperatures increased so as really to influence the tensile properties and cut down both the tensile strength and elastic limit at operating temperature, it is probable that the first steps taken were correspondingly to reduce working stresses so as to preserve the nominal factors and margins currently in use.

This was the era in which the creep test, Fig. 1, became widely discussed and rather commonly recognized. It was easy to go

---

[1] Structural Engineer, Turbine Engineering Divisions, General Electric Company. Fellow ASME.

Contributed by the Gas Turbine Power Division and presented at the Semi-Annual Meeting, St. Louis, Mo., June 19–23, 1950, of The American Society of Mechanical Engineers.

Note: Statements and opinions advanced in papers are to be understood as individual expressions of their authors and not those of the Society. Manuscript received at ASME Headquarters, February 16, 1950. Paper No. 50—SA-28.

[2] Numbers in parentheses refer to the list of References at the end of the paper.

from a reasoning that related working stresses to an elastic limit, to a criterion connecting working stress with a rate of deformation for some long but definitely stated period of service. Thus, in Germany came the DIN 35-hr creep test, while in America

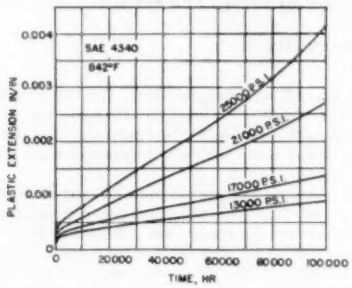

FIG. 1 CONSTANT-STRESS CREEP TEST

(This test enables proportioning of equipment so it will maintain shape throughout its life. It is important that conclusions be based upon tests at extensions tolerable in service so as to avoid faulty estimates based upon excessive strain-hardening. In steam turbines creep rates of 10^{-6} per hr and 10^{-5} per hr are used for proportioning parts. In boilers a creep rate of 10^{-7} per hr is used by the ASME Boiler Code for guidance. Precisely speaking, this test is run at constant load rather than constant stress, because ordinary service is at constant load.)

10^{-6} per hr and 10^{-7} per hr creep strengths were used based on 1000-hr tests.

INFLUENCE ON CHOICE OF WORKING STRESSES

The ASME Boiler Code, as recorded in the 1930 Jacobus paper (4), chose to base working stresses on-⅔ the stress which would cause a creep rate of 1 per cent per 100,000 hr. There was no subsequent published revision of that basis for selecting working stresses until 1949, when a statement was published (5) that Tables P-7 and U-2 of the Boiler Code limited *S*-values to 80 per cent of the stress, which would cause a creep rate of 1 per cent per 100,000 hr (which is 10^{-7} per hr). The 1950 edition of the Code for Unfired Pressure Vessels (6) announces that stresses in Table UG-23 "are based on 100 per cent of the stress to produce a creep rate of $^1/_{100}$ per cent per 1000 hours" (which is 10^{-7} per hr), and the values listed are 25 per cent higher across the board than in Table P-7. The spread in test data is here recognized by noting that the values so chosen are based upon a conservative average of many reported tests.

The discovery of the straight line log-log plot of stress versus time to rupture (7) with the corresponding sudden breaks, which occur without the warning afforded by necking, brought a new factor of importance to be reckoned with in designing for long-time service at high temperature, Fig. 2. A material which, at high temperature, has 50 per cent of its room-temperature tensile strength might break without any warning deformation after 100,000 hr under a stress no more than 5 per cent of its room-temperature tensile strength. It must be admitted that no long-time rupture tests have extended to 100,000 hr, but with the "knee" in the otherwise straight line passed somewhere between 100 and 1000 hr, tests have been run to 20,000 hr without further deviation from a straight line. In fact it would seem extremely rash to assume that the line might bend upward and try to level off in longer tests. It would seem more likely that the deterioration of the material might accelerate rather than slow down. In fact critics, who attempt to discount the importance of this test, sometimes claim that the more complex stress distribution in an actual structure should afford greater strength than resides in a simpler pull test. While this may be so, it seems to the author somewhat rash to assume this in advance of test proof and in the face of contrary evidence (2).

The importance of the long-time rupture test has been recognized by the ASME Boiler Code in the statements just referred to (5, 6), where it is stated that the existing values in Tables P-7 and U-2 were chosen not to exceed 50 per cent of the stress to produce rupture at the end of 100,000 hr, but that new values added to Tables P-7, U-2, and UG-23 will not exceed 100 per cent of the stress to produce rupture at the end of 100,000 hr. If actual stresses were really equal to an *S*-value set at the 100,000-hr rupture strength, the life of the equipment would be but 11 years without any margin of safety. The author believes that peacetime industrial equipment should have a plainly under-

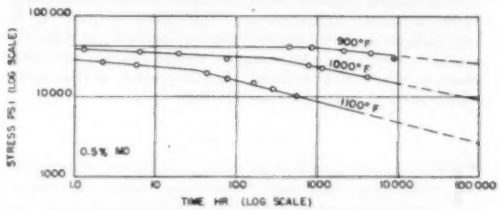

FIG. 2 LONG-TIME RUPTURE TEST AT HIGH TEMPERATURE

(At each temperature a series of bars loaded with progressively lower loads break after progressively longer periods. The log-log plot is a straight line except for the "knee" at 100 to 1000 hr. Long-time breaks occur without warning deformation at loads a small fraction of the room-temperature tensile strength. Extrapolated to form a basis for long-lived designs, a factor of safety of 3 to 1 or 2 to 1 on the 100,000-hr rupture strength is suggested as appropriate.)

standable factor of safety with reference to expected life, as distinguished from military weapons which properly may be designed on an expected-life basis without any other margins of safety. Furthermore, in the tables as at present constituted, it is not possible for the lay reader to know which values have been set at the 50 per cent level and which at the 100 per cent level. The subgroup which sets these figures is cognizant of this matter but so far has not completed a rational modernization of the figures.

Successful experience during the past 10 or 20 years is cited as evidence that the rupture test is of no significance, whereas the evidence of the test itself is to predict successful performance for about that long and longer where design stresses have been low or temperatures subnormal. It is now just about 100,000 hr (net operating time) since moly steels went into general use, and the evidence of the next 10 years should be studied as capable of yielding crucial information. If the materials operating with full stresses and temperatures continue to stand up, then the higher stress levels may be justified.

IMPORTANCE OF FORMULAS AND METHODS OF USE

It is important to note here that actual stresses and temperatures must be used in carrying out any valid analysis rather than the artificial formulas used in recognized codes for assuring safety. Thus, both the ASME Boiler Code and the ASA Code for Pressure Piping determine thickness by placing in a formula an allowable figure from a table. This practice adds one fixed slice to the thickness and one or more percentages, after which the next-larger even schedule may be selected. A check back may show the actual stress to be only one half or two thirds the nominal figure, thus increasing the actual safety factor by these hidden margins. Engineers who are intimately familiar with the application of these formulas are likely to be cognizant of this matter. But such tables are widely quoted and in danger of being

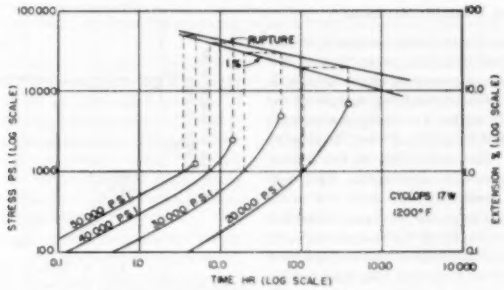

FIG. 3 SHORT-TIME RUPTURE TEST AT HIGH TEMPERATURE
(Run similarly to the test in Fig. 2, this test is used for proportioning short-lived equipment where early replacement is anticipated. Designs may be based upon minimum expected life without other protective margin. Because loadings are high, extensions are recorded and the life for 1 per cent deformation is indicated.)

used by others not so well informed as to how and where the safety margins are secured. Constructive progress is only possible as a result of sound analysis, and sound analysis is very difficult except by the use of real stresses rather than nominal values. Predictions of service performance over the forthcoming years can only be based on test if the formulas correspond closely with reality.

An illustration may help in understanding these "hidden" margins of safety which tend to conceal the true factor of safety or cloud its significance. A certain *S*-value may be close to the stress which, in a long-time tensile test, would cause rupture in 100,000 hr. The apparent safety factor for 11 years is, therefore, unity. In other words, there is no apparent margin, and it is difficult to understand why pipes 11 years old do not start to crack. However, when designed, the required thickness was computed from a formula which is based on an elastic stress somewhat higher than the stress which will persist. To this thickness was added an allowance for corrosion which takes a long time to occur, during most of which the stress is lower than recorded. Because mill tolerance might permit $^1/_8$ thinner pipe (along one side only), $^1/_7$ is added to the already oversize thickness. Then, because a 4-diam radius is used in bending with a consequent thinning of $^1/_8$ on the outside radius only, another $^1/_7$ is added to the pipe which has already been twice increased in thickness. It is, of course, very unlikely that both thin places would coincide. However, after this procedure is gone through, the next-larger even schedule size is adopted.

Examination of actual cases shows that the average stress in the pipe wall, statistically speaking, is likely to be anywhere from, say, 50 per cent to 80 per cent of the *S*-value. In other words there was a factor of safety of something over unity up to 2 relative to 100,000 hr but hidden in the procedure. In this connection it is necessary to bear in mind that a 2-to-1 factor in stress may mean as much as 10 to 1 in life, while as small a margin as 20 per cent stress reduction can effect an extra 100 per cent in life. These relationships show how difficult it is to analyze service for comparison with test and get convincingly significant results unless the formula used expresses significant quantities rather than nominal values.

In this connection it is interesting to note that the ASME Boiler Code, followed by the ASA Code for Pressure Piping, went from a formula which represented the average stress over the thickness of a pipe or drum to a formula based on elastic analysis, at a time when high-temperature pipes and drums definitely were entering the plastic range. There was a good reason for this because the older formula had been abused by the use of the outside diameter, and this abuse became very apparent as thicknesses increased. However, the present formula, which is fairly close to elastic analysis, goes only part way toward correcting this matter and still represents a stress which tends to decrease in service rather than the somewhat lower stress which must persist due to the loading.

It seems necessary to call attention to the fact that the oil-refining industry has made successful use for many years of the API-ASME Code (8), in which Table 1 gives allowable stresses at lower temperatures based upon $^1/_4$ the tensile strength, as compared with $^1/_5$ the tensile strength in Table P-7 of the Code for Power Boilers, and a correspondingly higher level of allowable stresses at high temperature. The evidence both of the creep test and the rupture test goes to show that a shorter period of useful life is expected at the higher allowable stress level. This whole question of expected useful life is not too well recognized in the rule books. Furthermore, a successful annual inspection is not necessarily a good assurance of a long expectation of life. In the rupture test, it is difficult to detect any deterioration of the material much before the actual break.

The reality of the long-time rupture test was well demonstrated in the 1930's by the extension of carbon steel up close to 1000 F in the mercury boiler. This led to plain rupture failure in tubes under too much longitudinal stress due to the weight of the liquid. This much had been learned prewar (9).

The advent of the jet engine during the war, born of wartime necessity, was made possible by recognizing the possibility of getting a short but adequate life for a military weapon by using very high design stresses corresponding to 100 to 1000 hr life, Fig. 3, instead of limiting stresses to a suitable factor of safety based on the 100,000-hr strength.

The exhaust-gas-driven turbine supercharger developed after the first world war was proportioned largely on short-time tensile tests at operating temperature. This was a good working possibility as was later learned, because that part of the rupture line to the left of the knee is more closely tied to the short-time tensile strength than to any long-time nominal figure beyond the knee of the curve. During the second world war direct use was made of the long-time rupture test in the development of the aircraft gas turbine. In fact the success of the gas-turbine development during this critical period was a direct tribute to the significance of the long-time rupture test in the range out to 1000 hr. For equipment with no longer expected life, the additional uncertainties of extrapolation for the prediction of performance longer than possible for test could be avoided.

Suggested Levels for Working Stresses

What then, are suitable levels for working stresses with reference to this test? Values currently in use range from a full 100 per cent of the test value in equipment designed for a definite life, to as low as $^1/_3$ the 100,000-hr value for equipment intended to have indefinite life. The author's company makes wide use of the 3-to-1 factor on the 100,000-hr strength for the proportioning of steam-turbine parts. The suitability of the former limit for military applications cannot be questioned. The margin of safety in the latter case eventually may turn out to be greater than necessary. When the long-time rupture strength is a minor fraction of the short-time tensile strength, such as $^1/_3$ or $^1/_{10}$, to take a 3-to-1 factor on this fraction is to give a short-time factor of safety as great as 15 or 30-to-1, and this may not be justifiable. Much high-temperature equipment undoubtedly has operated for a period of years with success because it has enjoyed a transitory factor of safety based on a well-proportioned initial design. Thus, a pressure vessel originally designed with a 5-to-1 factor of safety on the tensile strength may still be just safe at the end of 100,000 hr, if the corresponding long-time rupture strength is not less than $^1/_5$ the short-time tensile strength. From the time of discovery of the rupture test, the author's company has leaned toward ample safety factors. If service eventually shows these factors unnecessarily conservative, lower values will be used.

Perhaps the rupture test is of more importance in the simpler applications such as pressure vessels and piping, where distortion by itself is of little consequence. In such applications it is important not to crack or break open.

In high-speed rotating machines it is important to maintain dimension, both to avoid leakages and to maintain perfection of balance and consequent smooth operation. Here design values as low as the stress corresponding to 0.001 per cent per 1000 hr are currently in use by the author's company. This is a rate of 10^{-6} in. per in. per hr. For shrunk-on wheels this company estimates as well as it can from its tests the strength corresponding to a rate of 10^{-6} in. per in. per hr. Bailey and Roberts (10) mentioned this same rate as appropriate for wheels, and credited the choice to Baumann (11).

Creep-Test Procedures and Interpretations

Methods of determining the creep rate vary from the simple constant-stress test, which closely represents what goes on in a turbine shell or boiler drum under steady pressure or bucket at constant speed, to the relaxation test at constant total elastic-plus-plastic extension that simulates bolt action.

The "constant-stress" test, Fig. 1, is sometimes more accurately described as a "constant-load" test, but as ordinarily run it represents the condition of service, while the less representative but "true" constant-stress test differs less in result than the ordinary spread in test results. Of far greater importance is the total strain under which the test is run. The practice of plotting the strength based on the "minimum rate" attained after completion of all "initial creep" and before going into the "third-stage" creep, which leads to rupture, gives high strength values and presupposes that large distortions are characteristic of and allowable in the equipment.

The determination of creep rates in a test with a limited total extension corresponding to the conditions of service seems more appropriate to the author. Such a test is afforded by the "step-down" relaxation test, Fig. 4, which also may be used to evaluate bolting materials by the determination of their characteristic residual stresses.

A consideration of the most effective use of laboratory facilities also favors the use of the step-down test at a controlled extension.

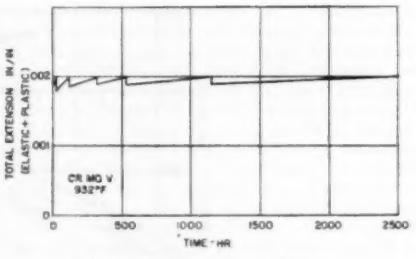

Fig. 4 Relaxation-Creep Test

(This form of creep test is run with constant total elastic-plus-plastic extension, such as occurs in a bolt where creep is replaced by elastic extension. This illustration shows the step-down type of test as run in an ordinary constant-stress testing machine by manual adjustment. The author's company uses the 10,000-hr residual stress for proportioning bolts.)

One bar tested in this manner at the desired extension yields as much applicable information as 3 or 4 bars tested under conditions of constant load which attain amounts of extension which are not applicable to a particular case. It is not to be denied that the several bars yield a greater amount of general information than the single bar. Furthermore, general information is useful for scientific studies of general behavior. However, for use in machines such tests frequently need a limitation not always recognized, namely, that they be run without exceeding the total strains tolerable in the equipment. Otherwise strain-hardening effects are present in some of the bars which may tend to vitiate conclusions that must be based on extrapolation. The importance of this matter was emphasized by Bailey at the very beginning of his classic paper (12).

Working Stresses for Bolts

The 10,000-hr residual strength determined with a total extension of 0.002 in. per in. is used by the author's company for proportioning bolts which may be conveniently retightened on an annual overhaul. Higher values could be used where more frequent tightening is both possible and not annoying. The importance and usefulness of "follow-up" elasticity in assuring effective flange bolting has been discussed in the First Progress Report of Project 16 of the ASME-ASTM Joint Committee on the Effect of Temperature on the Properties of Metals (13).

The *S*-values listed for bolting materials in Tables P-7 and U-2 of the Boiler Code have been set at the same level relative to the creep strength of the material as the *S*-values for the other materials, namely, 80 per cent of the stress to produce a creep rate of $^1/_{100}$ per cent per 1000 hr in Tables P-7 and U-2, and 100 per cent in Table UG-23. Such bolts require generous amounts of flange or other elasticity to assure maintenance of tightness. The Second Progress Report of Project 16 (14) showed that in a rigid flange it takes but 1000 hr for a bolt to relax to a stress corresponding to a creep rate of $^1/_{100}$ per cent per 1000 hr. Bolts in rigid flanges if intended to hold tight for long periods need to be proportioned for lower stresses than given in any of the Boiler Code tables.

Ductility and Elongation

What is a proper requirement as to ductility and how is it to be measured? The fact that large percentages of elongation were readily available in low-carbon steel made it natural enough to write this property into a specification because, obviously, something was the matter with such a steel if it did not have the elongation characteristic of itself. But this is another matter from saying that such large percentages of elongation generally were

more useful or assured greater safety than much smaller amounts, provided they were surely present.

Thus, local elastic stress concentrations are usually completely relieved by a yielding of $^1/_2$ per cent. It seems to call for a very special set of circumstances to make as much as 1 per cent of yielding really useful. Actually, thoughtful engineers note that it is the first $^1/_2$ of 1 per cent that is the most useful. Perhaps 2 per cent is as much as is ever really used in extreme cases. Furthermore, this is a requirement of service and needed at operating temperature. R. B. Smith (15) suggests 3 to 5 per cent as a suitable requirement for gas-turbine materials.

In a material which is to operate at high temperature levels, the most important reason for ductility at ordinary temperatures is to facilitate manufacture and handling. The difficulties of manufacture have been barriers of consequence in the progress toward materials good for high-temperature operation. However, man did not refuse to use window glass because panes could be so easily broken. However, the hardness is likely to lessen at high temperature, and the elongation in a short-time test is likely to increase.

On the other hand, the rupture which occurs at the end of a long period at high temperature is likely to be quite brittle in nature, occurring with little elongation beyond the creep in service. Notorious in this respect is the low-carbon steel which is so very ductile at room temperature. In other words, the familiar steels in which we place most confidence can be pretty treacherous at high temperature. We need to be careful not to reject, because of its room-temperature hardness, a material much better for high-temperature service. The inflexibility of existing codes and rule books in these matters constitutes a deterrent to progress, if not a definite hazard. Important as they are, bend tests and flattening tests are arbitrary. New materials should not be rejected because they differ at room temperature from what we are accustomed to. Instead, suitable limits should be set to recognize both the needs of safety and the urge to progress.

Notch Sensitivity

Closely allied to elongation is notch sensitivity which is, perhaps, most important in the fatigue test. An ordinary tensile test on a notched bar normally shows extra strength (based upon the net section at the notch), because necking down is prevented by the reinforcing effect of the material at either side of the notch. But in the long-time rupture test, where the break is brittle anyway, this strengthening effect may occur or may not, depending upon the material. The effect of a notch may similarly be great or little on the fatigue strength of a material. This is particularly important in the ability to resist vibratory stress, and, perhaps, equal in importance to the damping quality of the material. But strength to resist vibration is so specialized a quality and so closely connected with high-grade engineering design, that these properties are pretty much still in the hands of specialists and are not so widely discussed as are the more primary stresses in a structure.

"Impact" Tests

This discussion would not be complete without some mention of the use of Charpy or Izod impact tests for the securing of some indication of notch sensitivity. The fact that these tests combine two effects, namely, the sudden application of load and the presence of the notch, tends to obscure their utility and make rational interpretation difficult.

The direct applicability to equipment where sudden shock may occur is obvious, but there are many cases where breaks have occurred without shock, and the only significant quality has appeared to be a low Charpy value. This has led to a preference for a high Charpy material even though many applications have been entirely successful with low values.

It is well known that certain steels, which have high Charpy strength at high temperature and low values at subatmospheric temperatures, go through an uncertain range just at ordinary outdoor temperatures. This makes analysis of performance difficult. There is ample experience to show that low Charpy materials may be satisfactory. There is also ample evidence that high values can remove some unwelcome uncertainties. Therefore, it is certainly desirable to have a material whose uncertain transition-temperature range is below the temperatures at which it will have to be fabricated and used. However, it cannot now be said that this is a necessary requirement.

The internal damping of a metal is a precise measure of the plastic action which takes place during cyclic stressing at high frequency. Damping may be determined at very low stresses as well as very high, and at either low or high temperature. The Charpy test has a direct application in shock-resistant equipment. The damping test has a direct application in the limitation of mechanical resonance which will be discussed later. However, both these tests may have valuable lessons which have not yet been learned. Here is a field for fruitful investigation.

Temperature Strains

Cyclic fatigue stresses due to starting and stopping, or due to temperature or load cycles are primary effects that are widely considered. Based, for instance, upon complete reversal, how much creeping and "uncreeping" can a material stand? Ordinary carbon-moly pipe material (cold) has been bent back and forth through a strain of plus and minus $^1/_2$ per cent for 1000 cycles without showing any sign of a crack, and yet this strain when multiplied by the modulus of elasticity would be well beyond the tensile strength, Fig. 5. The lesson from this test is that so-called stresses due to thermal expansion are not necessarily harmful, and what is allowable must be found from quite a different sort of test from the ordinary high-speed fatigue test. The left part of Fig. 5 is a slow-speed fatigue or repeated creep test going far beyond the elastic limit and designed to furnish the needed information.

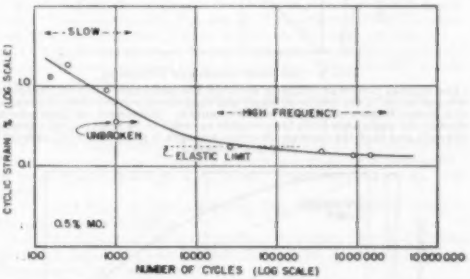

Fig. 5 Cyclic-Strain Test

(Plotted in terms of strain rather than stress, the conventional S-N fatigue diagram run at high speed has been extended to the left using 4-min cycles to avoid temperature effects. One thousand cycles on ordinary carbon-moly piping material with a strain of 0.55 per cent failed to start any crack, although this strain multiplied by the elastic modulus gives a figure well beyond the tensile strength.)

Commonly used procedures for designing expansion bends in high-temperature piping (16,17) add stresses due to thermal expansion (which tend to relax and anneal out in time due to creep) to very real bursting stresses which, if they change at all, tend to get slightly worse with time if any deformation occurs. It does not seem proper to the author to add together two effects

so entirely unlike both as regards origin and as regards consequence.

A more reasonable procedure is to assemble the piping so as to be free from thermal stress when hot, and to take the expansion stresses in the cold condition. This was recommended by R. W. Bailey long ago (12). Since tests show that high strains may be experienced many times without danger, the cold expansion stresses should be allowed more liberal limits, say, at least $^3/_4$ the elastic limit, if not actually a certain amount of plastic strain.

Cyclic Stress Plus Steady Stress

The relationships between rupture strength and fatigue strength at high temperature are not fully understood and more work needs to be done along these lines. Twenty-five years ago the author's company joined in sponsoring a series of fatigue tests at the Engineering Experiment Station of the University of Illinois, as a result of which Prof. H. F. Moore (18) published information from which it appeared desirable to redraw the Goodman diagram with the endurance limit for complete reversal equal to one half the tensile strength, and with the reduction in cyclic strength decreasing little if any as a consequence of small to moderate steady stresses, but with the upper line of the diagram eventually joining the tensile strength so as to indicate zero cyclic strength for a steady stress equal to the tensile strength (see Fig. 6). This is technically equivalent to the Gerber parabola (19, 20), Fig. 7.

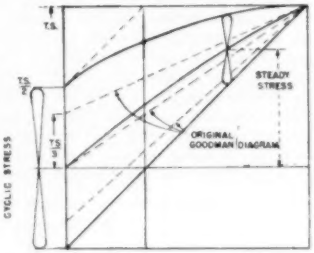

Fig. 6 Revised Goodman Diagram

(The original Goodman diagram assumed the endurance limit for complete reversal to be $^1/_3$ the tensile strength and that the safe cyclic stress decreased in a linear manner up to the tensile strength. University of Illinois tests showed the endurance limit for complete reversal to be nearer $^1/_2$ the tensile strength and that the decrease in cyclic strength is not great with moderate steady stresses.)

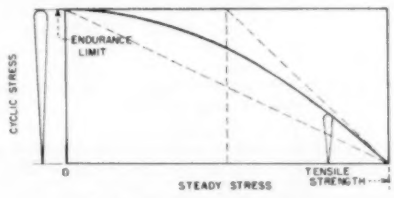

Fig. 7 The Gerber Parabola

(This diagram portrays in a different manner the same characteristics as shown by the revised Goodman diagram in Fig. 6.)

The author confesses to having frequently drawn a similar diagram for a limited life at high temperature by placing the point of the Gerber parabola at the long-time rupture strength for the required life and temperature, and then drawing backward to the endurance limit for complete reversal found by test at temperature, Fig. 8. However, reasonable as this may seem, the author admits it is pure conjecture, to be verified by test when tests become available. The difficulty is that such tests are very difficult to set up and run outside of actual service in a machine.

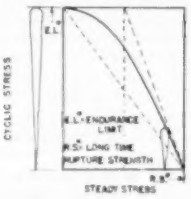

Fig. 8 High-Temperature Fatigue Diagram

(This conjectural diagram is suggested as a modification of the Gerber parabola suitable to represent high-temperature strength. The cyclic strength for complete reversal is found by test and may differ but little from low-temperature strength. The toe of the parabola is placed at the long-time rupture strength for the particular life instead of at the tensile strength.

Impact and Resonance Factors

Service in a machine is always a very complex matter. In bridge design an impact factor may represent the degree of suddenness with which a locomotive loading can come on a girder. A suddenly released load results in 100 per cent overswing about the condition of static equilibrium, and so ordinary impact factors range up to 100 per cent overload depending on the suddenness of the release. If there is velocity of application the overswing may exceed 100 per cent.

In comparison with sudden impact, the magnification of a static loading under conditions of simple resonance can be much more serious. Thus any form of periodic stimulus must be carefully avoided in high-speed rotating machines. In comparison with the 2-to-1 multiplier for sudden impact, the magnification factor for simple resonance with a sinusoidal stimulus is π/δ, where δ is the damping expressed as a fractional loss of amplitude per amplitude cycle or "log decrement." Where the stimulus is steady, as in the case of a stationary wave in a turbine wheel, the magnification at resonance is $2\pi/\delta$. If the irregularity in steam flow, whether axial or tangential, which gives rise to the vibration is a fraction β of the tangential power push on a bucket, the vibrational stress will be $2\pi\beta/\delta$ times the bending stress in the bucket that would be caused by the power push imagined as acting in the direction of the vibratory bending. The direction of bending may be axial or tangential, depending upon the direction of the irregularity and the type of vibratory motion which is resonant.

Supposing the ratio $\beta/\delta = 5$, the vibratory stress at precise and prolonged resonance would be $10\pi = 31$ times the static stress caused by the steady steam force applied in the direction of the vibratory bending. But this can occur only over an extremely

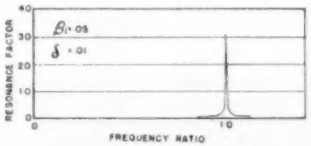

Fig. 9 Resonance Diagram

(This illustration is drawn for a special set of conditions to show circumstances that have to be taken into account in turbine design. For an irregularity factor $\beta = 5$ per cent and a damping factor $\delta = 1$ per cent the magnification at resonance is $10\pi = 31$. The diagram shows how extremely narrow is the speed range in which frictional damping is relied upon for satisfactory operation.)

narrow speed range, as illustrated in Fig. 9. With the stress so computed kept below the endurance limit of the material, the author's company finds its designs to have a satisfactory degree of reliability. Such buckets are said to have less than 100 per cent "load factor." The mortality of buckets has been found to increase with the square of the loading. Actually the chances of accidental resonance are low in constant-speed machines so that satisfactory performance has frequently been obtained with several times the standard loading. On the other hand, loadings are limited to lower values in variable-speed machines such as marine propulsion turbines.

The importance both of a smooth steam path and of using material possessed of a high degree of internal damping is evident, as also the advantage of using mechanical construction that involves friction.

Only the designer knows whether or not he has margins from resonance and the corresponding "dynamic damping" on which he can depend. Consequently, the valid analysis of the reliability of machine performance is practically impossible for anyone but the designer and, when he cannot rely on dynamic protection, he has to proceed on a statistical basis. Almen (21) has used statistical methods to good effect in describing the results of fatigue tests rather simpler than the behavior of a complicated machine. However, the viewpoint is much the same, and the results correspond surprisingly well with performance. Thus, using this line of reasoning, it is possible for the designer to "predict" a satisfactorily small level of "unpredictable" misfortunes.

Internal Stresses

Especially in citing such a reference as (21), it seems necessary to point out as Almen does that a condition of internal stress is not always detrimental but may indeed be highly beneficial. Thus, in localized areas, such as the fillets where a change of section or stress direction occurs, without the aid of any internal stress, there would be a high spot of local overstress where fatigue may choose to start a crack. In such a region, the existence of internal stresses in the form of a local surface compression balanced by a larger central region of mild tension can easily contribute greatly to improve the notch fatigue strength, or in other words to reduce the notch sensitivity.

While there is no question as to the wisdom of eliminating unsystematic internal stresses remaining after casting, forging, or welding during manufacture, examples of beneficial internal stresses may be given, such as the design shrinkage of a disk wheel on the shaft, or the cold pull up of a station pipe during assembly.

When designs are so made that the effects can be controlled and the figures compared with test results, then it is possible to proceed with confidence on a sound basis.

Conclusion

The object of this paper has been to provoke discussion of design stress levels and corresponding safety margins as they exist in high-temperature machinery and equipment.

The author believes that machines and equipment now being built and placed in service at temperatures of 900 to 1000 F and higher, have for the most part more adequate margins of safety relative to the strength of the materials at operating temperatures than did similar equipment built 20 years ago, before the common use of molybdenum-bearing steels and other heat-resisting alloys. Certainly this is true of steam turbines as built by the author's company. Such a conclusion is based upon the comparison of design stresses with test results using all applicable test methods. Without such use of test results, however arbitrary, there can be no satisfactory assurance of safe operation under advanced conditions.

Of course it is not to be expected that all classes of application would be identical in their requirements. On almost every subject it would be possible to stage a symposium or write another book. All the author has tried to do is to name illustrative figures and call attention to existing ranges of figures so as to invite critical comment.

Acknowledgment

In conclusion the author wishes to express his appreciation for the constructive criticism of Mr. A. W. Rankin during preparation of the text, and of Lieut. Col. A. W. Wheeler's interest in preparing the illustrations.

List of References

1 "Rules for the Classification and Construction of Steel Vessels," American Bureau of Shipping, 1949, sect. 33, Table 1.

2 "Bursting Tests of Steam-Turbine Disk Wheels," by E. L. Robinson, Trans. ASME, vol. 66, 1944, p. 373.

3 "Theory of Limit Design," by J. A. Van den Broek, Trans. ASCE, vol. 105, 1940, pp. 638–730.

4 "Working Stresses for Steels at High Temperatures," by D. S. Jacobus, Trans. ASME, vol. 52, 1930, paper FSP-52-35.

5 "ASME Boiler Code," *Mechanical Engineering*, vol. 71, 1949, p. 954.

6 "Code for Unfired Pressure Vessels," Sect. 8, ASME Boiler Code, 1950 edition, Appendix P.

7 "The Fracture of Carbon Steels at Elevated Temperatures," by A. E. White, C. L. Clark, and R. L. Wilson, Trans. ASM, vol. 25, Sept., 1937, pp. 863–888.

8 "API-ASME Code for Design, Construction, Inspection and Repair, Unfired Pressure Vessels for Petroleum Liquids and Gases," 4th edition, American Petroleum Institute, ASME, 1943.

9 "Failure of Low Carbon Steel Still Tubes," letter by R. H. Thielemann, *Metals and Alloys*, vol. 12, Sept., 1940, pp. 298–300.

10 "Testing of Materials for Service in High Temperature Steam Plant," by R. W. Bailey and A. M. Roberts, Proceedings of the IME, vol. 122, February, 1932, pp. 209–284.

11 "Some Considerations Affecting the Future Development of the Steam Cycle," by K. Baumann, Proceedings of the IME, Dec., 1930, pp. 1305–1396.

12 "The Utilization of Creep Test Data in Engineering Design," by R. W. Bailey, Proceedings of the IME, vol. 131, Nov., 1935, p. 191.

13 "The Resistance to Relaxation of Materials at High Temperature," by E. L. Robinson, Trans. ASME, vol. 61, 1939, pp. 543–554.

14 "High Temperature Bolting Materials," Project 16, Second Progress Report, prepared by E. L. Robinson, Trans. ASTM, vol. 48, 1948, pp. 214–235.

15 "Problems in the Mechanical Design of Gas Turbines," by R. B. Smith, *Journal of Applied Mechanics*, Trans. ASME, vol. 69, 1947, p. A-99.

16 "The Significance of, and Suggested Limits for, the Stress in Pipe Lines Due to the Combined Effects of Pressure and Expansion," by D. B. Rossheim and A. R. C. Markl, Trans. ASME, vol. 62, 1940, p. 443.

17 "ASA Code for Pressure Piping, Fabrication Details," chapt. 3, Expansion and Flexibility.

18 "An Investigation of the Fatigue of Metals," by H. F. Moore and T. M. Jasper, Bulletin No. 136, Engineering Experiment Station, University of Illinois, Series of 1922.

19 "The Fatigue of Metals," by H. F. Moore and J. B. Kommers, McGraw-Hill Book Company, Inc., New York., N. Y., 1927, p. 174.

20 "The Fatigue of Metals," by H. J. Gough, Scott Greenwood & Son, London, England, 1924, Fig. 36.

21 "Shot Blasting to Increase Fatigue Resistance," by J. O. Almen, *SAE Journal*, vol. 51, 1943, pp. 248–268.

Discussion

Perry R. Cassidy.[1] In his excellent paper Mr. Robinson refers to the concealment of true stress in Boiler Code formulas and mentions that actual stress in pipe walls may range from 50 to 80 per cent of the tabular value.

It may be of interest to show the actual pressure stress in super-

[1] Babcock & Wilcox Company, Boston, Mass. Mem. ASME.

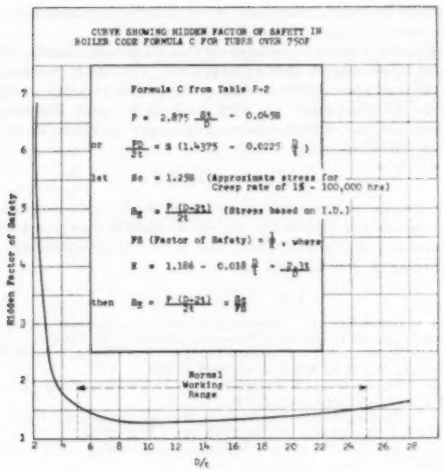

FIG. 10 CURVE SHOWING HIDDEN FACTOR OF SAFETY IN BOILER CODE FORMULA (C) FOR TUBES OVER 750 F

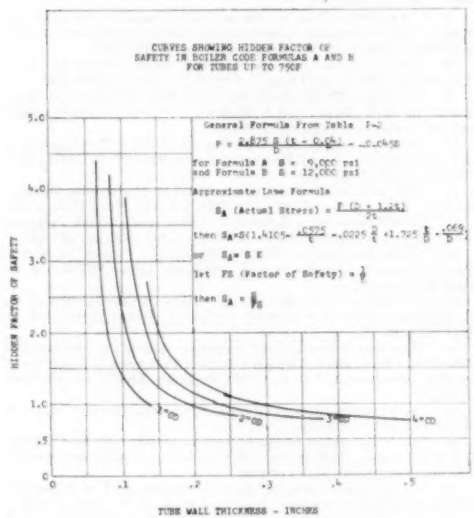

FIG. 10(*a*)

heater tubes operating in the creep range above 750 F. Formula (C) of Table P-2, ASME Power Boiler Code, governs. In Fig. 10 of this discussion a formula and curve are given to show the relationship of the actual stress due to pressure and the tabular stress × 1.25, which corresponds approximately to the stress to produce a creep of one per cent in 100,000 hr.

It will be noted that the maximum stress occurs at a $\frac{D}{t}$ value of 11 and the hidden factor of safety is about 1.25.

It is assumed that the pressure stress in the creep range is best represented by the Common formula using the inside diameter.

Fig. 10(*a*) shows the hidden factor of safety for boiler tubes in accordance with Formulas (A) and (B) of Table P-2 up to 750 F. The factors of safety shown are based upon the approximate Lamé formula for stress due to pressure only and do not include stress due to temperature differential resulting from heat input.

In the paper by R. W. Bailey, the author's reference (12) curves are given for the ratio of pressure stress to creep stress for heated tubes in order that the combined pressure and temperature stress shall not exceed the limiting creep stress selected. The curves for carbon-steel tubes with a stress of 1.5 to 5 tons per sq in and $b = 0.15$ give a temperature stress for $\frac{D}{t}$ of 12 of 0.08 × the creep stress for a heat input of 19,000 Btu per sq ft per hr, and for 38,000 Btu 0.16 × the creep stress.

Bailey uses the stress and temperature at the bore as criteria whereas the Boiler Code formula (C) uses the mean wall temperature of the tube, being slightly more conservative.

It is questionable as to how much consideration need be given to the differential temperature stress in convection superheaters as compared with radiant. In the creep range with time there will tend to be a relaxation of the higher stresses with accelerated strain rate in the primary creep range. The higher the temperature the greater this effect will be. Base-load boilers that operate continuously for long periods should be more favorable in this respect than boilers which are subject to frequent cycles of on and off.

The design of superheater tubes is more a question of experience than of formulas and theory. It is more a question of economics than of safety.

C. L. CLARK.[4] It is rather difficult to discuss a paper in which the author has covered his subject so completely and so well. Being a member of the Subcommittee on Stress Allowances for Ferrous Materials we are particularly pleased at Mr. Robinson's treatment of this matter and especially his remarks as to the importance of the expected life of the equipment in so far as allowable stresses are concerned.

The author's discussion of the various hidden factors of safety in high-temperature equipment should be carefully studied by all concerned in this field. As stated by the author, not only do these hidden factors cause discrepancies between laboratory data and service performance but for those applications in which weight limitations are of importance a thorough understanding of these factors may permit the use of lighter sections with the proper changes in the processing and fabrication of the equipment.

Mr. Robinson's preference for the stress-rupture test in the evaluation of steels for many high-temperature applications is very gratifying to us. We have long advocated this test and believe the information obtained from it to be more useful than that from the creep test for the majority of high-temperature applications. We do believe the author's statement "In the rupture test it is difficult to detect any deterioration of the material before the actual break" needs further explanation. A rupture test conducted on a specimen previously subjected to a rupture test but not carried to fracture, will show a decrease in fracture time corresponding to the length of the previous test if the temperature and stress were the same in both cases.

Another statement by the author ".... so-called stresses due to thermal expansion are not necessarily harmful...." should not be taken too literally and it is not believed that Mr. Robinson intended it should be. In our experiences we have seen just as

[4] Metallurgical Engineer, Special Steel Developments, Steel and Tube Division, The Timken Roller Bearing Company, Canton, Ohio. Mem. ASME.

many, if not more, high-temperature failures due to thermal-expansion stresses than to any other single cause.

There never has been, and may never be, agreement among engineers as to suitable hardness and ductility levels for materials for use at either room or elevated temperatures. There is no question but the materials can be too hard and thus fail prematurely due to their inability to adjust themselves to the applied stresses. To us the most important fact in this respect is for the designer to fully recognize the characteristics of the material with which he is dealing.

D. S. JACOBUS.[5] The author should be commended for making conservative recommendations and advocating advances through a review of procedures, the making of tests, comparisons, and by diverging from practice.

There is no better criterion in deciding safe stresses than the results secured in long-time service. It might seem that too-close an adherence to what has been done might hamper advances. Advances can, however, be made in this way and by studying the knowledge that has been gained on the subject.

My paper on "Working Stresses for Steel at High Temperatures," published in 1930, is referred to. This paper was prepared for the use of the ASME Boiler Code Committee and gave the stresses employed by the Babcock & Wilcox Company at that time. Most of the stresses given in the paper were those which had been used for a long time. For example, the stress of 8000 psi at 800 F for steel plate having a tensile strength of 55,000 to 65,000 lb per sq in., was based on that employed in an oil-cracking still which had been in use for over ten years before the paper was prepared, as well as in other stills which followed with the same working stress.

For a long time before my paper was presented, the ultimate strength at ordinary air temperatures was used for determining the allowable working stress for steel plate up to a temperature of 750 F. In my paper the allowable stress at 750 F was shaded down to allow for the falling off of the yield point and the proportional limit.

In the preliminary copy of the paper it was suggested that the allowable working stress be taken at two thirds that which would produce a rate of creep not exceeding one per cent in 10,000 hr. Parts of the preliminary copy were published in the supplement to the *Engineer* (London), March 28, 1930, which gave one per cent in 10,000 hours. In presenting my paper to the ASME, I changed 10,000 hours to 100,000 hr and said that the more conservative rule was suggested in view of the wide variations in the results of creep tests which had been reported.

The question of which creep rate should be used depends on the individual case. Some vessels may distort a considerable amount without reducing their safety while the distortion must be limited in others. The length of time the vessel will be used is another important feature. There are so many elements that should be considered that there is no general answer and each type of construction should be considered by itself.

We have a lot to learn about setting working stresses in the plastic range. It is well that someone with as broad an experience as the author has made available his knowledge of the many features that should be considered and that he will be able to analyze suggestions which are offered in such a way as to lead to further accomplishments.

T. MCLEAN JASPER.[6] In the concluding remarks of this paper the author states that it has been written to provoke discussion of design stress levels which are applicable to high-temperature machinery and equipment.

I fully agree with the introductory remarks that it is necessary to exploit various methods of testing. I would point out, however, that the tests being considered should bear on the functioning of a structure or material.

I disagree with the general idea that a tensile test is arbitrary in the sense that it is not applicable or needed. Wherever the failure point of a structure is at the ultimate strength then this value becomes highly important. Even the elastic limit or yield point may be arbitrary in many elastic problems involving collapse or vibrations because of the fact that the disaster point of many structures may be far below such values. However, a knowledge of the strength properties that an engineer uses is essential when designing any structure for service.

This statement leads me to approach the matter of various conditions or properties in materials which should dominate the selection of base points from which to calculate designs for operating conditions.

In general, the basing points should be different for different demands of service. These basing points should bear on the properties of shape as well as materials which are to be used in the designs and on the point at which the resulting structures can be considered to have reached the brink of complete or dangerous failure.

Factors of safety, therefore, should be based on different properties depending on the use of a structure or design. In simple language, for such items as pressure vessels, cables, chains, and many other structures the factor of safety should be based on the ultimate strength of the material used. This does not mean that the operating stress should be above, or even approaching, the elastic limit of the material used.

Structures whose failure point because of collapse or other reasons is below the elastic limit or yield point of a material, should be designed considering these physical properties plus the actual collapse or failure point as indicated by tests which consider their slenderness, i.e., $\frac{1}{r}$ in columns under load or $\frac{D}{t}$ in tubes under external pressure.

Structures which deal with vibrations like springs, steam-turbine rotating parts, automobile frames, airplane propellers, and the like need to be designed with consideration of $\frac{M}{EI}$ or the torsion equivalent in order that the allowable limits for riding qualities in automobiles, shock-absorbing properties in springs, close allowable tolerances in steam-turbine rotating parts, and stability factors in propeller blades can be sensibly designed.

In all of these problems the physical and elastic properties of the materials used are exceedingly important in order that the designing engineer may at least reach a safe and satisfactory structure. Needless to say that in the first instance cited, the physical property on which the safety factor should be based is the tensile strength. In the second, it should be the limit of elasticity properly applied, and in the last instance it should be an acceptable $\frac{M}{EI}$ for resilience and satisfactory physical properties including endurance.

I agree with the author that the theory of elasticity is very technical, but I do not imply that for this reason it is something to ignore or to apply with tongue in cheek. Without this theory and a capable engineer to apply it, we would still be minus many of the accomplishments which we now enjoy. The same remarks apply to the theory of least work or least action. These, unbeknown to the architects of antiquity, were the principles which they applied and a knowledge of this fact can and does greatly

[5] Past-President and Honorary Member ASME, Montclair, N. J.

[6] Chicago, Ill. Mem. ASME.

help us in our so-called indeterminate problems. Nature does most of its building by the quiet application of the principles of least work or least action.

Because of going to high and still higher temperatures of operation, we need to know the elastic and long-time strength and yield properties at these elevated temperatures of the materials we wish to use. These values are not obtained in a simple manner. A vast quantity of creep testing at elevated temperatures has been done and its application to service has been carried out with considerable success. These values are not sufficient for the most satisfactory gas-turbine and high-temperature jet designs. The long-time strength and the long-time elastic limit are very desirable at temperatures as high as 1800 F. for some materials and at lower temperatures for others. The moduli of elasticity and rigidity are equally important values to know at these high temperatures.

The choice of working stresses or the application of the best available material for a service is at present in considerable controversy. I agree most heartily with Mr. Robinson in the statement which implies that formulas should conform closely with reality. Safety factors should not contain a large degree of ignorance. They should be based mostly on the hazard and the variations encountered in service. Formulas derived mathematically without confirmation by physical testing are not completely usable. Returning to the discussion of least work and least action, nature's formulas are in most part simple and direct. This of course does not mean that, with several factors which may enter into many problems, the algebraic form of the equation which applies may not seem long.

From the author's discussion on working stress levels it is evident that he thinks largely of the steam turbine and its servicing units when elevated-temperature applications of stress values are being considered. These actual values seem low in the light of operating materials at considerably higher temperature values. Actually, long-time strength and elastic-limit values seem more easily applicable at the higher temperature values. The writer believes that moduli of elasticity and rigidity are not as high as those shown in the critical tables. There is much need for getting very reliable values of these properties. It is something which should take a considerable time and be done for the particular materials now being used for very high-temperature operations.

Practical approaches for the selection of bolt materials for high-temperature service find some vagaries in the creep method of testing. I am referring to the generally stated comments that high-alloy tungsten and molybdenum bolts which show lower creep values than those of 18 Cr 8 Ni composition of the same dimensions are superior in service.

The discussion of ductility in materials is difficult. In the hot-forging, cold-pressing, or shaping of materials, ductility requirements for these operations must be met. After the proper shape has been obtained ductility is of much less use in service than most engineers profess to think. Actually, ductility should be selected on values appropriate to good material for a desired metal strength. Generally, high-strength materials of a general composition are less ductile and more brittle than the low-strength materials. Our spring steels, for instance, which are used for the absorption of large-value repeated stresses are particularly lean in ductility. Our best-strength materials for very high-temperature service are generally very low in ductility. Ductility as a specified quality should represent good materials and no one can ask for a renegade ductility for a greatly desired material and expect to be doing a sensible thing. For instance, high ductility does not represent high fatigue values, high ductility at ordinary temperatures is rarely discovered in the best operating materials at very high temperatures. There are many anomalies. Many of us would like to have our cake and eat it also. The best engineer is going to select his materials on the basis that produces for him the essential, most needed results with the least expenditure and not be throttled by a test method which very often does not represent service needs.

The foregoing discussion applies also to notch sensitivity and impact tests. I am not implying that ignorance of these properties is advised. Too few full-size and time-consuming tests are made. We therefore often endeavor to imagine what will happen to our designs and structures rather than find out by putting them to a practical test.

We shirk from tedious or apparently expensive full-size testing in order to constantly load our structures with expenses of ignorance which straightforward discovery methods could eliminate. The result is an expensive method of avoiding the full-sized test method.

H. A. Wagner.[7] We are indeed indebted to the author for his able exposition of a subject which has been, and continues to be, most controversial. It is difficult to secure agreement on the subject of stress levels and factors of safety even among engineers interested in designing the same type of equipment for use in a specific industry. The long-standing difference in approach to setting allowable stresses for steam piping which exists between the Code for Pressure Piping and the ASME Boiler Code is cited as a case in point. Below 650 F, the Power Boiler Code assigns the same stress at all temperatures to —20 F, whereas the Piping Code permits an increasingly higher stress as the temperature decreases to 150 F. A full discussion of this entire subject by those interested should be helpful either in securing agreement, or in establishing legitimate differences which may exist in stress levels and safety factors in piping or equipment intended for high-temperature service.

With reference to the margin of safety involved between elastic limit and tensile strength mentioned in the paper, I have never been in complete agreement with the practice permitted by the Gas and Air Section of the Code for Pressure Piping wherein the elastic limit is taken as the sole design criterion. This has led to the process followed by some pipe mills of hydraulically expanding pipe so as to increase the transverse yield by cold work. A carbon steel having a normal yield point of about 42,000 psi may have its yield point raised to over 50,000 psi after expanding. This latter value is then used as a basis for gas-transmission pipeline design. The corresponding ultimate strength might be 60,000 psi, which leaves little margin for redistribution of stresses by local yielding. However, I know of no gas-line failures which have been attributed specifically to this factor.

It is indeed desirable to point out the hidden margins involved in computing wall thickness of pipes and pressure vessels as the author has done. On the other hand, factors on the other side of the ledger are: (1) nonhomogeneity of materials; and (2) lack of stability over long periods of time. Lack of uniformity of pipe and castings materials has been observed many times. With reference to lack of long-time stability, neither the rupture nor creep tests evaluate structural permanence. To assume that a 2000 hr, or even 10,000 hr, rupture test can be accurately extrapolated 30 to 150 fold to 300,000 hr seems hardly warranted for materials presently being used.

It seems to me that sufficient consideration has not been given in our discussions to the amount of deformation which can be tolerated in power piping. For valves, the allowable deformation is quite restricted since even slight warpage may result in misalignment of the seats which prevents tight closure of the valve. On the other hand, valves are complex structures for which stresses

[7] Chief Mechanical Engineer, Mechanical Engineering Division, Engineering Department, The Detroit Edison Company, Detroit, Mich. Mem. ASME.

cannot be accurately computed. It is customary practice to use the pipe wall-thickness formula to determine minimum thickness, to which is added 50 per cent to compensate for the shape.

For pipe, however, the long-time deformation may be of significance also, as embrittlement due to long-time exposure at high temperature may result in failure with as little as two per cent elongation. This has been observed by Bailey and others for carbon-moly and chrome-nickel-moly materials. If two to three per cent elongation on a long-time basis is considered the maximum which can be tolerated without failure, design predicated on a stress corresponding to a creep rate of 0.01 in. per in. per 1000 hr (1 per cent per 100,000 hr) can readily be justified for power piping.

With reference to local yielding affording relief to stress concentrations, this is particularly true for flanges, fillets, and the like. It is true also for pipe-line stresses which result from expansion. These should be carefully distinguished from transverse stresses resulting from internal pressure which are not relieved by local yielding. On the contrary, they may be intensified as a result of it as the author indicates. In determining the total longitudinal stresses in a pipe line, however, it seems proper to add the longitudinal stress resulting from the internal pressure to the longitudinal expansion stress to secure the total combined stress.

I believe it is generally recognized that room-temperature tests have little if any relation to the high-temperature characteristics of materials. Lacking an acceptable short-time test to evaluate high-temperature properties, however, it appears that the best we can do is to secure materials which, by room-temperature test, seem to be homogeneous, sound, with chemical and physical properties which seem to indicate that a high-quality product has been obtained. We could use to good advantage a short-time test which would quickly evaluate the long-time high-temperature characteristics of materials.

Author's Closure

The charts contributed by Mr. Cassidy showing the range of values possible for the hidden factor of safety in boiler tubes as provided for in Formulas C, A, and B are very welcome. While these extra margins of safety are provided by the formulation, there are still further margins provided by the procedure with reference to mill tolerance, thickening on the bends, and choice of schedule thickness. The procedure in these respects leads statistically to average stresses well below the nominal *S*-values, giving additional hidden margins.

The mode of analysis suggested by Mr. Cassidy would seem to invite further consideration. If it does not seem practicable to overhaul the formulations which form the backbone of the boiler code, it may be perfectly practicable to chart the relationships between primary stresses and nominal *S*-values, the latter being used for code compliance and the former for analysis of performance.

Dr. Clark pointed out that the author said too little in noting that it is difficult to detect any deterioration of the material before the actual break. Indubitably, as Dr. Clark points out, there is a "taxi meter" counting up the service from beginning to end of the life and it is never reset. The trouble is we cannot see the dial and have no warning of the end of the trip.

Dr. Clark also points out that the author's remarks about the seriousness of thermal expansion are too brief. The author does not believe that a figure arrived at by taking the product of thermal expansion and modulus of elasticity should be held within the same limits as a stress caused by internal pressure or centrifugal force. He believes these different influences should be separately limited and this can be accomplished in piping by 100 per cent cold springing.

Dr. Jacobus is to be credited with originating the modern attitude toward the evaluation of suitable working stresses in the high-temperature range. It is particularly gratifying to have his blessing on this attempt to contribute something further along these lines.

Mr. Jasper should be mentioned as the cosuthor of reference No. 18 which outlines some of the most important characteristics in the behavior of materials. As in the case of Dr. Clark's comments, Mr. Jasper's rounded out certain statements by the author which were too brief. In remarking that the tensile test is "arbitrary" the author had no intention of reflecting adversely upon the importance of this test. He concurs with Mr. Jasper and welcomes this amplification of a statement which might otherwise have conveyed an impression which was not intended.

Mr. Jasper's remarks about stability and the ability to resist a tendency to collapse are very pertinent and relate to a subject not covered by the author at all. As Mr. Jasper remarks farther on, the author has to confess that his background is turbine design.

As in the case of the tensile test, the author also concurs with Mr. Jasper in his remarks about elastic analysis. In deploring the use of elastic analysis where it is not applicable, the author does not wish to belittle at all the use of elastic analysis where it is the most proper means of proportioning.

The author particularly likes Mr. Jasper's remarks on ductility and agrees with him in his preference for full-sized tests.

Mr. Wagner's remarks lead the author to feel that he has, perhaps, called too much attention to the hidden margins of safety in code procedures, whereas there are offsetting factors "on the other side of the ledger." It is because of these matters that the author has favored a setup which would show a definite factor of safety of 2 to 1, all where it can be seen and not hidden in procedure. While Mr. Wagner deems it proper to add pressure and expansion stresses, the author would limit such propriety to the determination of the magnitude of the stress but not its degree of severity. He concurs as to the advantage of "a short-time test which would quickly evaluate the long-time high-temperature characteristics of materials" but recalls a remark attributed to Mark Twain that "the Lord himself cannot make a 3-year old colt in one year."

Upon rereading this paper a year and a half after making the first draft, the author is more than ever conscious of the brevity with which the subject matter is covered. He is grateful to the discussers who have amplified certain particular parts with their comments but he hopes that active discussions will go on along the lines suggested in order to perfect the controls being exercised through the several codes in use throughout the country.

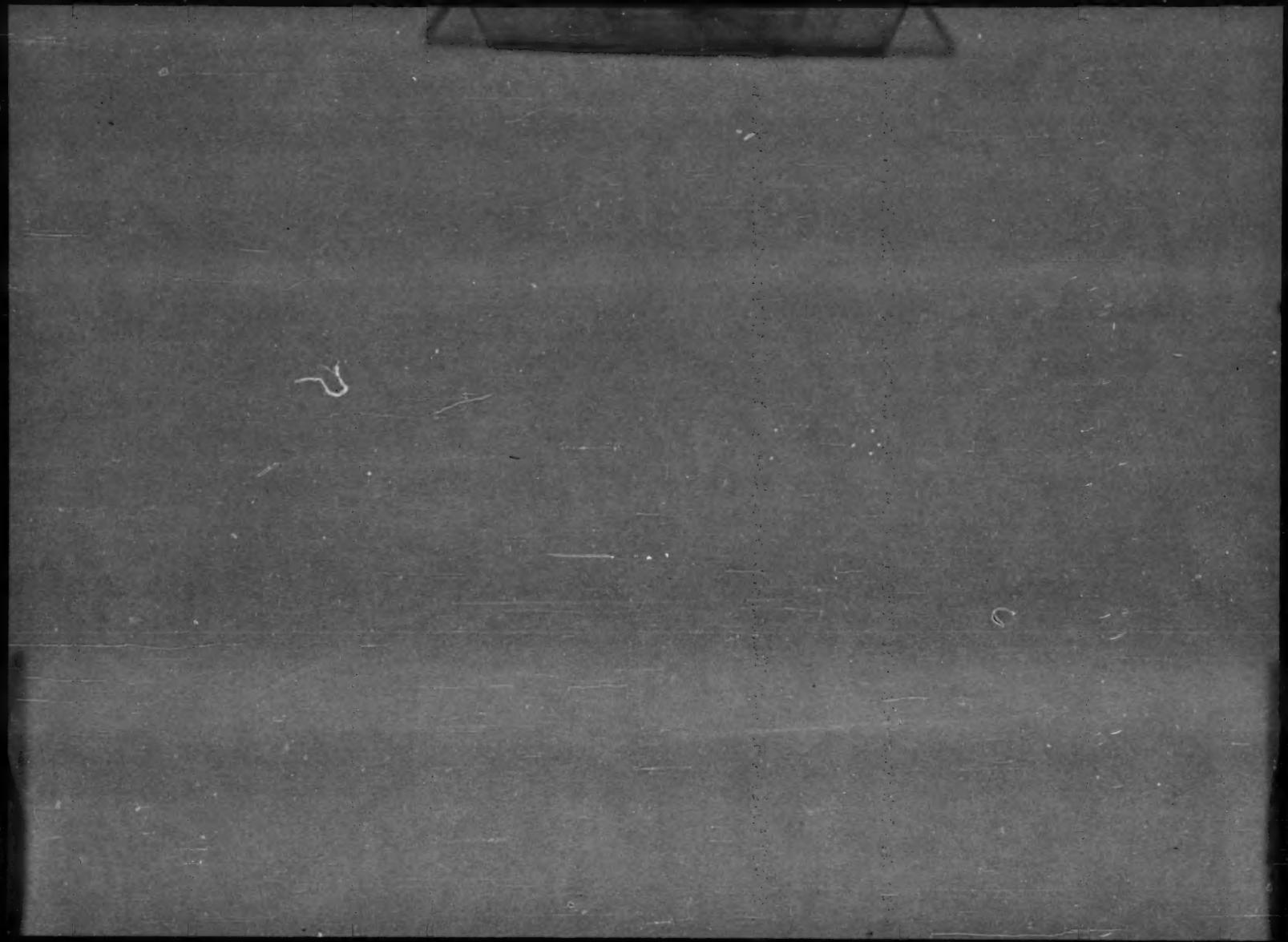

AN ASME PAPER

Its Preparation, Submission and Publication, and Presentation

To a large degree the papers prepared and presented under the ASME sponsorship are evidence by which its professional standing and leadership are judged. It follows, therefore, that to qualify for ASME sponsorship, a paper must not only present suitable subject matter, but it must be well written and conform to recognized standards of good English and literary style.

The pamphlet on "AN ASME PAPER" is designed to aid authors in meeting these requirements and to acquaint them with rules of the Society relating to the preparation and submission of manuscripts and accompanying illustrations. It also includes suggestions for the presentation of papers before Society meetings.

CONTENTS

Price 35¢. No discount allowed. *A remittance must accompany all orders for $2.00 or less. U. S. Postage Stamps are acceptable.*

THE AMERICAN SOCIETY OF MECHANICAL ENGINEERS

29 West 39th Street, New York 18, N. Y.